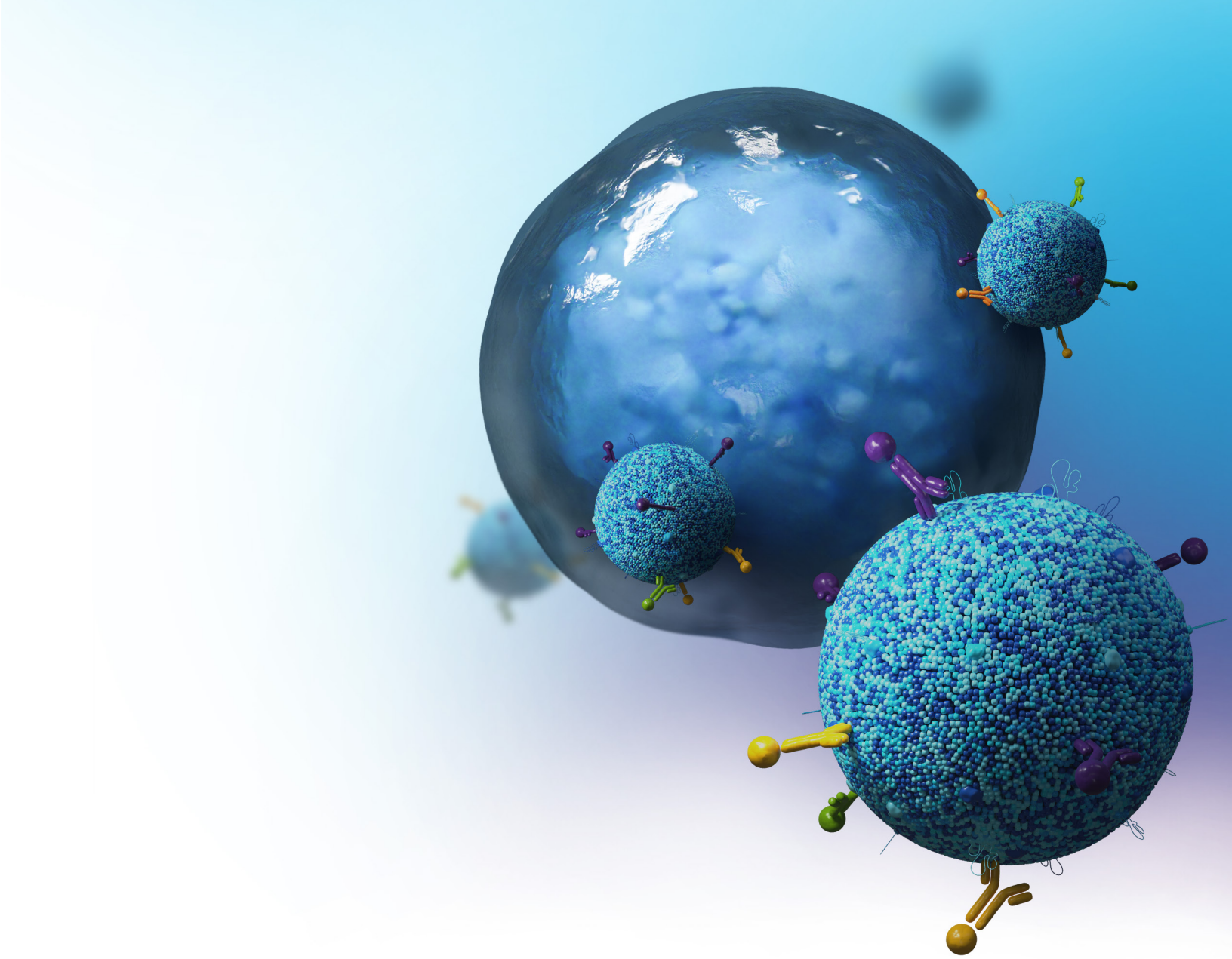

Characterization of Extracellular Vesicles as Messengers and Biomarkers

ARTICLE COLLECTION

WILEY

CURRENT PROTOCOLS
A Wiley Brand

WIREs
Wiley Interdisciplinary Reviews

Sponsored by:
NOVUS BIOLOGICALS
a bio-techne brand

NOVUS BIOLOGICALS
a bio-techne brand

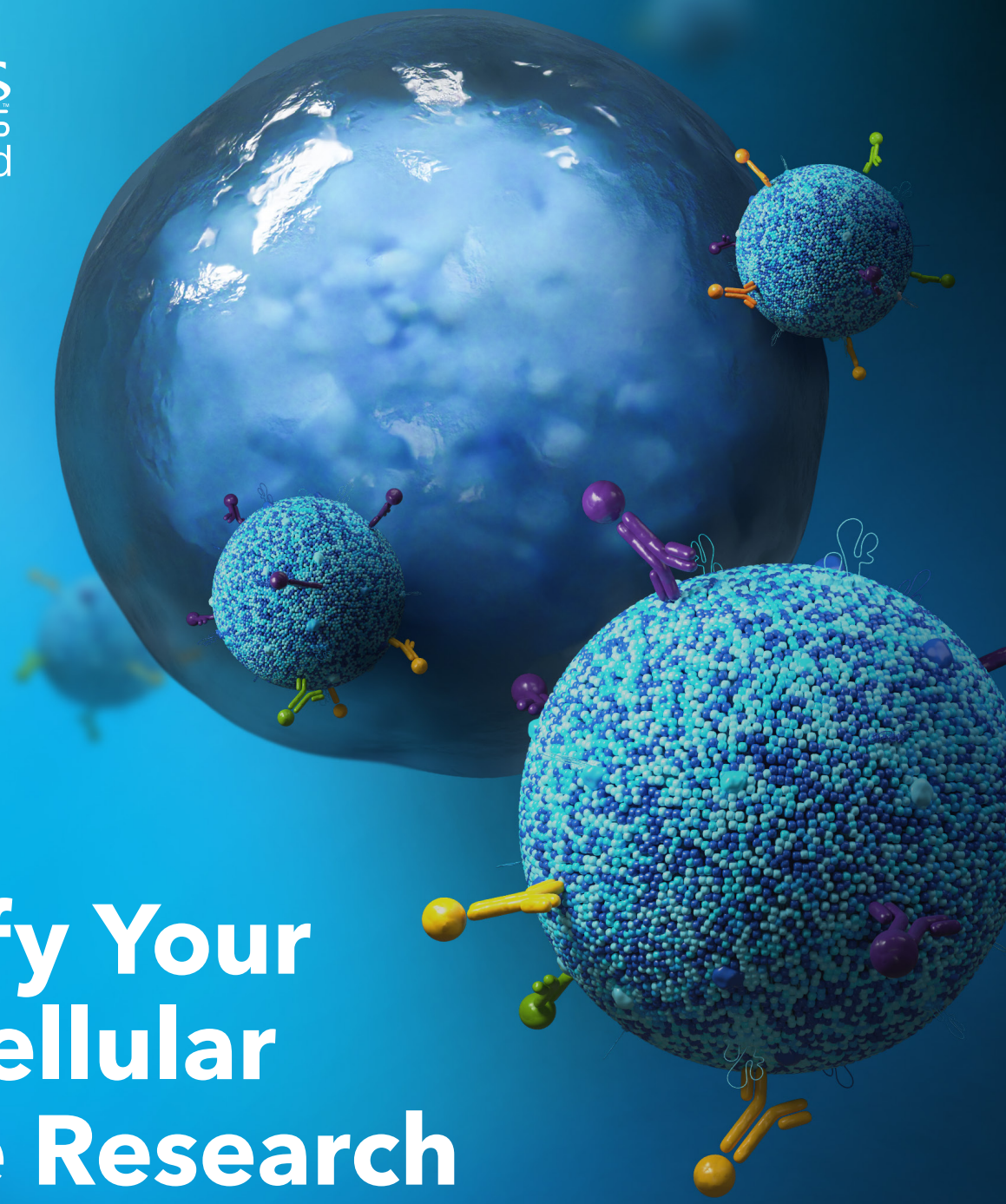

Simplify Your Extracellular Vesicle Research

Whether you are researching the basic biology of extracellular vesicles as intercellular messengers or their potential for use in disease diagnostics, discover how our curated products will help streamline both isolation and detection of these small but mighty nanoparticles.

EV Isolation

- SEC Columns
- TFF Filters
- EV Precipitation Solutions

EV Detection by Flow Cytometry

- Fluorescent Exosome Standards
- EV FACS kits

Learn more | www.novusbio.com/research-areas/cell-biology/exosome-research-tools

Contents

Introduction

Extracellular vesicles (EV) are nanometer-scale membranous particles that can carry and deliver a wide range of cargo, from proteins to genetic material. Investigations into these nanometer vesicles have intensified after the discovery that extracellular vesicles act as conduits of intercellular messages that can influence the activity of neighboring cells, both in normal physiological processes as well as pathophysiology. Furthermore, extracellular vesicles have shown significant promise as biomarkers to diagnose disease states. In this article collection, we present a series of reviews, research articles, and protocols on the fundamentals of EV biology, isolation, and the use of flow cytometry and imaging for characterization to serve as an educational resource for these small but mighty vesicles.

First, Couch et al (2021) presents a broad overview to the field of EV biology, summarizing key research and the emergence of the extracellular vesicle research community. In the review, the current state of the field as well as unresolved research questions are presented and discussed. The next review by De Sousa et al (2022) provides a thorough evaluation of various EV isolation methods and characterization techniques, as well as a discussion of the challenges of using EVs as biomarkers and therapeutic delivery vehicles. These techniques are essential knowledge for any EV biologist, whether in a research or clinical setting, because a complete understanding of the role of EVs requires isolation prior to characterization.

For EV characterization, flow cytometry has become one of the primary techniques used. A number of additional controls and optimizations are required to reliably and accurately report EV characterization data using flow cytometry, from sample injection rates to fluorescent detection limits. In Gorgun et al (2019), they detail a protocol and updated technical guidelines for researchers to follow to isolate and characterize of EVs from mesenchymal stromal cells (MSCs) using flow cytometry. Extracellular vesicles are increasingly of interest as biomarkers of disease and disease progression, especially for cancer. For solid tumors in particular, their use as an early indicator of disease onset and as a diagnostic tool has been heavily investigated. Li et al (2018) assess the use of micro-bead assisted flow cytometry as a method for the detection and molecular phenotyping of EVs in patient serum. They found that using this methodology they can obtain robust and reliable identification and characterization of EVs from breast cancer serum samples. Lastly, Han et al (2020) investigates a recent advancement in the ability to distinguish different types of EVs. Using total internal reflection (TIRF) microscopy to analyze tetraspanin colocalization, they identify different EV populations through direct visualization of differential marker expression at single vesicle resolution.

In summary, this article collection will educate the reader as to the current state of knowledge and ongoing research into extracellular vesicles. As isolation and characterization methods advance, understanding how extracellular vesicles function as integral components of intercellular signaling pathways will lead us to greater biological insights and potential therapeutics for human diseases.

By Jeremy Petravicz, PhD, Senior Editor,
Current Protocols

References

Couch, Y., Buzàs, E. I., Di Vizio, D., Gho, Y. S., Harrison, P., Hill, A. F., Lötvall, J., Raposo, G., Stahl, P. D., Théry, C., Witwer, K. W., & Carter, D. R. F. (2021). A brief history of nearly EV-erything – The rise and rise of extracellular vesicles. *J Extracell Vesicles*. 10, e12144. https://doi.org/10.1002/jev2.12144

De Sousa, K. P., Rossi, I., Abdullahi, M., Ramirez, M. I., Stratton, D., & Inal, J. M. (2022). Isolation and characterization of extracellular vesicles and future directions in diagnosis and therapy. *WIREs Nanomedicine and Nanobiotechnology,* e1835. https://doi.org/10.1002/wnan.1835

Gorgun, C., Reverberi, D., Rotta, G., Villa, F., Quarto, R., & Tasso, R. (2019). Isolation and flow cytometry characterization of extracellular-vesicle subpopulations derived from human mesenchymal stromal cells. *Current Protocols*, 48, e76. doi: https://doi.org/10.1002/cpsc.76

Li, W., Shao, B., Liu, C., Wang, H., Zheng, W., Kong, W., Liu, X., Xu, G., Wang, C., Li, H., Zhu, L., Yang, Y. Noninvasive Diagnosis and Molecular Phenotyping of Breast Cancer through Microbead-Assisted Flow Cytometry Detection of Tumor-Derived Extracellular Vesicles *Small Methods* 2018, 2, 1800122. https://doi.org/10.1002/smtd.201800122

Han, C, Kang, H, Yi, J, et al. Single-vesicle imaging and co-localization analysis for tetraspanin profiling of individual extracellular vesicles. *J Extracell Vesicles*. 2021; 10:e12047. https://doi.org/10.1002/jev2.12047

Received: 19 May 2021 | Revised: 6 August 2021 | Accepted: 28 August 2021

DOI: 10.1002/jev2.12144

REVIEW ARTICLE

A brief history of nearly EV-erything – The rise and rise of extracellular vesicles

Yvonne Couch[1] | **Edit I. Buzàs**[2,3,4] | **Dolores Di Vizio**[5] | **Yong Song Gho**[6] | **Paul Harrison**[7] | **Andrew F. Hill**[8] | **Jan Lötvall**[9] | **Graça Raposo**[10] | **Philip D. Stahl**[11] | **Clotilde Théry**[12] | **Kenneth W. Witwer**[13] | **David R. F. Carter**[14,15]

[1] Acute Stroke Programme, Radcliffe Department of Medicine, University of Oxford, John Radcliffe Hospital, Headley Way, Headington, Oxford, UK

[2] Department of Genetics, Cell- and Immunobiology, Semmelweis University, Budapest, Hungary

[3] ELKH-SE Immune-Proteogenomics Extracellular Vesicle Research Group, Budapest, Hungary

[4] HCEMM-SU Extracellular Vesicles Research Group, Budapest, Hungary

[5] Department of Surgery, Pathology & Laboratory Medicine, Cedars-Sinai Medical Center, Los Angeles, California, USA

[6] Department of Life Sciences, Pohang University of Science and Technology, Pohang, Republic of Korea

[7] Institute of Inflammation and Ageing, College of Medical and Dental Sciences, University of Birmingham, Edgbaston, Birmingham, UK

[8] Department of Biochemistry and Genetics, La Trobe Institute for Molecular Science, La Trobe University, Bundoora, Victoria, Australia

[9] Krefting Research Centre, Institute of Medicine Sahlgrenska Academy at University of Gothenburg, Gothenburg, Sweden

[10] Institut Curie, Paris Sciences et Lettres Research University, Centre National de la Recherche Scientifique UMR144, Structure and Membrane Compartments, Paris, France

[11] Department of Cell Biology, Washington University School of Medicine, St Louis, Missouri, USA

[12] INSERM U932, Institut CurieParis Sciences et Lettres Research University, Paris, France

[13] Molecular and Comparative Pathobiology and Neurology, and The Richman Family Precision Medicine Center of Excellence in Alzheimer's Disease, The Johns Hopkins University School of Medicine, Baltimore, Maryland, USA

[14] Department of Biological and Medical Sciences, Faculty of Health and Life Sciences, Oxford Brookes University, Oxford, UK

[15] Evox Therapeutics Limited, Oxford Science Park, Oxford OX4 4HG, UK

Correspondence
David RF Carter, Evox Therapeutics Limited, Oxford Science Park, Oxford, OX4 4HG, UK.
Email: dcarter@brookes.ac.uk

Funding information
BBSRC, Grant/Award Number: BB/P006205/1; Cancer Research UK, Grant/Award Number: A28052; Alzheimer's Research UK, Grant/Award Number: ARUK-RF2019B-004; NIH/NCI, Grant/Award Numbers: DDV: R01CA234557, R01CA218526, KWW: AI144997, DA047807, MH118164, CA241694; Michael J. Fox Foundation; Scar Free Foundation and the National Institute for Health Research (NIHR) Surgical Reconstruction and Microbiology Research Centre (SRMRC)

Abstract

Extracellular vesicles (EVs) are small cargo-bearing vesicles released by cells into the extracellular space. The field of EVs has grown exponentially over the past two decades; this growth follows the realisation that EVs are not simply a waste disposal system as had originally been suggested by some, but also a complex cell-to-cell communication mechanism. Indeed, EVs have been shown to transfer functional cargo between cells and can influence several biological processes. These small biological particles are also deregulated in disease. As we approach the 75th anniversary of the first experiments in which EVs were unknowingly isolated, it seems right to take stock and look back on how the field started, and has since exploded into its current state. Here we review the early experiments, summarise key findings that have propelled the field, describe the growth of an organised EV community, discuss the current state of the field, and identify key challenges that need to be addressed.

KEYWORDS
ectosome, exosome, extracellular vesicle, microparticle, microvesicle

1 | THE EARLY EXPERIMENTS

The experiments in which EVs were specifically identified as biological entities, with enzymatic and functional potential, began during the 1980s and 1990s. Prior to this period there are numerous studies that hint at potential structures that *would subsequently* be described as EVs, or that describe experiments in which we can retrospectively speculate *may have* involved the activity of EVs. In this sense the story of the origins of EV research arguably begins with the studies of coagulation.

As a topic this dates back to the mid-1600s and is covered in excellent reviews elsewhere (Hargett & Bauer, 2013; Quick, 1966). For the purposes of this article we will start with Chargaff and West and their studies on blood clotting, performed in New York in the 1940s. West was a clinician, with an on-going interest in anaemia and haemophilia, and Chargaff was a biochemist. Chargaff had begun a series of papers in 1936 in the Journal of Biological Chemistry entitled *Studies on the Chemistry of Blood Coagulation* and made an observation in paper XIX of the series – *Cell Structure and the Problem of Blood Coagulation* – which can be interpreted as the beginning of the field of EV biology. When spinning down blood to establish a centrifugation protocol to separate clotting factors from cells, Chargaff observed that "*the addition of the high speed sediment to the supernatant plasma brought about a very considerable shortening of the clotting time*" (Chargaff, 1945). Enigmatically he went on to say "*this will be discussed in detail on a later occasion*"; that later occasion turned out to be his paper published with Randolph West in 1946 on *The Biological Significance of the Thromboplastic Protein of Blood*. Here they discovered a 'particulate fraction' which sedimented at 31,000 *g* and had high clotting potential, as well as a 'thromboplastic protein'. The authors suggested that this fraction "*probably includes, in addition to the thromboplastic agent, a variety of minute breakdown products of blood corpuscles*" (Chargaff & West, 1946). However, it would be some years before these were specifically identified as EVs.

In fact, 17 years would pass until Peter Wolf described a "*material in minute particulate form, sedimentable by high-speed centrifugation and originating from platelets, but distinguishable from intact platelets*" which we now know as the EV fraction. Wolf published electron microscopy images of these particles, which he described as 'platelet dust' (Wolf, 1967). Following this, in 1971, Neville Crawford published further images of these vesicles—which were now being described as 'microparticles'—obtained from platelet-free plasma. Crawford also showed they contained lipid and carried cargo including ATP and contractile proteins (Crawford, 1971). These pioneering experiments with platelets were the first to describe the presence and coarse structure of such cell-free components and hinted at their potential biological importance.

Between the mid-1960s and early 1980s other early electron microscopy studies described structures consistent with the sub-micron size of EVs. In the summer of 1966, Sun described vesicle-like structures released from alveolar cells into the alveolar space (Sun, 1966). In the late 1960s, H. Clarke Anderson and Ermanno Bonucci described 'matrix vesicles'. These small membrane-bound vesicles of different sizes are embedded in the matrix of hypertrophic cartilage and could potentially play a role in bone mineralisation (Anderson, 1969; Bonucci, 1967). Nunez et al., and Gershon (1974) described the presence of small (1-10 nm) extracellular vesicles in the bat thyroid gland during arousal from hibernation (Nunez et al., 1974). In fact, this paper was one of the first to describe the presence of multivesicular bodies (MVBs) close to the apical membrane. The authors proposed that "*fusion of the outer or limiting membrane of the multivesicular body with the apical plasma membrane might lead to the release of the vesicles contained within the structure into the luminal space*" (Nunez et al., 1974). Indeed, we now define a subtype of EV, commonly called the exosome or small EV, as being formed when the endosomal MVB structure fuses with the plasma membrane, leading to the release of the intraluminal vesicles (for an illustration of the different types of EVs *see* Figure 1).

In addition to these experiments where vesicles were found in a happenstance manner, others were specifically looking for vesicles. Between 1950 and 1970 there were several researchers who were hoping to prove that viruses caused diseases beyond infection, specifically that they caused cancer. In looking for 'virus-like particles' in biofluids they often came across particulate matter (Levine et al., 1967; Seman et al., 1971) but could not identify anything they thought might actually be viral in nature (Dmochowski et al., 1968; Haguenau, 1959; Levine et al., 1967). Moreover, the particles seemed to be present in control fluids as well as those from cancer patients (Fawcett, 1956; Lunger et al., 1964; Prince & Adams, 1966). By the mid-1960s the consensus was that it was unlikely that particles found in biofluids were attributable to viruses but were rather an artefact of separation (Prince & Adams, 1966). Finally, in 1975 Dalton published a paper studying fractions of filtered and unfiltered foetal bovine serum and demonstrated that the sera held similar particles to an epithelial cell line. He put an end to the reign of the virus-like particle by saying that '*to call structures with the morphology of normally occurring vesicles of multivesicular bodies and of microvesicles associated with epithelial cells "virus-like" is unwarranted*' (Dalton, 1975).

Studies in other organisms suggested that vesicular structures extruded from cells were not unique to mammals. A study of *Ochromonas danica*, a flagellated alga, revealed the presence of a range of vesicles that could be visualised budding from cells and isolated by centrifugation (Aaronson et al., 1971). Preparations including EVs released by the yeast *Candida tropicalis* were shown to decrease growth of other cultures of yeast (Chigaleichik et al., 1977). Different kinds of vesicles were shown to be released by Corynebacterium, some of which were shown to induce cell agglutination (Vysotskii et al., 1977); Acinetobacter, which were seen to release phospholipid-rich EVs (Käppeli & Finnerty, 1979); and the gram negative bacteria, *Escherichia coli*, which was shown to produce EVs containing lipopolysaccharide complexes (Käppeli & Finnerty, 1979). Whilst these studies began to unravel the ultrastructure of cells and the potential existence of EVs the research had yet to gain the momentum to unite as a cohesive field.

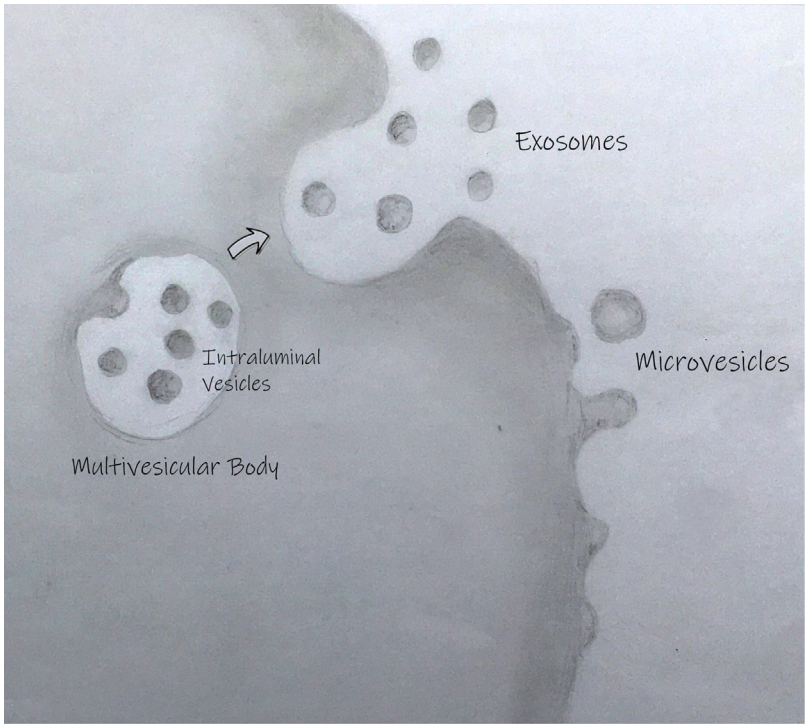

FIGURE 1 The primary routes of extracellular vesicle biogenesis. Exosomes are released from cells when a multivesicular body (which is formed when an early endosome matures and inwardly buds to form intraluminal vesicles) fuses with the plasma membrane. Ectosomes (more commonly called microvesicles and microparticles) are formed when the plasma membrane buds outwardly and pinches off. Cargo can be loaded into both intraluminal vesicles (which are released as exosomes) and ectosomes. Other types of vesicles such as apoptotic bodies (not shown) can be released by dying cells.

2 | THE START OF SOMETHING ~~BIG~~ SMALL

The early 1980s mark the start of the era of expansion and more specific understanding in EV research. Whilst the significant explosion of papers, theories, arguments about nomenclature and EV-related societies wouldn't begin for another 20 years or so, the cohesion began here. Two seminal and complementary papers published by the Johnstone and Stahl laboratories made a watertight case for the release of intraluminal vesicles from the cell, and defined them as exosomes (Harding et al., 1983; Pan & Johnstone, 1983). Whilst these papers are now considered seminal and the origins of our field, Rose herself felt the discovery to be happenstance, saying they had an '*Alice in Blunderland approach which led to the discovery of exosomes*' (Johnstone, 2005). Both laboratories were using reticulocyte maturation as a model; Stahl's group to investigate membrane trafficking, and Johnstone's lab to study the biochemistry of the plasma membrane. Their work showed that during reticulocyte maturation the transferrin receptor was lost via the release of vesicles. Cliff Harding, then an MD/PhD in the Stahl laboratory, produced some stunning EM images demonstrating that these vesicles were released from the lumen of MVBs upon fusion with the plasma membrane. Conceptually, the Harding et al. (1983) paper revealed the existence of a novel intracellular sorting and trafficking pathway, now referred to as the exosome secretion pathway. Although Trams et al., and Heine (1981) originally coined the term 'exosome' to describe EVs shed from the surface of the cell (Trams et al., 1981), Rose Johnstone applied the name to those vesicles specifically released following fusion of MVBs with the plasma membrane and in this context the name caught on (Johnstone et al., 1987; Witwer & Théry, 2019).

As well as defining one of the hallmarks of EV vernacular, an early lecture by Rose Johnstone may have been responsible for the global opinion of EVs as just 'waste disposal mechanisms' for the ensuing decade. In 1991 she gave the Jeanne Manery-Fisher Memorial Lecture which she titled *'Maturation of reticulocytes: formation of exosomes as a mechanism for shedding membrane proteins'* which was primarily based on her paper from the same year where she suggested that exosomes were a '*major route for externalization of obsolete membrane proteins*' (Johnstone et al., 1991). This paper demonstrated the presence of the transferrin receptor on exosomes, and the presence of the nucleoside transporter. The authors demonstrated that different cellular stresses resulted in the internalization and shedding of these membrane components at different times. Whilst they did not speculate on the mechanisms of this, the message that this was a way for the cells to shed 'obsolete' proteins stuck in the minds of researchers for some years to come.

Despite this, these early studies laid the foundation for the explosion of interest that followed over the next 35 years. In terms of the period between these seminal papers and the start of the massive expansion in EV research at the millennium, form seemed to come before function. Articles on platelet derived microparticles, microvesicles and exosomes dominated, with some important early advances in the understanding of the fundamental nature of EVs. These early studies demonstrated lateral diffusion of lipids and proteins in vesicle membranes (Gawrisch et al., 1986) and the presence and function of flippases (Vidal et al., 1989). Studies revealed glimpses of the iconic components of EVs we know today such as Rab, ARF (Vidal & Stahl, 1993) and the tetraspanins

(Escola et al., 1998). As early as 1986 there were concerns about storage of blood and its effects on the EV population (George et al., 1986). In addition to work on mammalian EVs, a wealth of knowledge was developed about bacterial EVs in studies from Liverpool on *Porphyromonas gingivalis* (Kay et al., 1990; Smalley & Birss, 1987; Smalley et al., 1988, 1989). These last papers demonstrated not only the presence of bacterial EVs but the interaction of these EVs with mammalian cells in the body (Kay et al., 1990).

During the 1980s and 1990s several articles reported the quantification of EVs, demonstrating altered EV numbers in disease. The phenomenon started around 1993 with a paper on elevated microparticles in transient brain ischemia and other infarctions (Lee et al., 1993), but goes on to be explored in diseases such as angina (Singh et al., 1995) and Crohn's (Powell et al., 1996). Papers describing the physical and biochemical characteristics of EVs also began to emerge. Rose Johnstone's 1989 paper demonstrated exosomes released from reticulocytes are enzymatically active (Johnstone et al., 1989). Membrane vesiculation was shown to be a potentially protective mechanism to prevent cell lysis (Iida et al., 1991), and a way of specifically exposing phosphatidyl serine to enhance clotting (Chang et al., 1993). It was also revealed that other active enzymes could exist in EVs (Fourcade et al., 1995). Outside the field of platelet biology, it was discovered that EVs from immune cells are capable of presenting antigen (Raposo et al., 1996). This last paper, in particular, was a watershed moment that caught the imagination of many and helped to catalyse increased interest in the field of EVs. It showed that EVs had the potential to be harnessed as anti-tumoral vaccines; indeed, this study led the Amigorena lab to investigate whether dendritic cells secrete EVs that, when loaded with tumor peptides, can eradicate tumours (Zitvogel et al., 1998), and led to clinical trials over the next decade (Escudier et al., 2005). Importantly, it showed that EVs could play functional roles in biological processes. Taken together, these ideas that EVs could have physiological roles, that they could be used as biomarkers, and that they could have therapeutic applications, led to the explosion of interest in EVs in the early 21st century.

3 | A ROSE BY ANY OTHER NAME

In 2018 Roy and colleagues performed a systematic survey of all the papers published in the field since 2000, demonstrating the exponential growth of the field since the millennium (Roy et al., 2018). This included not only thousands of papers but also patent applications and grant funding. The specific search criteria to isolate key papers for this current review identified 1017 articles published in the 15 years between 1985 and 2000, and more than four times that number in the 10 years to 2010. The issue, still plaguing the field today, although vastly improving (Witwer & Théry, 2019), was the issue of nomenclature (Box 1) (Gould & Raposo, 2013; Witwer & Théry, 2019). Of the > 4000 papers from 2000 to 2010 the most popular search term was 'microparticles'. This proves challenging as a search criterium because not only can it refer to platelet microparticles, but also microparticles of iron oxide (frequently used as an imaging agent) and synthetic microparticles for drug delivery. Sifting out the relevant papers remained challenging. During this period 'exosomes' remained more popular than 'microvesicles' or 'ectosomes' (respectively 945, 664 and 261 papers; though it should also be noted that the term 'exosome' also describes RNA-processing machinery). The term 'extracellular vesicles' was barely seen at all with a mere 31 papers.

In the decade following the year 2000 the first reviews began to be published in the field of EV biology (Denzer et al., 2000; Schartz et al., 2002). The growing community of researchers started to explore the nature of EVs in more depth, investigating the proteome of EVs from various cell types (Bard et al., 2004; Théry et al., 2001; Wubbolts et al., 2003) as well as the lipidome (Subra et al., 2007). Cytokines were shown to be shed via EVs (Mackenzie et al., 2001) and EVs derived from immune cells were found to play a key role in the function of the immune system (Skokos et al., 2003; Van Niel, 2003). The increased interest in tumor-derived EVs (Wolfers et al., 2001), combined with new knowledge of the role of EVs in the immune system, led to their potential as anti-tumor therapy (Chaput et al., 2003). As the decade winds down, the real expansion in EV research began. Papers began to demonstrate the functional effects of EVs in vivo, protecting animal models from disease (Colino & Snapper, 2007). The functional transfer of nucleic acids was demonstrated (Ratajczak et al., 2006; Skog et al., 2008; Valadi et al., 2007), and a report that plant cells can use EVs as a means of communication was also published (An et al., 2007). The increased interest in EV-based therapy was merged with burgeoning interest in stem cells as therapy, and 2009 saw the emergence of a plethora of papers on mesenchymal stem cell (MSC)-derived vesicles (Bruno et al., 2009), further increasing the therapeutic opportunities afforded by EVs.

Some key EV milestones from 1940 to 2010 are summarised in Figure 2. From 2010 to today the expansion of the field has been enormous. EVs have been shown to be involved in numerous biological processes across many species, and they contribute to a plethora of diseases when deregulated. It would be unfair to pick out individual contributions to this latest decade of work as it has become so diverse and specialised, and the reader is directed to more recent reviews (Mathieu et al., 2019; Raposo & Stahl, 2019; Welsh et al., 2020).

The early 2000s also saw the first organized EV meetings take place, and the regular meetings of the International Society for Extracellular Vesicles (ISEV) now have thousands of participants working in a multitude of disciplines from all over the world. Now came the time to organize these disparate researchers and bring them together with a common purpose.

BOX 1 – EV NOMENCLATURE

In the early years of the field, a variety of terms were used to describe the structures that were observed, including 'extracellular microvesicles', 'microparticles, 'pequenas particulas' (small particles), and 'virus-like particles'. The term 'exosome' was first used in the context of EVs by Trams *et al* (Trams et al., 1981) to describe vesicles that are produced directly by outward budding at the plasma membrane. Later, Rose Johnstone used the term 'exosome' to describe vesicles released following the fusion of MVBs with the plasma membrane (Johnstone et al., 1987), and this has become ISEV's recommended term for this type of vesicle (Théry et al., 2018). As the field grew, and understanding of the variety of biogenesis pathways increased, it became clear that distinct and precise nomenclature was required (Gould & Raposo, 2013). It was suggested that the catch-all term 'extracellular vesicles' should be used to describe non-replicating structures that are delimited by a lipid bilayer (György et al., 2011), and this was formalised into the current recommendations within the MISEV guidelines (Théry et al., 2018). Confusion in nomenclature can arise due to the assignment of arbitrary size ranges for different types of vesicle; in fact, the proposed names for different types of EVs are based on biogenesis pathways (Théry et al., 2018) (see also figure 1). The range of terms used to describe the different types of EV continues to grow, and authors should clearly define what type of EV they are referring to (Théry et al., 2018; Witwer & Théry, 2019). The issue of EV nomenclature has caused controversy over the years, and not all researchers agree with current recommendations (Witwer & Théry, 2019). The use of the term 'exosome' as a general term for EVs continues to pervade the literature (Roy et al., 2018), despite the fact that most (if not all) EV samples contain a heterogeneous mixture of vesicle types (Van Deun et al., 2017). This prevalence for the term 'exosomes' to describe EVs may be due to the anecdotally reported perception of exosomes as a more 'desirable' term, particularly in the context of industrial applications of EVs (Witwer & Théry, 2019). Similarly, the terms ectocytosis (Stein & Luzio, 1991), proposed to design specifically release of EVs from the plasma membrane, and ectosomes for such EVs (Cocucci & Meldolesi, 2015; Hess et al., 1999), are still less commonly used than the term 'microvesicles' for plasma membrane-derived vesicles. It is therefore important that the field continues to discuss the best way to describe these exciting extracellular voyagers, and clear reporting is crucial to reduce confusion in nomenclature.

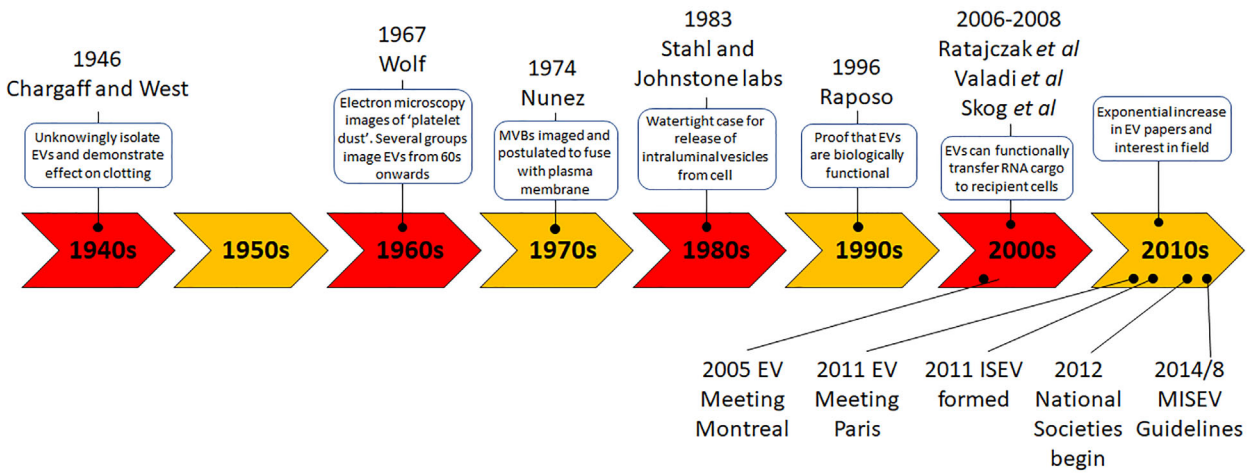

FIGURE 2 Timeline of selected milestones in the EV field

4 | BRINGING ORDER TO THE CHAOS

The first international meeting for EVs (called exosomes at the time) was organised by Rose Johnstone and held in Montreal in 2005 (Couzin, 2005). An international meeting in 2010 in Oxford focused on advances in methodologies for measuring EVs (including new biophysical approaches such as Nanoparticle Tracking Analysis (Dragovic et al., 2011), which led to the publication of the first book on EVs (Harrison et al., 2014). A seminal moment came at a vibrant (and oversubscribed) international meeting organised by Clotilde Théry and Graça Raposo, held in Paris in 2011. At this meeting of over 200 attendees, Jan Lötvall (who fortunately was allowed to attend despite a late registration!) proposed the formation of an International Society to represent the interests of the field. Following extensive consultations with members of the community, the International Society for Extracellular Vesicles (ISEV) was formed in 2011. The first ISEV meeting was held in 2012, in Gothenburg, Sweden,

and attracted more than 400 participants and was also oversubscribed. Subsequent ISEV annual meetings in Boston (2013), Rotterdam (2014, 2016), Washington (2015), Toronto (2017), Barcelona (2018) and Kyoto (2019) saw rapid growth in attendee numbers with over 1000 attendees recorded for the last 2 years. With the eruption of a global pandemic in 2020, the ISEV meeting went virtual, holding its first international online conference to great success. The society also organises and supports a variety of other focused workshops and surveys that lead to 'position papers' (Hill et al., 2013; Lener et al., 2015; Mateescu et al., 2017; Russell et al., 2019; Witwer et al., 2013), survey outputs (Gardiner et al., 2016; Soekmadji et al., 2018), and meeting reports (Araldi et al., 2012; Clayton et al., 2018; Hu et al., 2017; Soares et al., 2017), many of which are published in the society's 'Journal of Extracellular Vesicles' (JEV) (Lötvall et al., 2012). These have played an important role in helping to collate and focus the efforts of the field. This is perhaps best exemplified by the publication of 'Minimal Information for Studies of EVs' (MISEV) guidelines in 2014 (Lötvall et al., 2014), which has been more recently reviewed, in 2018 (Théry et al., 2018). ISEV has therefore provided an effective platform for researchers around the world to come together and share their work on EVs.

As the EV field expands, so too does the number of researchers in each country. This has led to the formation of numerous 'National Societies' or local networks who conduct their own local meetings and support EV research within their own countries. For a field where for many years there was considerable scepticism about whether EVs were just cellular debris, local support networks capable of validating findings and sharing new ideas, reagents, models and techniques, are crucial. These networks began in the US in 2012 with the American Society for Exosomes and Microvesicles and expanded from there; the Grupo Español de Innovación e Invesigación en Vesículas Extracelulares (in 2012), the UK, French and German Societies for EVs (in 2018), are but a few of the many national groups working together with the common goal of forwarding EV research. These National Societies help to coordinate national meetings and support regional networks of EV researchers, providing opportunities for newcomers to the field to network with established labs. Together with ISEV they provide an important support mechanism in the rich research ecosystem for the field.

ISEV has also strived to produce educational material for those new to the EV field. This includes the production of two popular and free Massive Open Online Courses (Lässer et al., 2016), the production of a 3D animated video on EV function, and posters on the basics of EVs (Nieuwland et al., 2018). This not only helps give new researchers perspective on the field, but also helps with some of the challenges and disputes the field has had, and continues to have, regarding standardization and nomenclature.

5 | CHALLENGES

The proliferation of EV research around the world has propelled the field forwards at an ever-increasing pace, but this brings with it a different set of problems. The EV field, as with science more generally, may suffer from a lack of reproducibility (Begley & Ellis, 2012; Neuhaus et al., 2017). This is exacerbated by the relatively young state of the field and the 'hype', which drives accelerated publication of 'exciting' new findings. The technical challenges and position papers from ISEV and other international groups have been outlined comprehensively elsewhere (Ramirez et al., 2018). Below are some of the major issues the field continues to contend with.

6 | STANDARDISATION AND REPORTING

There is no universal agreement on many aspects of methodology in EV research, including the best methodology for enrichment, and protocols vary between laboratories (Gardiner et al., 2016). In the 1990s the International Society on Thrombosis and Haemostasis (ISTH) vascular biology subcommittee (SSC) initiated the discussion and early standardization efforts of microparticle measurements. The SSC has continued to publish important articles on pre-analytical variables, inter-laboratory studies and standardization of flow cytometry. On-going standardization and collaboration between the ISTH SSC, ISAC (International society for advancement of cytometry) and ISEV continue. A recent consortium-effort to catalogue EV research revealed a total of 1,742 experiments with 190 different isolation methods and 1,038 unique protocols to isolate EVs (Van Deun et al., 2017). While it is too early to pronounce which methodology is 'right or wrong', the heterogeneity in approach and frequent lack of complete reporting make comparing and interpreting the results of different studies more difficult and reaching general conclusions more challenging. This is further compounded by a lack of experimental reference materials and controls that can be reliably used to standardise experiments between labs. Initiatives such as EV-TRACK (Van Deun et al., 2017), the MISEV guidelines (Théry et al., 2018), EV databases (Kalra et al., 2012; Simpson et al., 2012), attempts to generate reference materials (Welsh et al., 2020). ISEV taskforces and ISEV workshops on 'Rigour and Reproducibility' aim to address these issues, but transparency in reporting and standardisation of methodology remain two of the greatest challenges for this nascent field.

7 | TECHNICAL CHALLENGES

There are many technical challenges associated with working on EVs which are detailed well elsewhere (Ramirez et al., 2018). Briefly, there are several techniques available for isolating EVs; they all have pros and cons, and the best choice depends on the intended downstream applications, the type of EV of interest, and level of homogeneity required (Gardiner et al., 2016). However, there is still a need to develop improved methodology to enrich higher yields, with greater homogeneity, faster time, and lower cost. The challenge is because the fluids that EVs are enriched from are typically complex matrices containing multiple contaminants, often of similar size and/or density (Ramirez et al., 2018). Improved tools are also required for characterising and quantifying EVs. A key problem here is the relatively small size of most EVs, which makes specifically counting and characterising EVs a challenge, and there is currently no perfect instrument for quantifying and characterising EVs. Another issue is their relative paucity of material when isolating EVs. To obtain sufficient material for testing using most 'bulk methods' (in which material from multiple vesicles is aggregated for testing), such as Western blotting, a lot of EVs are required. More sensitive methods are therefore required to make EV characterisation less onerous on laboratories. 'Single-EV' methodology must be developed and improved to allow a greater range of experiments to be performed and new insights generated into EV biology. Finally, improved in vivo methods are required for studying the biology of EVs. These challenges, amongst many others, are being addressed by multiple labs around the world, and as these technical issues are addressed our ability to test hypotheses about EV function will improve.

8 | UNANSWERED BIOLOGICAL QUESTIONS

There are some areas of EV biology where more is known, and some where almost nothing is known (Soekmadji et al., 2018). One area that needs addressing is the lack of suitable markers for specifically identifying different types of EVs. Some excellent work has been done to address this (Jeppesen et al., 2019; Kowal et al., 2016; Zhang et al., 2018). However, due in most part to the overlap in EV biogenesis mechanisms and the overlap in size and density of different EV types, it has proven difficult to generate reliable markers for different EV subtypes. Despite this, several laboratories have shown that different subtypes of EVs may exist, with different cargo, release mechanisms, and different functions (Goberdhan et al., 2019; Willms et al., 2016; Yeung et al., 2018). Better understanding of these subpopulations is a key goal for EV research over the coming decade. Another area in need of further work is EV uptake, and in particular, how EVs functionally deliver cargo to recipient cells (Mulcahy et al., 2014; Russell et al., 2019). This is thought to be a fairly low-efficiency process, and it is understood that a significant number of EVs go to the lysosome, where they presumably are destroyed (Russell et al., 2019). The development of novel in vitro and in vivo systems for modelling EV transfer and cargo release is therefore another priority for the field. An increased understanding of cargo delivery would not only help us to understand EV biology, but it would help us to engineer vesicles specifically to avoid lysosomal destruction, resulting in the rapid emergence of strong EV therapeutic platforms.

9 | CONCLUSIONS AND FUTURE PERSPECTIVES

Since the early electron microscopy and biochemistry studies from the 1940s through to the 1980s, the EV field has rapidly progressed. The range of functions that have been assigned to EV grows by the week. The reasons for this increased interest are manifold. The idea that these small messengers can carry cargo from one cell and deliver it for functional use by another cell is a highly attractive one that has captured the imagination. The results of many studies confirm the work of early pioneers in the field, indicating an important functional role for EVs in cell-to-cell communication. Their roles in many biological processes, and their deregulation in disease have fuelled further interest. EVs have been found in every biological fluid tested thus far (Carollo et al., 2019; Garcia-Contreras et al., 2017; Jansen & Li, 2017; Lee et al., 2019; Li et al., 2019; Meng et al., 2019; O'farrell & Yang, 2019) so perhaps the greatest translational prospect for them lies in their diagnostic, prognostic and therapeutic abilities (Box 2). They have the potential to be modified for the delivery of therapeutic cargo in the treatment of different disorders (Clemmens & Lambert, 2018; Melling et al., 2019; Wiklander et al., 2019). Both their therapeutic and diagnostic potential stems from their ability to protect cargo in circulation, and their functionality as natural cell-to-cell transporters of multiple complex biological cargo.

In the coming years we expect the increase in EV research observed over the past two decades to continue. This will carry on yielding incremental improvements in our knowledge of EV biology, and the translational benefits will follow.

°°

BOX 2 EVS IN DIAGNOSTICS AND THERAPEUTICS

- The growth of the EV field has been accompanied by a growth in patents to use EVs as diagnostic markers, and therapeutic delivery vehicles. Between 2000 and 2020 there were > 500 patents filed in the US which included any of the various terms for EVs (Roy et al., 2018). As a more specific example of their use, between 2000–2020 > 30 clinical trials specified using EVs, either as diagnostic tools or as therapeutics, mainly in the field of cancer biology.
- There are two major ways that EVs might be useful as biomarkers for disease. Firstly in the acute setting as *diagnostic* markers, to determine whether someone has had an ischemic or a haemorrhagic stroke for example. And secondly in the *prognostic* setting, to help determine the course of a disease such as cancer, or the responsiveness of a patient to, for example, anti-depressant therapy. The first CLIA/FDA approved diagnostic test using EVs is the EPI ExoDx platform, a rule-out test for prostate cancer which uses gene expression to determine whether patients are positive for cancer-specific markers (Mckiernan et al., 2018).
- The potential for EVs as therapeutics is vast. EVs can potentially be engineered to deliver specific therapeutics, including proteins and RNA. Non-engineered EVs, for example those produced from MSCs, also have the potential to be used in a therapeutic context. The first clinical trials using EVs as therapeutics used autologous EVs derived from patient dendritic cells and demonstrated that EVs are capable of boosting the immune response to lung cancer in both phase I and phase II/III studies (Besse et al., 2016; Escudier et al., 2005; Morse et al., 2005). Several more trials have since been established studying the potential of several types of EVs, from autologous EVs to plant-derived EVs in diseases from cancer to stroke (Nassar et al., 2016; Wiklander et al., 2019). While challenges remain, the potential of EVs in diagnostic and therapeutic is beginning to be unlocked and there is much excitement for the translational applications of EVs in the coming decades.

ACKNOWLEDGEMENTS AND FUNDING

DRFC is supported by the BBSRC (BB/P006205/1) and Cancer Research UK (A28052). YC is supported by Alzheimer's Research UK (ARUK-RF2019B-004). PH is funded by the Scar Free Foundation and the National Institute for Health Research (NIHR) Surgical Reconstruction and Microbiology Research Centre (SRMRC). DDV is supported by NIH/NCI (R01 CA234557 and R01CA218526). KWW is supported in part by the US National Institutes of Health (AI144997, DA047807, MH118164, CA241694) and the Michael J. Fox Foundation. We thank Ben Carter for his artistic rendition of EV biogenesis in Figure 1. We thank ISEV for supporting this work.

CONFLICT OF INTEREST

Edit Buzas: Shere Gene Tharapeutics Inc. Boston, MA, US. Advisory Board Member. David Carter: Evox Therapeutics Ltd, Employee. Yong Song Gho: Founder and CEO of Rosetta Exosome, INC. Philip Stahl, Graca Raposo, Kenneth Witwer and Yvonne Couch: no conflicts of interest.

ORCID

Yvonne Couch https://orcid.org/0000-0002-5623-5568

REFERENCES

Aaronson, S., Behrens, U., Orner, R., & Haines, T. H. (1971). Ultrastructure of intracellular and extracellular vesicles, membranes, and myelin figures produced by Ochromonas danica. *Journal of Ultrastructure Research*, *35*(5), 418–430.

An, Q., Van Bel, A. J. E., & Hückelhoven, R. (2007). Do plant cells secrete exosomes derived from multivesicular bodies? *Plant Signaling & Behavior*, *2*(1), 4–7.

Anderson, H. C. (1969). Vesicles associated with calcification in the matrix of epiphyseal cartilage. *Journal of Cell Biology*, *41*(1), 59–72.

Araldi, E., Krämer-Albers, E.-M., Hoen, E. N.-T., Peinado, H., Psonka-Antonczyk, K. M., Rao, P., Van Niel, G., Yáñez-Mó, M., & Nazarenko, I. (2012). International Society for Extracellular Vesicles: First annual meeting, April 17–21, 2012: ISEV-2012. *Journal of Extracellular Vesicles*, *1*, 19995.

Bard, M. P., Hegmans, J. P., Hemmes, A., Luider, T. M., Willemsen, R., Severijnen, L.-A. A., Van Meerbeeck, J. P., Burgers, S. A., Hoogsteden, H. C., & Lambrecht, B. N. (2004). Proteomic analysis of exosomes isolated from human malignant pleural effusions. *American Journal of Respiratory Cell and Molecular Biology*, *31*(1), 114–121.

Begley, C. G., & Ellis, L. M. (2012). Drug development: Raise standards for preclinical cancer research. *Nature*, *483*(7391), 531–533.

Besse, B., Charrier, M., Lapierre, V., Dansin, E., Lantz, O., Planchard, D., Le Chevalier, T., Livartoski, A., Barlesi, F., Laplanche, A., Ploix, S., Vimond, N., Peguillet, I., Théry, C., Lacroix, L., Zoernig, I., Dhodapkar, K., Dhodapkar, M., Viaud, S., & Chaput, N. (2016). Dendritic cell-derived exosomes as maintenance immunotherapy after first line chemotherapy in NSCLC. *Oncoimmunology*, *5*(4), e1071008.

Bonucci, E. (1967). Fine structure of early cartilage calcification. *Journal of Ultrastructure Research*, *20*(1), 33–50.

Bruno, S., Grange, C., Deregibus, M. C., Calogero, R. A., Saviozzi, S., Collino, F., Morando, L., Busca, A., Falda, M., Bussolati, B., Tetta, C., & Camussi, G. (2009). Mesenchymal stem cell-derived microvesicles protect against acute tubular injury. *Journal of the American Society of Nephrology*, *20*(5), 1053–1067.

Carollo, E., Paris, B., Samuel, P., Pantazi, P., Bartelli, T. F., Dias-Neto, E., Brooks, S. A., Pink, R. C., & Carter, D. R. F. (2019). Detecting ovarian cancer using extracellular vesicles: Progress and possibilities. *Biochemical Society Transactions*, *47*(1), 295–304.

Chang, C. P., Zhao, J., Wiedmer, T., & Sims, P. J. (1993). Contribution of platelet microparticle formation and granule secretion to the transmembrane migration of phosphatidylserine. *Journal of Biological Chemistry*, *268*(10), 7171–7178.

Chaput, N., Schartz, N. E. C., Andre, F., & Zitvogel, L. (2003). Exosomes for immunotherapy of cancer. *Advances in Experimental Medicine and Biology*, *532*, 215–221.

Chargaff, E. J. (1945). Cell structure and the problem of blood coagulation. *160*(1), 351–359.

Chargaff, E., & West, R. (1946). The biological significance of the thromboplastic protein of blood. *Journal of Biological Chemistry*, *166*(1), 189–197.

Chigaleichik, A. G., Belova, L. A., Grishchenko, V. M., & Rylkin, S. S. (1977). Several properties of the extracellular vesicles of Candida tropicalis yeasts grown on n-alkanes. *Mikrobiologiia*, *46*(3), 467–471.

Clayton, A., Buschmann, D., Byrd, J. B., Carter, D. R. F., Cheng, L., Compton, C., Daaboul, G., Devitt, A., Falcon-Perez, J. M., Gardiner, C., Gustafson, D., Harrison, P., Helmbrecht, C., Hendrix, A., Hill, A., Hoffman, A., Jones, J. C., Kalluri, R., Kang, J. Y., … Nieuwland, R. (2018). Summary of the ISEV workshop on extracellular vesicles as disease biomarkers, held in Birmingham, UK, during December 2017. *Journal of Extracellular Vesicles*, *7*(1), 1473707.

Clemmens, H., & Lambert, D. W. (2018). Extracellular vesicles: Translational challenges and opportunities. *Biochemical Society Transactions*, *46*(5), 1073–1082.

Cocucci, E., & Meldolesi, J. (2015). Ectosomes and exosomes: Shedding the confusion between extracellular vesicles. *Trends in Cell Biology*, *25*(6), 364–372.

Colino, J., & Snapper, C. M. (2007). Dendritic cell-derived exosomes express a Streptococcus pneumoniae capsular polysaccharide type 14 cross-reactive antigen that induces protective immunoglobulin responses against pneumococcal infection in mice. *Infection and Immunity*, *75*(1), 220–230.

Couzin, J. (2005). Cell biology: The ins and outs of exosomes. *Science*, *308*(5730), 1862–1863.

Crawford, N. (1971). The presence of contractile proteins in platelet microparticles isolated from human and animal platelet-free plasma. *British Journal of Haematology*, *21*(1), 53–69.

Dalton, A. J. (1975). Microvesicles and vesicles of multivesicular bodies versus "virus-like" particles. *Journal of the National Cancer Institute*, *54*(5), 1137–1148.

Denzer, K., Kleijmeer, M. J., Heijnen, H. F., Stoorvogel, W., & Geuze, H. J. (2000). Exosome: From internal vesicle of the multivesicular body to intercellular signaling device. *Journal of Cell Science*, *113*(Pt 19), 3365–3374.

Dmochowski, L., Langford, P. L., Williams, W. C., Liebelt, A. G., & Liebelt, R. A. (1968). Electron microscopic and bioassay studies of milk from mice of high and low mammary-cancer and high and low leukemia strains. *Journal of the National Cancer Institute*, *40*(6), 1339–1358.

Dragovic, R. A., Gardiner, C., Brooks, A. S., Tannetta, D. S., Ferguson, D. J. P., Hole, P., Carr, B., Redman, C. W. G., Harris, A. L., Dobson, P. J., Harrison, P., & Sargent, I. L. (2011). Sizing and phenotyping of cellular vesicles using nanoparticle tracking analysis. *Nanomedicine*, *7*(6), 780–788.

Escola, J.-M., Kleijmeer, M. J., Stoorvogel, W., Griffith, J. M., Yoshie, O., & Geuze, H. J. (1998). Selective enrichment of tetraspan proteins on the internal vesicles of multivesicular endosomes and on exosomes secreted by human B-lymphocytes. *Journal of Biological Chemistry*, *273*(32), 20121–20127.

Escudier, B., Dorval, T., Chaput, N., André, F., Caby, M.-P., Novault, S., Flament, C., Leboulaire, C., Borg, C., Amigorena, S., Boccaccio, C., Bonnerot, C., Dhellin, O., Movassagh, M., Piperno, S., Robert, C., Serra, V., Valente, N., Le Pecq, J.-B., … Zitvogel, L. (2005). Vaccination of metastatic melanoma patients with autologous dendritic cell (DC) derived-exosomes: Results of the first phase I clinical trial. *Journal of translational medicine*, *3*(1), 10.

Fawcett, D. W. (1956). Electron microscope observations on intracellular virus-like particles associated with the cells of the Lucke renal adenocarcinoma. *The Journal of Biophysical and Biochemical Cytology*, *2*(6), 725–742.

Fourcade, O., Simon, M.-F., Viodé, C., Rugani, N., Leballe, F., Ragab, A., Fournié, B., Sarda, L., & Chap, H. (1995). Secretory phospholipase A2 generates the novel lipid mediator lysophosphatidic acid in membrane microvesicles shed from activated cells. *Cell*, *80*(6), 919–927.

Garcia-Contreras, M., Brooks, R. W., Boccuzzi, L., Robbins, P. D., & Ricordi, C. (2017). Exosomes as biomarkers and therapeutic tools for type 1 diabetes mellitus. *European Review for Medical and Pharmacological Sciences*, *21*(12), 2940–2956.

Gardiner, C., Vizio, D. D., Sahoo, S., Théry, C., Witwer, K. W., Wauben, M., & Hill, A. F. (2016). Techniques used for the isolation and characterization of extracellular vesicles: Results of a worldwide survey. *Journal of Extracellular Vesicles*, *5*, 32945.

Gawrisch, K., Stibenz, D., Möps, A., Arnold, K., Linss, W., & Halbhuber, K.-J. (1986). The rate of lateral diffusion of phospholipids in erythrocyte microvesicles. *Biochimica Et Biophysica Acta*, *856*(3), 443–447.

George, J., Pickett, E., & Heinz, R. (1986). Platelet membrane microparticles in blood bank fresh frozen plasma and cryoprecipitate. *Blood*, *68*(1), 307–309.

Goberdhan, D., Fan, S.-J., Kroeger, B., Marie, P. P., Bridges, E., Mason, J. D., Mccormick, K., Zois, C., Sheldon, H., Alham, N. K., Johnson, E., Elis, M., Stefana, I., Mendes, C. C., Wainwright, M., Cunningham, C., Hamdy, F., Morris, J. F., Harris, A. L., & Wilson, C. (2019). Glutamine deprivation regulates the origin and function of cancer cell exosomes. 859447.

Gould, S. J., & Raposo, G. (2013). As we wait: Coping with an imperfect nomenclature for extracellular vesicles. *Journal of Extracellular Vesicles*, *2*, 20389.

György, B., Szabó, T. G., Pásztói, M., Pál, Z., Misják, P., Aradi, B., László, V., Pállinger, É., Pap, E., Kittel, Á., Nagy, G., Falus, A., & Buzás, E. I. (2011). Membrane vesicles, current state-of-the-art: Emerging role of extracellular vesicles. *Cellular and Molecular Life Sciences*, *68*(16), 2667–2688.

Haguenau, F. (1959). Cancer of the breast in the female. Comparative electron microscope and optical microscope study. *Bulletin De L Association Francaise Pour L Etude Du Cancer*, *46*, 177–211.

Harding, C., Heuser, J., & Stahl, P. (1983). Receptor-mediated endocytosis of transferrin and recycling of the transferrin receptor in rat reticulocytes. *Journal of Cell Biology*, *97*(2), 329–339.

Hargett, L. A., & Bauer, N. N. (2013). On the origin of microparticles: From "platelet dust" to mediators of intercellular communication. *Pulmonary Circulation*, *3*(2), 329–340.

Harrison, P., Gardiner, C., & Sargent, I. L. (2014). *Extracellular vesicles in health and disease*. Pan Stanford Publishing, Singapore, CRC Press.

Hess, C., Sadallah, S., Hefti, A., Landmann, R., & Schifferli, J. A. (1999). Ectosomes released by human neutrophils are specialized functional units. *Journal of Immunology*, *163*(8), 4564–4573.

Hill, A. F., Pegtel, D. M., Lambertz, U., Leonardi, T., O'driscoll, L., Pluchino, S., Ter-Ovanesyan, D., & Nolte-'T Hoen, E. N. M. (2013). ISEV position paper: Extracellular vesicle RNA analysis and bioinformatics. *Journal of Extracellular Vesicles*, *2*, 22859.

Hu, G., Yelamanchili, L., Kashanchi, S., Haughey, F., Bond, N., Witwer, V. C., Pulliam, K. W., & Buch, S. (2017). Proceedings of the 2017 ISEV symposium on "HIV, NeuroHIV, drug abuse, & EVs". *Journal of Neurovirology*, *23*(6), 935–940.

Iida, K., Whitlow, M. B., & Nussenzweig, V. (1991). Membrane vesiculation protects erythrocytes from destruction by complement. *Journal of Immunology*, *147*(8), 2638–2642.

Jansen, F., & Li, Q. (2017). Exosomes as diagnostic biomarkers in cardiovascular diseases. *Advances in Experimental Medicine and Biology*, *998*, 61–70.

Jeppesen, D. K., Fenix, A. M., Franklin, J. L., Higginbotham, J. N., Zhang, Q., Zimmerman, L. J., Liebler, D. C., Ping, J., Liu, Q., Evans, R., Fissell, W. H., Patton, J. G., Rome, L. H., Burnette, D. T., & Coffey, R. J. (2019). Reassessment of exosome composition. *Cell*, *177*(2), 428–445 e18.

Johnstone, R. M. (2005). Revisiting the road to the discovery of exosomes. *Blood Cells, Molecules & Diseases*, *34*(3), 214–219.

Johnstone, R. M., Adam, M., Hammond, J. R., Orr, L., & Turbide, C. (1987). Vesicle formation during reticulocyte maturation. Association of plasma membrane activities with released vesicles (exosomes). *Journal of Biological Chemistry*, *262*(19), 9412–9420.

Johnstone, R. M., Mathew, A., Mason, A. B., & Teng, K. (1991). Exosome formation during maturation of mammalian and avian reticulocytes: Evidence that exosome release is a major route for externalization of obsolete membrane proteins. *Journal of Cellular Physiology*, *147*(1), 27–36.

Johnstone, R. m., Bianchini, A., & Teng, K. (1989). Reticulocyte maturation and exosome release: Transferrin receptor containing exosomes shows multiple plasma membrane functions. *Blood*, *74*(5), 1844–1851.

Kalra, H., Simpson, R. J., Ji, H., Aikawa, E., Altevogt, P., Askenase, P., Bond, V. C., Borràs, F. E., Breakefield, X., Budnik, V., Buzas, E., Camussi, G., Clayton, A., Cocucci, E., Falcon-Perez, J. M., Gabrielsson, S., Gho, Y. S., Gupta, D., Harsha, H. C., … Mathivanan, S. (2012). Vesiclepedia: A compendium for extracellular vesicles with continuous community annotation. *Plos Biology*, *10*(12), e1001450.

Käppeli, O., & Finnerty, W. R. (1979). Partition of alkane by an extracellular vesicle derived from hexadecane-grown Acinetobacter. *Journal of Bacteriology*, *140*(2), 707–712.

Kay, H. M., Birss, A. J., & Smalley, J. W. (1990). Interaction of extracellular vesicles of Bacteroides gingivalis W50 with human polymorphonuclear leucocytes. *Fems Microbiology Letters*, *60*(1-2), 69–73.

Kowal, J., Arras, G., Colombo, M., Jouve, M., Morath, J. P., Primdal-Bengtson, B., Dingli, F., Loew, D., Tkach, M., & Théry, C. (2016). Proteomic comparison defines novel markers to characterize heterogeneous populations of extracellular vesicle subtypes. *Proceedings of the National Academy of Sciences of the United States of America*, *113*(8), E968–E977.

Lässer, C., Théry, C., Buzás, E. I., Mathivanan, S., Zhao, W., Gho, Y. S., & Lötvall, J. (2016). The international society for extracellular vesicles launches the first massive open online course on extracellular vesicles. *Journal of Extracellular Vesicles*, *5*, 34299.

Lee, S., Mankhong, S., & Kang, J.-H. (2019). Extracellular vesicle as a source of Alzheimer's biomarkers: Opportunities and challenges. *International Journal of Molecular Sciences*, *20*(7), 1728.

Lee, Y. J., Jy, W., Horstman, L. L., Janania, J., Reyes, Y., Kelley, R. E., & Ahn, Y. S. (1993). Elevated platelet microparticles in transient ischemic attacks, lacunar infarcts, and multiinfarct dementias. *Thrombosis Research*, *72*(4), 295–304.

Lener, T., Gimona, M., Aigner, L., Börger, V., Buzas, E., Camussi, G., Chaput, N., Chatterjee, D., Court, F. A., Portillo, H. A. D., O'driscoll, L., Fais, S., Falcon-Perez, J. M., Felderhoff-Mueser, U., Fraile, L., Gho, Y. S., Görgens, A., Gupta, R. C., Hendrix, A., & Giebel, B. (2015). Applying extracellular vesicles based therapeutics in clinical trials - an ISEV position paper. *Journal of Extracellular Vesicles*, *4*, 30087.

Levine, P. H., Horoszewicz, J. S., Grace, J. T., Chai, L. S., Ellison, R. R., & Holland, J. F. (1967). Relationship between clinical status of leukemic patients and virus-like particles in their plasma. *Cancer*, *20*(10), 1563–1577.

Li, Y., Yin, Z., Fan, J., Zhang, S., & Yang, W. (2019). The roles of exosomal miRNAs and lncRNAs in lung diseases. *Signal Transduction and Targeted Therapy*, *4*, 47.

Lötvall, J., Hill, A. F., Hochberg, F., Buzás, E. I., Di Vizio, D., Gardiner, C., Gho, Y. S., Kurochkin, I. V., Mathivanan, S., Quesenberry, P., Sahoo, S., Tahara, H., Wauben, M. H., Witwer, K. W., & Théry, C. (2014). Minimal experimental requirements for definition of extracellular vesicles and their functions: A position statement from the International Society for Extracellular Vesicles. *Journal of Extracellular Vesicles*, *3*, 26913.

Lötvall, J., Rajendran, L., Gho, Y.-S., Thery, C., Wauben, M., Raposo, G., Sjöstrand, M., Taylor, D., Telemo, E., & Breakefield, X. O. (2012). The launch of Journal of Extracellular Vesicles (JEV), the official journal of the International Society for Extracellular Vesicles - about microvesicles, exosomes, ectosomes and other extracellular vesicles. *Journal of Extracellular Vesicles*, *1*, 18514.

Lunger, P. D., Lucas, J. C., & Shipkey, F. H. (1964). The ultramorphology of milk fractions for normal and breast cancer patients. A preliminary report. *Cancer*, *17*, 549–557.

Mackenzie, A., Wilson, H. L., Kiss-Toth, E., Dower, S. K., North, R. A., & Surprenant, A. (2001). Rapid secretion of interleukin-1beta by microvesicle shedding. *Immunity*, *15*(5), 825–835.

Mateescu, B., Kowal, E. J. K., Van Balkom, B. W. M., Bartel, S., Bhattacharyya, S. N., Buzás, E. I., Buck, A. H., De Candia, P., Chow, F. W. N., Das, S., Driedonks, T. A. P., Fernández-Messina, L., Haderk, F., Hill, A. F., Jones, J. C., Van Keuren-Jensen, K. R., Lai, C. P., Lässer, C., Di Liegro, I., … Nolte-'T Hoen, E, N. M. (2017). Obstacles and opportunities in the functional analysis of extracellular vesicle RNA - an ISEV position paper. *Journal of Extracellular Vesicles*, *6*(1), 1286095.

Mathieu, M., Martin-Jaular, L., Lavieu, G., & Théry, C. (2019). Specificities of secretion and uptake of exosomes and other extracellular vesicles for cell-to-cell communication. *Nature Cell Biology*, *21*(1), 9–17.

Mckiernan, J., Donovan, M. J., Margolis, E., Partin, A., Carter, B., Brown, G., Torkler, P., Noerholm, M., Skog, J., Shore, N., Andriole, G., Thompson, I., & Carroll, P. (2018). A prospective adaptive utility trial to validate performance of a novel urine exosome gene expression assay to predict high-grade prostate cancer in patients with prostate-specific antigen 2–10ng/ml at initial biopsy. *European Urology*, *74*(6), 731–738.

Melling, G. E., Carollo, E., Conlon, R., Simpson, J. C., & Carter, D. R. F. (2019). The challenges and possibilities of extracellular vesicles as therapeutic vehicles. *European Journal of Pharmaceutics and Biopharmaceutics*, *144*, 50–56.

Meng, Y., Sun, J., Wang, X., Hu, T., Ma, Y., Kong, C., Piao, H., Yu, T., & Zhang, G. (2019). Exosomes: A promising avenue for the diagnosis of breast cancer. *Technology in Cancer Research & Treatment*, *18*, 153303381882142.

Morse, M. A., Garst, J., Osada, T., Khan, S., Hobeika, A., Clay, T. M., Valente, N., Shreeniwas, R., Sutton, M., Delcayre, A., Hsu, D.-H., Le Pecq, J.-B., & Lyerly, H. K. (2005). A phase I study of dexosome immunotherapy in patients with advanced non-small cell lung cancer. *Journal of Translational Medicine*, *3*(1), 9.

Mulcahy, L. A., Pink, R. C., & Carter, D. R. F. (2014). Routes and mechanisms of extracellular vesicle uptake. *Journal of Extracellular Vesicles*, *3*, 24641.

Nassar, W., El-Ansary, M., Sabry, D., Mostafa, M. A., Fayad, T., Kotb, E., Temraz, M., Saad, A.-N., Essa, W., & Adel, H. (2016). Umbilical cord mesenchymal stem cells derived extracellular vesicles can safely ameliorate the progression of chronic kidney diseases. *Biomaterials Research*, *20*, 21.

Neuhaus, A. A., Couch, Y., Hadley, G., & Buchan, A. M. (2017). Neuroprotection in stroke: The importance of collaboration and reproducibility. *Brain*, *140*(8), 2079–2092.

Nieuwland, R., Falcon-Perez, J. M., Soekmadji, C., Boilard, E., Carter, D., & Buzas, E. I. (2018). Essentials of extracellular vesicles: Posters on basic and clinical aspects of extracellular vesicles. *Journal of Extracellular Vesicles*, *7*(1), 1548234.

Nunez, E. A., Wallis, J., & Gershon, M. D. (1974). Secretory processes in follicular cells of the bat thyroid. 3. The occurrence of extracellular vesicles and colloid droplets during arousal from hibernation. *American Journal of Anatomy*, *141*(2), 179–201.

O'farrell, H. E., & Yang, I. A. (2019). Extracellular vesicles in chronic obstructive pulmonary disease (COPD). *Journal of Thoracic Disease*, *11*(17), S2141–S2154.

Pan, B.-T., & Johnstone, R. M. (1983). Fate of the transferrin receptor during maturation of sheep reticulocytes in vitro: Selective externalization of the receptor. *Cell*, *33*(3), 967–978.

Powell, J. J., Harvey, R. S., & Thompson, R. P. (1996). Microparticles in Crohn's disease–has the dust settled? *Gut*, *39*(2), 340–341.

Prince, A. M., & Adams, W. R. (1966). Virus-like particles in human plasma and serum: Role of platelet lysosomes. *Journal of the National Cancer Institute*, *37*(2), 153–166.

Quick, A. J. (1966). *Hemorrhagic diseases and thrombosis*.. Philadelphia, Lea & Febiger.
Ramirez, M. I., Amorim, M. G., Gadelha, C., Milic, I., Welsh, J. A., Freitas, V. M., Nawaz, M., Akbar, N., Couch, Y., Makin, L., Cooke, F., Vettore, A. L., Batista, P. X., Freezor, R., Pezuk, J. A., Rosa-Fernandes, L., Carreira, A. C. O., Devitt, A., Jacobs, L., … Dias-Neto, E. (2018). Technical challenges of working with extracellular vesicles. *Nanoscale*, *10*(3), 881–906.
Raposo, G., Nijman, H. W., Stoorvogel, W., Liejendekker, R., Harding, C. V., Melief, C. J., & Geuze, H. J. (1996). B lymphocytes secrete antigen-presenting vesicles. *Journal of Experimental Medicine*, *183*(3), 1161–1172.
Raposo, G., & Stahl, P. D. (2019). Extracellular vesicles: A new communication paradigm? *Nature Reviews Molecular Cell Biology*, *20*(9), 509–510.
Ratajczak, J., Miekus, K., Kucia, M., Zhang, J., Reca, R., Dvorak, P., & Ratajczak, M. Z. (2006). Embryonic stem cell-derived microvesicles reprogram hematopoietic progenitors: Evidence for horizontal transfer of mRNA and protein delivery. *Leukemia*. *20*(5), 847–856.
Roy, S., Hochberg, F. H., & Jones, P. S. (2018). Extracellular vesicles: The growth as diagnostics and therapeutics; a survey. *Journal of Extracellular Vesicles*, *7*(1), 1438720.
Russell, A. E., Sneider, A., Witwer, K. W., Bergese, P., Bhattacharyya, S. N., Cocks, A., Cocucci, E., Erdbrügger, U., Falcon-Perez, J. M., Freeman, D. W., Gallagher, T. M., Hu, S., Huang, Y., Jay, S. M., Kano, S. I., Lavieu, G., Leszczynska, A., Llorente, A. M., Lu, Q., … Vader, P. (2019). Biological membranes in EV biogenesis, stability, uptake, and cargo transfer: An ISEV position paper arising from the ISEV membranes and EVs workshop. *Journal of Extracellular Vesicles*, *8*(1), 1684862.
Schartz, N. E., Chaput, N., André, F., & Zitvogel, L. (2002). From the antigen-presenting cell to the antigen-presenting vesicle: The exosomes. *Current Opinion in Molecular Therapeutics*, *4*(4), 372–381.
Seman, G., Gallager, H. S., Lukeman, J. M., & Dmochowski, L. (1971). Studies on the presence of particles resembling RNA virus particles in human breast tumors, pleural effusions, their tissue cultures, and milk. *Cancer*, *28*(6), 1431–1442.
Simpson, R. J., Kalra, H., & Mathivanan, S. (2012). ExoCarta as a resource for exosomal research. *Journal of Extracellular Vesicles*, *1*, 18374.
Singh, N., Gemmell, C. H., Daly, P. A., & Yeo, E. L. (1995). Elevated platelet-derived microparticle levels during unstable angina. *Canadian Journal of Cardiology*, *11*(11), 1015–1021.
Skog, J., Würdinger, T., Van Rijn, S., Meijer, D. H., Gainche, L., Curry, W. T., Carter, B. S., Krichevsky, A. M., & Breakefield, X. O. (2008). Glioblastoma microvesicles transport RNA and proteins that promote tumour growth and provide diagnostic biomarkers. *Nature Cell Biology*, *10*(12), 1470–1476.
Skokos, D., Botros, H. G., Demeure, C., Morin, J., Peronet, R., Birkenmeier, G., Boudaly, S., & Mécheri, S. (2003). Mast cell-derived exosomes induce phenotypic and functional maturation of dendritic cells and elicit specific immune responses in vivo. *Journal of Immunology*, *170*(6), 3037–3045.
Smalley, J. W., & Birss, A. J. (1987). Trypsin-like enzyme activity of the extracellular membrane vesicles of Bacteroides gingivalis W50. *Journal of General Microbiology*, *133*(10), 2883–2894.
Smalley, J. W., Birss, A. J., & Shutteworth, C. A. (1988). The degradation of type I collagen and human plasma fibronectin by the trypsin-like enzyme and extracellular membrane vesicles of Bacteroides gingivalis W50. *Archives of Oral Biology*, *33*(5), 323–329.
Smalley, J. W., Shuttleworth, C. A., & Birss, A. J. (1989). Collagenolytic activity of the extracellular vesicles of Bacteroides gingivalis W50 and an avirulent variant W50/BE1. *Archives of Oral Biology*, *34*(7), 579–583.
Soares, R. P., Xander, P., Costa, A. O., Marcilla, A., Menezes-Neto, A., Del Portillo, H., Witwer, K., Wauben, M., Hoen, E. N.-'T., Olivier, M., Criado, M. F., da Silva, L. L. P., Baqui, M. M. A., Schenkman, S., Colli, W., Alves, M. J. M., & Ferreira, K. S., Puccia, R., Nejsum, P., … Torrecilhas, A. C. (2017). Highlights of the Sao Paulo ISEV workshop on extracellular vesicles in cross-kingdom communication. *Journal of Extracellular Vesicles*, *6*(1), 1407213.
Soekmadji, C., Hill, A. F., Wauben, M. H., Buzás, E. I., Di Vizio, D., Gardiner, C., Lötvall, J., Sahoo, S., & Witwer, K. W. (2018). Towards mechanisms and standardization in extracellular vesicle and extracellular RNA studies: Results of a worldwide survey. *Journal of Extracellular Vesicles*, *7*(1), 1535745.
Stein, J. M., & Luzio, J. P. (1991). Ectocytosis caused by sublytic autologous complement attack on human neutrophils. The sorting of endogenous plasma-membrane proteins and lipids into shed vesicles. *Biochemical Journal*, *274*(Pt 2), 381–386.
Subra, C., Laulagnier, K., Perret, B., & Record, M. (2007). Exosome lipidomics unravels lipid sorting at the level of multivesicular bodies. *Biochimie*, *89*(2), 205–212.
Sun, C. N. (1966). Lattice structures and osmiophilic bodies in the developing respiratory tissue of rats. *Journal of Ultrastructure Research*, *15*(3), 380–388.
Théry, C., Boussac, M., Véron, P., Ricciardi-Castagnoli, P., Raposo, G., Garin, J., & Amigorena, S. (2001). Proteomic analysis of dendritic cell-derived exosomes: A secreted subcellular compartment distinct from apoptotic vesicles. *Journal of Immunology*, *166*(12), 7309–7318.
Théry, C., Witwer, K. W., Aikawa, E., Alcaraz, M. J., Anderson, J. D., Andriantsitohaina, R., Antoniou, A., Arab, T., Archer, F., Atkin-Smith, G. K., Ayre, D. C., Bach, J.-M., Bachurski, D., Baharvand, H., Balaj, L., Baldacchino, S., Bauer, N. N., Baxter, A. A., Bebawy, M., & Zuba-Surma, E. K. (2018). Minimal information for studies of extracellular vesicles 2018 (MISEV2018): A position statement of the International Society for Extracellular Vesicles and update of the MISEV2014 guidelines. *Journal of Extracellular Vesicles*, *7*(1), 1535750.
Trams, E. G., Lauter, C. J., Salem, N. Jr., & Heine, U. (1981). Exfoliation of membrane ecto-enzymes in the form of micro-vesicles. *Biochimica Et Biophysica Acta*, *645*(1), 63–70.
Valadi, H., Ekström, K., Bossios, A., Sjöstrand, M., Lee, J. J., & Lötvall, J. O. (2007). Exosome-mediated transfer of mRNAs and microRNAs is a novel mechanism of genetic exchange between cells. *Nature Cell Biology*, *9*(6), 654–659.
Van Deun, J., Mestdagh, P., Agostinis, P., Akay, Ö., Anand, S., Anckaert, J., Martinez, Z. A., Baetens, T., Beghein, E., Bertier, L., Berx, G., Boere, J., Boukouris, S., Bremer, M., Buschmann, D., Byrd, J. B., Casert, C., Cheng, L., Cmoch, A., & Hendrix, A. (2017). EV-TRACK: Transparent reporting and centralizing knowledge in extracellular vesicle research. *Nature Methods*, *14*(3), 228–232.
Van Niel, G. (2003). Intestinal epithelial exosomes carry MHC class II/peptides able to inform the immune system in mice. *Gut*, *52*(12), 1690–1697.
Vidal, M. J., & Stahl, P. D. (1993). The small GTP-binding proteins Rab4 and ARF are associated with released exosomes during reticulocyte maturation. *European Journal of Cell Biology*, *60*(2), 261–267.
Vidal, M., Sainte-Marie, J., Philippot, J. R., & Bienvenue, A. (1989). Asymmetric distribution of phospholipids in the membrane of vesicles released during in vitro maturation of guinea pig reticulocytes: Evidence precluding a role for aminophospholipid translocase. *Journal of Cellular Physiology*, *140*(3), 455–462.
Vysotskii, V. V., Mazurova, I. K., & Shmeleva, E. A. (1977). Extracellular material of some representatives of the genus Corynebacterium (the electron microscopic aspect). *Zhurnal Mikrobiologii, Epidemiologii I Immunobiologii*, *8*, 90–95.
Welsh, J. A., Pol, E., Bettin, B. A., Carter, D. R. F., Hendrix, A., Lenassi, M., Langlois, M. A., Llorente, A., Nes, A. S., Nieuwland, R., Tang, V., Wang, L., Witwer, K. W., & Jones, J. C. (2020). Towards defining reference materials for measuring extracellular vesicle refractive index, epitope abundance, size and concentration. *Journal of Extracellular Vesicles*, *9*(1), 1816641.
Wiklander, O. P. B., Brennan, M. Á., Lötvall, J., Breakefield, X. O., & El Andaloussi, S. (2019). Advances in therapeutic applications of extracellular vesicles. *Science Translational Medicine*, *11*(492), eaav8521.

Willms, E., Johansson, H. J., Mäger, I., Lee, Y., Blomberg, K. E. M., Sadik, M., Alaarg, A., Smith, C. I. E., Lehtiö, J., El Andaloussi, S., Wood, M. J. A., & Vader, P. (2016). Cells release subpopulations of exosomes with distinct molecular and biological properties. *Scientific Reports*, *6*, 22519.

Witwer, K. W., Buzás, E. I., Bemis, L. T., Bora, A., Lässer, C., Lötvall, J., Nolte-'T Hoen, E. N., Piper, M. G., Sivaraman, S., Skog, J., Théry, C., Wauben, M. H., & Hochberg, F. (2013). Standardization of sample collection, isolation and analysis methods in extracellular vesicle research. *Journal of Extracellular Vesicles*, *2*, 20360.

Witwer, K. W., & Théry, C. (2019). Extracellular vesicles or exosomes? On primacy, precision, and popularity influencing a choice of nomenclature. *Journal of Extracellular Vesicles*, *8*(1), 1648167.

Wolf, P. (1967). The nature and significance of platelet products in human plasma. *British Journal of Haematology*, *13*(3), 269–288.

Wolfers, J., Lozier, A., Raposo, G., Regnault, A., Théry, C., Masurier, C., Flament, C., Pouzieux, S., Faure, F., Tursz, T., Angevin, E., Amigorena, S., & Zitvogel, L. (2001). Tumor-derived exosomes are a source of shared tumor rejection antigens for CTL cross-priming. *Nature Medicine*, *7*(3), 297–303.

Wubbolts, R., Leckie, R. S., Veenhuizen, P. T. M., Schwarzmann, G., Möbius, W., Hoernschemeyer, J., Slot, J.-W., Geuze, H. J., & Stoorvogel, W. (2003). Proteomic and biochemical analyses of human B cell-derived exosomes. Potential implications for their function and multivesicular body formation. *Journal of Biological Chemistry*, *278*(13), 10963–10972.

Yeung, V., Webber, J. P., Dunlop, E. A., Morgan, H., Hutton, J., Gurney, M., Jones, E., Falcon-Perez, J., Tabi, Z., Errington, R., & Clayton, A. (2018). Rab35-dependent extracellular nanovesicles are required for induction of tumour supporting stroma. *Nanoscale*, *10*(18), 8547–8559.

Zhang, H., Freitas, D., Kim, H. S., Fabijanic, K., Li, Z., Chen, H., Mark, M. T., Molina, H., Martin, A. B., Bojmar, L., Fang, J., Rampersaud, S., Hoshino, A., Matei, I., Kenific, C. M., Nakajima, M., Mutvei, A. P., Sansone, P., Buehring, W., … Lyden, D. (2018). Identification of distinct nanoparticles and subsets of extracellular vesicles by asymmetric flow field-flow fractionation. *Nature Cell Biology*, *20*(3), 332–343.

Zitvogel, L., Regnault, A., Lozier, A., Wolfers, J., Flament, C., Tenza, D., Ricciardi-Castagnoli, P., Raposo, G., & Amigorena, S. (1998). Eradication of established murine tumors using a novel cell-free vaccine: Dendritic cell-derived exosomes. *Nature Medicine*, *4*(5), 594–600.

Received: 16 March 2022 | Revised: 23 June 2022 | Accepted: 30 June 2022

DOI: 10.1002/wnan.1835

ADVANCED REVIEW

WIREs NANOMEDICINE AND NANOBIOTECHNOLOGY WILEY

Isolation and characterization of extracellular vesicles and future directions in diagnosis and therapy

Karina P. De Sousa[1] | **Izadora Rossi**[2,3] | **Mahamed Abdullahi**[2] | **Marcel Ivan Ramirez**[3,4] | **Dan Stratton**[5] | **Jameel Malhador Inal**[1,2]

[1]Bioscience Research Group, School of Life and Medical Sciences, University of Hertfordshire, Hertfordshire, UK

[2]School of Human Sciences, London Metropolitan University, London, UK

[3]Federal University of Paraná, Curitiba, Brazil

[4]Carlos Chagas Institute (ICC), Curitiba, Brazil

[5]Open University, The School of Life, Health and Chemical Sciences, Milton Keynes, UK

Correspondence
Dan Stratton, Open University, The School of Life, Health and Chemical Sciences, Milton Keynes, UK.
Email: dan.stratton@open.ac.uk

Jameel Malhador Inal, School of Human Sciences, London Metropolitan University, London, UK.
Email: j.inal@londonmet.ac.uk

Funding information
HEFCE QR; CAPES-PrinT

Edited by: Gareth Williams, Associate Editor and Gregory Lanza, Co-Editor-in-Chief

Abstract

Extracellular vesicles (EVs) are a unique and heterogeneous class of lipid bilayer nanoparticles secreted by most cells. EVs are regarded as important mediators of intercellular communication in both prokaryotic and eukaryotic cells due to their ability to transfer proteins, lipids and nucleic acids to recipient cells. In addition to their physiological role, EVs are recognized as modulators in pathological processes such as cancer, infectious diseases, and neurodegenerative disorders, providing new potential targets for diagnosis and therapeutic intervention. For a complete understanding of EVs as a universal cellular biological system and its translational applications, optimal techniques for their isolation and characterization are required. Here, we review recent progress in those techniques, from isolation methods to characterization techniques. With interest in therapeutic applications of EVs growing, we address fundamental points of EV-related cell biology, such as cellular uptake mechanisms and their biodistribution in tissues as well as challenges to their application as drug carriers or biomarkers for less invasive diagnosis or as immunogens.

This article is categorized under:

Diagnostic Tools > Biosensing

Therapeutic Approaches and Drug Discovery > Nanomedicine for Oncologic Disease

Therapeutic Approaches and Drug Discovery > Nanomedicine for Infectious Disease

KEYWORDS

EV analysis, EV characterization, EV therapeutics, extracellular vesicles, isolation methods

1 | INTRODUCTION

Extracellular vesicles (EVs) are lipid bilayer vesicles released in an evolutionary conserved manner by cells, from prokaryotes to higher eukaryotes and plants (Stotz et al., 2022; Yáñez-Mó et al., 2015). This review will focus on exosomes and

microvesicles (MVs), two subgroups of EVs, as therapeutic applications of apoptotic bodies (large EVs [lEVs]) are still in their infancy (T. K. Phan et al., 2020). The biogenesis of exosomes involves endocytosis and formation of multivesicular bodies (MVBs) containing intraluminal vesicles (ILVs) formed by the internal budding of the endosomal membrane. ILVs can be degraded by fusion of MVBs with lysosomes or secreted into the extracellular space by fusion of MVBs with the plasma membrane (PM). From then on, these vesicles are considered "exosomes," having a diameter that varies from 30 to 200 nm. The protein topology in exosomes remains the same as in the PM of the releasing cell. On the other hand, MVs are released directly into the extracellular matrix through the external budding of the PM and are heterogeneous in size, ranging from 100 nm to 1 μm (Kalra et al., 2016; Van Niel et al., 2018). Biogenesis pathways for budding MVs are still being elucidated (Catalano & O'Driscoll, 2019; Kholia et al., 2015; Sedgwick & D'Souza-Schorey, 2018). The overlap of physical characteristics (such as size) between MVs and exosomes, added to the lack of specific markers that differentiate them, has made it challenging to study these two populations individually. Therefore, the International Society for Extracellular Vesicles (ISEV) advocates the use of the generic term "extracellular vesicle" (EV), unless authors can establish specific markers of subcellular origin that are reliable in their experimental models or can name them based on operational terms for the EV subtypes they refer to, such as the use of lEVs (which would mostly correspond to MVs) and small EVs (sEVs, mostly exosomes).

The first function attributed to exosomes following their discovery (Harding et al., 1983; Pan et al., 1985) was the elimination of unwanted cellular proteins (Johnstone et al., 1987). Currently, exosomes and MVs are implicated with a variety of biological processes, including tissue remodeling, transport of intercellular material, metabolic regulation, protein removal and trafficking, among others (Iraci et al., 2016). Although their physiological role in homeostasis is recognized, the main interest has been to investigate EV participation in pathological conditions, such as cancer (M. P. Bebelman et al., 2018), autoimmune diseases (Antwi-Baffour et al., 2010; J. Tian et al., 2020), infections (Antwi-Baffour et al., 2019; Caobi et al., 2020; Cestari et al., 2012; De Sousa et al., 2022; Evans-Osses et al., 2017; Joffe et al., 2016; Rodrigues et al., 2018; Rossi et al., 2021), and neurodegenerative disorders (Lange et al., 2017; Xiao et al., 2021).

These functions are performed by transferring encoded information and bioactive molecules in the form of cytokines, lipids, genetic material, proteins, peptides, and other macromolecular elements to recipient cells (van Niel et al., 2018). EVs are stable structures, their contents being protected from degradation processes. They are easily taken up by many cell types and can act locally or circulate through various body fluids, including blood and lymph, resulting in a systemic response (Mathieu et al., 2019). They have been shown to display homing capacity (Cesi et al., 2016), are able to cross the blood–brain barrier (Morad et al., 2019), and are nonimmunogenic (Cestari et al., 2012; Villa et al., 2019). These characteristics make EVs very attractive acellular, biocompatible agents for drug delivery, immune mediation, cancer therapy and even for regenerative medicine (Fais et al., 2016). Furthermore, EVs may provide a means for minimally invasive diagnostics and therapeutics. Attesting to the interest in these vesicles, there are currently a number of studies appraising their various clinical uses (C. Choi, 2022; T. H. Phan et al., 2022).

2 | METHODS FOR THE ISOLATION OF EVs

EVs can be studied both in vitro and in vivo, and are found in many biofluids (blood, milk, saliva, urine, amniotic fluid, semen, cerebrospinal fluid, ascites) (Bano et al., 2021), demonstrating their role in cellular communication between distant body compartments.

The specific method used to isolate EVs greatly influences the yield and purity of isolated samples. Numerically, it is generally accepted that freshly acquired and processed samples yield higher numbers of vesicles, but this is not always possible. In addition, EV isolation is complicated not only by their nanosize but also by contaminants which may be co-isolated with EVs (including cellular debris and interfering components: lipoproteins, protein complexes, aggregates) (Ramirez et al., 2018). Importantly, it has been shown that different isolation methods greatly impact the downstream analyses of EV cargo and physicochemical properties (S. Sharma et al., 2020; van Deun et al., 2014). The scientific community, mainly led by ISEV, has made efforts to standardize good practices for obtaining and characterizing EVs (Lötvall et al., 2014; Théry et al., 2018).

2.1 | Ultracentrifugation-based methods for EV isolation

Historically, ultracentrifugation protocols are the most widely used methods for EV isolation, both from cell culture media and body fluids. In fact, it is estimated that this method accounts for 81% of all EV isolations (Gardiner

et al., 2016), as ultracentrifugation requires very little technical expertise, is an affordable technique over time and obviates the need for expensive and mechanistically unclear commercial EV isolation kits (X. Zhang et al., 2020). The process separates EVs from the other materials present in the sample based on their volume and physical properties using differential sequential centrifugation cycles at 4°C with forces of up to 120,000*g* applied directly to samples, there being little or no need for pretreatment of samples. Isolated EVs can be stored at 4°C until further analysis and should be used as soon as possible thereafter. Looking forward, EV analysis directly from samples, without the need to isolate them first, is an obvious goal.

Simple differential ultracentrifugation is a suitable method for concentrating EVs, but improvements to the technique have been introduced in order to obtain preparations of higher purity. In particular, buoyant density centrifugation methods (also known as isopycnic separation and zone centrifugation) adjusted to the specific density of EVs (1.13–1.19 g/ml) are often used to separate them from potential co-isolated contaminants (Szatanek et al., 2015). This method yields single EV banding at their characteristic density zone, making collection of the vesicles simple. To achieve separation based on EV density (rather than weight), either a cushion or a gradient method can be used, reportedly with little effect on the number of vesicles collected (Yamashita et al., 2016). For both methods, solutions of sucrose or iodixanol are the most commonly used, but the use of iodixanol offers several advantages over sucrose solutions. Iodixanol is less viscous and thus easier to handle, metabolically inert and non-toxic to cells and due to its lower osmolality is a better preservative of EV integrity and functionality (K. Li, Wong, et al., 2018).

In comparison to ultracentrifugation, density gradient centrifugation has been shown to produce preparations with higher purity and yield (Duong et al., 2019; van Deun et al., 2014); however, this method is labor-intensive, time-consuming, and not suitable for high-throughput applications. Furthermore, the method is more suitable for large sample volumes than for the processing of clinical samples. Importantly, it has also been observed that EVs isolated by ultracentrifugation show impaired functionality (Mol et al., 2017) or form aggregates (Linares et al., 2015), potentially linked to the damaging forces exerted on the vesicles during centrifugation at high speed.

2.2 | Size exclusion-based EV isolation

EVs can be isolated according to size and one of the most popular methods by which to do this is ultrafiltration (also termed microfiltration). This technique employs simple membrane filters with specific size exclusion limits (using pore diameters of 0.1, 0.22, or 0.45 μm in general), through which EVs in suspension are filtered (Grant et al., 2011) or in combination with other EV isolation methodologies (Stam et al., 2021), providing a fast and inexpensive method for separating EVs from bigger elements (Konoshenko et al., 2018). In our opinion, the term ultrafiltration should be confined to use of pore sizes below 0.1 μm, which are more commonly used to remove viruses. The EV preparations resulting from ultrafiltration consist of free-standing single particles, not aggregates, which is favorable for downstream analysis. Additionally, ultrafiltration greatly reduces the likelihood of rupturing EVs, since the vesicles are not subject to the same forces and pressure required by ultracentrifugation methods; this likely explains why ultrafiltration recovers significantly more EVs than ultracentrifugation (Grant et al., 2011; Lobb et al., 2015; Yu et al., 2018). However, EV preparations obtained by ultrafiltration are often contaminated with molecules of a diameter similar to that of EVs, rendering the method less adequate for downstream proteomic analysis if used alone (Inal et al., 2013). To counter this, and due to the ease of combining ultrafiltration with ultracentrifugation, these two methods are often used together (Parimon et al., 2018; Y. Xu, Qin, et al., 2017).

Hydrostatic filtration dialysis techniques have likewise been used for processing larger sample volumes, as an alternative to direct ultrafiltration. This method has been shown to produce preparations that are enriched in EVs by up to 100 times when compared to ultracentrifugation-based techniques and is less labor-intensive and cheaper (Musante et al., 2014, 2017; R. Xu, Simpson, & Greening, 2017).

Size-exclusion chromatography is becoming increasingly popular to isolate EVs by fractionation, resulting in preparations of high purity (Benedikter et al., 2017; Lozano-Ramos et al., 2015). With this method, samples are filtered through a porous stationary phase; sample components with small hydrodynamic radii are able to pass faster through the pores and are thus eluted quickly, while those components with larger radii are excluded from entering the pores. Again, this method has been used in combination with ultracentrifugation (Onódi et al., 2018; Rood et al., 2010) and/or ultrafiltration (Benedikter et al., 2017; Nordin et al., 2015), with the added benefit of having a relatively low cost and short isolation time. Although generally accepted as a good method for EV isolation, concerns related to vesicle deformation and rupture have been raised, but these problems can be minimized by selecting the appropriate stationary

fractionation column and the use of gravity alone to perform the chromatography separation. Accordingly, it has been shown that size-exclusion chromatography can produce a high yield isolation while preserving biophysical and functional properties of the isolated vesicles (Foers et al., 2018; Gámez-Valero et al., 2016; Hirschberg et al., 2021; Mol et al., 2017).

Asymmetrical flow field-flow fractionation (AF4) systems may represent an improvement to size-exclusion chromatography. While both methods work on the principle of size exclusion, the AF4 technique makes a parabolic flow run along a porous rectangular axis channel, carrying the sample and distributing particulate components based on their diffusivity: smaller particles diffuse further and are eluted earlier than larger ones (B. Wu et al., 2020). Successful EV isolations were obtained with this technique showing that it requires a smaller volume of starting material than in conventional chromatography and is able to produce EV preparations of high purity (Kang et al., 2008).

2.3 | EV isolation by precipitation

Another alternative to ultracentrifugation is the use of precipitation methods. This technique, allows vesicle aggregates to be easily formed upon the addition to the sample of water-excluding polymers such as polyethylene glycol (PEG) (García-Romero et al., 2019; Weng et al., 2016) or lectins (Samsonov et al., 2016; Shtam et al., 2017) which force less soluble components out of solution allowing them to be subsequently precipitated by low-speed centrifugation (Deregibus et al., 2016; Niu et al., 2017; Serrano-Pertierra et al., 2019). Alternatively, the protein organic solvent precipitation (PROSPR) method (Gallart-Palau et al., 2015), and the commercially available Total Exosome Isolation Reagent (ThermoFisher Scientific) have been proposed as inexpensive and quick protocols for EV isolation. This approach uses organic solvents to remove unwanted soluble proteins from complex biological fluids such as plasma, leaving behind a supernatant enriched in double-membrane vesicles in suspension; the vesicles can easily be collected and separated by centrifugation. This approach reportedly produces high-purity vesicle preparations suitable for downstream proteomic analysis, as serum albumin and other highly abundant plasma proteins are removed with the hydrophilic phase (Gallart-Palau et al., 2015). The precipitation of EVs in culture supernatants with sodium acetate has also been shown to be a simple and inexpensive method. When isolated by this "salting-out" technique, EVs are reportedly indistinguishable from those purified by ultracentrifugation (Brownlee et al., 2014).

Precipitation is an inexpensive method for EV isolation, with the added advantages of being easy to use, not requiring any specialized equipment, and being scalable for large sample sizes (Ludwig et al., 2018). However, the likelihood of co-precipitating non-EV material (such as protein aggregates, polymeric materials, other vesicles, or lipoparticles) is high. For this reason, several currently available commercial kits which rely on this method for EV isolation have introduced preisolation and postisolation steps aimed at minimizing contamination with subcellular particles and polymeric materials. Nevertheless, there are conflicting studies suggesting that those co-purified molecules may not have a negative impact on the functional properties of isolated EV samples (Ludwig et al., 2018) and others suggesting that precipitation methods may be particularly detrimental to the biological activity of EVs (Baranyai et al., 2015), especially considering the potential cytotoxic effect and reduced viability observed in some cell lines following treatment with vesicles isolated using PEG and/or PROSPR precipitation (Gámez-Valero et al., 2016).

2.4 | Immunoaffinity capture-based EV isolation methods

Although a rigorous definition of specific EV markers remains unclear, specific immunoaffinity techniques have been developed to take advantage of the presence of certain surface proteins and receptors (Brambilla et al., 2021; Brett et al., 2017; Ostenfeld et al., 2016; J. M. Wang et al., 2021). These techniques can easily complement other isolation methods, while offering increased efficiency, specificity and integrity in the recovery of EVs from complex and viscous fluids (Zarovni et al., 2015). Moreover, immunoaffinity methods are easy and fast to execute, and compatible with routine laboratory equipment. Immunoaffinity capture assays may, however, be negatively affected by antibody availability and the presence of these markers in the whole population (Gandham et al., 2020; Greening et al., 2015). Ideally, biomarkers should be solely or mainly expressed on the surface of the EVs and should also be fully membrane-bound (without soluble variants) (P. Li et al., 2017). It may also be necessary to have a combination of markers to increase the chance of isolating a specific subpopulation of EVs.

Immunoaffinity assays aimed at isolating EVs can employ submicron-sized antibody-coated magnetic beads to increase the specificity, sensitivity, and yield of the isolation. This improvement is a consequence of the larger surface area, no sample volume limitations, and a near-homogeneous capturing process (S. Chen, Shiesh, et al., 2020; Z. Chen, Yang, et al., 2020; Liangsupree et al., 2021; Zarovni et al., 2015). To apply this method of isolation, the immunomagnetic beads are first coated with antibodies against the EV-associated surface molecules; next, they are incubated with the sample, forming EV-magnetic bead complexes. Finally, the application of a magnetic field induces the movement of the complexes and separates them from the sample (Liangsupree et al., 2021). With this strategy, Zarovni et al. (2015) improved the recovery rate of vesicles from plasma samples by 10- to 15-fold, when compared to ultracentrifugation. Another study combined ultracentrifugation, ultrafiltration, and magnetic immunoaffinity capture to isolate EVs, resulting in a high-yield homogenous population of EVs that subsequently underwent a successful proteomic analysis (Mathivanan et al., 2010).

This approach therefore has obvious advantages: it is specific to the point of extracting subpopulations of EVs based on the expression of target markers; it ensures the integrity of the extracted EVs irrespective of vesicle size; it is relatively easy and quick to perform. However, it has been argued that this method cannot be applied to all sample types or all downstream analyses, as: (a) it is difficult to elute the EVs from the magnetic beads and (b) the non-neutral pH and nonphysiological salt concentrations applied by this method may affect the biological activity of the EVs. A solution to the problem of eluting the EVs from the magnetic beads has been proposed (Nakai et al., 2016; Yoshida et al., 2017), by exploring the specific interaction between Tim4, an EV binding molecule, and phosphatidylserine molecules naturally present on the surface of EVs. The binding of these two molecules is Ca^{2+}-dependent, and intact EVs can easily be detached from Tim4 with the addition of Ca^{2+} chelators to yield high purity preparations. The authors have furthermore suggested that this approach can be adapted to ELISA and flow cytometry assays (Nakai et al., 2016). To further enhance the capacity of immunoaffinity assays for the isolation of EVs, several groups are developing exciting and comprehensive methods that couple magnetic immunocapture with mass spectrometry (MS; Ueda et al., 2014), multiplex bead-based platforms (Koliha et al., 2016), on-chip devices (Kang et al., 2020), nanowires (Dong et al., 2019; Lim, Choi, Lee, Han, et al., 2019), nanoplasmon-enhanced scattering and dark field microscopy (Wan et al., 2019), as well as surface-enhanced Raman scattering (Kwizera et al., 2018), among others. These may prove powerful techniques to expand EV research and its clinical applications, including point-of-care testing for diagnostics.

2.5 | EV isolation based on microfluidic technologies

Microfluidic systems can be defined as integrated systems possessing two or more devices assembled into parallel autonomous operation. Usually, one or more devices are units composed of a network of microchannels, which can be interconnected, and are able to handle small volumes of media (Gholizadeh et al., 2017; Narayanamurthy et al., 2020). Because of this ability, microfluidic devices can often reproduce complex analytical processes on a microscale, with high accuracy and specificity. Additional specialized elements can then be added for facilitating fluid movement or expanding the number of available analyses (Guo et al., 2018).

Microfluidic-based technologies are used for a myriad of applications, and have more recently been applied to EV research. These methods tap into both the physical and biochemical properties of EVs at microscales and usually combine high throughput with molecular detection capacity (Z. Chen, Yang, et al., 2020; Iliescu et al., 2019). Just recently, microfluidic analysis using as little as 2 μl of plasma (with no further processing) successfully detected tumor-associated biomarkers in a subpopulation of EVs (P. Zhang et al., 2019), attesting to the potentially ultrasensitive power of microfluidics-based technologies.

At present, EV isolation methods that are based on microfluidics are classified into three categories: size-based, immunoaffinity-based, or dynamic. Moreover, size-based EV separation devices include nanofilters, nanoarrays, and nanoporous membranes (Iliescu et al., 2019). The latter has been shown to constitute a simple strategy to isolate vesicles from whole blood samples. A study by Davies et al. (2012) showed that EVs can be isolated directly from whole blood filtered through a nanoporous membrane into a microfluidic device using electrophoresis to force the vesicles through the membrane, thus increasing the efficiency of the isolation. A similar design by Rho et al. (2013), using negative pressure instead of an electrical current to drive the blood in the microfluidic circuit, proved to be less specific and less sensitive.

Nanofilter and nanoarray systems have been used in conjunction with unique mechanisms developed around microfluidic systems, aiming to address the issues of sample volume, reagent consumption, overall cost, and processing

time that often surround EV isolation protocols. These mechanisms include acoustic manipulation (K. Lee et al., 2015; M. Wu et al., 2017); nanowire-based traps (Lim, Choi, Lee, Kim, et al., 2019; Z. Wang et al., 2013); nano-sized deterministic lateral displacement (J. T. Smith et al., 2018); viscoelastic flow (Liu et al., 2017); and microscale nuclear magnetic resonance (Shao et al., 2012).

Despite the potential of microfluidics-based technologies to isolate and analyze EVs and EV components in an integrated and user-friendly manner (Bernstein et al., 2021), there are still some problems to be resolved, namely those concerning the viscosity of some biological samples (which can block the microfluidic channels) and the small sample volumes used (which can be detrimental in cases where the target protein or biomarker is expressed in low concentrations).

2.6 | Commercial kits for EV isolation

Several companies have developed quick and easy EV isolation kits in order to minimize the limitations of time and sample volume of the conventional methods; however, the reliability and specificity of these kits vary and they are not always the most economical solution. Generally, commercial kits for EV isolation/analysis tend to be relatively expensive, with the added constraint of only allowing analysis of a small number of samples.

Enderle et al. (2015) compared the RNA yield of EVs isolated using conventional ultracentrifugation and the commercial ExoRNeasy Serum/Plasma Maxi Kit (QIAGEN, Germany), which is an immunoaffinity kit. Results showed no difference in the concentration of intact vesicles recovered by the two methods, and the RNA yield obtained was also equivalent. Balaj et al. (2015) compared the recovery rate and RNA yield of EVs isolated by a protocol developed in-house (using heparinized agarose) against conventional ultracentrifugation, and also against the ExoQuick™-TC commercial kit (System Bioscience) which is a polymeric precipitation kit. Results showed that the vesicles isolated using heparinized agarose were morphologically similar to those obtained by standard ultracentrifugation and the RNA content did not significantly differ between the three methods. Paolini et al. (2016) tested the purity and biological function of EVs isolated by simple and gradient ultracentrifugation against those isolated by the commercial one-step precipitation kit Exo PK (Invitrogen). Their results showed that the preparations obtained by gradient centrifugation were of higher purity and biological activity.

In summary, while commercially available kits represent an attractive alternative for the quick and less labor-intensive isolation of EVs, problems concerning their present lack of specificity will need to be addressed before they can be routinely used.

2.7 | Other methods and future perspectives for EV isolation

Due to the explosion of interest in the study and application of EVs as novel therapeutic targets, biomarkers and nano-sized biocompatible drug carriers, among other uses (Bazzan et al., 2021), innovative advances in the development of techniques for the isolation of these vesicles are frequently being reported in the literature. For example, a strategy for the specific isolation of EVs from relatively small volumes of human serum has recently been proposed which takes advantage of the naturally reversible, high affinity binding between titanium oxide and the phosphate groups on the surface of the lipid bilayer of EVs (Gao et al., 2019). This protocol produced a high-purity isolation with good recovery of EVs which could then either be eluted to obtain intact EVs or directly lysed for downstream proteomic analysis.

3 | CURRENT METHODS FOR THE CHARACTERIZATION OF EVs

After isolation, EVs are often characterized by size, concentration, presence of protein markers, protein concentration, and other components. However, not all types of characterization are necessarily included in all studies and data obtained by different methods can differ significantly. These factors, associated with the lack of sufficient methodological information, make it difficult to compare different studies within the field (Théry et al., 2018).

As with other groups, we believe that existing EV isolation techniques, the majority of which are used in basic research, will become more efficient when they begin to be used in clinical applications (Gowen et al., 2020; Inal, 2020;

O. Wiklander et al., 2019), particularly if isolation techniques are coupled with integrated multiplexed analysis able to perform EV analyses. This still remains a major challenge as, despite the great advances in EV isolation methodology, techniques that allow efficient, quick and cost-effective detection, quantification, and characterization/analysis of EVs are lagging behind. Accordingly, EV characterization is still a matter of debate and remains a challenge, no consensus, for example, yet being reached about EV-specific markers.

The methodologies used to characterize EVs by quantity/abundance, size, or content/composition vary according to the subsequent analyses. Figure 1 outlines a flow of the study of EVs, from isolation to their characterization by various approaches. Interestingly, much work has been dedicated to comparing different methodologies, reinforcing the importance of technical knowledge of the instruments, awareness of analytical variables, and recognition of instrument settings when analyzing EV populations (Akers et al., 2016; Erdbrügger & Lannigan, 2016). In this section, we will consider the most used techniques and their potential application in characterizing EVs (Gardiner et al., 2016) in terms of physical and biochemical characteristics. As the methods are not specific for EV subtypes (MVs or exosomes), the term "EVs" will be used to cover all populations. In addition, these methods are not exclusive to the analysis of EVs, but adapted for this field, meaning there is a large scope for optimization to enable adequate evaluation of EVs.

3.1 | Single EV analysis

The characterization of EVs with their small size and low refractive index makes detection by light scattering methods, such as conventional flow cytometry difficult. In addition, they are heterogeneous in size, and there may be interference from lipoproteins and protein aggregates of similar size. The antigen density in EVs is often low and a very large amount of EVs may be required to be detectable by techniques such as ELISA and western blotting. Thus, single-particle analysis can help further delineate heterogeneous and complex populations of EVs into subgroups better defined by physicochemical and molecular characteristics. The main single-particle analysis techniques in the field of EVs are nanoparticle tracking analysis (NTA), microscopy (electron microscopy [EM], cryo-EM, atomic force microscopy, and high-resolution microscopy), resistive pulse sensing, high-resolution flow cytometry, and Raman spectroscopy (Chiang & Chen, 2019).

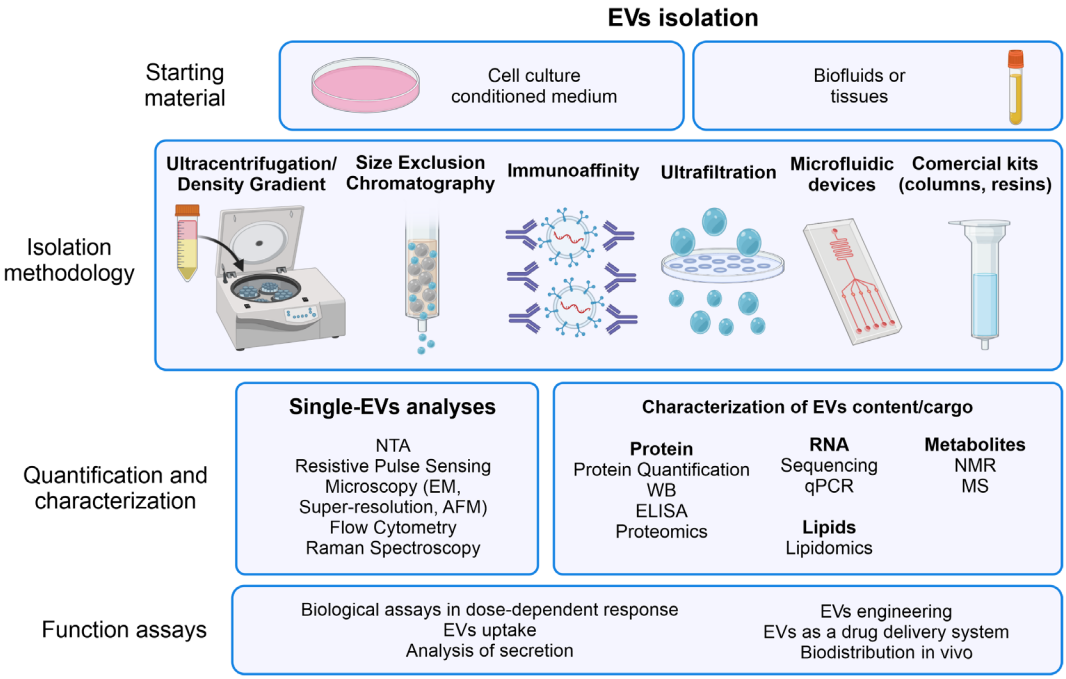

FIGURE 1 Schematic representation of the workflow for isolation and characterization of EVs, with the most used methods in each step. AFM, atomic force microscopy; EM, electron microscopy; MS, mass spectrometry; NMR, nuclear magnetic resonance; NTA, nanoparticle tracking analysis; WB, Western blotting. Image created using BioRender (https://app.biorender.com/)

3.1.1 | Nanoparticle tracking analysis

NTA is one of the most used methods in EV research, as it provides parameters of concentration and particle size. This technique combines laser light scattering microscopy with a camera, which allows the visualization and recording of nanoparticles in solution. In this system, vesicles of about 30–1 μm are driven by a flow and the NTA software tracks the Brownian motion of individual particles and calculates their size and total concentration. This technique has been particularly important to assess the release of subpopulations of EVs, generally categorized into lEVs and sEVs, respectively (Crescitelli et al., 2020; Durcin et al., 2017; Gavinho et al., 2020; Théry et al., 2018; Yekula et al., 2020).

The NanoSight instrument incorporates a laser and camera for detecting fluorescent particles. This property has been exploited to determine the phenotype of vesicle subpopulations according to their labeling with specific antibodies or fluorescent markers (Desgeorges et al., 2020; Dragovic et al., 2011; Thane et al., 2019). Furthermore, Baldwin et al. (2017) showed that it is possible to use this fluorescence property of NTA to determine the content of miR-21 targets contained in lung cancer-derived EVs and their stoichiometry in relation to the total EV population. The assay was designed using a mixture of tumor cell-derived EVs that fuse with cationic lipoplex nanoparticles, the latter containing (encapsulated) fluorescently labeled microRNAs (miRNA)-specific molecular beacons. These are fluorophore quenched oligonucleotide hybridization probes whose fluorescence is restored upon binding to a target nucleic acid sequence. After mixing the EVs with the particles carrying the molecular beacons, a combination of light scattering and fluorescence nanoparticle tracking was used to identify the proportion of the total EV population that contained the target miRNA transcripts. This type of experiment opens new avenues for the identification of specific targets carried by vesicles and presents a more sensitive alternative than cytometry, which loses sensitivity with vesicles below 100 nm, such as most exosomes (Pasalic et al., 2016).

3.1.2 | Microscopy techniques for EV imaging

EV imaging helps researchers to understand physical properties of EVs, their morphology, mechanism of release and uptake, and enables detection of biomarkers expressed on the EV surface (Fertig et al., 2014; Han et al., 2021; Höög & Lötvall, 2015; Morelli et al., 2004; Sorrells et al., 2021; Szempruch et al., 2016). EM, for example, played a key role in the first descriptions of the presence of MVBs inside cells (Harding et al., 1983) and has still been used in the field of EV investigation due to the images of high resolution (ranging from 1 to 3 nm for transmission electron microscopy (TEM) and approximately 5 nm for scanning EM). In addition, using immunogold-labeling, TEM can further reveal EV proteins, which can help in the understanding of the role of these vesicles (Marcilla et al., 2012; Shi et al., 2019).

The electron microscope has, however, its drawbacks, which include loss of material during extensive sample preparation, lack of multiparametric phenotyping and low throughput capacity. In the field of EVs, one of the problems of this methodology is the possible alteration in morphology, particularly of exosomes during preparation, resulting in the characteristic "cup-shape" (Lobb et al., 2015). This has been suggested to be an artifact caused by sample dehydration, since cryo-EM results have shown that EVs have a perfectly spherical structure in aqueous solution (Conde-Vancells et al., 2008; Kadiu et al., 2012). Indeed, the preparative steps of chemical fixation, dehydration, observation under vacuum, and electron beam radiation damage could all interfere with an important feature of EVs. Some alternatives have been proposed, including the use of protein-rich material (such as matrigel or albumin) or some inert polysaccharides (such as agarose or methylcellulose) to protect against material loss and keep the EVs preserved during the fixation processes. In addition, some groups have used negatively stained whole mount preparation, in which EVs are adsorbed onto a metal grid, chemically fixed and negatively stained prior to observation (Ramirez et al., 2018).

As a result, there has been a great advance in microscopy techniques that are being explored for the visualization of EVs, such as cryo-EM, electron tomography EM, atomic force microscopy (AFM), confocal microscopy, and super resolution microscopy, each with their own resolving power and specific advantages and disadvantages (reviewed by Chuo et al., 2018).

Cryo-EM does not use staining or chemical fixation procedures and samples are directly applied onto an EM grid, vitrified and visualized. In this preparation, water is transformed into a glass-like state without the formation of ice crystals. Cryo-immobilizing allows biological structures to be preserved in their native hydrated state, thus avoiding artifacts commonly caused by conventional fixation. Cryo-EM also allows 3D tomographic data collection thus enabling the spatial visualization of more complex structures (Höög & Lötvall, 2015; Votteler et al., 2016; Yang et al., 2020; Yuana et al., 2013). Similar to conventional TEM, cryo-EM can be combined with immunogold labeling, providing data on the presence of certain molecules carried by EVs (Brisson et al., 2017; Goughnour et al., 2020).

AFM uses a microscopic physical probe to scan through the surface of specimens and detects the morphology of the sample in three-dimensional space, obtaining information from the very weak interaction between the probe and the sample surface. By recording the probe position during the scan, AFM generates topographic images of the samples with a resolution limit around 1 nm, which allows imaging of most EVs (Bairamukov et al., 2021; Kim et al., 2019).

The term super resolution microscopy refers to an assortment of various imaging approaches including single-molecule localization microscopy, which encompasses both stochastic optical reconstruction microscopy and photo-activated localization microscopy. In conventional fluorescence microscopy, every fluorophore in a sample is activated, meaning that closely grouped fluorescence emitters cannot be resolved due to overlapping point-spread functions. Single-molecule localization microscopy exploits the temporal gap between activation-deactivation cycles of nearby molecules to detect their spatial separation (F. Colombo et al., 2021). As a result, it is possible to reconstruct the position of each emitter with a spatial resolution of ≤20 nm by combining thousands of frames (Rust et al., 2006). It was shown that different fluorescent dyes or conjugated antibodies can provide a good definition of EVs using this technique (C. Chen et al., 2016; Nizamudeen et al., 2018; Skovronova et al., 2021). This methodology shows a great sensitivity for EVs, where cancer-specific markers can be detected on single EVs isolated from body fluids, a very difficult detection by conventional techniques.

3.1.3 | EV concentration, size, and charge by resistive pulse sensing

Tunable resistive pulse sensing (TRPS) provides reliable and fast particle-by-particle measurement of EV size and concentration distribution. In TRPS, a tunable submicron-sized pore separates two fluid chambers, one containing the sample to be analyzed, the other an electrolyte solution. By applying a voltage across the membrane, a flow of ions is induced. Once a particle moves through the nanopore, the flow of ions is altered resulting in a brief "resistive pulse" which is recorded by the instrument. When a particle passes through the pore causing a change in voltage, the magnitude of this pulse is proportional to the volume of the particle traversing the pore, and the blockade rate is directly related to the particle concentration (Maas et al., 2017; Vogel et al., 2016).

An adaptation of this technique is microfluidic resistive pulse sensing (MRPS). MRPS differentiates itself from TRPS in that MRPS uses cartridges that have rigid, precalibrated pores made of polydimethylsiloxane, while TRPS uses sensing pores of polyurethane that can be stretched to tune the pore size. MRPS allows control flow of samples through the constriction using controlled pressure (Cimorelli et al., 2021). Some protocols are already available for measuring EVs using variations of the resistive pulse sensing technique (Coumans et al., 2014; Maas et al., 2014; Vogel et al., 2016) with equipment available on the market, for example, IZON qNano (Izon Science Ltd) and nCS1™ instrument (Spectradyne LLC).

3.1.4 | Single EV analysis by flow cytometry

One method for high-throughput multi-parametric analysis and quantification of EVs is flow cytometry. Flow cytometry is a technology that records both the scattering and fluorescence signals generated by individual particles as they are illuminated by a laser beam while passing through a nozzle. The intensity of detected light is reported as forward light scatter and side light scatter (SLS). The quantity of light scattered forward is proportional to the diameter, while SLS indicates morphology and inner anatomy of EVs (Lannigan & Erdbruegger, 2017; Lucchetti et al., 2020). One of the great advantages of flow cytometry is the ability to analyze multiple labels on individual particles and to identify various types and subsets. Despite its wide application, some limiting factors make it difficult to use in the field of EVs. These include the small size of EVs, resulting in a low sensitivity to discriminate them using most popular flow cytometry equipment (or even to discriminate them from background signals). This low fluorescence being emitted by labeled EVs is due to the low number of antigens per particle and limited feasibility of post-stain washing to reduce background fluorescence (Inglis et al., 2015; Lannigan & Erdbruegger, 2017). Therefore, the correct application of cytometry often requires special equipment or at least specific components for the detection of small particles, such as beads. Despite this, some studies have brought solutions to these problems and optimized systems and protocols can elevate the detection limit, as commented later in this article under future directions (D. Choi et al., 2019; Görgens et al., 2019; Morales-Kastresana et al., 2017; Nolan & Duggan, 2018; Y. Tian et al., 2018).

3.1.5 | EV purity and composition by Raman spectroscopy

Vibrational spectroscopies, and in particular Raman spectroscopy are attractive tools for the study of EVs providing an overall biochemical characterization without labeling or targeting any previously known marker at the single-particle level (K. Lee, Fraser, et al., 2018; Morasso et al., 2020). A source of high-intensity light is applied to the sample, and incident photons are scattered by molecules. The frequency and intensity of scattered radiations reveal the quality and quantity of the sample, respectively (Butler et al., 2016). An interesting study showed that, by means of Raman spectroscopy, a fingerprint of the amyloid-beta (Aβ) peptide (one of the hallmarks of Alzheimer's disease) was present in the cargo of sEVs derived from a cell culture model and from midbrain organoids. These findings open a positive path for the investigation of EVs in the identification of biomarkers of neurological disorders, such as toxic proteins (Imanbekova et al., 2021).

One approach that has been used in the field of nanoparticles is laser Tweezer Raman spectroscopy, which combines optical trapping with Raman probing. Optical tweezers consist of using a diffraction limited beam to stably trap a particle in three dimensions creating a net force that brings them to the axial center of the incident laser (Enciso-Martinez et al., 2020). This technique has already been used to characterize EVs in several biological models (Kruglik et al., 2019; Z. J. Smith et al., 2015; Tatischeff et al., 2012).

3.2 | Characterization of EV content

3.2.1 | Protein content of EVs

Proteins present in EVs may provide clues about biological functions and their effects in cell communication. Therefore, many groups have chosen to characterize EVs from the point of view of proteins. Initially, a basic method can be applied to quantify the total protein content, such as the Coomassie Brilliant Blue G-250 assay (also called Bradford assay) or the bicinchoninic acid assay (Théry et al., 2018). Both rely on quantification of proteins by absorbance measurement of a colored complex between a reagent and the protein, based on a calibration curve of known concentrations. EV total protein dosage data can be associated with other applied characterization methods, providing interesting correlations such as the protein per nanoparticle ratio (De Sousa et al., 2022). It is important to emphasize that problems in the purification of EVs will impact the amount of proteins dosed, since contaminants can be measured and generate a bias. In addition, it must be ensured that the EVs are broken (by the action of detergents or freeze–thaw cycles) prior to dosing in order to have a total value of proteins both inside and in the membrane of the vesicles.

The search for EV markers is extensive, but fails to differentiate subpopulations of particles. Some of the markers that had been suggested in past years (such as HSP70, flotillin-1, TSG101, CD63) are not present in every/each vesicle or can be found in both sEV and lEV (M. Colombo et al., 2013; Crescitelli et al., 2020; Kowal et al., 2016; Yoshioka et al., 2013). Due to this, there is no single protein or combination of proteins that can be recommended as universal EVs markers. The demonstration of the enrichment of molecules present in EVs and absence (or depletion) of putative contaminants is a good alternative in the biochemical characterization of EVs. The lack of specific markers brings a change in the naming of EVs: unless authors can establish specific markers of subcellular origin that are reliable in their experimental systems, authors should consider using "operational terms" for EV subtypes, as referred to earlier in this review (Théry et al., 2018).

Proteomics technologies have provided a significant contribution to the field of EVs, allowing the creation of large-scale profiling of proteins secreted through EVs, which can be confirmed later with other methodologies, such as western blotting. Several works have used proteomics to identify differences in the EVs of biological samples from patients and to quantify the presence of some peptides compared to healthy individuals. Notably, one study showed that EVs derived from the serum of breast cancer patients can differentiate the molecular subtypes of breast cancer (such as triple-negative or *HER2*) using a proteomic approach (Rontogianni et al., 2019). This shows the prospect of their use as non-invasive biopsies for diagnosis and management of cancer patients.

3.2.2 | RNA content of EVs

The presence of RNA inside EVs has attracted the attention of researchers since these nucleic acids are protected from degradation in the extracellular environment and can be delivered intact to recipient cells (Hinger et al., 2018;

O'Brien et al., 2020), even between different species (or kingdoms) (Stanton, 2021). These RNA populations include various protein-coding transcripts (mRNAs) and many types of noncoding RNAs, including miRNAs, long noncoding RNAs, circular RNAs, small nucleolar RNAs, small nuclear RNAs, transfer RNAs, ribosomal RNAs, and piwi-interacting RNAs (O'Brien et al., 2020). Many groups have been dedicated to understanding the mechanisms of this RNA packing/loading within EVs and the differences in RNA profiles between different cell types or conditions (Ge et al., 2019; Y. Li et al., 2019). The RNA content varies greatly according to the physiological state of the cells and differs substantially from the cellular RNA content (in types of RNA and relative concentrations of specific RNA sequences) (Baglio et al., 2015; Bayer-Santos et al., 2014; Guduric-Fuchs et al., 2012; Skog et al., 2008). Some database and community-contributed catalogues of molecules identified in EVs have emerged in the past years, such as Vesiclepedia (Kalra et al., 2012), Exocarta (Mathivanan & Simpson, 2009), exRNA (Murillo et al., 2019), and ExoRBase (Lai et al., 2022).

Some difficulties arise in establishing the functionality of RNA in EVs. Firstly, overexpression systems that increase the amounts of a particular RNA in EVs can result in supraphysiological levels of the RNA in the source cells, affecting their physiological behavior (O'Brien et al., 2020). Also, contaminating EVs, such as those present in fetal bovine serum, can also carry RNA and confuse interpretations. To avoid the contamination with non-intravesicular RNAs, ISEV recommends performing a proteinase and RNAse treatment before RNA extraction. In the same way as for other characterization approaches, the methodology of isolation of EVs can influence the purity of the material found and the RNA content.

The RNA content of EVs has been studied extensively using high-throughput RNA-Seq and is commonly validated using reverse transcriptase quantitative polymerase chain reaction (RT-qPCR) analysis (Everaert et al., 2019). One of the difficulties of working with EV-derived RNA is the low yield of material, which is often below the detection limit of the most common quantification techniques, such as fluorimetry. This can be overcome by vacuum concentrating all the RNA extracted from EVs prior to analysis.

There is a concerted effort to find diagnostic and prognostic markers based on the detection of mRNAs in EVs. Detection of these biomarkers in biofluids in different disorders will avoid more invasive tests (Castellanos-Rizaldos et al., 2018; Cha et al., 2020; de Gonzalo-Calvo et al., 2016). In fact, these advances are already present in the clinic today, for example, for the prognostic evaluation of prostate tumors with urine samples (Bio-Test Prostate Techne ExoDx; Tutrone et al., 2020).

3.2.3 | Lipid content of EVs

Lipids are relevant components of EVs, constituting a significant fraction of the total EV volume (especially in sEVs), considering a membrane thickness of about 5 nm (Kreimer et al., 2015). Lipids in EVs form a protective barrier for their cargo and can carry markers derived from their cell of origin. They also participate in membrane fusion events and biomolecule delivery. Hundreds of lipid varieties have been identified in EVs in several reports; cholesterol, phosphatidylcholine, phosphatidylserine, and sphingomyelin derivatives are among the most commonly detected (Brzozowski et al., 2018; Haraszti et al., 2016; Llorente et al., 2013; Skotland et al., 2020). EVs tend to have a higher lipid:protein ratio and a different lipid content than their parent cells (Haraszti et al., 2016; Llorente et al., 2013; Lydic et al., 2015; Skotland et al., 2019; Sun et al., 2019; Subra et al., 2007). The description of both the relative and the absolute values of lipid classes in different EVs provides interesting information about the composition of these particles and can be explored through quantitative lipidomics (S. Chen et al., 2019; Sun et al., 2019). There are several reports describing how to perform quantitative lipidomic studies and the recommended extraction methods. Also, there are some methods used for total quantification of lipids in EVs (such as sulfo-phospho-vanillin assay [SPVA], fluorescent dyes that incorporate into membrane bilayers or Fourier transform infrared spectroscopy), but they have their limitations in sensitivity for detection of some types of lipids (Théry et al., 2018).

Brzozowski et al. (2018) identified differences in the relative abundance of lipid species in EVs derived from three prostate cell lines (one non-tumorigenic, one tumorigenic and another metastatic) by the approach of quantitation of molecular lipid species by target lipidomics. Other work also found differences in the lipid composition of EVs derived from different breast cancer cell lines and showed that the contents differed from their cell of origin (Nishida-Aoki, Izumi, et al., 2020).

3.2.4 | Metabolite content of EVs

Metabolites are a type of small molecule (with a molecular weight <2 kDa) being the downstream products of various biological reactions. They can be steroid hormones, amino acids, metabolic intermediates of nutrient and lipid anabolism, among other molecular species. Despite participating in almost all cellular processes, these are the least studied components of EVs to date.

Two main analytical methodologies are mostly applied for characterizing metabolites in EVs: nuclear magnetic resonance (NMR) spectroscopy and high-resolution MS. Čuperlović-Culf et al. (2020) evaluated the metabolome of sEVs derived from different glioblastoma cells by NMR spectroscopy. A clear difference was seen between the metabolic profiles of the cells when comparing EVs and conditioned media. Another study performed a metabolomic analysis of EVs derived from pancreatic cancer cells (PANC-1) cultured under different oxygen concentrations, as hypoxia contributes to the malignant behavior of these cells (Hayasaka et al., 2021). This work also showed that the metabolite profile of the EVs were different in relation to the cell of origin. A total of 140 hydrophilic metabolites were detected in sEVs and it was observed that the metabolomic profile of sEVs changed under hypoxic stress and that there was an increase in the metabolites involved in angiogenesis.

4 | FUNCTIONAL ASSAYS AND BIOLOGICAL CHARACTERIZATION OF EVs TOWARD DEVELOPING EVs AS THERAPEUTICS

Although the physical and biochemical characterization of EVs is important, only functional assays can provide answers about the real role of EVs in biological systems. The study of EVs can take place both in vitro and in vivo and has been explored in different areas of knowledge from basic cell biology to immunology, pathology, among others. Certain questions can guide the definition of an appropriate model to test hypotheses about EVs: (i) What is the origin of EVs and what is the secretion stimulus? (ii) What are the approximate physiological amounts of secreted EVs? (iii) Which EV populations are being evaluated (e.g., only lEVs, only sEVs or only EVs containing a certain epitope)? (iv) Which tests can provide answers about the role of EVs in this biological model?

In most cases, the EVs are studied within limited conditions and the results cannot always be extrapolated to other models. Also, it is important to emphasize the need for adequate controls for each experiment using, for example, EVs from healthy cells or cells not exposed to treatments. Figure 2 shows the long path from the characterization of EVs toward their translational application.

4.1 | Assays to ascertain functional capacity of EVs, toward developing EV-based therapies

4.1.1 | Biological responses modulated by EVs

In the EV field, there are a range of biological assays which have been used to understand the function of EVs and their suitability for therapeutic use (Nguyen et al., 2020). These include assays for inducing transformation and differentiation in cells (Ansa-Addo et al., 2010; Ismail et al., 2013), change in permissiveness to infection by pathogens, cell migration, and changes in cytokine release or triggering of secondary signals. It is further recommended that these trials be performed on progressive doses of EVs to show dose dependence.

4.1.2 | Cellular uptake of EVs

Cells appear to take up EVs by a variety of pathways, including clathrin-dependent endocytosis, caveolin-mediated endocytosis, macropinocytosis, phagocytosis, and direct fusion to PM (Mulcahy et al., 2014). Indeed, it seems likely that a heterogeneous population of EVs may gain entry into a cell via more than one route. The analysis of the capture of fluorescently labeled EVs in the presence of a series of drugs that inhibit these internalization pathways can clarify the EV uptake mechanism and also monitor their intracellular trafficking after entry (Lange et al., 2016).

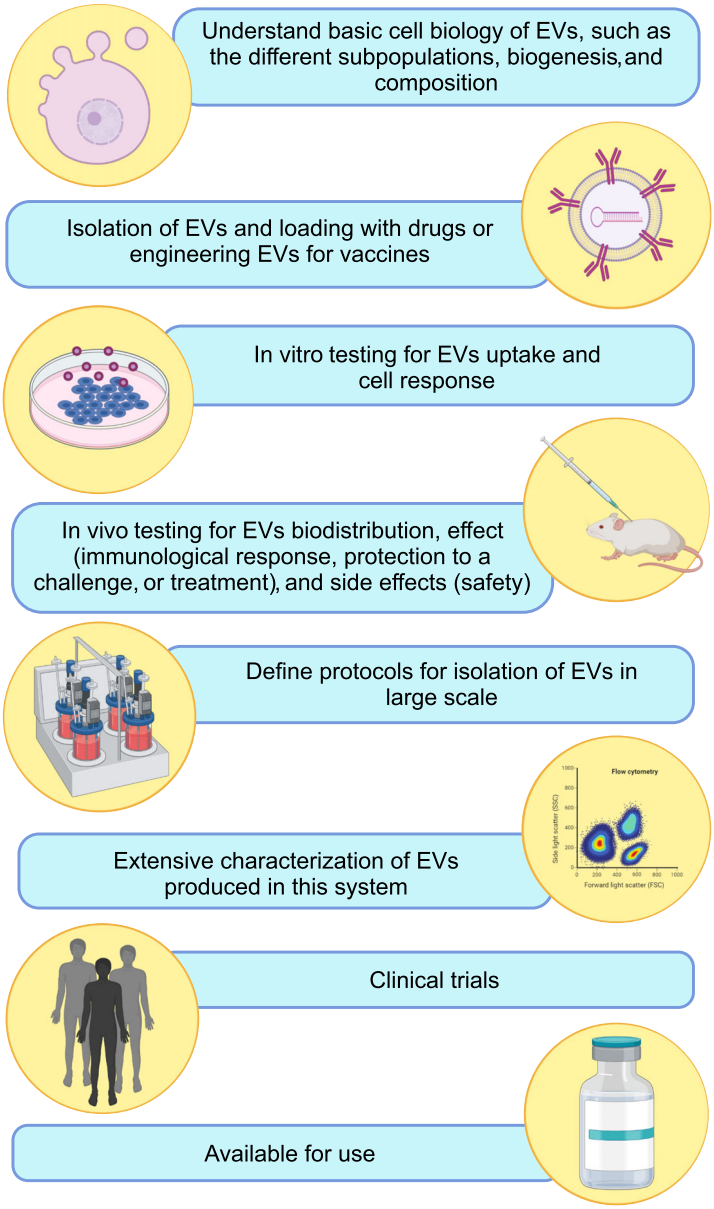

FIGURE 2 Steps toward the translational application of extracellular vesicles (EVs), from basic research to market arrival. Image created using BioRender (https://app.biorender.com/)

4.1.3 | In vivo biodistribution of EVs

Understanding the in vivo fate of EVs is of utmost importance for future therapeutic applications. Using different approaches, it was shown that the biodistribution of EVs was influenced by the route of administration and the origin of the EVs (Gupta et al., 2020; Nishida-Aoki, Tominaga, et al., 2020; Royo et al., 2019; O. P. Wiklander et al., 2015). Using EVs fluorescently labeled with DiR (1,1′-Dioctadecyl-3,3,3′,3′-Tetramethylindotricarbocyanine Iodide) or CD63-EGFP-labeled EVs, O. P. Wiklander et al. (2015) showed that 24 h after EV injection, the main sites with detected fluorescence were the liver, spleen, lungs, and gastrointestinal tract. This study also evaluated the targeting of EVs derived from cells transfected with the fusion protein LAMP2b-RVG which targets the Rabies virus glycoprotein (RVG) peptide to the EV membrane (RVG-coupled species are more readily addressed to the brain, due to the presence of nicotinic acetylcholine receptor). The DiR-labeled EVs were injected intravenously into the animals and, interestingly, the RVG-EVs displayed a significantly increased signal in the brain compared to the non-RVG (mock) EV group. This work has also shown that there is a propensity for tumor tissues to capture injected EVs, possibly due to the high vascularization

of the tumor and the permeability of the vasculature in the region(Wiklander et al., 2015). This opens a possibility for anti-tumor therapies delivered by EVs, especially if optimized using different cell sources and target inclusion.

Royo et al. (2019) showed that EVs derived from proliferative liver cells accumulate mainly in the liver and lungs in mice after a short period (15 min). After treating the EVs with neuraminidase (an enzyme that digests the terminal sialic acid residues of glycoproteins), their accumulation in the lungs was greater than that of untreated EVs. Furthermore, when the EVs were injected through the hock, the neuraminidase-treated vesicles distributed better to the axillary lymph nodes than the untreated EVs.

4.1.4 | EVs as a drug delivery system

EVs have features that qualify them as a potential drug delivery system, some of which have been previously described. These include that EVs carry and protect a wide range of biomolecules and are able to deliver them to recipient cells; they are distributed through the circulation with a certain stability to reach different organs, including crossing the blood–brain barrier. They can be engineered to optimize delivery to certain tissues and have a high level of biocompatibility (Elsharkasy et al., 2020). Despite its advantages, there are technical obstacles to the use of EVs in the clinic, such as the ability to upscale the production and isolation of EVs. Escudé Martinez de Castilla et al. (2021) provide a very complete systematic review of preclinical studies involving EVs as drug carriers, including the most used procedures for encapsulation of active pharmaceutical ingredients in EVs, routes of administration and purity estimation. Greater understanding of EVs, as well as comparative analysis of EVs to other synthetic delivery vehicles (such as liposomes, lipid nanoparticles, and polymeric micelles) can provide answers about the future use of EVs as a drug delivery system (Moore et al., 2017).

5 | FUTURE DIRECTIONS FOR EV ISOLATION AND CHARACTERIZATION

It is expected that further development of the methods currently in use for EV isolation and characterization will allow for ever more detailed dissection of EV biogenesis, and promote a better understanding of their content and functional properties. Each technique presents benefits and weaknesses, and the selection of any particular isolation method presents a multifactorial problem. It is therefore worth considering the optimization of certain methods to, for example, improve detection limits and resolution.

5.1 | Optimization of flow cytometric techniques for EV analysis

Recent research has led to the construction of customized high-sensitivity flow cytometers that can detect single vesicles, as well as enumerate, size, and recognize molecular markers. A high-sensitivity flow cytometer was reported by Stoner et al. (2016) using parts from commercially available equipment and integrated optimized sample preparation using fluorescent membrane staining. This method termed vesicle flow cytometry (VFC) combined an optical bench, photomultiplier tube detector and fluorescence detector (Stoner et al., 2016). This custom-made VFC was used to assess several fluorescent probes and determined that the voltage sensing dye di-8-ANEPPS emitted fluorescence in relation to the surface area of the vesicle enabling the measurement of its size and concentration. The estimated size of vesicles identified using this method was in the range of 70–80 nm, and the authors theorized that an increase in sensitivity could reduce the detection limit to <40 nm. Nevertheless, it was found that the VFC results regarding vesicle size and concentration were in agreement with those obtained by NTA. VFC could also detect a subpopulation of CD61-positive vesicles from platelet-rich plasma demonstrating a greater resolution attributed to increased laser power, decreased flow, and increased duration of signal integration (Stoner et al., 2016).

Further optimization of flow cytometric instruments has been reported for the detection and quantification of single particles using fluorescence-labeled vesicles for calibration, rather than submicron sizing beads. Imaging flow cytometry (IFCM) integrates imaging cameras with conventional flow cytometers (Headland et al., 2014). The signals generated with IFCM are examined through a digital microscope to produce quantitative imaging data detected with a charged coupled device camera. Görgens et al. (2019) reported an optimized IFCM method. Using enhanced green fluorescent protein (eGFP) fused with CD63-labeled vesicles derived from monocytic THP-1 cells, eGFP-CD63 vesicles were

used as a reference material to modify various parameters to increase the contrast between background noise and vesicle signals. At present, researchers use polystyrene and silica beads of known sizes to calibrate flow cytometers for the detection of EVs but while this has provided superior and consistent flow cytometric methods in EVs analysis, the beads lack the physical characteristics that EVs possess such as different refractive indices. This optimized IFCM method was shown to detect and quantify single vesicles and vesicle subpopulations from a heterogeneous population without the need of prior vesicle purification or isolation of samples.

Nano-flow cytometry (NFCM) is an emerging technology that can detect nanosized particles such as viruses and EVs. It can detect, in real time, light elastically scattered by single nanosized silica and gold particles as small as 24 and 7 nm in diameter, respectively (S. Zhu et al., 2014). The high sensitivity of NFCM was attributed to a decrease in the sample volume, the reduced sample stream diameter and reduced size of the laser beam contact site, as well as the higher laser energy and an increased particle contact time with the laser beam. As a recent application of NFCM it has been used to define subpopulations of EVs from cancer cells (D. Choi et al., 2019) and in nanomedicine to determine the size and content of individual liposomes carrying doxorubicin (C. Chen et al., 2021). Simultaneous fluorescence detection allowed for the measurement of the size distribution and payload of individual liposomes and the results showed variations in vesicle size and content.

Ma et al. (2016) used NFCM for a label-free detection of viruses, with diameters of 27 nm, as well as distinguishing them in a mixture, through the quantification of ultraweak elastically scattered light from single-virus particles. NFCM was also able to identify distinct physical differences of the viral particle such as the position of tail fibers of the bacteriophage PP01, distinguishing empty capsids from mature virions and the content of capsids with and without enclosed DNA. This technology is particularly important for distinguishing virions and similarly sized EVs.

5.2 | Emerging techniques for EV analysis

The potential application of EVs in medicine (particularly nanomedicine) is clear but their use in a clinical setting is still hampered by the limitations of methods currently available, for vesicle isolation, detection, and characterization. The new technologies being developed seek to integrate different approaches, especially those based in antibody labeling or capturing. Advances in the analytical tools used in EV research are leading to improvements in generated data, particularly data that can characterize individual vesicle details such as size, concentration, and protein expression. Efforts are also directed to create inexpensive, rapid, reproducible assays that can be applied to clinical settings without the need for extensive preparation of EVs from bodily fluids. One promising field is biosensing technology that seeks to combine current conventional methods with lab-on-chip devices to facilitate EV analysis. Biosensors are analytical instruments that detect and/or quantify biomarkers by producing signals related to the concentration of an analyte (Bhalla et al., 2018). These biosensors are composed of a biological receptor that provides specificity and a transducer that converts biological signals into electrical data (Naresh & Lee, 2021). Biosensors are generally grouped based on the type of transducer they use: electrochemical, fluorescence, or optical.

5.2.1 | Electrochemical biosensing systems for EV analysis

Electrochemical biosensing technology is an emerging field in EV analysis, with several variations employed. For example, an electrochemical sensor-based system, named integrated magneto-electrochemical sensor (iMEX) was reported to quickly isolate and detect exosomes in clinical samples (Jeong et al., 2016). The system is based on the specific isolation of exosomes with magnetic beads attached to anti-CD63, CD81, and CD9 antibodies and the electrochemical detection of exosomal proteins (Jeong et al., 2016). It has eight detection channels each with a potentiostat to measure the electrical current. Individual potentiostats are attached to a digital-to-analog converter, analog-to-digital converter, a multiplexer, and a micro-controller. The system was designed as a handheld unit with a value of <£50. It aims firstly to capture exosomes with magnetic beads followed by the binding of secondary antibody with horseradish peroxidase (HRP) and the addition of a chromogenic electron-mediator, tetramethylbenzidine (TMB). This produces an electrical current which is then detected, enabling the iMEX system to detect exosomes at a sensitivity of $<10^5$ from a minimal specimen volume of 10 μl and generating results in 1 h (Jeong et al., 2016). iMEX was customized to detect exosomes in blood from ovarian cancer patients. The selected markers, CD63, EpCAM, CD24, and CA125 along with their respective IgG-controls were measured simultaneously. The results of the profiling of the plasma samples showed exosomes from

cancer patients had higher levels of EpCAM and CD24 expression in comparison to non-cancer patients. An advantage of the iMEX system is the detection of a subpopulation of exosomes from liquid samples, without the need for isolation methods such as ultracentrifugation or filtration (Jeong et al., 2016).

Electrochemical sensors can also be utilized in the characterization of the nucleic acid content of exosomes. Shao et al. (2015) described a microfluidic platform called the immuno-magnetic exosome RNA (iMER) system which combines immunomagnetic exosome separation, RNA purification, and real-time PCR. iMER operates based on the capture of exosomes with magnetic beads coated with anti-EGFRvIII antibodies. After the addition of patient blood samples to the system only exosomes with the targeted markers are isolated on the chip. The captured exosomes are then lysed to release mRNAs that are then absorbed onto glass beads via electrostatic interactions. The mRNAs undergo amplification and quantitation by the on-chip PCR. The iMER system was used to analyze the mRNA profiles of glioblastoma-derived exosomes from human blood, glioblastoma cells, and used to assess the efficacy of drug treatment (Shao et al., 2015). The level of mRNA expression of O6-methylguanine DNA methyltransferase and alkylpurine-DNA-N-glycosylase enzymes involved in reversing DNA damage from temozolomide correlated with drug resistance (Shao et al., 2015). The iMER system has several advantages over other conventional methods including simplicity (quick turnaround time, typically 2 h), sensitivity, portability, and the ability to work with small specimen volumes (~100 μl).

5.2.2 | Surface plasmon resonance, quartz crystal microbalance, and opto-fluidic smartphone for detection and characterization of EVs

Surface plasmon resonance (SPR) and quartz crystal microbalance (QCM) have common features including the use of gold film sensors to detect mass change that they are label-free and that they transport sample in solvent across the sensor by means of a flow system. However, while SPR is an optical technique, mass changes being monitored based on a plasmonic principle (changes in light-sensor interaction), the QCM measures change in mass based on the change in frequency of oscillations of the (gold-plated) quartz crystal (thus, a mechanical technique).

SPR sensors represent a new method in EV detection and characterization with the advantage of label-free detection and minimal sample processing. The SPR sensor-based method called the nano-plasmonic exosome (nPLEX) assay first developed by Im et al. (2014) showed the quantitative detection and characterization of exosomes from the ascitic fluid of ovarian cancer patients. nPLEX is centered on the transmission of SPR through periodic nanohole arrays located on an opaque gold film. The nanohole arrays are each equipped with capturing antibodies against exosomal markers. Upon exosome binding, shifts or intensity changes occur in the transmission spectral peaks related to the levels of the target markers. Using the nPLEX assay the protein expression of exosomes collected from the ascites of cancer and non-cancer patients were profiled. The nPLEX assay was able to distinguish between exosomes from ovarian cancer patients with elevated protein expression of EpCAM and CD24 in comparison with non-cancer patients (Im et al., 2014). The nPLEX assay showed sensitivities 10-fold higher than western blot and chemiluminescence ELISA and was used to monitor the response to chemotherapy in ovarian cancer patients. Ascitic fluid was collected before and after chemotherapeutic treatment and the nPLEX assay used to show that patients responding to treatment had lower levels of exosomal EpCAM and CD24 or both compared to non-responding patients (Im et al., 2014). In a further improvement of nPLEX, by using gold nanoholes rather than glass, increased sensitivity enabled multiplexed analysis of target surface and internal markers on single EVs (Min et al., 2020).

The QCM is a highly sensitive mass sensing acoustic biosensor. Either adhered or adsorbed to the surface of the sensor, changes in mass are detected in this piezoelectric device by changes in frequency of the gold-coated quartz crystal and related by the Sauerbrey equation (Stratton et al., 2014). We previously used QCM with dissipation (QCM-D) to monitor EV release from primary endothelial and fibroblast cells stimulated with agents affecting the cytoskeleton.

This was demonstrated as a real-time loss in mass, giving an indication of the kinetics of EV biogenesis (2.4×10^6 EVs released from 10^5 prostate cancer cells over 1000s; 1.4 EVs per cell per minute). Similar estimates have been given by others (M. Bebelman et al., 2020; Verweij et al., 2018). The QCM has also been used to monitor EV release (from PC12 and NG108-15 cells) after stimulation with increased potassium and by spontaneous endocytosis (Cans et al., 2001) or to study the absorption properties of red cell EVs (Románszki et al., 2020).

Another adaptation of this technology for EV research involves characterization of EV markers by QCM-D. Although highly sensitive, compared to other methods, it is expensive and labor-intensive requiring preparation of samples on assembled monolayers and of IgGs covalently immobilized on the sensor surface (Priglinger et al., 2021). With a view to making EV characterisation by QCM technology more accessible, therefore, (QCM coupled with impedance,

QCM-I) represents an improvement which was further linked to atomic force microscopy (AFM). This sensitive and label-free immuno-sensing method required minimal sample preparation, and enabled detection of mesenchymal stem cell (MSC) EVs via EV and MSC markers, the further use of AFM allowing the distinction of EVs and non-vesicular particles (Priglinger et al., 2021).

An optofluidic smart phone-based device called the mobile exosome detector (μMED) was developed by Ko et al. (2016) that can capture and analyze exosomes following mild traumatic brain injury using in vitro and murine models. The μMED is a handheld diagnostic device utilizing a smartphone camera for fluorometric data acquisition. The μMED device is based on a key innovation that uses both negative and positive selection of exosomes using immunocapture microbeads to isolate on-chip. The positive and negative microbeads are incubated with serum for 30 min in an on-chip compartment. The sample is then passed through the device using negative pressure which leads to the capture of the negative selection microbeads on a porous membrane and the remaining uncaptured exosomes pass through. Downstream, the sample interacts with positive selection microbeads on a porous membrane where the exosomes of interest are captured. The depletion of exosomes that are not derived from brain cells is achieved through negative selection. This leaves only brain-derived exosomes for analysis through immunolabeling with anti-CD81 tagged microbeads. The signal from the captured exosomes is amplified using HRP-conjugated antibodies against glutamate receptor 2, a marker for mild traumatic brain injury. The intensity of the fluorescence signal is acquired on the smartphone device via the camera. The μMED device enables the isolation of brain-derived exosomes from mice serum without the need for ultracentrifugation which is time consuming and requires large equipment. In addition, the μMED device was shown to be a cheap, quick, and portable instrument to detect mild traumatic brain injury in comparison to expensive conventional procedures such brain MRI. The authors suggest the μMED device can be used as a point of care test due to the wide availability of smartphones.

5.2.3 | Fluorescence-based techniques for single vesicle analysis

A fluorescence-based lab-on-a-chip platform was described by Deschout et al. (2014) to accurately measure vesicle size and concentration in interstitial fluid from human breast cancer tumors. Deschout et al. produced a microfluidic device which incorporated light sheet illumination for fluorescence single-particle tracking analysis (FSPT). FSPT was previously reported to measure the size range and concentration of vesicles that are fluorescently tagged in bodily fluids without vesicle isolation or purification. The innovative combination of light sheet illumination with FSPT allows for the reduction of background noise which is a well-known problem due to limited contrast occurring because of unbound fluorescent dyes or out of focus particles in FSPT.

Another, fluorescence-based technique recently developed called single EV analysis (SEA) allows for the multiplexed measurement of biomarkers on single EVs (K. Lee, Fraser, et al., 2018). The SEA technique operates first with the immobilization of EVs on a microfluidic device with subsequent lab-on-a-chip immunostaining and imaging of the captured EVs. Immunostaining is accomplished with fluorescent antibodies against EV markers such as CD9, CD63, and CD81 or cancer markers, in this particular study from three glioblastoma cell lines overexpressing EGFRvIII, EGFR, or IDH1-R132. Imaging of the immobilized EVs was performed in cycles for three different biomarkers in successive rounds by quenching the fluorochromes and then repeating the staining process for the other markers. The intensity of fluorescence was measured on single EVs generating data on total vesicle counts and protein composition. Using SEA, Lee et al. discovered variations in EV markers and tumor markers on EVs. For instance, EVs derived from the Gli36 cell line overexpressing EGFRvIII were observed to be more positive for CD9, a marker for EVs than was found on other cell lines. Moreover, EVs exhibited a difference in tumor marker expression from the three cell lines studied. As anticipated, the EVs from the Gli36 cell line overexpressing EGFRvIII had a significant subpopulation positive for EGFRvIII (67%) whereas the EVs derived from Gli36-IDH1-132H cell line had a small subpopulation positive for IDH1-R132.

5.2.4 | Paper-based platforms for EV analysis

Paper-based platforms are being actively researched as cheap, quick, portable, and simple analytical tools in clinical settings and point-of-care testing (X. Chen et al., 2018). A paper-based aptasensor utilizes luminescence resonance energy transfer (LRET) from the upconversion of nanoparticles to nanorods which enables the detection

and quantification of EVs. LRET is a spectroscopic technique that measures the distance and changes in distance between a donor and acceptor attached to a protein (Zoghbi & Altenberg, 2018). LRET is based on the resonance energy transfer between two spectroscopic probes in close proximity due to the overlap of the emission spectrum of the donor and the absorption spectrum of the acceptor (Dolino et al., 2014). The paper-based aptasensor was fabricated by dividing the DNA aptamer sequence of the CD63 protein into two sections. One section is immobilized on the paper while the other section is attached to gold nanorods and mixed with EVs for application onto the paper. The presence of EVs triggers the merging of the two sections of the aptamer with CD63 protein present on the particle surface to form a complex that reduces the distance between the nanoparticles and nanorods inducing luminescence resonance energy transfer. The green luminescence emitted by the nanoparticles is quenched and this change in the intensity of the luminescence emissions is captured by an imaging camera. The detection of EVs is calculated using the quenching rate and upconversion luminescence and the concentration of particles (X. Chen et al., 2018). This paper-based aptasensor developed by Chen et al. was reported to be highly sensitive with a limit of detection of 1.1×10^3 particles/μl and was performed in 30 min proving to be a suitable assay in clinical settings.

6 | CONCLUSIONS AND FUTURE DIRECTIONS

This review has included classical methods that have been used by laboratories throughout the world to isolate, detect and characterize EVs. We also have critically analyzed some of the challenges that further development of EV technologies face. With a view to developing EV-based liquid biopsy, the field still needs to overcome low yields and purity, high costs, overly complex procedures, and lack of standardization. Ideally EV isolation should not be a prerequisite for analysis and the field must strive for an integrated procedure that would be quicker, requiring fewer steps. Novel methodologies open up the possibility of detecting EVs from small clinical samples. The electrochemical biosensor systems such as iMEX quantifying EVs from μl samples of unprocessed plasma are a positive move promising liquid biopsy as a point-of-care in cancer diagnostics and in monitoring response to treatment. With EVs being found in bodily fluids, especially urine and saliva, the noninvasive nature of these methods means that EV-based liquid biopsy holds amazing promise for personalized medicine, but all the models and protocols mentioned in this review will still need extensive preclinical experience to prove reliability.

Looking ahead, molecular cargoes of EVs must be more fully characterized, both in health and disease, as this will help us better understand the role EVs play in disease progression. One of the biggest challenges facing the field is assigning different biological functions according to EV subtype. Although some such differences of function have been ascribed to certain sEV and lEV populations, this knowledge will require better characterization of EV subtypes based on mode of biogenesis or specific composition. It is also likely that there will be tailored isolation/purification procedures according to what EVs are being used for, for example, whether for diagnostics or therapy. For use in therapy, EV isolation is likely to require more rigorous and large-scale methodologies than are needed for diagnostics. Eventually, however, it is likely that integrated technological advances will arrive enabling detection of markers without prior EV isolation.

AUTHOR CONTRIBUTIONS

Karina De Sousa: Conceptualization (lead); writing – original draft (lead); writing – review and editing (equal). **Izadora Rossi:** Writing – original draft (lead); writing – review and editing (equal). **Mahamed Abdullahi:** Writing – original draft (equal). **Marcel Ivan Ramirez:** Writing – review and editing (equal). **Dan Stratton:** Writing – review and editing (equal). **Jameel Malhador Inal:** Conceptualization (equal); supervision (equal); writing – original draft (equal); writing – review and editing (equal).

ACKNOWLEDGMENTS

This work was part funded by HEFCE QR funding to Jameel Malhador Inal. Izadora Rossi received funding from CAPES. Marcel Ivan Ramirez is a fellow from National Council for scientific and Technological Development (CNPq) Brazil.

CONFLICT OF INTEREST

The authors have declared no conflicts of interest for this article.

DATA AVAILABILITY STATEMENT

Data sharing is not applicable to this article as no new data were created or analyzed in this study.

ORCID

Karina P. De Sousa https://orcid.org/0000-0002-1418-0669
Jameel Malhador Inal https://orcid.org/0000-0002-7200-0363

RELATED WIREs ARTICLE

Progress in extracellular vesicle biology and their application in cancer medicine

REFERENCES

Akers, J. C., Ramakrishnan, V., Nolan, J. P., Duggan, E., Fu, C. C., Hochberg, F. H., Chen, C. C., & Carter, B. S. (2016). Comparative analysis of technologies for quantifying extracellular vesicles (EVs) in clinical cerebrospinal fluids (CSF). *PLoS One*, *11*(2), e0149866.

Ansa-Addo, E. A., Lange, S., Stratton, D., Antwi-Baffour, S., Cestari, I., Ramirez, M. I., McCrossan, M. V., & Inal, J. M. (2010). Human plasma membrane-derived vesicles halt proliferation and induce differentiation of THP-1 acute monocytic leukemia cells. *Journal of Immunology*, *185*(9), 5236–5246.

Antwi-Baffour, S., Kholia, S., Aryee, Y. K., Ansa-Addo, E. A., Stratton, D., Lange, S., & Inal, J. M. (2010). Human plasma membrane-derived vesicles inhibit the phagocytosis of apoptotic cells—Possible role in SLE. *Biochemical and Biophysical Research Communications*, *398*(2), 278–283.

Antwi-Baffour, S., Malibha-Pinchbeck, M., Stratton, D., Jorfi, S., Lange, S., & Inal, J. (2019). Plasma mEV levels in Ghanain malaria patients with low parasitaemia are higher than those of healthy controls, raising the potential for parasite markers in mEVs as diagnostic targets. *Journal of Extracellular Vesicles*, *9*(1), 1697124.

Baglio, S. R., Rooijers, K., Koppers-Lalic, D., Verweij, F. J., Pérez Lanzón, M., Zini, N., Naaijkens, B., Perut, F., Niessen, H. W. M., Baldini, N., & Pegtel, D. M. (2015). Human bone marrow-and adipose-mesenchymal stem cells secrete exosomes enriched in distinctive miRNA and tRNA species. *Stem Cell Research & Therapy*, *6*(1), 1–20.

Bairamukov, V., Bukatin, A., Landa, S., Burdakov, V., Shtam, T., Chelnokova, I., Fedorova, N., Filatov, M., & Starodubtseva, M. (2021). Biomechanical properties of blood plasma extracellular vesicles revealed by atomic force microscopy. *Biology*, *10*(1), 4.

Balaj, L., Atai, N. A., Chen, W., Mu, D., Tannous, B. A., Breakefield, X. O., Skog, J., & Maguire, C. A. (2015). Heparin affinity purification of extracellular vesicles. *Scientific Reports*, *5*(1), 1–15.

Baldwin, S., Deighan, C., Bandeira, E., Kwak, K. J., Rahman, M., Nana-Sinkam, P., Lee, L. J., & Paulaitis, M. E. (2017). Analyzing the miRNA content of extracellular vesicles by fluorescence nanoparticle tracking. *Nanomedicine: Nanotechnology, Biology and Medicine*, *13*(2), 765–770.

Bano, R., Ahmad, F., & Mohsin, M. (2021). A perspective on the isolation and characterization of extracellular vesicles from different biofluids. *Royal Society of Chemistry Advances*, *11*(32), 19598–19615.

Baranyai, T., Herczeg, K., Onódi, Z., Voszka, I., Módos, K., Marton, N., Nagy, G., Mäger, I., Wood, M. J., el Andaloussi, S., Pálinkás, Z., Kumar, V., Nagy, P., Kittel, Á., Buzás, E. I., Ferdinandy, P., & Giricz, Z. (2015). Isolation of exosomes from blood plasma: Qualitative and quantitative comparison of ultracentrifugation and size exclusion chromatography methods. *PLoS One*, *10*(12), e0145686.

Bayer-Santos, E., Lima, F. M., Ruiz, J. C., Almeida, I. C., & da Silveira, J. F. (2014). Characterization of the small RNA content of *Trypanosoma cruzi* extracellular vesicles. *Molecular and Biochemical Parasitology*, *193*(2), 71–74.

Bazzan, E., Tinè, M., Casara, A., Biondini, D., Semenzato, U., Cocconcelli, E., Balestro, E., Damin, M., Radu, C. M., Turato, G., Baraldo, S., Simioni, P., Spagnolo, P., Saetta, M., & Cosio, M. G. (2021). Critical review of the evolution of extracellular vesicles' knowledge: From 1946 to today. *International Journal of Molecular Sciences*, *22*, 6417.

Bebelman, M., Bun, P., Huveneers, S., van Niel, G., Pegtel, D., & Verweij, F. (2020). Real-time imaging of multivesicular body–plasma membrane fusion to quantify exosome release from single cells. *Nature Protocols*, *15*(1), 102–121.

Bebelman, M. P., Smit, M. J., Pegtel, D. M., & Baglio, S. R. (2018). Biogenesis and function of extracellular vesicles in cancer. *Pharmacology & Therapeutics*, *188*, 1–11.

Benedikter, B. J., Bouwman, F. G., Vajen, T., Heinzmann, A. C., Grauls, G., Mariman, E. C., Wouters, E. F. M., Savelkoul, P. H., Lopez-Iglesias, C., Koenen, R. R., Rohde, G. G. U., & Stassen, F. R. M. (2017). Ultrafiltration combined with size exclusion chromatography efficiently isolates extracellular vesicles from cell culture media for compositional and functional studies. *Scientific Reports*, *7*(1), 1–13.

Bernstein, D. E., Piedad, J., Hemsworth, L., West, A., Johnston, I. D., Dimov, N., Inal, J. M., & Vasdev, N. (2021). Prostate cancer and microfluids. *Urologic Oncology*, *39*(8), 455–470.

Bhalla, N., Chiang, H. J., & Shen, A. Q. (2018). Cell biology at the interface of nanobiosensors and microfluidics. In *Methods in Cell Biology* (Vol. 148, pp. 203–227). Academic Press.

Brambilla, D., Sola, L., Ferretti, A. M., Chiodi, E., Zarovni, N., Fortunato, D., Criscuoli, M., Dolo, V., Giusti, I., Murdica, V., Kluszczyńska, K., Czernek, L., Düchler, M., Vago, R., & Chiari, M. (2021). EV separation: Release of intact extracellular vesicles immunocaptured on magnetic particles. *Analytical Chemistry*, *93*(13), 5476–5483.

Brett, S. I., Lucien, F., Guo, C., Williams, K. C., Kim, Y., Durfee, P. N., Brinker, C. J., Chin, J. I., Yang, J., & Leong, H. S. (2017). Immunoaffinity based methods are superior to kits for purification of prostate derived extracellular vesicles from plasma samples. *The Prostate*, *77*(13), 1335–1343.

Brisson, A. R., Tan, S., Linares, R., Gounou, C., & Arraud, N. (2017). Extracellular vesicles from activated platelets: A semiquantitative cryo-electron microscopy and immuno-gold labeling study. *Platelets*, *28*(3), 263–271.

Brownlee, Z., Lynn, K. D., Thorpe, P. E., & Schroit, A. J. (2014). A novel "salting-out" procedure for the isolation of tumor-derived exosomes. *Journal of Immunological Methods*, *407*, 120–126.

Brzozowski, J. S., Jankowski, H., Bond, D. R., McCague, S. B., Munro, B. R., Predebon, M. J., Scarlett, C. J., Skelding, K. A., & Weidenhofer, J. (2018). Lipidomic profiling of extracellular vesicles derived from prostate and prostate cancer cell lines. *Lipids in Health and Disease*, *17*(1), 1–12.

Butler, H. J., Ashton, L., Bird, B., Cinque, G., Curtis, K., Dorney, J., Esmonde-White, K., Fullwood, N. J., Gardner, B., Martin-Hirsch, P. L., Walsh, M. J., McAinsh, M. R., Stone, N., & Martin, F. L. (2016). Using Raman spectroscopy to characterize biological materials. *Nature Protocols*, *11*(4), 664–687.

Caobi, A., Nair, M., & Raymond, A. D. (2020). Extracellular vesicles in the pathogenesis of viral infections in humans. *Viruses*, *12*(10), 1200.

Cans, A.-S., Höök, F., Shupliakov, O., Ewing, A. G., Eriksson, P. S., Brodin, L., & Orwar, O. (2001). Measurement of the dynamics of exocytosis and vesicle retrieval at cell populations using a quartz crystal microbalance. *Analytical Chemistry*, *73*(24) 5805–5811.

Castellanos-Rizaldos, E., Grimm, D. G., Tadigotla, V., Hurley, J., Healy, J., Neal, P. L., Sher, M., Venkatesan, R., Karlovich, C., Raponi, M., Krug, A., Noerholm, M., Tannous, J., Tannous, B. A., Raez, L. E., & Skog, J. K. (2018). Exosome-based detection of EGFR T790M in plasma from non–small cell lung cancer patients. *Clinical Cancer Research*, *24*(12), 2944–2950.

Catalano, M., & O'Driscoll, L. (2019). Inhibiting extracellular vesicles formation and release: A review of EV inhibitors. *Journal of Extracellular Vesicles*, *9*(1), 1703244.

Cesi, G., Walbrecq, G., Margue, C., & Kreis, S. (2016). Transferring intercellular signals and traits between cancer cells: Extracellular vesicles as "homing pigeons". *Cell Communication and Signaling*, *14*(1), 1–12.

Cestari, I., Ansa-Addo, E., Deolindo, P., Inal, J. M., & Ramirez, M. I. (2012). *Trypanosoma cruzi* immune evasion mediated by host cell-derived microvesicles. *Journal of Immunology*, *188*(4), 1942–1952.

Cha, B. S., Park, K. S., & Park, J. S. (2020). Signature mRNA markers in extracellular vesicles for the accurate diagnosis of colorectal cancer. *Journal of Biological Engineering*, *14*(1), 1–9.

Chen, C., Sun, M., Wang, J., Su, L., Lin, J., & Yan, X. (2021). Active cargo loading into extracellular vesicles: Highlights the heterogeneous encapsulation behaviour. *Journal of Extracellular Vesicles*, *10*(13), e12163.

Chen, C., Zong, S., Wang, Z., Lu, J., Zhu, D., Zhang, Y., & Cui, Y. (2016). Imaging and intracellular tracking of cancer-derived exosomes using single-molecule localization-based super-resolution microscope. *American Chemical Society Applied Materials & Interfaces*, *8*(39), 25825–25833.

Chen, S., Datta-Chaudhuri, A., Deme, P., Dickens, A., Dastgheyb, R., Bhargava, P., Bi, H., & Haughey, N. J. (2019). Lipidomic characterization of extracellular vesicles in human serum. *Journal of Circulating Biomarkers*, *8*, 1849454419879848.

Chen, S., Shiesh, S. C., Lee, G. B., & Chen, C. (2020). Two-step magnetic bead-based (2MBB) techniques for immunocapture of extracellular vesicles and quantification of microRNAs for cardiovascular diseases: A pilot study. *PLoS One*, *15*(2), e0229610.

Chen, X., Lan, J., Liu, Y., Li, L., Yan, L., Xia, Y., Wu, F., Li, C., Li, S., & Chen, J. (2018). A paper-supported aptasensor based on upconversion luminescence resonance energy transfer for the accessible determination of exosomes. *Biosensors and Bioelectronics*, *102*, 582–588.

Chen, Z., Yang, Y., Yamaguchi, H., Hung, M. C., & Kameoka, J. (2020). Isolation of cancer-derived extracellular vesicle subpopulations by a size-selective microfluidic platform. *Biomicrofluidics*, *14*(3), 034113.

Chiang, C. Y., & Chen, C. (2019). Toward characterizing extracellular vesicles at a single-particle level. *Journal of Biomedical Science*, *26*(1), 1–10.

Choi, C. (2022). Therapeutic exosomes for various human diseases: Special issue of BMB reports in 2022. *BMB Reports*, *55*(1), 1–2.

Choi, D., Montermini, L., Jeong, H., Sharma, S., Meehan, B., & Rak, J. (2019). Mapping subpopulations of cancer cell-derived extracellular vesicles and particles by nano-flow cytometry. *ACS Nano*, *13*(9), 10499–10511.

Chuo, S. T. Y., Chien, J. C. Y., & Lai, C. P. K. (2018). Imaging extracellular vesicles: Current and emerging methods. *Journal of Biomedical Science*, *25*(1), 1–10.

Cimorelli, M., Nieuwland, R., Varga, Z., & van der Pol, E. (2021). Standardized procedure to measure the size distribution of extracellular vesicles together with other particles in biofluids with microfluidic resistive pulse sensing. *PLoS One*, *16*(4), e0249603.

Colombo, F., Norton, E. G., & Cocucci, E. (2021). Microscopy approaches to study extracellular vesicles. *Biochimica et Biophysica Acta*, *1865*(4), 129752.

Colombo, M., Moita, C., van Niel, G., Kowal, J., Vigneron, J., Benaroch, P., Manel, N., Moita, L. F., Théry, C., & Raposo, G. (2013). Analysis of ESCRT functions in exosome biogenesis, composition and secretion highlights the heterogeneity of extracellular vesicles. *Journal of Cell Science*, *126*(24), 5553–5565.

Conde-Vancells, J., Rodriguez-Suarez, E., Embade, N., Gil, D., Matthiesen, R., Valle, M., Elortza, F., Lu, S. C., Mato, J. M., & Falcon-Perez, J. M. (2008). Characterization and comprehensive proteome profiling of exosomes secreted by hepatocytes. *Journal of Proteome Research*, *7*(12), 5157–5166.

Coumans, F. A., van der Pol, E., Böing, A. N., Hajji, N., Sturk, G., van Leeuwen, T. G., & Nieuwland, R. (2014). Reproducible extracellular vesicle size and concentration determination with tunable resistive pulse sensing. *Journal of Extracellular Vesicles*, *3*(1), 25922.

Crescitelli, R., Lässer, C., Jang, S. C., Cvjetkovic, A., Malmhäll, C., Karimi, N., Höög, J. L., Johansson, I., Fuchs, J., Thorsell, A., Gho, Y. S., Olofsson Bagge, R., & Lötvall, J. (2020). Subpopulations of extracellular vesicles from human metastatic melanoma tissue identified by quantitative proteomics after optimized isolation. *Journal of Extracellular Vesicles*, *9*(1), 1722433.

Čuperlović-Culf, M., Khieu, N. H., Surendra, A., Hewitt, M., Charlebois, C., & Sandhu, J. K. (2020). Analysis and simulation of glioblastoma cell lines-derived extracellular vesicles metabolome. *Metabolites*, *10*(3), 88.

Davies, R. T., Kim, J., Jang, S. C., Choi, E. J., Gho, Y. S., & Park, J. (2012). Microfluidic filtration system to isolate extracellular vesicles from blood. *Lab on a Chip*, *12*(24), 5202–5210.

de Gonzalo-Calvo, D., Cenarro, A., Civeira, F., & Llorente-Cortes, V. (2016). microRNA expression profile in human coronary smooth muscle cell-derived microparticles is a source of biomarkers. *Clinica e Investigacion en Arteriosclerosis*, *28*(4), 167–177.

De Sousa, K. P., Potriquet, J., Mulvenna, J., Sotillo, J., Groves, P. L., Loukas, A., Apte, S. H., & Doolan, D. L. (2022 Jan). Proteomic identification of the contents of small extracellular vesicles from in vivo *Plasmodium yoelii* infection. *International Journal for Parasitology*, *52*(1), 35–45.

Deregibus, M. C., Figliolini, F., D'antico, S., Manzini, P. M., Pasquino, C., de Lena, M., Tetta, C., Brizzi, M. F., & Camussi, G. (2016). Charge-based precipitation of extracellular vesicles. *International Journal of Molecular Medicine*, *38*(5), 1359–1366.

Deschout, H., Raemdonck, K., Stremersch, S., Maoddi, P., Mernier, G., Renaud, P., Jiguet, S., Hendrix, A., Bracke, M., Van den Broecke, R., & Röding, M. (2014). On-chip light sheet illumination enables diagnostic size and concentration measurements of membrane vesicles in biofluids. *Nanoscale*, *6*(3), 1741–1747.

Desgeorges, A., Hollerweger, J., Lassacher, T., Rohde, E., Helmbrecht, C., & Gimona, M. (2020). Differential fluorescence nanoparticle tracking analysis for enumeration of the extracellular vesicle content in mixed particulate solutions. *Methods*, *177*, 67–73.

Dolino, D. M., Ramaswamy, S. S., & Jayaraman, V. (2014). Luminescence resonance energy transfer to study conformational changes in membrane proteins expressed in mammalian cells. *Journal of Visualized Experiments*, *91*, 51895.

Dong, J., Zhang, R. Y., Sun, N., Smalley, M., Wu, Z., Zhou, A., Chou, S. J., Jan, Y. J., Yang, P., Bao, L., Qi, D., Tang, X., Tseng, P., Hua, Y., Xu, D., Kao, R., Meng, M., Zheng, X., Liu, Y., … Zhu, Y. (2019). Bio-inspired nanovilli chips for enhanced capture of tumor-derived extracellular vesicles: Toward non-invasive detection of gene alterations in non-small cell lung cancer. *ACS Applied Materials & Interfaces*, *11*(15), 13973–13983.

Dragovic, R. A., Gardiner, C., Brooks, A. S., Tannetta, D. S., Ferguson, D. J., Hole, P., Carr, B., Redman, C. W. G., Harris, A. L., Dobson, P. J., Harrison, P., & Sargent, I. L. (2011). Sizing and phenotyping of cellular vesicles using nanoparticle tracking analysis. *Nanomedicine: Nanotechnology, Biology and Medicine*, *7*(6), 780–788.

Duong, P., Chung, A., Bouchareychas, L., & Raffai, R. L. (2019). Cushioned-density gradient ultracentrifugation (C-DGUC) improves the isolation efficiency of extracellular vesicles. *PLoS One*, *14*(4), e0215324.

Durcin, M., Fleury, A., Taillebois, E., Hilairet, G., Krupova, Z., Henry, C., Truchet, S., Trötzmüller, M., Köfeler, H., Mabilleau, G., Hue, O., Andriantsitohaina, R., Martin, P., & le Lay, S. (2017). Characterisation of adipocyte-derived extracellular vesicle subtypes identifies distinct protein and lipid signatures for large and small extracellular vesicles. *Journal of Extracellular Vesicles*, *6*(1), 1305677.

Elsharkasy, O. M., Nordin, J. Z., Hagey, D. W., de Jong, O. G., Schiffelers, R. M., Andaloussi, S. E., & Vader, P. (2020). Extracellular vesicles as drug delivery systems: Why and how? *Advanced Drug Delivery Reviews*, *159*, 332–343.

Enciso-Martinez, A., van der Pol, E., Lenferink, A. T., Terstappen, L. W., Van Leeuwen, T. G., & Otto, C. (2020). Synchronized Rayleigh and Raman scattering for the characterization of single optically trapped extracellular vesicles. *Nanomedicine: Nanotechnology, Biology and Medicine*, *24*, 102109.

Enderle, D., Spiel, A., Coticchia, C. M., Berghoff, E., Mueller, R., Schlumpberger, M., Sprenger-Haussels, M., Shaffer, J. M., Lader, E., Skog, J., & Noerholm, M. (2015). Characterization of RNA from exosomes and other extracellular vesicles isolated by a novel spin column-based method. *PLoS One*, *10*(8), e0136133.

Erdbrügger, U., & Lannigan, J. (2016). Analytical challenges of extracellular vesicle detection: A comparison of different techniques. *Cytometry Part A*, *89*(2), 123–134.

Escudé Martinez de Castilla, P., Tong, L., Huang, C., Sofias, A. M., Pastorin, G., Chen, X., Storm, G., Schiffelers, R. M., & Wang, J. W. (2021). Extracellular vesicles as a drug delivery system: A systematic review of preclinical studies. *Advanced Drug Delivery Reviews*, *175*, 113801.

Evans-Osses, I., Mojoli, A., Monguió-Tortajada, M., Marcilla, A., Aran, V., Amorim, M., Inal, J., Borràs, F. E., & Ramirez, M. I. (2017 Mar). Microvesicles released from *Giardia intestinalis* disturb host-pathogen response in vitro. *European Journal of Cell Biology*, *96*(2), 131–142.

Everaert, C., Helsmoortel, H., Decock, A., Hulstaert, E., van Paemel, R., Verniers, K., Nuytens, J., Anckaert, J., Nijs, N., Tulkens, J., Dhondt, B., Hendrix, A., Mestdagh, P., & Vandesompele, J. (2019). Performance assessment of total RNA sequencing of human biofluids and extracellular vesicles. *Scientific Reports*, *9*(1), 1–16.

Fais, S., O'Driscoll, L., Borras, F. E., Buzas, E., Camussi, G., Cappello, F., Carvalho, J., Cordeiro da Silva, A., del Portillo, H., el Andaloussi, S., Ficko Trček, T., Furlan, R., Hendrix, A., Gursel, I., Kralj-Iglic, V., Kaeffer, B., Kosanovic, M., Lekka, M. E., Lipps, G., … Giebel, B. (2016). Evidence-based clinical use of nanoscale extracellular vesicles in nanomedicine. *ACS Nano*, *10*(4), 3886–3899.

Fertig, E. T., Gherghiceanu, M., & Popescu, L. M. (2014). Extracellular vesicles release by cardiac telocytes: Electron microscopy and electron tomography. *Journal of Cellular and Molecular Medicine*, *18*(10), 1938–1943.

Foers, A. D., Chatfield, S., Dagley, L. F., Scicluna, B. J., Webb, A. I., Cheng, L., Hill, A. F., Wicks, I. P., & Pang, K. C. (2018). Enrichment of extracellular vesicles from human synovial fluid using size exclusion chromatography. *Journal of Extracellular Vesicles*, *7*(1), 1490145.

Gallart-Palau, X., Serra, A., Wong, A. S. W., Sandin, S., Lai, M. K., Chen, C. P., Kon, O. L., & Sze, S. K. (2015). Extracellular vesicles are rapidly purified from human plasma by PRotein Organic Solvent PRecipitation (PROSPR). *Scientific Reports*, *5*(1), 1–12.

Gámez-Valero, A., Monguió-Tortajada, M., Carreras-Planella, L., Franquesa, M., Beyer, K., & Borràs, F. E. (2016). Size-exclusion chromatography-based isolation minimally alters extracellular Vesicles' characteristics compared to precipitating agents. *Scientific Reports*, *6*(1), 1–9.

Gandham, S., Su, X., Wood, J., Nocera, A. L., Alli, S. C., Milane, L., Zimmerman, A., Amiji, M., & Ivanov, A. R. (2020). Technologies and standardization in research on extracellular vesicles. *Trends in Biotechnology*, *38*(10), 1066–1098.

Gao, F., Jiao, F., Xia, C., Zhao, Y., Ying, W., Xie, Y., Guan, X., Tao, M., Zhang, Y., Qin, W., & Qian, X. (2019). A novel strategy for facile serum exosome isolation based on specific interactions between phospholipid bilayers and TiO2. *Chemical Science*, *10*(6), 1579–1588.

García-Romero, N., Madurga, R., Rackov, G., Palacín-Aliana, I., Núñez-Torres, R., Asensi-Puig, A., Carrión-Navarro, J., Esteban-Rubio, S., Peinado, H., González-Neira, A., González-Rumayor, V., Belda-Iniesta, C., & Ayuso-Sacido, A. (2019). Polyethylene glycol improves current methods for circulating extracellular vesicle-derived DNA isolation. *Journal of Translational Medicine*, *17*(1), 1–11.

Gardiner, C., Vizio, D. D., Sahoo, S., Théry, C., Witwer, K. W., Wauben, M., & Hill, A. F. (2016). Techniques used for the isolation and characterization of extracellular vesicles: Results of a worldwide survey. *Journal of Extracellular Vesicles*, *5*(1), 32945.

Gavinho, B., Sabatke, B., Feijoli, V., Rossi, I. V., da Silva, J. M., Evans-Osses, I., Palmisano, G., Lange, S., & Ramirez, M. I. (2020). Peptidylarginine deiminase inhibition abolishes the production of large extracellular vesicles from *Giardia intestinalis*, affecting host-pathogen interactions by hindering adhesion to host cells. *Frontiers in Cellular and Infection Microbiology*, *10*, 417.

Ge, X., Meng, Q., Zhuang, R., Yuan, D., Liu, J., Lin, F., Fan, H., & Zhou, X. (2019). Circular RNA expression alterations in extracellular vesicles isolated from murine heart post ischemia/reperfusion injury. *International Journal of Cardiology*, *296*, 136–140.

Gholizadeh, S., Draz, M. S., Zarghooni, M., Sanati-Nezhad, A., Ghavami, S., Shafiee, H., & Akbari, M. (2017). Microfluidic approaches for isolation, detection, and characterization of extracellular vesicles: Current status and future directions. *Biosensors and Bioelectronics*, *91*, 588–605.

Görgens, A., Bremer, M., Ferrer-Tur, R., Murke, F., Tertel, T., Horn, P. A., Thalmann, S., Welsh, J. A., Probst, C., Guerin, C., Boulanger, C. M., Jones, J. C., Hanenberg, H., Erdbrügger, U., Lannigan, J., Ricklefs, F. L., el-Andaloussi, S., & Giebel, B. (2019). Optimisation of imaging flow cytometry for the analysis of single extracellular vesicles by using fluorescence-tagged vesicles as biological reference material. *Journal of Extracellular Vesicles*, *8*(1), 1587567.

Goughnour, P. C., Park, M. C., Kim, S. B., Jun, S., Yang, W. S., Chae, S., Cho, S., Song, C., Lee, J. H., Hyun, J. K., Kim, B. G., Hwang, D., Jung, H. S., Gho, Y. S., & Kim, S. (2020). Extracellular vesicles derived from macrophages display glycyl-tRNA synthetase 1 and exhibit anti-cancer activity. *Journal of Extracellular Vesicles*, *10*(1), e12029.

Gowen, A., Shahjin, F., Chand, S., Odegaard, K. E., & Yelamanchili, S. V. (2020). Mesenchymal stem cell-derived extracellular vesicles: Challenges in clinical applications. *Frontiers in Cell and Developmental Biology*, *8*, 149.

Grant, R., Ansa-Addo, E., Stratton, D., Antwi-Baffour, S., Jorfi, S., Kholia, S., Krige, L., Lange, S., & Inal, J. (2011). A filtration-based protocol to isolate human plasma membrane-derived vesicles and exosomes from blood plasma. *Journal of Immunological Methods*, *371*(1–2), 143–151.

Greening, D. W., Xu, R., Ji, H., Tauro, B. J., & Simpson, R. J. (2015). A protocol for exosome isolation and characterization: Evaluation of ultracentrifugation, density-gradient separation, and immunoaffinity capture methods. In *Proteomic profiling* (pp. 179–209). Humana Press.

Guduric-Fuchs, J., O'Connor, A., Camp, B., O'Neill, C. L., Medina, R. J., & Simpson, D. A. (2012). Selective extracellular vesicle-mediated export of an overlapping set of microRNAs from multiple cell types. *BioMed Central Genomics*, *13*(1), 1–14.

Guo, S. C., Tao, S. C., & Dawn, H. (2018). Microfluidics-based on-a-chip systems for isolating and analysing extracellular vesicles. *Journal of Extracellular Vesicles*, *7*(1), 1508271.

Gupta, D., Liang, X., Pavlova, S., Wiklander, O. P., Corso, G., Zhao, Y., Saher, O., Bost, J., Zickler, A. M., Piffko, A., Maire, C. L., Ricklefs, F. L., Gustafsson, O., Llorente, V. C., Gustafsson, M. O., Bostancioglu, R. B., Mamand, D. R., Hagey, D. W., Görgens, A., ... el Andaloussi, S. (2020). Quantification of extracellular vesicles in vitro and in vivo using sensitive bioluminescence imaging. *Journal of Extracellular Vesicles*, *9*(1), 1800222.

Han, C., Kang, H., Yi, J., Kang, M., Lee, H., Kwon, Y., Jung, J., Lee, J., & Park, J. (2021). Single-vesicle imaging and co-localization analysis for tetraspanin profiling of individual extracellular vesicles. *Journal of Extracellular Vesicles*, *10*(3), e12047.

Haraszti, R. A., Didiot, M. C., Sapp, E., Leszyk, J., Shaffer, S. A., Rockwell, H. E., Gao, F., Narain, N. R., DiFiglia, M., Kiebish, M. A., Aronin, N., & Khvorova, A. (2016). High-resolution proteomic and lipidomic analysis of exosomes and microvesicles from different cell sources. *Journal of Extracellular Vesicles*, *5*(1), 32570.

Harding, C., Heuser, J., & Stahl, P. (1983). Receptor-mediated endocytosis of transferrin and recycling of the transferrin receptor in rat reticulocytes. *The Journal of Cell Biology*, *97*(2), 329–339.

Hayasaka, R., Tabata, S., Hasebe, M., Ikeda, S., Ohnuma, S., Mori, M., Soga, T., Tomita, M., & Hirayama, A. (2021). Metabolomic analysis of small extracellular vesicles derived from pancreatic cancer cells cultured under normoxia and hypoxia. *Metabolites*, *11*(4), 215.

Headland, S. E., Jones, H. R., D'Sa, A. S., Perretti, M., & Norling, L. V. (2014). Cutting-edge analysis of extracellular microparticles using ImageStream(X) imaging flow cytometry. *Scientific Reports*, *4*, 5237.

Hinger, S. A., Cha, D. J., Franklin, J. L., Higginbotham, J. N., Dou, Y., Ping, J., Shu, L., Prasad, N., Levy, S., Zhang, B., Liu, Q., Weaver, A. M., Coffey, R. J., & Patton, J. G. (2018). Diverse long RNAs are differentially sorted into extracellular vesicles secreted by colorectal cancer cells. *Cell Reports*, *25*(3), 715–725.

Hirschberg, Y., Schildermans, K., van Dam, A., Sterck, K., Boonen, K., Nelissen, I., Vermeiren, Y., & Mertens, I. (2021). Characterizing extracellular vesicles from cerebrospinal fluid by a novel size exclusion chromatography method. *Alzheimer's & Dementia*, *17*, e051264.

Höög, J. L., & Lötvall, J. (2015). Diversity of extracellular vesicles in human ejaculates revealed by cryo-electron microscopy. *Journal of Extracellular Vesicles*, *4*(1), 28680.

Iliescu, F. S., Vrtačnik, D., Neuzil, P., & Iliescu, C. (2019). Microfluidic technology for clinical applications of exosomes. *Micromachines*, *10*(6), 392.

Im, H., Shao, H., Park, Y. I., Peterson, V. M., Castro, C. M., Weissleder, R., & Lee, H. (2014). Label-free detection and molecular profiling of exosomes with a nano-plasmonic sensor. *Nature Biotechnology*, *32*(5), 490–495.

Imanbekova, M., Suarasan, S., Rojalin, T., Mizenko, R. R., Hilt, S., Mathur, M., Lepine, P., Nicouleau, M., Mohamed, N. V., Durcan, T. M., Carney, R. P., Voss, J. C., & Wachsmann-Hogiu, S. (2021). Identification of amyloid beta in small extracellular vesicles via Raman spectroscopy. *Nanoscale Advances*, *3*(14), 4119–4132.

Inal, J. M. (2020). Decoy ACE2-expressing extracellular vesicles that competitively bind SARS-CoV-2 as a possible COVID-19 therapy. *Clinical Science*, *134*(12), 1301–1304.

Inal, J. M., Kosgodage, U., Azam, S., Stratton, D., Antwi-Baffour, S., & Lange, S. (2013). Blood/plasma secretome and microvesicles. *Biochimica et Biophysica Acta*, *1834*(11), 2317–2325.

Inglis, H. C., Danesh, A., Shah, A., Lacroix, J., Spinella, P. C., & Norris, P. J. (2015). Techniques to improve detection and analysis of extracellular vesicles using flow cytometry. *Cytometry Part A*, *87*(11), 1052–1063.

Iraci, N., Leonardi, T., Gessler, F., Vega, B., & Pluchino, S. (2016). Focus on extracellular vesicles: Physiological role and signalling properties of extracellular membrane vesicles. *International Journal of Molecular Sciences*, *17*(2), 171.

Ismail, N., Wang, Y., Dakhlallah, D., Moldovan, L., Agarwal, K., Batte, K., Shah, P., Wisler, J., Eubank, T. D., Tridandapani, S., Paulaitis, M. E., Piper, M. G., & Marsh, C. B. (2013). Macrophage microvesicles induce macrophage differentiation and miR-223 transfer. *Blood*, *121*(6), 984–995.

Jeong, S., Park, J., Pathania, D., Castro, C. M., Weissleder, R., & Lee, H. (2016). Integrated magneto–electrochemical sensor for exosome analysis. *American Chemical Society Nano*, *10*(2), 1802–1809.

Joffe, L. S., Nimrichter, L., Rodrigues, M. L., & Del Poeta, M. (2016). Potential roles of fungal extracellular vesicles during infection. *MSphere*, *1*(4), e00099-16.

Johnstone, R. M., Adam, M., Hammond, J. R., Orr, L., & Turbide, C. (1987). Vesicle formation during reticulocyte maturation. Association of plasma membrane activities with released vesicles (exosomes). *Journal of Biological Chemistry*, *262*(19), 9412–9420.

Kadiu, I., Narayanasamy, P., Dash, P. K., Zhang, W., & Gendelman, H. E. (2012). Biochemical and biologic characterization of exosomes and microvesicles as facilitators of HIV-1 infection in macrophages. *The Journal of Immunology*, *189*(2), 744–754.

Kalra, H., Drummen, G. P., & Mathivanan, S. (2016). Focus on extracellular vesicles: Introducing the next small big thing. *International Journal of Molecular Sciences*, *17*(2), 170.

Kalra, H., Simpson, R. J., Ji, H., Aikawa, E., Altevogt, P., Askenase, P., Bond, V. C., Borràs, F. E., Breakefield, X., Budnik, V., Buzas, E., Camussi, G., Clayton, A., Cocucci, E., Falcon-Perez, J. M., Gabrielsson, S., Gho, Y. S., Gupta, D., Harsha, H. C., … Mathivanan, S. (2012). Vesiclepedia: A compendium for extracellular vesicles with continuous community annotation. *PLoS Biology*, *10*(12), e1001450.

Kang, D., Oh, S., Ahn, S. M., Lee, B. H., & Moon, M. H. (2008). Proteomic analysis of exosomes from human neural stem cells by flow field-flow fractionation and nanoflow liquid chromatography−tandem mass spectrometry. *Journal of Proteome Research*, *7*(8), 3475–3480.

Kang, Y. T., Hadlock, T., Jolly, S., & Nagrath, S. (2020). Extracellular vesicles on demand (EVOD) chip for screening and quantification of cancer-associated extracellular vesicles. *Biosensors and Bioelectronics*, *168*, 112535.

Kholia, S., Jorfi, S., Thompson, P. R., Causey, C. P., Nicholas, A. P., Inal, J. M., & Lange, S. (2015). A novel role for peptidylarginine deiminases in microvesicle release reveals therapeutic potential of PAD inhibition in sensitizing prostate cancer cells to chemotherapy. *Journal of Extracellular Vesicles*, *4*, 26192.

Kim, S. Y., Khanal, D., Kalionis, B., & Chrzanowski, W. (2019). High-fidelity probing of the structure and heterogeneity of extracellular vesicles by resonance-enhanced atomic force microscopy infrared spectroscopy. *Nature Protocols*, *14*(2), 576–593.

Ko, J., Hemphill, M. A., Gabrieli, D., Wu, L., Yelleswarapu, V., Lawrence, G., Pennycooke, W., Singh, A., Meaney, D. F., & Issadore, D. (2016). Smartphone-enabled optofluidic exosome diagnostic for concussion recovery. *Scientific Reports*, *6*(1), 1–12.

Koliha, N., Wiencek, Y., Heider, U., Jüngst, C., Kladt, N., Krauthäuser, S., Johnston, I. C. D., Bosio, A., Schauss, A., & Wild, S. (2016). A novel multiplex bead-based platform highlights the diversity of extracellular vesicles. *Journal of Extracellular Vesicles*, *5*(1), 29975.

Konoshenko, M. Y., Lekchnov, E. A., Vlassov, A. V., & Laktionov, P. P. (2018). Isolation of extracellular vesicles: General methodologies and latest trends. *BioMed Research International*, *2018*, 1–27.

Kowal, J., Arras, G., Colombo, M., Jouve, M., Morath, J. P., Primdal-Bengtson, B., Dingli, F., Loew, D., Tkach, M., & Théry, C. (2016). Proteomic comparison defines novel markers to characterize heterogeneous populations of extracellular vesicle subtypes. *Proceedings of the National Academy of Sciences*, *113*(8), E968–E977.

Kreimer, S., Belov, A. M., Ghiran, I., Murthy, S. K., Frank, D. A., & Ivanov, A. R. (2015). Mass-spectrometry-based molecular characterization of extracellular vesicles: Lipidomics and proteomics. *Journal of Proteome Research*, *14*(6), 2367–2384.

Kruglik, S. G., Royo, F., Guigner, J. M., Palomo, L., Seksek, O., Turpin, P. Y., Tatischeff, I., & Falcón-Pérez, J. M. (2019). Raman tweezers microspectroscopy of circa 100 nm extracellular vesicles. *Nanoscale*, *11*(4), 1661–1679.

Kwizera, E. A., O'Connor, R., Vinduska, V., Williams, M., Butch, E. R., Snyder, S. E., Chen, X., & Huang, X. (2018). Molecular detection and analysis of exosomes using surface-enhanced Raman scattering gold nanorods and a miniaturized device. *Theranostics*, *8*(10), 2722–2738.

Lai, H., Li, Y., Zhang, H., Hu, J., Liao, J., Su, Y., Li, Q., Chen, B., Li, C., Wang, Z., Li, Y., Wang, J., Meng, Z., Huang, Z., & Huang, S. (2022). exoRBase 2.0: An atlas of mRNA, lncRNA and circRNA in extracellular vesicles from human biofluids. *Nucleic Acids Research*, *50*(D1), D118–D128.

Lange, S., Gallagher, M., Kholia, S., Kosgodage, U. S., Hristova, M., Hardy, J., & Inal, J. M. (2017). Peptidylarginine deiminases-roles in cancer and neurodegeneration and possible avenues for therapeutic intervention via modulation of exosome and microvesicle (EMV) release? *International Journal of Molecular Sciences*, *18*(6), 1196.

Lange, S., Kosgodage, U., & Inal, J. M. (2016). Non-phagocytic epithelial cells take up microvesicles by macropinocytosis (PF7.09). *Journal of Extracellular Vesicles*, *5*, 34.

Lannigan, J., & Erdbruegger, U. (2017). Imaging flow cytometry for the characterization of extracellular vesicles. *Methods*, *112*, 55–67.

Lee, K., Fraser, K., Ghaddar, B., Yang, K., Kim, E., Balaj, L., Chiocca, E. A., Breakefield, X. O., Lee, H., & Weissleder, R. (2018). Multiplexed profiling of single extracellular vesicles. *ACS Nano*, *12*(1), 494–503.

Lee, K., Shao, H., Weissleder, R., & Lee, H. (2015). Acoustic purification of extracellular microvesicles. *American Chemical Society Nano*, *9*(3), 2321–2327.

Lee, W., Nanou, A., Rikkert, L., Coumans, F. A., Otto, C., Terstappen, L. W., & Offerhaus, H. L. (2018). Label-free prostate cancer detection by characterization of extracellular vesicles using Raman spectroscopy. *Analytical Chemistry*, *90*(19), 11290–11296.

Li, K., Wong, D. K., Hong, K. Y., & Raffai, R. L. (2018). Cushioned-density gradient ultracentrifugation (C-DGUC): A refined and high performance method for the isolation, characterization, and use of exosomes. *Methods in Molecular Biology*, *1740*, 69–83.

Li, P., Kaslan, M., Lee, S. H., Yao, J., & Gao, Z. (2017). Progress in exosome isolation techniques. *Theranostics*, *7*(3), 789–804.

Li, Y., Zhao, J., Yu, S., Wang, Z., He, X., Su, Y., Guo, T., Sheng, H., Chen, J., Zheng, Q., Li, Y., Guo, W., Cai, X., Shi, G., Wu, J., Wang, L., Wang, P., He, X., & Huang, S. (2019). Extracellular vesicles long RNA sequencing reveals abundant mRNA, circRNA, and lncRNA in human blood as potential biomarkers for cancer diagnosis. *Clinical Chemistry*, *65*(6), 798–808.

Liangsupree, T., Multia, E., & Riekkola, M. L. (2021). Modern isolation and separation techniques for extracellular vesicles. *Journal of Chromatography A*, *1636*, 461773.

Lim, J., Choi, M., Lee, H., Han, J. Y., & Cho, Y. (2019). A novel multifunctional nanowire platform for highly efficient isolation and analysis of circulating tumor-specific markers. *Frontiers in Chemistry*, *6*, 664.

Lim, J., Choi, M., Lee, H., Kim, Y. H., Han, J. Y., Lee, E. S., & Cho, Y. (2019). Direct isolation and characterization of circulating exosomes from biological samples using magnetic nanowires. *Journal of Nanobiotechnology*, *17*(1), 1–12.

Linares, R., Tan, S., Gounou, C., Arraud, N., & Brisson, A. R. (2015). High-speed centrifugation induces aggregation of extracellular vesicles. *Journal of Extracellular Vesicles*, *4*(1), 29509.

Liu, C., Guo, J., Tian, F., Yang, N., Yan, F., Ding, Y., Wei, J., Hu, G., Nie, G., & Sun, J. (2017). Field-free isolation of exosomes from extracellular vesicles by microfluidic viscoelastic flows. *American Chemical Society Nano*, *11*(7), 6968–6976.

Llorente, A., Skotland, T., Sylvänne, T., Kauhanen, D., Róg, T., Orłowski, A., Vattulainen, I., Ekroos, K., & Sandvig, K. (2013). Molecular lipidomics of exosomes released by PC-3 prostate cancer cells. *Biochimica et Biophysica Acta (BBA)-Molecular and Cell Biology of Lipids*, *1831*(7), 1302–1309.

Lobb, R. J., Becker, M., Wen Wen, S., Wong, C. S., Wiegmans, A. P., Leimgruber, A., & Möller, A. (2015). Optimized exosome isolation protocol for cell culture supernatant and human plasma. *Journal of Extracellular Vesicles*, *4*(1), 27031.

Lötvall, J., Hill, A. F., Hochberg, F., Buzás, E. I., di Vizio, D., Gardiner, C., Gho, Y. S., Kurochkin, I. V., Mathivanan, S., Quesenberry, P., Sahoo, S., Tahara, H., Wauben, M. H., Witwer, K. W., & Théry, C. (2014). Minimal experimental requirements for definition of extracellular vesicles and their functions: A position statement from the International Society for Extracellular Vesicles. *Journal of Extracellular Vesicles*, *3*(1), 26913.

Lozano-Ramos, I., Bancu, I., Oliveira-Tercero, A., Armengol, M. P., Menezes-Neto, A., Portillo, H. A. D., Lauzurica-Valdemoros, R., & Borràs, F. E. (2015). Size-exclusion chromatography-based enrichment of extracellular vesicles from urine samples. *Journal of Extracellular Vesicles*, *4*(1), 27369.

Lucchetti, D., Battaglia, A., Ricciardi-Tenore, C., Colella, F., Perelli, L., de Maria, R., Scambia, G., Sgambato, A., & Fattorossi, A. (2020). Measuring extracellular vesicles by conventional flow cytometry: Dream or reality? *International Journal of Molecular Sciences*, *21*(17), 6257.

Ludwig, A. K., de Miroschedji, K., Doeppner, T. R., Börger, V., Ruesing, J., Rebmann, V., Durst, S., Jansen, S., Bremer, M., Behrmann, E., Singer, B. B., Jastrow, H., Kuhlmann, J. D., el Magraoui, F., Meyer, H. E., Hermann, D. M., Opalka, B., Raunser, S., Epple, M., ... Giebel, B. (2018). Precipitation with polyethylene glycol followed by washing and pelleting by ultracentrifugation enriches extracellular vesicles from tissue culture supernatants in small and large scales. *Journal of Extracellular Vesicles*, *7*(1), 1528109.

Lydic, T. A., Townsend, S., Adda, C. G., Collins, C., Mathivanan, S., & Reid, G. E. (2015). Rapid and comprehensive 'shotgun'lipidome profiling of colorectal cancer cell derived exosomes. *Methods*, *87*, 83–95.

Ma, L., Zhu, S., Tian, Y., Zhang, W., Wang, S., Chen, C., Wu, L., & Yan, X. (2016). Label-free analysis of single viruses with a resolution comparable to that of electron microscopy and the throughput of flow cytometry. *Angewandte Chemie International Edition*, *55*(35), 10239–10243.

Maas, S. L., Broekman, M. L., & Vrij, J. D. (2017). Tunable resistive pulse sensing for the characterization of extracellular vesicles. In *Exosomes and microvesicles* (pp. 21–33). Humana Press.

Maas, S. L., De Vrij, J., & Broekman, M. L. (2014). Quantification and size-profiling of extracellular vesicles using tunable resistive pulse sensing. *Journal of Visualized Experiments*, *92*, e51623.

Marcilla, A., Trelis, M., Cortés, A., Sotillo, J., Cantalapiedra, F., Minguez, M. T., Valero, M. L., Sánchez del Pino, M. M., Muñoz-Antoli, C., Toledo, R., & Bernal, D. (2012). Extracellular vesicles from parasitic helminths contain specific excretory/secretory proteins and are internalized in intestinal host cells. *PLoS One*, *7*(9), e45974.

Mathieu, M., Martin-Jaular, L., Lavieu, G., & Théry, C. (2019). Specificities of secretion and uptake of exosomes and other extracellular vesicles for cell-to-cell communication. *Nature Cell Biology*, *21*(1), 9–17.

Mathivanan, S., Lim, J. W., Tauro, B. J., Ji, H., Moritz, R. L., & Simpson, R. J. (2010). Proteomics analysis of A33 immunoaffinity-purified exosomes released from the human colon tumor cell line LIM1215 reveals a tissue-specific protein signature. *Molecular & Cellular Proteomics*, *9*(2), 197–208.

Mathivanan, S., & Simpson, R. J. (2009). ExoCarta: A compendium of exosomal proteins and RNA. *Proteomics*, *9*(21), 4997–5000.

Min, J., Son, T., Hong, J. S., Cheah, P. S., Wegemann, A., Murlidharan, K., Weissleder, R., Lee, H., & Im, H. (2020). Plasmon-enhanced biosensing for multiplexed profiling of extracellular vesicles. *Advanced Biosystems*, *4*(12), e2000003.

Mol, E. A., Goumans, M. J., Doevendans, P. A., Sluijter, J. P., & Vader, P. (2017). Higher functionality of extracellular vesicles isolated using size-exclusion chromatography compared to ultracentrifugation. *Nanomedicine: Nanotechnology, Biology and Medicine*, *13*(6), 2061–2065.

Moore, C., Kosgodage, U., Lange, S., & Inal, J. M. (2017). The emerging role of exosome and microvesicle- (EMV-) based cancer therapeutics and immunotherapy. *International Journal of Cancer*, *141*(3), 428–436.

Morad, G., Carman, C. V., Hagedorn, E. J., Perlin, J. R., Zon, L. I., Mustafaoglu, N., Park, T. E., Ingber, D. E., Daisy, C. C., & Moses, M. A. (2019). Tumor-derived extracellular vesicles breach the intact blood–brain barrier via transcytosis. *American Chemical Society Nano*, *13*(12), 13853–13865.

Morales-Kastresana, A., Telford, B., Musich, T. A., McKinnon, K., Clayborne, C., Braig, Z., Rosner, A., Demberg, T., Watson, D. C., Karpova, T. S., Freeman, G. J., DeKruyff, R. H., Pavlakis, G. N., Terabe, M., Robert-Guroff, M., Berzofsky, J. A., & Jones, J. C. (2017). Labeling extracellular vesicles for nanoscale flow cytometry. *Scientific Reports*, *7*(1), 1–10.

Morasso, C. F., Sproviero, D., Mimmi, M. C., Giannini, M., Gagliardi, S., Vanna, R., Diamanti, L., Bernuzzi, S., Piccotti, F., Truffi, M., Pansarasa, O., Corsi, F., & Cereda, C. (2020). Raman spectroscopy reveals biochemical differences in plasma derived extracellular vesicles from sporadic amyotrophic lateral sclerosis patients. *Nanomedicine: Nanotechnology, Biology and Medicine*, *29*, 102249.

Morelli, A. E., Larregina, A. T., Shufesky, W. J., Sullivan, M. L., Stolz, D. B., Papworth, G. D., Zahorchak, A. F., Logar, A. J., Wang, Z., Watkins, S. C., Falo, L. D., Jr., & Thomson, A. W. (2004). Endocytosis, intracellular sorting, and processing of exosomes by dendritic cells. *Blood*, *104*(10), 3257–3266.

Mulcahy, L. A., Pink, R. C., & Carter, D. R. F. (2014). Routes and mechanisms of extracellular vesicle uptake. *Journal of Extracellular Vesicles*, *3*(1), 24641.

Murillo, O. D., Thistlethwaite, W., Rozowsky, J., Subramanian, S. L., Lucero, R., Shah, N., Jackson, A. R., Srinivasan, S., Chung, A., Laurent, C. D., Kitchen, R. R., Galeev, T., Warrell, J., Diao, J. A., Welsh, J. A., Hanspers, K., Riutta, A., Burgstaller-Muehlbacher, S., Shah, R. V., … Milosavljevic, A. (2019). exRNA atlas analysis reveals distinct extracellular RNA cargo types and their carriers present across human biofluids. *Cell*, *177*(2), 463–477.

Musante, L., Tataruch, D., Gu, D., Benito-Martin, A., Calzaferri, G., Aherne, S., & Holthofer, H. (2014). A simplified method to recover urinary vesicles for clinical applications and sample banking. *Scientific Reports*, *4*(1), 1–11.

Musante, L., Tataruch-Weinert, D., Kerjaschki, D., Henry, M., Meleady, P., & Holthofer, H. (2017). Residual urinary extracellular vesicles in ultracentrifugation supernatants after hydrostatic filtration dialysis enrichment. *Journal of Extracellular Vesicles*, *6*(1), 1267896.

Nakai, W., Yoshida, T., Diez, D., Miyatake, Y., Nishibu, T., Imawaka, N., Naruse, K., Sadamura, Y., & Hanayama, R. (2016). A novel affinity-based method for the isolation of highly purified extracellular vesicles. *Scientific Reports*, *6*(1), 1–11.

Narayanamurthy, V., Jeroish, Z. E., Bhuvaneshwari, K. S., Bayat, P., Premkumar, R., Samsuri, F., & Yusoff, M. M. (2020). Advances in passively driven microfluidics and lab-on-chip devices: A comprehensive literature review and patent analysis. *Royal Society of Chemistry Advances*, *10*(20), 11652–11680.

Naresh, V., & Lee, N. (2021). A review on biosensors and recent development of nanostructured materials-enabled biosensors. *Sensors*, *21*(4), 1109.

Nguyen, V., Witwer, K. W., Verhaar, M. C., Strunk, D., & van Balkom, B. (2020). Functional assays to assess the therapeutic potential of extracellular vesicles. *Journal of Extracellular Vesicles*, *10*(1), e12033.

Nishida-Aoki, N., Izumi, Y., Takeda, H., Takahashi, M., Ochiya, T., & Bamba, T. (2020). Lipidomic analysis of cells and extracellular vesicles from high-and low-metastatic triple-negative breast cancer. *Metabolites*, *10*(2), 67.

Nishida-Aoki, N., Tominaga, N., Kosaka, N., & Ochiya, T. (2020). Altered biodistribution of deglycosylated extracellular vesicles through enhanced cellular uptake. *Journal of Extracellular Vesicles*, *9*(1), 1713527.

Niu, Z., Pang, R. T., Liu, W., Li, Q., Cheng, R., & Yeung, W. S. (2017). Polymer-based precipitation preserves biological activities of extracellular vesicles from an endometrial cell line. *PLoS One*, *12*(10), e0186534.

Nizamudeen, Z., Markus, R., Lodge, R., Parmenter, C., Platt, M., Chakrabarti, L., & Sottile, V. (2018). Rapid and accurate analysis of stem cell-derived extracellular vesicles with super resolution microscopy and live imaging. *Biochimica et Biophysica Acta (BBA)-Molecular Cell Research*, *1865*(12), 1891–1900.

Nolan, J. P., & Duggan, E. (2018). Analysis of individual extracellular vesicles by flow cytometry. *Flow Cytometry Protocols*, *1678,* 79–92.

Nordin, J. Z., Lee, Y., Vader, P., Mäger, I., Johansson, H. J., Heusermann, W., Wiklander, O. P. B., Hällbrink, M., Seow, Y., Bultema, J. J., Gilthorpe, J., Davies, T., Fairchild, P. J., Gabrielsson, S., Meisner-Kober, N. C., Lehtiö, J., Smith, C. I. E., Wood, M. J. A., & Andaloussi, S. E. L. (2015). Ultrafiltration with size-exclusion liquid chromatography for high yield isolation of extracellular vesicles preserving intact biophysical and functional properties. *Nanomedicine: Nanotechnology, Biology and Medicine*, *11*(4), 879–883.

O'Brien, K., Breyne, K., Ughetto, S., Laurent, L. C., & Breakefield, X. O. (2020). RNA delivery by extracellular vesicles in mammalian cells and its applications. *Nature Reviews Molecular Cell Biology*, *21*(10), 585–606.

Onódi, Z., Pelyhe, C., Terézia Nagy, C., Brenner, G. B., Almási, L., Kittel, Á., Manček-Keber, M., Ferdinandy, P., Buzás, E. I., & Giricz, Z. (2018). Isolation of high-purity extracellular vesicles by the combination of iodixanol density gradient ultracentrifugation and bind-elute chromatography from blood plasma. *Frontiers in Physiology*, *9*, 1479.

Ostenfeld, M. S., Jensen, S. G., Jeppesen, D. K., Christensen, L. L., Thorsen, S. B., Stenvang, J., Hvam, M. L., Thomsen, A., Mouritzen, P., Rasmussen, M. H., Nielsen, H. J., Ørntoft, T. F., & Andersen, C. L. (2016). miRNA profiling of circulating EpCAM+ extracellular vesicles: Promising biomarkers of colorectal cancer. *Journal of Extracellular Vesicles*, *5*(1), 31488.

Pan, B. T., Teng, K., Wu, C., Adam, M., & Johnstone, R. M. (1985). Electron microscopic evidence for externalization of the transferrin receptor in vesicular form in sheep reticulocytes. *The Journal of Cell Biology*, *101*(3), 942–948.

Paolini, L., Zendrini, A., Noto, G. D., Busatto, S., Lottini, E., Radeghieri, A., Dossi, A., Caneschi, A., Ricotta, D., & Bergese, P. (2016). Residual matrix from different separation techniques impacts exosome biological activity. *Scientific Reports*, *6*(1), 1–11.

Parimon, T., Garrett, N. E., III, Chen, P., & Antes, T. J. (2018). Isolation of extracellular vesicles from murine bronchoalveolar lavage fluid using an ultrafiltration centrifugation technique. *Journal of Visualized Experiments*, *141*, e58310.

Pasalic, L., Williams, R., Siupa, A., Campbell, H., Henderson, M. J., & Chen, V. M. (2016). Enumeration of extracellular vesicles by a new improved flow cytometric method is comparable to fluorescence mode nanoparticle tracking analysis. *Nanomedicine: Nanotechnology, Biology and Medicine*, *12*(4), 977–986.

Phan, T. H., Kim, S. Y., Rudge, C., & Chrzanowski, W. (2022). Made by cells for cells—Extracellular vesicles as next-generation mainstream medicines. *Journal of Cell Science*, *135*(1), jcs259166.

Phan, T. K., Ozkocak, D. C., & Poon, I. K. H. (2020). Unleashing the therapeutic potential of apoptotic bodies. *Biochemical Society Transactions*, *48*(5), 2079–2088.

Priglinger, E., Strasser, J., Buchroithner, B., Weber, F., Wolbank, S., Auer, D., Grasmann, E., Arzt, C., Sivun, D., Grillari, J., Jacak, J., Preiner, J., & Gimona, M. (2021). Label-free characterization of an extracellular vesicle-based therapeutic. *Journal of Extracellular Vesicles*, *10*(12), e12156.

Ramirez, M. I., Amorim, M. G., Gadelha, C., Milic, I., Welsh, J. A., Freitas, V. M., Nawaz, M., Akbar, N., Couch, Y., Makin, L., Cooke, F., Vettore, A. L., Batista, P. X., Freezor, R., Pezuk, J. A., Rosa-Fernandes, L., Carreira, A. C. O., Devitt, A., Jacobs, L., … Dias-Neto, E. (2018). Technical challenges of working with extracellular vesicles. *Nanoscale*, *10*(3), 881–906.

Rho, J., Chung, J., Im, H., Liong, M., Shao, H., Castro, C. M., Weissleder, R., & Lee, H. (2013). Magnetic nanosensor for detection and profiling of erythrocyte-derived microvesicles. *ACS Nano*, *7*(12), 11227–11233.

Rodrigues, M., Fan, J., Lyon, C., Wan, M., & Hu, Y. (2018). Role of extracellular vesicles in viral and bacterial infections: Pathogenesis, diagnostics, and therapeutics. *Theranostics*, *8*(10), 2709–2721.

Románszki, L., Varga, Z., Mihály, J., Keresztes, Z., & Thompson, M. (2020). Electromagnetic piezoelectric acoustic sensor detection of extracellular vesicles through interaction with detached vesicle proteins. *Biosensors*, *10*(11), 173.

Rontogianni, S., Synadaki, E., Li, B., Liefaard, M. C., Lips, E. H., Wesseling, J., Wu, W., & Altelaar, M. (2019). Proteomic profiling of extracellular vesicles allows for human breast cancer subtyping. *Communications Biology*, *2*(1), 1–13.

Rood, I. M., Deegens, J. K., Merchant, M. L., Tamboer, W. P., Wilkey, D. W., Wetzels, J. F., & Klein, J. B. (2010). Comparison of three methods for isolation of urinary microvesicles to identify biomarkers of nephrotic syndrome. *Kidney International*, *78*(8), 810–816.

Rossi, I. V., Nunes, M. A. F., Vargas-Otalora, S., da Silva Ferreira, T. C., Cortez, M., & Ramirez, M. I. (2021). Extracellular vesicles during TriTryps infection: Complexity and future challenges. *Molecular Immunology*, *132*, 172–183.

Royo, F., Cossío, U., de Angulo, A. R., Llop, J., & Falcon-Perez, J. M. (2019). Modification of the glycosylation of extracellular vesicles alters their biodistribution in mice. *Nanoscale*, *11*(4), 1531–1537.

Rust, M. J., Bates, M., & Zhuang, X. (2006). Stochastic optical reconstruction microscopy (STORM) provides sub-diffraction-limit image resolution. *Nature Methods*, *3*(10), 793–796.

Samsonov, R., Shtam, T., Burdakov, V., Glotov, A., Tsyrlina, E., Berstein, L., Nosov, A., Evtushenko, V., Filatov, M., & Malek, A. (2016). Lectin-induced agglutination method of urinary exosomes isolation followed by mi-RNA analysis: Application for prostate cancer diagnostic. *The Prostate*, *76*(1), 68–79.

Sedgwick, A. E., & D'Souza-Schorey, C. (2018). The biology of extracellular microvesicles. *Traffic*, *19*(5), 319–327.

Serrano-Pertierra, E., Oliveira-Rodríguez, M., Rivas, M., Oliva, P., Villafani, J., Navarro, A., Blanco-López, M., & Cernuda-Morollón, E. (2019). Characterization of plasma-derived extracellular vesicles isolated by different methods: A comparison study. *Bioengineering*, *6*(1), 8.

Shao, H., Chung, J., Balaj, L., Charest, A., Bigner, D. D., Carter, B. S., Hochberg, F. H., Breakefield, X. O., Weissleder, R., & Lee, H. (2012). Protein typing of circulating microvesicles allows real-time monitoring of glioblastoma therapy. *Nature Medicine*, *18*(12), 1835–1840.

Shao, H., Chung, J., Lee, K., Balaj, L., Min, C., Carter, B. S., Hochberg, F. H., Breakefield, X. O., Lee, H., & Weissleder, R. (2015). Chip-based analysis of exosomal mRNA mediating drug resistance in glioblastoma. *Nature Communications*, *6*(1), 1–9.

Sharma, S., LeClaire, M., Wohlschlegel, J., & Gimzewski, J. (2020). Impact of isolation methods on the biophysical heterogeneity of single extracellular vesicles. *Scientific Reports*, *10*(1), 1–11.

Shi, C., Ulke-Lemée, A., Deng, J., Batulan, Z., & O'Brien, E. R. (2019). Characterization of heat shock protein 27 in extracellular vesicles: A potential anti-inflammatory therapy. *The Federation of American Societies for Experimental Biology Journal*, *33*(2), 1617–1630.

Shtam, T. A., Burdakov, V. S., Landa, S. B., Naryzhny, S. N., Bairamukov, V. Y., Malek, A. V., Orlov, Y. N., & Filatov, M. V. (2017). Aggregation by lectin-methodical approach for effective isolation of exosomes from cell culture supernatant for proteome profiling. *Tsitologiia*, *59*(1), 5–12.

Skog, J., Würdinger, T., van Rijn, S., Meijer, D. H., Gainche, L., Sena-Esteves, M., Curry, W. T., Jr., Carter, B. S., Krichevsky, A. M., & Breakefield, X. O. (2008). Glioblastoma microvesicles transport RNA and proteins that promote tumour growth and provide diagnostic biomarkers. *Nature Cell Biology*, *10*(12), 1470–1476.

Skotland, T., Hessvik, N. P., Sandvig, K., & Llorente, A. (2019). Exosomal lipid composition and the role of ether lipids and phosphoinositides in exosome biology. *Journal of Lipid Research*, *60*(1), 9–18.

Skotland, T., Sagini, K., Sandvig, K., & Llorente, A. (2020). An emerging focus on lipids in extracellular vesicles. *Advanced Drug Delivery Reviews*, *159*, 308–321.

Skovronova, R., Grange, C., Dimuccio, V., Deregibus, M. C., Camussi, G., & Bussolati, B. (2021). Surface marker expression in small and medium/large mesenchymal stromal cell-derived extracellular vesicles in naive or apoptotic condition using orthogonal techniques. *Cell*, *10*(11), 2948.

Smith, J. T., Wunsch, B. H., Dogra, N., Ahsen, M. E., Lee, K., Yadav, K. K., Weil, R., Pereira, M. A., Patel, J. V., Duch, E. A., Papalia, J. M., Lofaro, M. F., Gupta, M., Tewari, A. K., Cordon-Cardo, C., Stolovitzky, G., & Gifford, S. M. (2018). Integrated nanoscale deterministic lateral displacement arrays for separation of extracellular vesicles from clinically-relevant volumes of biological samples. *Lab on a Chip*, *18*(24), 3913–3925.

Smith, Z. J., Lee, C., Rojalin, T., Carney, R. P., Hazari, S., Knudson, A., Lam, K., Saari, H., Ibañez, E. L., Viitala, T., Laaksonen, T., Yliperttula, M., & Wachsmann-Hogiu, S. (2015). Single exosome study reveals subpopulations distributed among cell lines with variability related to membrane content. *Journal of Extracellular Vesicles*, *4*(1), 28533.

Sorrells, J. E., Martin, E. M., Aksamitiene, E., Mukherjee, P., Alex, A., Chaney, E. J., Marjanovic, M., & Boppart, S. A. (2021). Label-free characterization of single extracellular vesicles using two-photon fluorescence lifetime imaging microscopy of NAD (P) H. *Scientific Reports*, *11*(1), 1–12.

Stam, J., Bartel, S., Bischoff, R., & Wolters, J. C. (2021). Isolation of extracellular vesicles with combined enrichment methods. *Journal of Chromatography. B, Analytical Technologies in the Biomedical and Life Sciences*, *1169*, 122604.

Stanton, B. A. (2021). Extracellular vesicles and host–pathogen interactions: A review of inter-kingdom signaling by small noncoding RNA. *Genes*, *12*(7), 1010.

Stoner, S. A., Duggan, E., Condello, D., Guerrero, A., Turk, J. R., Narayanan, P. K., & Nolan, J. P. (2016). High sensitivity flow cytometry of membrane vesicles. *Cytometry Part A*, *89*(2), 196–206.

Stotz, H., Brotherton, D., & Inal, J. (2022). Communication is key: Extracellular vesicles as mediators of infection and defence during host–microbe interactions in animals and plants. *Federation of European Microbiological Societies Microbiology Reviews*, *46*(1), fuab044.

Stratton, D., Lange, S., Kholia, S., Jorfi, S., Antwi-Baffour, S., & Inal, J. (2014). Label-free real-time acoustic sensing of microvesicle release from prostate cancer (PC3) cells using a Quartz rystal Microbalance. *Biochemical and Biophysical Research Communications*, *453*(3), 619–624.

Subra, C., Laulagnier, K., Perret, B., & Record, M. (2007). Exosome lipidomics unravels lipid sorting at the level of multivesicular bodies. *Biochimie*, *89*(2), 205–212.

Sun, Y., Saito, K., & Saito, Y. (2019). Lipid profile characterization and lipoprotein comparison of extracellular vesicles from human plasma and serum. *Metabolites*, *9*(11), 259.

Szatanek, R., Baran, J., Siedlar, M., & Baj-Krzyworzeka, M. (2015). Isolation of extracellular vesicles: Determining the correct approach. *International Journal of Molecular Medicine*, *36*(1), 11–17.

Szempruch, A. J., Sykes, S. E., Kieft, R., Dennison, L., Becker, A. C., Gartrell, A., Martin, W. J., Nakayasu, E. S., Almeida, I. C., Hajduk, S. L., & Harrington, J. M. (2016). Extracellular vesicles from *Trypanosoma brucei* mediate virulence factor transfer and cause host anemia. *Cell*, *164*(1–2), 246–257.

Tatischeff, I., Larquet, E., Falcón-Pérez, J. M., Turpin, P. Y., & Kruglik, S. G. (2012). Fast characterisation of cell-derived extracellular vesicles by nanoparticles tracking analysis, cryo-electron microscopy, and Raman tweezers microspectroscopy. *Journal of Extracellular Vesicles*, *1*(1), 19179.

Thane, K. E., Davis, A. M., & Hoffman, A. M. (2019). Improved methods for fluorescent labeling and detection of single extracellular vesicles using nanoparticle tracking analysis. *Scientific Reports*, *9*(1), 1–13.

Théry, C., Witwer, K. W., Aikawa, E., Alcaraz, M. J., Anderson, J. D., Andriantsitohaina, R., Antoniou, A., Arab, T., Archer, F., Atkin-Smith, G. K., Ayre, D. C., Bach, J. M., Bachurski, D., Baharvand, H., Balaj, L., Baldacchino, S., Bauer, N. N., Baxter, A. A., Bebawy, M., … Zuba-Surma, E. K. (2018). Minimal information for studies of extracellular vesicles 2018 (MISEV2018): A position statement of the International Society for Extracellular Vesicles and update of the MISEV2014 guidelines. *Journal of Extracellular Vesicles*, *7*(1), 1535750.

Tian, J., Casella, G., Zhang, Y., Rostami, A., & Li, X. (2020). Potential roles of extracellular vesicles in the pathophysiology, diagnosis, and treatment of autoimmune diseases. *International Journal of Biological Sciences*, *16*(4), 620–632.

Tian, Y., Ma, L., Gong, M., Su, G., Zhu, S., Zhang, W., Wang, S., Li, Z., Chen, C., Li, L., Wu, L., & Yan, X. (2018). Protein profiling and sizing of extracellular vesicles from colorectal cancer patients via flow cytometry. *ACS Nano*, *12*(1), 671–680.

Tutrone, R., Donovan, M. J., Torkler, P., Tadigotla, V., McLain, T., Noerholm, M., Skog, J., & McKiernan, J. (2020). Clinical utility of the exosome based ExoDx Prostate (IntelliScore) EPI test in men presenting for initila Biopsy with a PSA 2–10 ng/mL. *Prostate Cancer Prostatic Disease*, *23*(4) 607–614.

Ueda, K., Ishikawa, N., Tatsuguchi, A., Saichi, N., Fujii, R., & Nakagawa, H. (2014). Antibody-coupled monolithic silica microtips for high throughput molecular profiling of circulating exosomes. *Scientific Reports*, *4*(1), 1–9.

van Deun, J., Mestdagh, P., Sormunen, R., Cocquyt, V., Vermaelen, K., Vandesompele, J., Bracke, M., de Wever, O., & Hendrix, A. (2014). The impact of disparate isolation methods for extracellular vesicles on downstream RNA profiling. *Journal of Extracellular Vesicles*, *3*(1), 24858.

Van Niel, G., d'Angelo, G., & Raposo, G. (2018). Shedding light on the cell biology of extracellular vesicles. *Nature Reviews Molecular Cell Biology*, *19*(4), 213–228.

Verweij, F., Bebelman, M., Jimenez, C., Garcia-Vallejo, J., Janssen, H., Neefjes, J., Knol, J., de Goeij-De Haas, R., Piersma, S., Baglio, S., & Verhage, M. (2018). Quantifying exosome secretion from single cells reveals a modulatory role for GPCR signaling. *Journal of Cell Biology*, *217*(3), 1129–1142.

Villa, F., Quarto, R., & Tasso, R. (2019). Extracellular vesicles as natural, safe and efficient drug delivery systems. *Pharmaceutics*, *11*(11), 557.

Vogel, R., Coumans, F. A., Maltesen, R. G., Böing, A. N., Bonnington, K. E., Broekman, M. L., Broom, M. F., Buzás, E. I., Christiansen, G., Hajji, N., Kristensen, S. R., Kuehn, M. J., Lund, S. M., Maas, S. L. N., Nieuwland, R., Osteikoetxea, X., Schnoor, R., Scicluna, B. J., Shambrook, M., … Pedersen, S. (2016). A standardized method to determine the concentration of extracellular vesicles using tunable resistive pulse sensing. *Journal of Extracellular Vesicles*, *5*(1), 31242.

Votteler, J., Ogohara, C., Yi, S., Hsia, Y., Nattermann, U., Belnap, D. M., King, N. P., & Sundquist, W. I. (2016). Designed proteins induce the formation of nanocage-containing extracellular vesicles. *Nature*, *540*(7632), 292–295.

Wan, M., Amrollahi, P., Sun, D., Lyon, C., & Hu, T. Y. (2019). Using nanoplasmon-enhanced scattering and low-magnification microscope imaging to quantify tumor-derived exosomes. *Journal of Visualized Experiments*, *147*, e59177.

Wang, J. M., Li, Y. J., Wu, J. Y., Cai, J. X., Wen, J., Xiang, D. X., Hu, X. B., & Li, W. Q. (2021). Comparative evaluation of methods for isolating small extracellular vesicles derived from pancreatic cancer cells. *Cell & Bioscience*, *11*(1), 1–13.

Wang, Z., Wu, H. J., Fine, D., Schmulen, J., Hu, Y., Godin, B., Zhang, J. X., & Liu, X. (2013). Ciliated micropillars for the microfluidic-based isolation of nanoscale lipid vesicles. *Lab on a Chip*, *13*(15), 2879–2882.

Weng, Y., Sui, Z., Shan, Y., Hu, Y., Chen, Y., Zhang, L., & Zhang, Y. (2016). Effective isolation of exosomes with polyethylene glycol from cell culture supernatant for in-depth proteome profiling. *Analyst*, *141*(15), 4640–4646.

Wiklander, O., Brennan, M. Á., Lötvall, J., Breakefield, X. O., & El Andaloussi, S. (2019). Advances in therapeutic applications of extracellular vesicles. *Science Translational Medicine*, *11*(492), eaav8521.

Wiklander, O. P., Nordin, J. Z., O'Loughlin, A., Gustafsson, Y., Corso, G., Mäger, I., Vader, P., Lee, Y., Sork, H., Seow, Y., Heldring, N., Alvarez-Erviti, L., Smith, C. I. E., le Blanc, K., Macchiarini, P., Jungebluth, P., Wood, M. J. A., & Andaloussi, S. E. L. (2015). Extracellular vesicle in vivo biodistribution is determined by cell source, route of administration and targeting. *Journal of Extracellular Vesicles*, *4*(1), 26316.

Wu, B., Chen, X., Wang, J., Qing, X., Wang, Z., Ding, X., Xie, Z., Niu, L., Guo, X., Cai, T., Guo, X., & Yang, F. (2020). Separation and characterization of extracellular vesicles from human plasma by asymmetrical flow field-flow fractionation. *Analytica Chimica Acta*, *1127*, 234–245.

Wu, M., Ouyang, Y., Wang, Z., Zhang, R., Huang, P. H., Chen, C., Li, H., Li, P., Quinn, D., Dao, M., Suresh, S., Sadovsky, Y., & Huang, T. J. (2017). Isolation of exosomes from whole blood by integrating acoustics and microfluidics. *Proceedings of the National Academy of Sciences of the United States of America*, *114*(40), 10584–10589.

Xiao, Y., Wang, S. K., Zhang, Y., Rostami, A., Kenkare, A., Casella, G., Yuan, Z. Q., & Li, X. (2021). Role of extracellular vesicles in neurodegenerative diseases. *Progress in Neurobiology*, *201*, 102022.

Xu, R., Simpson, R. J., & Greening, D. W. (2017). A protocol for isolation and proteomic characterization of distinct extracellular vesicle subtypes by sequential centrifugal ultrafiltration. In *Exosomes and microvesicles* (pp. 91–116). Humana Press.

Xu, Y., Qin, S., An, T., Tang, Y., Huang, Y., & Zheng, L. (2017). MiR-145 detection in urinary extracellular vesicles increase diagnostic efficiency of prostate cancer based on hydrostatic filtration dialysis method. *The Prostate*, *77*(10), 1167–1175.

Yamashita, T., Takahashi, Y., Nishikawa, M., & Takakura, Y. (2016). Effect of exosome isolation methods on physicochemical properties of exosomes and clearance of exosomes from the blood circulation. *European Journal of Pharmaceutics and Biopharmaceutics*, *98*, 1–8.

Yáñez-Mó, M., Siljander, P. R. M., Andreu, Z., Bedina Zavec, A., Borràs, F. E., Buzas, E. I., Buzas, K., Casal, E., Cappello, F., Carvalho, J., Colás, E., Cordeiro-da Silva, A., Fais, S., Falcon-Perez, J. M., Ghobrial, I. M., Giebel, B., Gimona, M., Graner, M., Gursel, I., … de Wever, O. (2015). Biological properties of extracellular vesicles and their physiological functions. *Journal of Extracellular Vesicles*, *4*(1), 27066.

Yang, J. E., Rossignol, E. D., Chang, D., Zaia, J., Forrester, I., Raja, K., Winbigler, H., Nicastro, D., Jackson, W. T., & Bullitt, E. (2020). Complexity and ultrastructure of infectious extracellular vesicles from cells infected by non-enveloped virus. *Scientific Reports*, *10*(1), 1–18.

Yekula, A., Minciacchi, V. R., Morello, M., Shao, H., Park, Y., Zhang, X., Muralidharan, K., Freeman, M. R., Weissleder, R., Lee, H., Carter, B., Breakefield, X. O., di Vizio, D., & Balaj, L. (2020). Large and small extracellular vesicles released by glioma cells in vitro and in vivo. *Journal of Extracellular Vesicles*, *9*(1), 1689784.

Yoshida, T., Ishidome, T., & Hanayama, R. (2017). High purity isolation and sensitive quantification of extracellular vesicles using affinity to TIM4. *Current Protocols in Cell Biology*, *77*(1), 3–45.

Yoshioka, Y., Konishi, Y., Kosaka, N., Katsuda, T., Kato, T., & Ochiya, T. (2013). Comparative marker analysis of extracellular vesicles in different human cancer types. *Journal of Extracellular Vesicles*, *2*(1), 20424.

Yu, L. L., Zhu, J., Liu, J. X., Jiang, F., Ni, W. K., Qu, L. S., Ni, R. Z., Lu, C. H., & Xiao, M. B. (2018). A comparison of traditional and novel methods for the separation of exosomes from human samples. *BioMed Research International*, *2018*, 1–9.

Yuana, Y., Koning, R. I., Kuil, M. E., Rensen, P. C., Koster, A. J., Bertina, R. M., & Osanto, S. (2013). Cryo-electron microscopy of extracellular vesicles in fresh plasma. *Journal of Extracellular Vesicles*, *2*(1), 21494.

Zarovni, N., Corrado, A., Guazzi, P., Zocco, D., Lari, E., Radano, G., Muhhina, J., Fondelli, C., Gavrilova, J., & Chiesi, A. (2015). Integrated isolation and quantitative analysis of exosome shuttled proteins and nucleic acids using immunocapture approaches. *Methods*, *87*, 46–58.

Zhang, P., Zhou, X., He, M., Shang, Y., Tetlow, A. L., Godwin, A. K., & Zeng, Y. (2019). Ultrasensitive detection of circulating exosomes with a 3D-nanopatterned microfluidic chip. *Nature Biomedical Engineering*, *3*(6), 438–451.

Zhang, X., Borg, E. G. F., Liaci, A. M., Vos, H. R., & Stoorvogel, W. (2020). A novel three step protocol to isolate extracellular vesicles from plasma or cell culture medium with both high yield and purity. *Journal of Extracellular Vesicles*, *9*(1), 1791450.

Zhu, J., Zhang, J., Ji, X., Tan, Z., & Lubman, D. M. (2021). Column-based technology for CD9-HPLC immunoaffinity isolation of serum extracellular vesicles. *Journal of Proteome Research*, *20*(10), 4901–4911.

Zhu, S., Ma, L., Wang, S., Chen, C., Zhang, W., Yang, L., Hang, W., Nolan, J. P., Wu, L., & Yan, X. (2014). Light-scattering detection below the level of single fluorescent molecules for high-resolution characterization of functional nanoparticles. *ACS Nano*, *8*(10), 10998–11006.

Zoghbi, M. E., & Altenberg, G. A. (2018). Luminescence resonance energy transfer spectroscopy of ATP-binding cassette proteins. *Biochimica et Biophysica Acta (BBA)-Biomembranes*, *1860*(4), 854–867.

Isolation and Flow Cytometry Characterization of Extracellular-Vesicle Subpopulations Derived from Human Mesenchymal Stromal Cells

Cansu Gorgun,[1,2,5] Daniele Reverberi,[3,5] Gianluca Rotta,[4] Federico Villa,[2] Rodolfo Quarto,[1,2] and Roberta Tasso[1,2,6]

[1]Department of Experimental Medicine, University of Genova, Genova, Italy
[2]U.O. Cellular Oncology, IRCCS Ospedale Policlinico San Martino, Genova, Italy
[3]U.O. Molecular Pathology, IRCCS Ospedale Policlinico San Martino, Genova, Italy
[4]BD Biosciences, Milano, Italy
[5]These authors contributed equally to this work.
[6]Corresponding author: *robertatasso@gmail.com*

This unit describes protocols for isolating subpopulations of extracellular vesicles (EVs) purified from human adipose tissue–derived mesenchymal stromal cells by density gradient centrifugation and for characterizing them by flow cytometry (FCM). Determining the optimal strategy for isolating EVs is a critical step toward retrieving the maximal amount while ensuring the recovery of different vesicular subtypes. The first protocol details density gradient centrifugation to isolate both exosomes and microvesicles. In the second protocol, characterization of EV subpopulations by FCM is depicted, taking advantage of non-conventional modalities, in accordance with the latest technical indications. The procedures described here can be easily reproduced and can be employed regardless of the cell type used to obtain EVs.

Keywords: exosomes • extracellular vesicles • flow cytometry • mesenchymal stromal cells • microvesicles

INTRODUCTION

For many years, mesenchymal stromal cells (MSCs) have been considered a central cell source for regenerative-medicine applications due to these cells' multipotent properties. In the last decade, MSCs have also received great attention for their marked paracrine activity (Caplan & Dennis, 2006), exerted via both soluble factors and extracellular vesicles (EVs). In particular, given the array of signals carried by vesicles through horizontal transfer of molecules, EVs have assumed an emerging role (Rani, Ryan, Griffin, & Ritter, 2015; Sicco et al., 2017).

EVs comprise a heterogeneous mixture of membrane-surrounded structures that consists of different subpopulations. The main vesicular types include exosomes (50 to 160 nm in diameter), microvesicles (160 to 900 nm), and apoptotic bodies (>900 nm) (Willms

CURRENT PROTOCOLS
A Wiley Brand

Current Protocols in Stem Cell Biology e76, Volume 48
Published in Wiley Online Library (wileyonlinelibrary.com).
doi: 10.1002/cpsc.76

et al., 2016). It has been demonstrated that the EV subpopulations possess different densities and that their cargo and functional properties can vary, thus drawing attention to the importance of considering all the subtypes released by a specific cell source (Kowal et al., 2016; Lässer, Jang, & Lötvall, 2018; Tkach, Kowal, & Théry, 2018). Differential centrifugation is one of the most commonly used methods for EV isolation in laboratory practice. However, it is generally used to isolate smaller EVs, whereas larger vesicles, such as shedding microvesicles, are partially eliminated during this experimental procedure, causing loss of heterogeneity (Tkach, Kowal, & Théry, 2018). Therefore, many attempts have been made to ameliorate both isolation techniques and characterization methods. Advanced flow cytometry (FCM) is one of the most promising approaches, as it can be used to analyze a large range of particle diameters <1 μm; in contrast, conventional FCM is useful for appropriately discriminating only larger particles (e.g., platelets) (Van Der Vlist, Nolte, Stoorvogel, Arkesteijn, & Wauben, 2012; Welsh, Holloway, Wilkinson, & Englyst, 2017).

In this unit, a methodology for isolation of human MSC–derived EV subpopulations by density gradient centrifugation (Basic Protocol 1) is optimized for applications beyond those detailed in our previously published paper (Lo Sicco, Reverberi, Pascucci, & Tasso, 2018), where our intent was to isolate a mixed population of EVs without taking into consideration the different subtypes. Vesicular characterization by FCM is explained in Basic Protocol 2, taking advantage of recently developed technologies. Compared to our previously published paper (Lo Sicco et al., 2018), here, we propose a more accurate FCM characterization that allows proper discrimination between different-sized vesicular subpopulations.

BASIC PROTOCOL 1

ISOLATION OF DIFFERENT SUBSETS OF MESENCHYMAL STROMAL CELL–DERIVED EXTRACELLULAR VESICLES

Cells release different types of EVs: exosomes, microvesicles, and apoptotic bodies. Each EV subset is characterized by a defined molecular composition and specific biological functions. Understanding whether the heterogeneous ensemble or a single EV subpopulation is responsible for the properties exerted by EVs is a topic of widespread interest (Tkach et al., 2018). In this protocol, we describe a useful method for dissecting EV heterogeneity based on density gradient ultracentrifugation (Fig. 1). Compared to our previously published paper (Lo Sicco et al., 2018), where a mixed population of vesicles was considered, here, we propose an advanced isolation protocol, useful for isolating microvesicles from exosomes.

Materials

MSC-conditioned serum-free medium
OptiPrep buffer (see recipe)
OptiPrep Density Gradient Medium [60% (w/v) stock solution, Sigma-Aldrich, D1556]
10% (w/v) and 20% (w/v) OptiPrep solutions (OptiPrep Density Gradient Medium in OptiPrep buffer)
Filtered (with 0.22-μm filter) 1× Dulbecco's phosphate-buffered saline (D-PBS), without calcium and magnesium
Distilled water

50-ml conical centrifuge tubes
Refrigerated tabletop centrifuge, 4°C
Open-top polypropylene ultracentrifugation tubes, 38.5 ml, 25 × 89 mm (SW28, Beckman Coulter, 326823), and 5.2 ml, 13 × 51 mm (SW55Ti, Beckman Coulter, 328819)

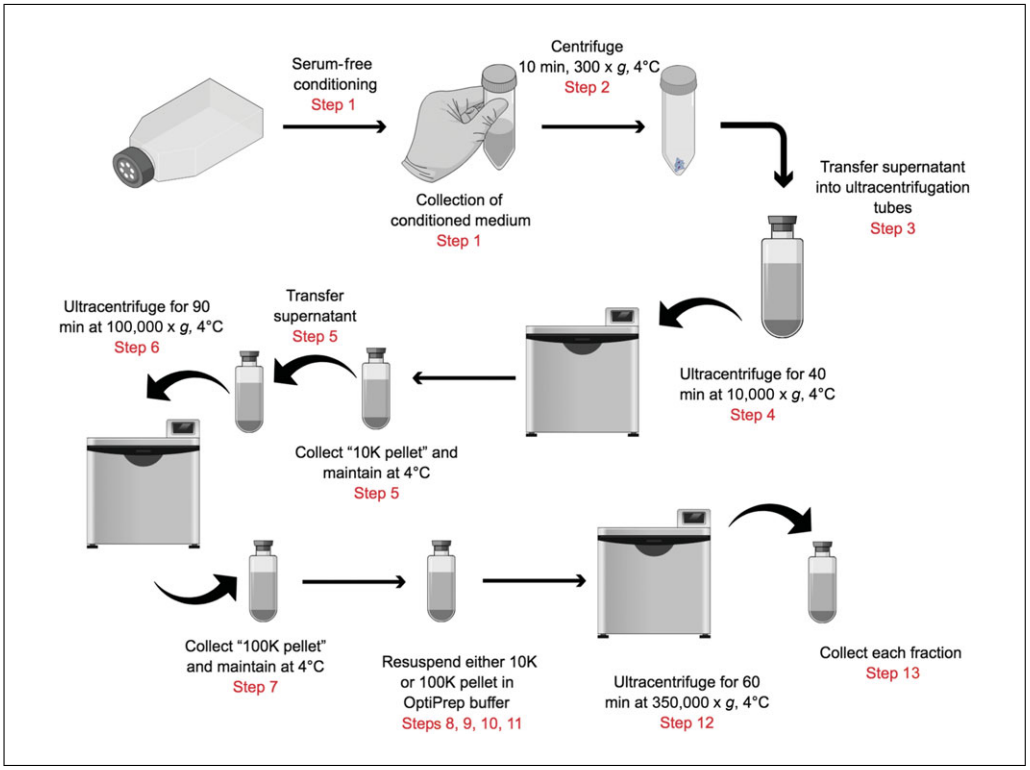

Figure 1 Schematic depicting the experimental steps for isolating different subsets of extracellular vesicles.

Ultracentrifuge (Optima XPN, Beckman Coulter)
Swinging-bucket rotors 28 and 55Ti (SW28 and SW55Ti, Beckman Coulter)
Low-binding collection tube
Refractometer

Additional reagents and equipment for harvesting MSC-conditioned medium (Lo Sicco et al., 2018)

Isolation of extracellular-vesicle subpopulations

1. Harvest MSC-conditioned serum-free medium as previously described (Lo Sicco et al., 2018) and transfer to 50-ml conical centrifuge tubes.

   It is recommended to prolong serum-free incubation from 24 hr to 48, 72, or 96 hr if using primary cell cultures to obtain a sufficient amount of vesicles for further analysis. We use a serum-free conditioning timeframe of 96 hr.

2. Centrifuge 10 min at 300 × *g*, 4°C, to remove cell debris.
3. Transfer supernatants into SW28 open-top polypropylene ultracentrifugation tubes.
4. Ultracentrifuge 40 min at 10,000 × *g*, 4°C, using SW28 rotor.
5. At the end of the centrifugation, carefully transfer supernatants into new SW28 tubes and reserve pellets ("10K pellets").
6. Ultracentrifuge supernatants for 90 min at 100,000 × *g*, 4°C, using SW28 rotor.
7. Discard new supernatants and reserve any pellets that have formed ("100K pellets").
8. Resuspend 10K or 100K pellets in 1.4 ml OptiPrep buffer each. Carefully transfer each resuspended pellet into an SW55Ti open-top polypropylene ultracentrifugation tube.

9. Add 1.4 ml OptiPrep Density Gradient Medium (60% stock solution) to both 10K and 100K resuspended pellets and mix carefully by pipetting up and down (30% final concentration).

10. Carefully add 1.2 ml of 20% OptiPrep solution on top of 30% solution, without disturbing the bottom layer.

    It is recommended to prepare an intermediate solution of OptiPrep (40%) for generating the 20% and 10% OptiPrep solutions.

    Add the different OptiPrep solutions slowly down the wall of the tube. Drop-by-drop addition could cause disruption of the continuous gradient layers.

11. Carefully add 1.1 ml of 10% OptiPrep solution on top of 20% solution, again without disturbing the bottom layer.

12. Ultracentrifuge 60 min at 350,000 × *g*, 4°C, using SW55Ti rotor.

    During placement in the rotor, the tubes should not be shaken.

13. Carefully remove tubes from the rotor. Collect each fraction starting from top of the tube.

    Ten fractions (455 µl/fraction) will be formed.

    To calculate the density of each fraction, proceed directly to step 18; otherwise, move to the next step.

14. To remove any trace of OptiPrep, transfer each fraction into a new SW55Ti tube and wash by adding 3.5 ml filtered 1× D-PBS and mixing well by pipetting up and down.

15. Ultracentrifuge 90 min at 100,000 × *g*, 4°C, using SW55Ti rotor.

16. Remove supernatants by turning each tube upside down and let pellets dry for a few minutes.

17. Resuspend pellet derived from each fraction in a small volume (50 to 100 µl) of an appropriate buffer (e.g., D-PBS or serum-free medium) to allow maximal vesicle retrieval and transfer solution into a low-binding collection tube.

Density assessment

18. Prepare a standard curve of OptiPrep Density Gradient Medium diluted in OptiPrep buffer to different concentrations: 50%, 40%, 30%, 20%, and 10% (see Internet Resources).

    The density of exosomes (high-density vesicles) ranges between 1.18 and 1.19 g/ml, whereas the density of larger (low-density) vesicles ranges between 1.09 and 1.10 g/ml. The protocol described for density assessment can be used for analyzing EVs derived from any cell type. In the case of MSC-derived EVs, low-density vesicles recovered after either 10K or 100K centrifugation float mostly in fraction 2 (F2) and F3 (F2+F3), and high-density vesicles recovered after either 10K or 100K centrifugation float in F5, F6, and F7 (F5+F6+F7). The following steps have been formulated considering these fractions.

19. Before starting the density assessment, initialize refractometer with 220 µl distilled water.

    The refractive index (RI) of the distilled water should be 1.333.

20. Measure RI values of the appropriate fractionated gradients from step 13 or 17, selected according to the annotation to step 18.

After each measurement, the refractometer should be carefully cleaned with distilled water and lens-cleaning papers.

21. Measure RI values of the standards prepared in step 18.

22. Create a linear calibration curve plotting RI of each standard versus OptiPrep concentration to infer the corresponding densities. Fit a line to data and use resulting equation to convert the readings of the fractions obtained in step 20 into concentrations.

FLOW CYTOMETRY SETUP, ACQUISITION, AND ANALYSIS

BASIC PROTOCOL 2

In recent years, the progress attained in the field of EV research has drastically changed methodological approaches based on multiparameter FCM. Despite being one of the most promising techniques for EV characterization, its successful use implies accurate setup of the instrument (Welsh et al., 2017).

Several technical precautions have to be considered to standardize the protocol, limit nonspecific background, and avoid possible artifacts. Setting the trigger parameter on fluorescent signals and optimizing the sheath-fluid pressure and the sample injection pressure are just some of the precautions that must be considered before starting EV analysis. As a whole, these technical expedients are useful when analyzing events falling in areas close to the sensitivity limit of the instrument and are normally referred to as "non-conventional FCM", "high-resolution FCM", or "next-generation FCM" (Arraud, Gounou, Turpin, & Brisson, 2016).

Given increasing interest in discriminating different-sized EVs, the appropriate setup of "last-generation" flow cytometers, together with the use of a mixture of fluorescent beads of varying diameters, is critical for correct analysis (Van der Pol et al., 2014).

Here, we describe a useful protocol for characterization of MSC-derived EV subtypes, taking advantage of a non-conventional FCM modality and the latest published technical indications (Poncelet et al., 2015). Compared to our previously published article (Lo Sicco et al., 2018), here, we propose an updated and advanced method to accurately identify and characterize vesicles with diameters <1 μm.

Materials

FACS Flow Sheath Solution (BD Biosciences)
FACS Clean Solution (BD Biosciences)
Sterile distilled water
70% (v/v) ethanol
FACS Rinse Solution (BD Biosciences)
EV suspension buffer (PBS/EDTA): filtered 1× D-PBS (see below) with 2 mM EDTA
Cytometer Setup and Tracking (CS&T) beads (BD Biosciences)
Filtered (with 0.22-μm filter) 1× D-PBS, without calcium and magnesium
Mixture of fluorescent beads of varying diameters [e.g., Megamix-Plus FSC and Megamix-Plus SSC (BioCytex)]
Selected EV fraction suspensions (see Basic Protocol 1, steps 18 and 20)
CFSE: Vybrant CFDA SE Cell Tracer Kit (Invitrogen, V12883)
Fluorochrome-conjugated antibodies and isotype-control antibodies:
    PE-Cy^{TM}7 Mouse Anti-Human CD63 (BD Biosciences, 561982)
    PE Mouse Anti-Human CD9 (BD Biosciences, 555372)
    BV421 Mouse Anti-Human CD81 (BD Biosciences, 740079)
    BV421 Mouse Anti-Human CD3 Clone UCHT1 (BD Biosciences, 562426)

PE-Cy™7 Mouse IgG1 κ Isotype Control (BD Biosciences, 557872)
PE Mouse IgG1, Clone 40 Isotype Control (BD Biosciences, 345816)

BD FACSAria II equipped with three lasers (405, 488, and 640 nm), nine fluorescence channels (respectively 2-5-2), Automated Cell Deposition Unit, closed-loop nozzle, 130-µm nozzle tip, and workstation or equivalent digital flow cytometer of same brand
FACSDiva software, v8.0
Sterile disposable 5-ml FACS tubes
TruCount tubes (BD Biosciences)

Flow cytometer preparation

1. Twenty-four hours before acquisition, check fluidic levels of the BD FACSAria II instrument and replenish fluids (FACS Flow Sheath solution, FACS Clean Solution, sterile distilled water, and 70% ethanol) and/or empty waste, if needed. Thirty minutes before acquisition, start up workstation and FACSDiva software and switch on instrument for laser warmup.

2. Connect fluid line to the sheath tank, purge air from all fluid filters to avoid air bubbles, and run a fluidic startup with closed-loop nozzle inserted.

   The presence of air bubbles could induce acquisition of artifacts.

   If using a BD FACSAria, the closed-loop nozzle must be used only for washing steps.

3. Ensure that sheath fluid is sterile and that 0.22-µm filter associated with the sheath fluid is intact and perfectly functioning.

4. Clean flow chamber as follows: at least three times with FACS Clean Solution, three times with FACS Rinse Solution, and five times with sterile distilled water. After starting up the fluidics, test for both instrument cleanliness and absence of bubbles by sequentially acquiring sterile distilled water and EV suspension buffer (PBS/EDTA) in sterile disposable 5-ml FACS tubes.

   All cleaning solutions should be freshly prepared and filtered with 0.22-µm filters.

   During acquisition of the distilled water as well as EV suspension buffer, the optical limit of the instrument must be visible in the bottom left part of the dot plot (FSC-H vs. SSC-H). All acquisitions have to be performed using sterile FACS tubes.

5. After removal of the closed-loop nozzle, use a 130-µm nozzle tip to minimize sheath flow pressure in the flow cell chamber and to reduce speed of particles interacting with the laser beam.

   The sample flow rate has to be as slow as possible. For this reason, the dilution of the EV suspension needs to be accurately optimized to avoid the "swarming effect" (see Critical Parameters and Troubleshooting) or loss of signal.

   If using a BD FACSAria II, the 130-µm nozzle corresponds to 10 psi of sheath flow pressure (default value). The lowest sample flow rate is 10 µl/min. To avoid formation of bubbles, the sheath tank should be filled the day before the experiment, and fluidic startup must be the first operative configuration performed.

6. Test flow cytometer's performance according to the manufacturer's instructions using CS&T beads (one drop of beads in 350 µl filtered 1× D-PBS) with flow cytometer in "CST mode".

   CS&T beads allow testing of optical and electronic efficiency (relative fluorescence detection efficiency, or Qr) and measurement of relative background noise (Br). All parameters are statistically paired (robust standard deviation, or rSD) with a multiparameter baseline (three drops of same bead suspension in 0.5 ml D-PBS) recorded for a

longer time. Using CS&T beads, we have attained repeatability and standardization of all experiments, allowing us to set the optimal voltage gain for each considered fluorescence channel.

7. Repeat step 5 and re-test cleanliness of the flow chamber by acquiring sterile distilled water.

   After CS&T testing (step 6), cleaning of the flow chamber is a very important step to ensure elimination of residual fluorescent beads, which could create artifacts. In general, the cleanliness of the instrument should be frequently checked.

Adjustment of instrument settings

8. Select and check fluorescence channels (i.e., FITC for CFSE, PE-Cy7 for blue laser at 488 nm, APC for red laser at 633 nm, and BV-421 for violet laser at 405 nm).

   It is recommended to select fluorochromes that emit at a greater distance to reduce spillover phenomena in adjacent fluorescence channels. The quantum efficiency and brightness of fluorochromes must be always inversely related to the density of surface-antigen markers according to the basic rules of multiparameter cytometry.

9. Scatter on SSC, which is preferential to FSC.

   Due to Rayleigh scattering (Shapiro, 2005), smaller particles have a size similar to the wavelength of the blue laser (488 nm), which defines physical characteristics.

10. Because the fluorescent intensity of small particles is very low, use electronic "Height" (-H) parameter rather than the "Area" (-A) parameter to allow optimal signal detection.

11. Draw a starting dot plot (FITC-H vs. SSC-H).

    It is recommended to select fluorescent beads and fluorescent dye (used to detect intact EVs) detected in the same fluorescence channel (e.g., CFSE and FITC-conjugated Megamix-Plus beads).

    All dot plots must be visualized in logarithmic mode and with bi-exponential values.

12. Select threshold on the fluorescence channel instead of physical scatter.

    This is strongly recommended. The threshold on the fluorescence channel is not widely used, but it allows one to avoid background noise in the analysis and, consequently, to set a more targeted dimensional gate (Kormelink et al., 2016).

    The clusters corresponding to the different-sized beads (100, 160, 200, 240, 300, 500, and 900 nm) have to be visualized over the threshold triggering. In this way, it is possible to draw a correct "dimensional gate", excluding both background signal (smaller than the 100-nm cloud) and particles >900 nm.

    It is also recommended to avoid use of serum-containing media, such as FACS buffer supplemented with serum, in order to analyze only the vesicles of interest, and not vesicles potentially contained in serum.

13. Prepare a mixture of fluorescent beads of varying diameters in EV suspension buffer following the beads' manufacturer's instructions. Load FACS tube and adjust FL1 gain voltage until visualization of the small cloud corresponding to 900-nm beads in the upper right part of the dot plot.

    For the beads, we use both types of Megamix-Plus beads (FSC and SSC) mixed together

14. Draw a histogram reporting SSC-H channel to clearly visualize the peaks generated by the fluorescent beads.

    This will allow delineation of the gate(s) of interest in the desired size range (Fig. 2).

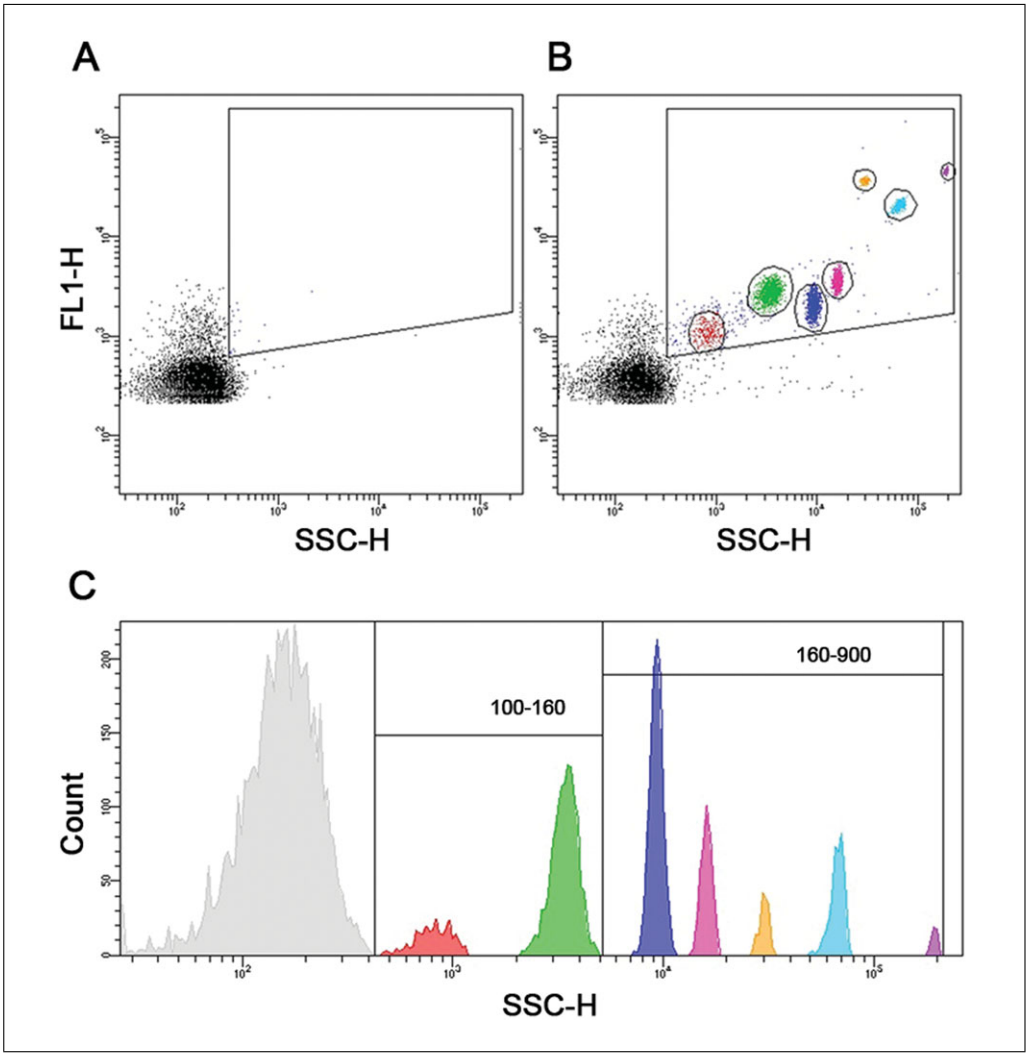

Figure 2 Representative bidimensional dot plots (FL1-H vs. SSC-H, in logarithmic scale) representing (**A**) the extracellular-vesicle suspension buffer (PBS/EDTA; blank control), useful to delineate a dimensional gate excluding background (black) and (**B**) the fluorescent suspension and relative sub-gating in the dimensional gate (red: 100 nm, green: 160 nm, blue: 200 nm, pink: 240 nm, light orange: 300 nm, cyan: 500 nm, and purple: 900 nm). (**C**) Visualization as SSC-H histogram peaks of the various dimensions of Megamix beads (gray: background).

Sample preparation and acquisition

15. Transfer selected EV fraction suspensions into FACS tubes.

16. Prepare a 10 mM CFSE stock solution following manufacturer's instructions. To reach the appropriate final concentration (1 μM) in steps 17 to 19, prepare an intermediate, 100 μM CFSE solution (1:100) by diluting stock solution in EV suspension buffer.

    In order to avoid formation of aggregates, centrifuge the intermediate CFSE solution for 30 sec at 10,000 rpm.

17. Load a control tube containing a selected EV fraction suspension (see step 15) stained with CFSE (e.g., 1 μl intermediate solution in 100 μl; 1 μM final CFSE concentration) at 4°C (Fig. 3A).

    When performing this step, it is recommended to set the sample injection chamber to 4°C for ≥30 min before acquisition. The tube has to be considered as the correct control to verify CFSE specificity. Indeed, only at room temperature is CFSE able to passively

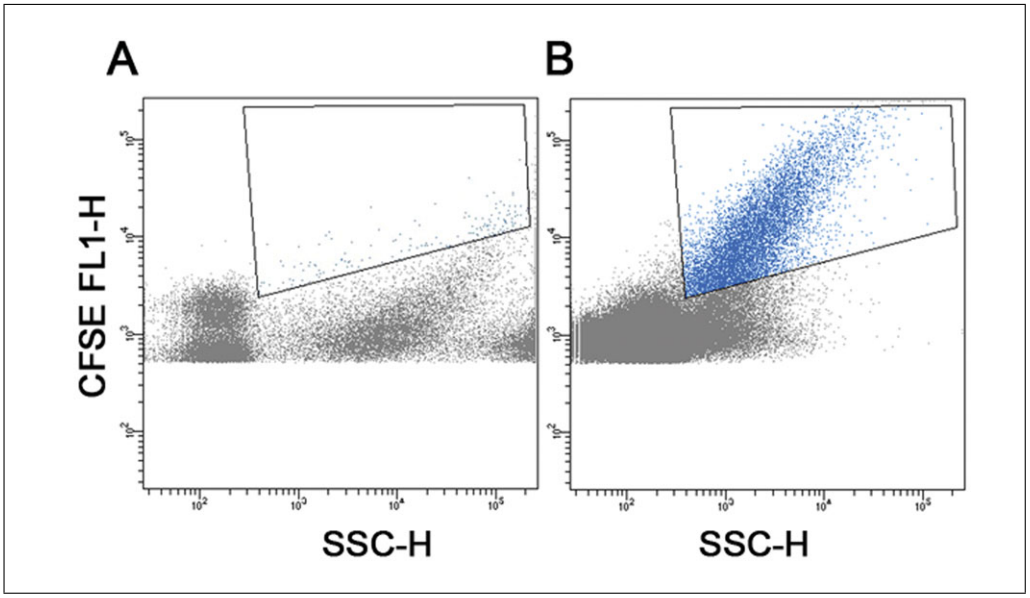

Figure 3 Control for CFSE specificity. (**A**) Dot plot for vesicles stained with CFSE at 4°C. (**B**) Dot plot for vesicles stained with CFSE at room temperature (25°C).

diffuse within vesicles; inside each vesicle, the acetate groups of CFSE are cleaved by intra-vesicular esterases, and the molecules are converted to fluorescent esters. At 4°C, the resulting cloud of particles must be under the level (in the FL1 intensity channel) of the dimensional gate.

18. Load a tube containing a selected EV fraction suspension (see step 15) stained with CFSE as in step 17 but at room temperature to set correct dimensional gate (Fig. 3B).

19. After setting the correct dimensional gate, obtain an accurate visualization of EVs by labeling the samples from step 15 with CFSE (see steps 17 and 18) together with specific fluorochrome-conjugated antibodies for 15 min at room temperature. Acquire all stained samples, recording ~50,000 events.

    Before any analysis involving use of antibodies, run an experiment with the corresponding isotype-control antibodies (together with the considered fluorescent dye, e.g., CFSE). Draw a histogram for each fluorescence channel and verify the absence of spillover, autofluorescence, and nonspecificity.

    The accurate titration of antibodies and the use of related isotype controls are critical steps for successful implementation of the FCM procedure. Each antibody and its corresponding isotype control must be used at the same concentration (w/v). An optimal antibody concentration allows acquisition of events outside the gate of the background, avoiding over-saturation (Fig. 4).

20. Check and remove fluorescent spillover by compensation, acquiring a single-color tube for each channel, creating a compensation matrix using program application tools, and later applying the matrix to each sample tube.

    To use several fluorochrome-associated antibodies at the same time, generate a "Compensation Setup" matrix, mixing one drop of compensation particles binding any light chain–bearing immunoglobulin (specific for the primary antibody used) and one drop of negative-control particles that have no binding capacity together with the fluorochrome-conjugated antibodies. The use of compensation particles [e.g., CompBeads (BD Biosciences)] will clearly provide distinct positive and negative (background fluorescence) populations that can be used to set compensation levels manually or automatically using instrument setup software.

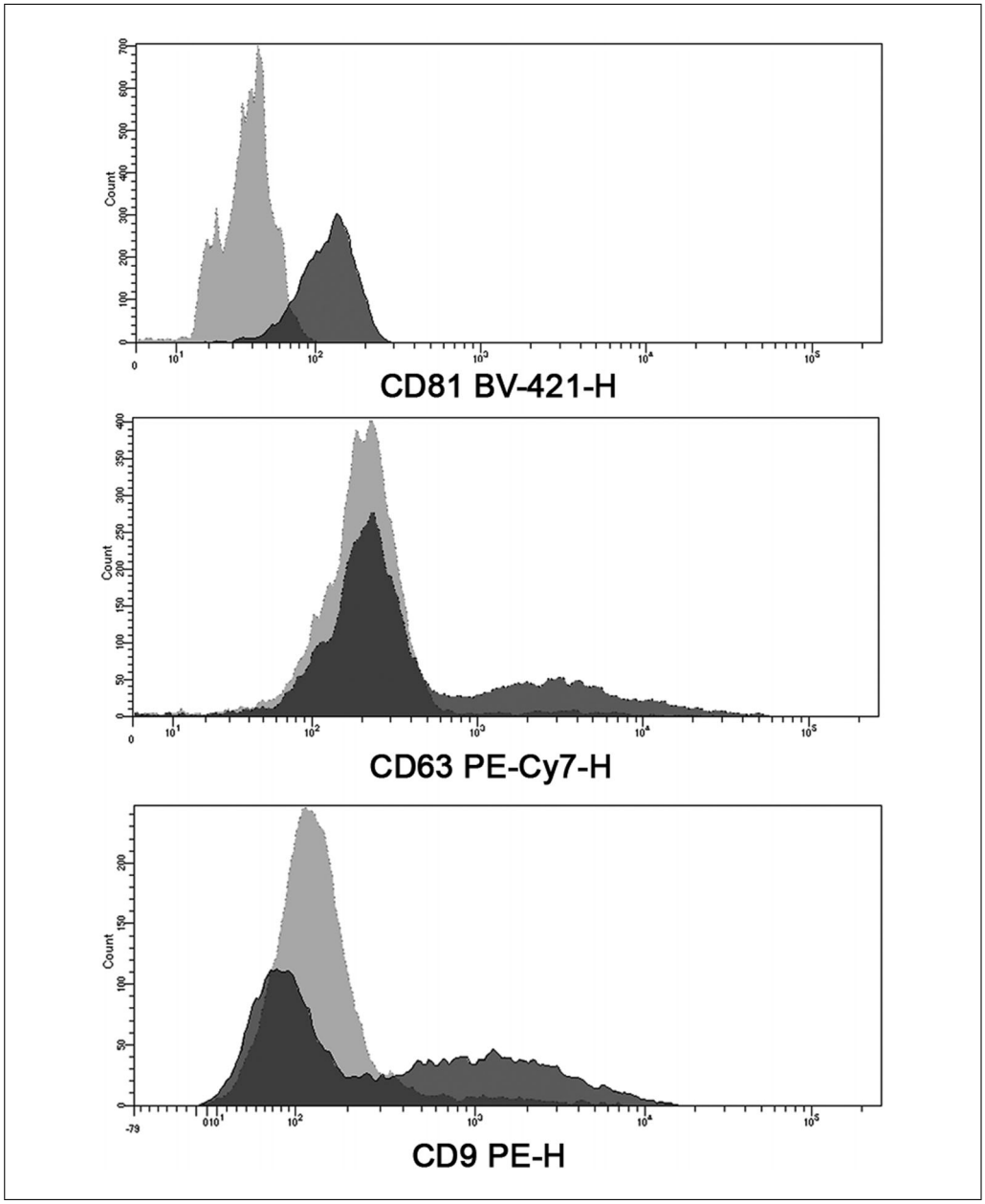

Figure 4 Flow cytometry analysis of mesenchymal stromal cell–derived extracellular vesicles. The presented data are from one representative experiment analyzing the vesicles present in a 100K pellet. The areas under the black lines identify cells reacting with CD81 (upper panel), CD63 (middle panel), and CD9 (bottom panel). The areas under the gray lines indicate the interactions of cells with corresponding nonreactive immunoglobulin of the same isotype.

21. Obtain an absolute count of labeled EVs contained in each tube using TruCount tubes (Fig. 5): Dissolve lyophilized pellet of beads (with a known concentration) contained in each TruCount tube in a known volume of labeled EVs. By FCM analysis, determine absolute number of EVs/μl by comparing vesicular events to bead events (as a reference number, it is recommended to record 10,000 events included in the gate of the beads) and dividing the number of positive EV events by the number of bead events and multiplying by the TruCount bead concentration.

    As previously described (Lo Sicco et al., 2018), TruCount tubes are commercially available tubes containing a known number of beads that are usually used in FCM strategies for determining absolute counts of leukocytes in blood. TruCount beads perfectly match a 4-μm-dimension gate, and use of TruCount tubes has been adopted to obtain absolute

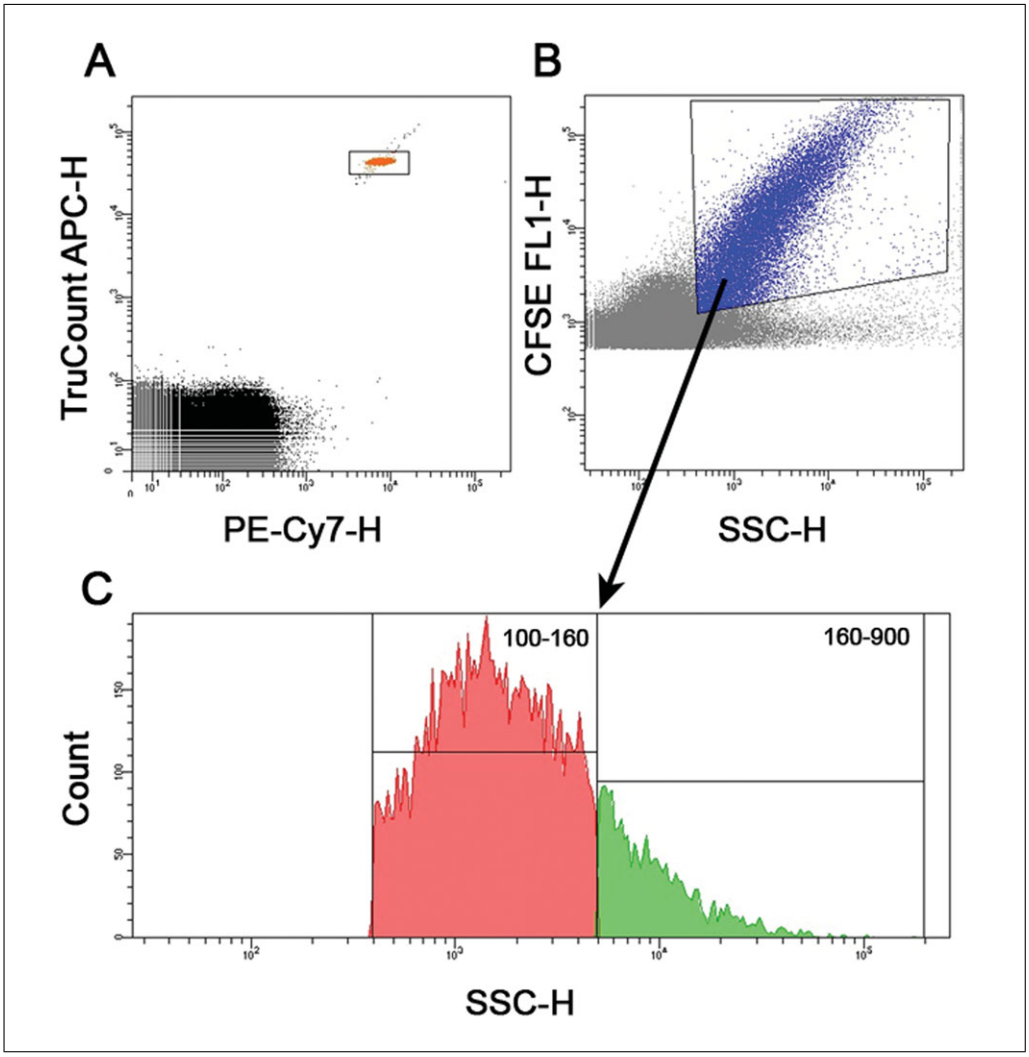

Figure 5 (**A**) A known number of TruCount beads (orange) is gated to obtain an absolute count of other subpopulations. (**B**) After exclusion of TruCount beads (gray), extracellular vesicles can be counted in a dimensional gate (blue) in FL1-H vs. SSC-H. (**C**) Using the reference of a mixture of fluorescent beads of varying diameters, we can visualize extracellular-vesicle sub-gates within CFSE-positive events (red: from 100 nm up to 160 nm; green: from 160 nm up to 900 nm) in an SSC-H histogram.

quantification of EVs. TruCount and sample preparation must be very accurate, with mixing by repeated pipetting to avoid clump formation and volume loss.

22. At the end of each experiment, sequentially load tubes containing FACS Clean Solution, FACS Rinse Solution, or sterile distilled water for ≥3 min/tube. Then, run fluidics shutdown and sterilize all fluidic parts of flow cytometer with 70% ethanol so that the equipment will be ready for the next run.

REAGENTS AND SOLUTIONS

OptiPrep buffer

0.25 M sucrose
1 mM EDTA
10 mM Tris, pH 8.0
Adjust pH to 7.4
Store ≤1 month at 4°C

COMMENTARY

Background Information

For many years, MSCs have been considered a remarkable cell source for regenerative-medicine applications. More recently, a paradigm shift has emerged, suggesting that these cells' beneficial effects are often due to the cells' paracrine activity (Caplan, 2009). Given that MSCs have a regulatory phenotype and respond actively to environmental signals, their secretory activity can be deeply modulated (da Silva Meirelles, Fontes, Covas, & Caplan, 2009; Ulivi, Tasso, Cancedda, & Descalzi, 2014). In this context, EVs are recognized as important components of the MSC secretome, and a growing body of literature has examined the regenerative potential of MSC-derived EVs using different approaches (Konala et al., 2016).

The term "extracellular vesicle" defines a heterogeneous population of exosomes, microvesicles, and apoptotic bodies. During traditional EV isolation, discarding the pellet after 10K centrifugation or filtering the supernatant with a 0.22-μm filter could in part exclude larger vesicles, such as shedding microvesicles, from further analysis. However, recent papers have highlighted the importance of considering different subtypes, which may have different functional properties (Kowal et al., 2016; Lässer et al., 2018; Willms, Cabañas, Mäger, Wood, & Vader, 2018). For this reason, it is becoming increasingly important to develop and optimize useful protocols to isolate the different subpopulations, avoiding the possibility of losing subtypes.

Several methods have been adopted to count and characterize EVs (e.g., nanoparticle tracking analysis, electron microscopy, resistive pulse sensing), but there is still considerable confusion about the definition of EV phenotype and the standardization of protocols for analysis (Erdbrügger & Lannigan, 2016). All the methodologies present difficulties and limitations, ranging from low sensitivity to very high cost to poor statistical validation. Last-generation FCM could become a methodology of choice, characterized by crucial advantages: relatively low cost, multiparameter phenotyping, and good statistical robustness of the data due to a large number of events being analyzed at the same time.

Critical Parameters and Troubleshooting

Some critical issues may affect different aspects of the protocols presented in this unit. One of these is the starting amount of vesicles (Basic Protocol 1) necessary to perform downstream analysis (Basic Protocol 2). Indeed, we have observed that primary cultures release fewer vesicles than cell lines do. Given that excessive expansion of primary cultures could lead to cellular senescence and permanent phenotypic and functional changes, it is not recommended to increase the cells' passage number in order to obtain more secreting cells. A possible approach to augment the amount of secreted EVs is to prolong the serum-free conditioning timeframe. However, we strongly recommend checking both cell viability and early/late apoptotic markers when optimizing this timeframe.

Another crucial aspect that should be taken into account is the selection of fractions based on density gradient separation (Basic Protocol 1). It is highly recommended to use "wettable" ultracentrifuge tubes when preparing OptiPrep density gradients. The use of non-wettable tubes could in fact cause disruption of the density layers (Wallace, 1969). As mentioned in Basic Protocol 1, we perform the experimental procedure with polypropylene tubes instead of the widely used polyallomer tubes.

Moreover, sample preparation for FCM (Basic Protocol 2) must be systematic: the choice and purity of buffers, the concentrations of particles, the fluorescent dyes used to discriminate intact vesicles, and the titration of the antibodies as well as the isotype controls have to be considered with great care. The final concentration of EVs is in fact a crucial factor in avoiding the "swarming effect": when the concentration of nano-sized particles is too high, the cytometer is no longer able to discriminate single events, thus generating artifacts. The opposite can also happen: when the particles are too diluted or are stained with an improper concentration of antibody, they can remain "embedded" in the background signal.

In Basic Protocol 2, it is also very important to check the injection pressure of the sample in the chamber (sample flow rate) and the pressure of the transport liquid (sheath flow pressure), which creates the laminar flow. Both pressures must be as low as possible in order to slow down the flow of the vesicles.

A troubleshooting guide is presented in Table 1.

Table 1 Troubleshooting Guide for Isolation and Flow Cytometry Characterization of Extracellular-Vesicle Subpopulations Derived From Human Mesenchymal Stromal Cells

Problem	Possible cause	Solution
No vesicles in the selected fractions	Wrong fractions were selected	Check the refractometer values and repeat the measurement.
	Vesicle amount is not enough for density gradient centrifugation	Increase the cell number or the serum-free conditioning timeframe.
	Wrong ultracentrifuge tubes were selected	Ensure that the tubes are polypropylene (wettable).
High background during flow cytometry	PBS/EDTA solution is contaminated	Filter the solution with a 0.22-µm filter.
	Vesicle amount is too high	Optimize the vesicle concentration prior to analysis by flow cytometry.
	Antibody concentration is too high	Perform antibody titration to determine the suitable concentration for your samples.

Anticipated Results

This unit has highlighted the critical and key points in the basic protocols. If the protocols are followed as indicated, optimal results are warranted. These protocols can be adapted to isolate and characterize EV subpopulations from cell types other than MSCs.

Time Considerations

The time necessary for preparation of cells and conditioned medium can vary depending on cell type and serum-free conditioning timeframe, as indicated in the Critical Parameters section. As stated in step 1 of Basic Protocol 1, we have optimized the serum-free conditioning timeframe for MSCs to be 96 hr. The time spent on EV isolation is ∼8 hr, and density measurement requires ∼2 hr, including calculations (from RI to density; Basic Protocol 1). Flow cytometer preparation takes ∼2 hr, and FCM characterization of isolated vesicles takes ∼3 hr, with variation based on the number of antibodies to be tested (Basic Protocol 2).

Acknowledgments

This project has received funding from the European Union's Horizon 2020 research and innovation program under Marie Sklodowska-Curie grant agreement no. 721432 (to C. G.) and from the Italian Ministry of Health via "Young Investigator Grant"-GR-2013-02357519 (to R. T.).

Literature Cited

Arraud, N., Gounou, C., Turpin, D., & Brisson, A. R. (2016). Fluorescence triggering: A general strategy for enumerating and phenotyping extracellular vesicles by flow cytometry. *Cytometry Part A*, *89*(2), 184–195. doi: 10.1002/cyto.a.22669.

Caplan, A. I. (2009). Why are MSCs therapeutic? New data: new insight. *The Journal of Pathology*, *217*(2), 318–324. doi: 10.1002/path.2469.

Caplan, A. I., & Dennis, J. E. (2006). Mesenchymal stem cells as trophic mediators. *Journal of Cellular Biochemistry*, *98*(5), 1076–1084. doi: 10.1002/jcb.20886.

da Silva Meirelles, L., Fontes, A. M., Covas, D. T., & Caplan, A. I. (2009). Mechanisms involved in the therapeutic properties of mesenchymal stem cells. *Cytokine & Growth Factor Reviews*, *20*(5–6), 419–427. doi: 10.1016/j.cytogfr.2009.10.002.

Erdbrügger, U., & Lannigan, J. (2016). Analytical challenges of extracellular vesicle detection: a comparison of different techniques. *Cytometry Part A*, *89*(2), 123–134. doi: 10.1002/cyto.a.22795.

Konala, V. B., Mamidi, M. K., Bhonde, R., Das, A. K., Pochampally, R., & Pal, R. (2016). The current landscape of the mesenchymal stromal cell secretome: a new paradigm for cell-free regeneration. *Cytotherapy*, *18*(1), 13–24. doi:10.1016/j.jcyt.2015.10.008.

Kormelink, T. G., Arkesteijn, G. J., Nauwelaers, F. A., van den Engh, G., Nolte-'t Hoen, E. N., & Wauben, M. H. (2016). Prerequisites for the analysis and sorting of extracellular vesicle subpopulations by high-resolution flow cytometry. *Cytometry Part A*, *89*(2), 135–147. doi: 10.1002/cyto.a.22644.

Kowal, J., Arras, G., Colombo, M., Jouve, M., Morath, J. P., Primdal-Bengtson, B., … Théry, C. (2016). Proteomic comparison defines novel markers to characterize heterogeneous populations of extracellular vesicle subtypes. *Proceedings of the National Academy of Sciences*, *113*(8), E968–E977. doi: 10.1073/pnas.1521230113.

Lässer, C., Jang, S. C., & Lötvall, J. (2018). Subpopulations of extracellular vesicles and their therapeutic potential. *Molecular Aspects of Medicine*, *60*, 1–14. doi: 10.1016/j.mam.2018.02.002.

Lo Sicco, C., Reverberi, D., Pascucci, L., & Tasso, R. (2018). A method for isolating and characterizing mesenchymal stromal cell-derived extracellular vesicles. *Current Protocols in Stem Cell Biology*, *46*, e55. doi: 10.1002/cpsc.55.

Poncelet, P., Robert, S., Bailly, N., Garnache-Ottou, F., Bouriche, T., Devalet, B., ... Mullier, F. (2015). Tips and tricks for flow cytometry-based analysis and counting of microparticles. *Transfusion and Apheresis Science*, *53*(2), 110–126. doi: 10.1016/j.transci.2015.10.008.

Rani, S., Ryan, A. E., Griffin, M. D., & Ritter, T. (2015). Mesenchymal stem cell-derived extracellular vesicles: Toward cell-free therapeutic applications. *Molecular Therapy*, *23*(5), 812–823. doi: 10.1038/mt.2015.44.

Shapiro, H. M. (2005). *Practical Flow Cytometry*. Hoboken, NJ: John Wiley & Sons.

Sicco, C. L., Reverberi, D., Balbi, C., Ulivi, V., Principi, E., Pascucci, L., ... Franzin, C. (2017). Mesenchymal stem cell-derived extracellular vesicles as mediators of anti-inflammatory effects: Endorsement of macrophage polarization. *Stem Cells Translational Medicine*, *6*(3), 1018–1028. doi: 10.1002/sctm.16-0363.

Tkach, M., Kowal, J., & Théry, C. (2018). Why the need and how to approach the functional diversity of extracellular vesicles. *Philosophical Transactions of the Royal Society B*, *373*(1737), 20160479. doi: 10.1098/rstb.2016.0479.

Ulivi, V., Tasso, R., Cancedda, R., & Descalzi, F. (2014). Mesenchymal stem cell paracrine activity is modulated by platelet lysate: induction of an inflammatory response and secretion of factors maintaining macrophages in a proinflammatory phenotype. *Stem Cells and Development*, *23*(16), 1858–1869. doi: 10.1089/scd.2013.0567.

Van der Pol, E., Coumans, F., Grootemaat, A., Gardiner, C., Sargent, I., Harrison, P., ... Nieuwland, R. (2014). Particle size distribution of exosomes and microvesicles determined by transmission electron microscopy, flow cytometry, nanoparticle tracking analysis, and resistive pulse sensing. *Journal of Thrombosis and Haemostasis*, *12*(7), 1182–1192. doi: 10.1111/jth.12602.

Van der Vlist, E. J., Nolte, E. N., Stoorvogel, W., Arkesteijn, G. J., & Wauben, M. H. (2012). Fluorescent labeling of nano-sized vesicles released by cells and subsequent quantitative and qualitative analysis by high-resolution flow cytometry. *Nature Protocols*, *7*(7), 1311–1326.

Wallace, H. (1969). Preparation of polyallomer centrifuge tubes for density gradients. *Analytical Biochemistry*, *32*(2), 334–339.

Welsh, J. A., Holloway, J. A., Wilkinson, J. S., & Englyst, N. A. (2017). Extracellular vesicle flow cytometry analysis and standardization. *Frontiers in Cell and Developmental Biology*, *5*, 78. doi: 10.3389/fcell.2017.00078.

Willms, E., Cabañas, C., Mäger, I., Wood, M. J. A., & Vader, P. (2018). Extracellular vesicle heterogeneity: subpopulations, isolation techniques, and diverse functions in cancer progression. *Frontiers in Immunology*, *9*, 738. doi: 10.3389/fimmu.2018.00738.

Willms, E., Johansson, H. J., Mäger, I., Lee, Y., Blomberg, K. E. M., Sadik, M., ... Andaloussi, S. E. (2016). Cells release subpopulations of exosomes with distinct molecular and biological properties. *Scientific Reports*, *6*, 22519. doi: 10.1038/srep22519.

Internet Resources

http://www.axis-shield-density-gradient-media.com/S09.pdf

A guide to checking the density of OptiPrep in buffers.

Noninvasive Diagnosis and Molecular Phenotyping of Breast Cancer through Microbead-Assisted Flow Cytometry Detection of Tumor-Derived Extracellular Vesicles

Wenzhe Li, Bin Shao, Changliang Liu, Huayi Wang, Wangshu Zheng, Weiyao Kong, Xiaoran Liu, Guobin Xu, Chen Wang, Huiping Li, Ling Zhu,* and Yanlian Yang**

Blood-based detection and molecular phenotyping are highly desired for the early diagnosis and dynamic monitoring of cancer. Extracellular vesicles (EVs) carry molecular information from the cells of origin and are biomarkers of cancer. However, the detection and molecular analysis of EVs has been challenging due to their nanoscaled size. Here, an assessment of the detection and molecular phenotyping of serum EVs based on microbead-assisted flow cytometry is established. The clinical utility of this method is validated in the diagnosis and human epidermal growth factor receptor 2 (HER2) phenotyping of breast cancer. Good correlation between the status of epithelial cell adhesion molecule (EpCAM) and HER2 expression in EVs and in the cells of origin is found. Both EpCAM+ and HER2+ EVs are demonstrated to be effective diagnostic markers of breast cancer with high sensitivity and specificity. EV-based HER2 phenotyping is consistent with tissue-based HER2 phenotyping by immunohistochemistry and can be used as a surrogate for the invasive tissue assessments. The microbead-assisted flow cytometry assessment of EVs enables rapid and noninvasive detection and molecular phenotyping of cancer and would help to personalized treatment and cancer survival.

1. Introduction

Despite the great progress made in medical imaging and systemic adjuvant therapy, the morbidity and mortality of breast cancer remain high.[1] Establishment of noninvasive blood-based assessments is highly desired for the diagnosis and prognosis of breast cancer. Epithelial cell adhesion molecule (EpCAM) and human epidermal growth factor receptor 2 (HER2) are two important diagnostic markers in breast cancer that participate in the diagnosis and classification of breast cancer into different molecular subtypes that exhibit different treatment responses.[2] Additionally, HER2 is a common therapeutic marker that plays a vital role in guiding therapeutic strategies. Current clinically applied HER2 phenotyping is mainly based on immunohistochemistry (IHC) or fluorescence in situ hybridization (FISH) analyses of tumor tissue obtained from surgery or puncture biopsies.[3] However, the HER2 status may change during tumor progression and cancer treatment due to genetic drift, intratumoral heterogeneity and selective pressure of therapies.[4] Single-needle aspiration biopsy may cause evaluation bias due to intratumoral heterogeneity.[4d,5] These changes and differences are difficult to be captured by current tissue assessments and, therefore, largely affect the efficacy of targeted therapies due to the difficulty in reconducting biopsies, especially for patients who have undergone tumor resection.[6] Blood-based molecular phenotyping, in this regard, enables dynamic and integral monitoring of HER2 expression and will be beneficial for personalized cancer management. Recent studies have reported the acquisition or loss of HER2 in circulating tumor cells (CTCs) from breast cancer patients compared with primary tumor tissue assessments[4a,7]

W. Li, C. Liu, H. Wang, W. Zheng, Prof. C. Wang, Dr. L. Zhu, Prof. Y. Yang
CAS Key Laboratory of Standardization and Measurement for Nanotechnology
CAS Key Laboratory of Biological Effects of Nanomaterials and Nanosafety
CAS Center for Excellence in Nanoscience
National Center for Nanoscience and Technology
Beijing 100190, China
E-mail: zhul@nanoctr.cn; yangyl@nanoctr.cn

The ORCID identification number(s) for the author(s) of this article can be found under https://doi.org/10.1002/smtd.201800122.

DOI: 10.1002/smtd.201800122

W. Li
Academy for Advanced Interdisciplinary Studies
Peking University
Beijing 100871, China

Dr. B. Shao, Dr. W. Kong, Dr. X. Liu, Prof. H. Li
Key Laboratory of Carcinogenesis and Translational Research (Ministry of Education/Beijing)
Department of Breast Oncology
Peking University Cancer Hospital & Institute
Beijing 100142, China
E-mail: lihuiping@bjcancer.org, huipingli2012@hotmail.com

Prof. G. Xu
Clinical Laboratory
Peking University Cancer Hospital & Institute
Beijing 100142, China

and indicated that the interconversion between HER2+ and HER2− CTC subpopulations may be responsible for disease progression and drug resistance.[7] These studies demonstrated the importance of blood-based dynamic HER2 phenotyping in the personalized treatment of breast cancer. However, the clinical application of HER2 phenotyping in CTCs is limited due to the small number of CTCs in the blood and difficulties in isolating CTCs from the complicated blood samples.[8]

EVs are endosomal-derived membrane vesicles (30–150 nm in diameter) widely present in body fluids. Unlike CTCs that are rare (usually one to several/ml blood) in the blood, EVs are abundant (>10^8 vesicles mL^{-1} serum), making them a desirable specimen type for clinical assessment.[9] EVs are secreted by various cell types, including tumor cells, and carry membrane proteins, cytosol proteins, and nucleic acids from their cells of origin.[10] Therefore, they can be used for the detection and molecular characterization of diseases, including cancer. It was reported that EpCAM and HER2 are present in EVs from breast cancer cell lines and in body fluids from breast cancer patients.[11] The HER2 status in tumor-derived EVs could reflect that in the source breast cancer cells,[12] suggesting the practicability of EVs as tissue surrogates to investigate the HER2 status. Nevertheless, EV-based HER2 phenotyping of breast cancer is rare. Sina et al. observed increased HER2+ EVs from sera in HER2+ patients compared with HER2− patients and healthy controls by surface plasmon resonance (SPR).[13] However, no threshold was established in this study. The specificity and sensitivity of this assessment were not evaluated. Other reliable EV-based HER2 phenotyping methods still need to be developed.

The detection and molecular analysis of EVs have been challenging due to the nanoscaled size of EVs and difficulties in their purification from complicated samples such as serum or plasma. Strategies have been taken to enrich and detect EVs. These include micro- or nanopillar arrays for the separation of EVs,[14] magnetic bead-assisted microfluidic chip for the on-chip analysis of RNA and proteins in EVs,[9b,15] and label-free detection of EVs with SPR sensors.[16] Microbead-assisted flow cytometry is an important technique. EVs alone can rarely be analyzed by flow cytometry because their nanoscaled size exceeds the detection limit of flow cytometry. This is overcome by adhering EVs onto antibody-coated microsized magnetic/latex beads[17] or microsized latex beads directly,[18] followed by staining the captured EVs with fluorescent-labeled antibodies that target the membrane proteins in EVs to yield detectable signals for the subsequent flow cytometry analysis. This method was successfully applied to clinical assessments to diagnose pancreatic cancer using glypican-1 positive EVs.[18] These valuable studies have laid the solid foundation to apply this microbead-assisted flow cytometry in EV detection. The molecular phenotyping of various cancers based on this technique should be feasible if the correlations between the expression of molecular markers in EVs and disease progression or prognosis are built up in clinical samples.

Here, we establish an assessment for the detection and molecular phenotyping of cancer serum EVs using microbead-assisted flow cytometry and evaluate the validity of this assessment in the diagnosis and HER2 phenotyping of breast cancer. We find that the expression statuses of EpCAM and HER2 in EVs well represent those in the cancer cells of origin. Both EpCAM+ and HER2+ EVs are effective biomarkers to detect breast cancer with high sensitivity and specificity. HER2+ EVs can well distinguish HER2+ patients from HER2− patients and healthy individuals. This EV-based HER2 phenotyping is consistent with HER2 phenotyping in the tumor tissues evaluated by IHC, suggesting that this EV-based HER2 phenotyping method can be used as a surrogate for traditional invasive tissue assessments. These results show the significant efficacy of microbead-assisted flow cytometry in analyzing tumor-derived EVs. This rapid and noninvasive assessment holds great potential in the diagnosis and molecular phenotyping of cancer and would be beneficial to personalized treatment and, eventually, cancer survival.

2. Results

2.1. Microbead-Assisted Flow Cytometry for Tumor-Derived EV Detection and Molecular Phenotyping

We first chose different human breast cancer cell lines to establish a method for the detection and HER2 phenotyping of breast cancer EVs: MDA-MB-468 (basal epithelial), MCF-7 (luminal A), and SK-BR-3 (HER2 overexpression, HER2-OE). The expression level of EpCAM and HER2 in the cell lines was investigated using flow cytometry analysis. As expected, all three breast cancer cell lines exhibited high expression levels of EpCAM compared with the nontumor mammary epithelial cell line MCF-10A (**Figure 1**a; Figure S1 upper lane, Supporting Information), in accordance with the previous findings showing that EpCAM was overexpressed in most human epithelial carcinomas, including breast cancer.[19] The basal epithelial cell line MDA-MB-468 showed higher expression levels of EpCAM than the other two breast cancer cell lines (Figure 1a; Figure S1 upper lane, Supporting Information). This was also as expected because EpCAM was shown to be an indicator of

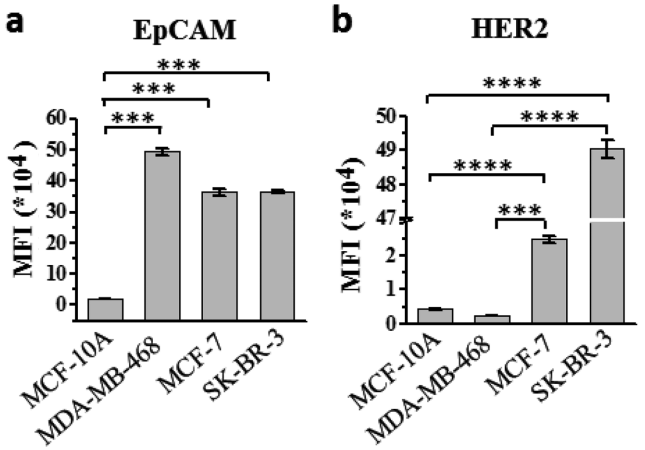

Figure 1. Expression of EpCAM and HER2 in different breast cancer cell lines. Expression levels of a) EpCAM and b) HER2 in the mammary epithelial cell line MCF-10A and the three breast cancer cell lines MDA-MB-468, MCF-7, and SK-BR-3, calculated from the mean fluorescence intensities in flow cytometry analysis. The data are presented as the means ± S.D. ($n = 3$). ***$p < 0.001$, ****$p < 0.0001$ (Student's t-test).

tumor malignancy and to be associated with the poor prognosis of breast cancer,[20] and the basal-like subtype displayed a poorer prognosis than the other subtypes of breast cancer.[21] The expression level of HER2 was the highest in the HER2-OE cell line SK-BR-3, moderate in the luminal A cell line MCF-7, and lowest in the basal epithelial cell line MDA-MB-468 and nontumor mammary epithelial cell line MCF-10A (Figure 1b; Figure S1 lower lane, Supporting Information), suggesting that the three breast cancer cell lines had different expression levels of HER2 and can be used as a model system for evaluating the HER2 phenotyping of breast cancer-derived EVs.

After evaluating the expression of EpCAM and HER2 in the cell lines, we investigated the expression of these two proteins in cell-derived EVs. EVs were isolated from each cell line by differential centrifugation modified from a previously described method.[18] Transmission electron microscopy (TEM), nanoparticle tracking analysis (NTA), and dynamic light scattering (DLS) were performed to examine the structure and size of the purified EVs. The electron microscopy images revealed that the purified EVs exhibited a saucer-like morphology of EVs, as previously described (**Figure 2**a; Figure S2a, Supporting Information).[10a,22] Size distribution analysis by NTA and DLS showed an average diameter of 100–150 nm (Figure 2b; Figure S2b, Supporting Information), similar to the previously reported size of EVs.[23] The expression of EpCAM and HER2 in EVs was analyzed by flow cytometry and western blotting. To further evaluate the purity of the sample and estimate the influence of protein contamination on the expression level of proteins as assessed by flow cytometry and western blotting, we calculated the particle/protein ratio of the isolated EV sample as previously described.[24] Particle counting was performed by NTA (Figure S3, Supporting Information), and the protein

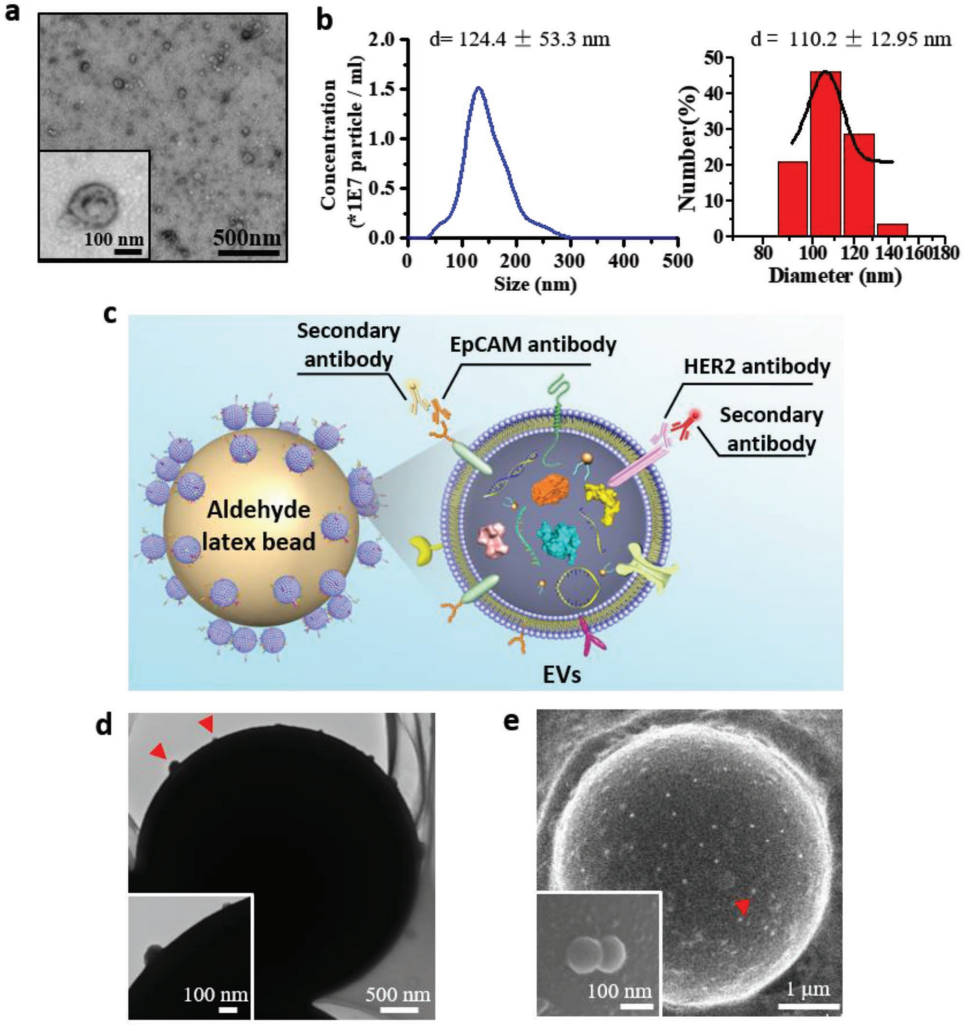

Figure 2. Aldehyde microbead enrichment and flow cytometry analysis of EVs. a) Transmission electron microscopy (TEM) images of EVs released from SK-BR-3 cells. b) Size distribution of EVs released from SK-BR-3 cells analyzed by nanoparticle tracking analysis (NTA) (left) and dynamic light scattering (DLS) (right). c) Schematic illustration of flow cytometry analysis of EVs utilizing aldehyde microbead enrichment. To enrich EVs, 4 µm aldehyde/sulfate latex beads were used. The captured EVs were stained with the antibodies specific to the membrane proteins on the EVs for flow cytometry analysis. d) TEM images of the capture of EVs derived from SK-BR-3 cells on the aldehyde latex bead. Inset: zoom in TEM image of the EVs bound to the aldehyde latex bead as indicated with the red arrowheads. e) Scanning electron microscopy (SEM) images of the capture of EVs derived from SK-BR-3 cells on the aldehyde latex bead. Inset: zoom in SEM image of the EVs bound to the aldehyde latex bead as indicated with the red arrow.

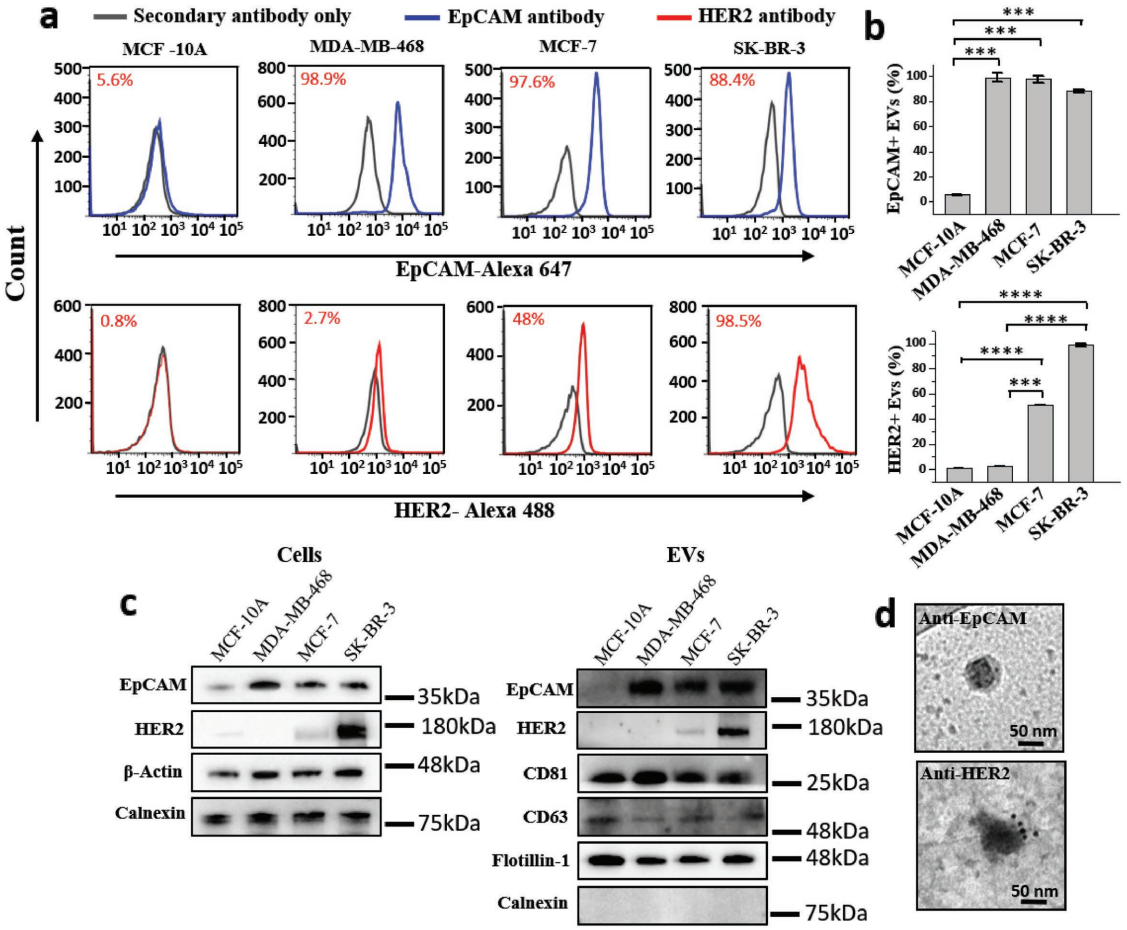

Figure 3. EpCAM and HER2 exhibit different expression levels in EVs from different breast cancer cell lines. a) Flow cytometry analysis of EpCAM+ (upper) and HER2+ (down) EV-bound beads in the mammary epithelial cell line MCF-10A and the three breast cancer cell lines MDA-MB-468, MCF-7, and SK-BR-3. b) Percentage of EpCAM+ (upper) and HER2+ (lower) EV-bound beads in the mammary epithelial cell line MCF-10A and the three breast cancer cell lines MDA-MB-468, MCF-7, and SK-BR-3, as analyzed by flow cytometry. The data are presented as the means ± S.D. ($n = 3$). ***$p < 0.001$, ****$p < 0.0001$ (Student's t-test). c) Western blot analysis of the expression of EpCAM and HER2 in the mammary epithelial cell line MCF-10A and the three breast cancer cell lines MDA-MB-468, MCF-7, and SK-BR-3, using β-Actin and calnexin as positive controls (left), and the expression of EpCAM and HER2 in EVs isolated from the four cell lines, using CD81, CD63, and flotillin-1 as positive controls and calnexin as the negative control (right). The blots were cropped from their original images, and the full-length blots are presented in Figure S4 in the Supporting Information. d) Immunogold TEM images of EpCAM (left) and HER2 (right) in EVs from SK-BR-3 cells.

concentration was determined by the bicinchoninic acid (BCA) assay. We found that the particle/protein ratio in EVs isolated from cell culture medium was ≈2×10^{10} particles μg^{-1} of protein (Figure S3, Supporting Information), equal to the medium-to-high vesicular purity as guided by Webber et al,[24] indicating that protein expression as determined by flow cytometry and western blotting was mainly from the expression of proteins in EVs. The nanoscaled size of EVs has limited the application of flow cytometry in the molecular analysis of EVs. To this end, strategies have been taken by adhering EVs onto the micro-sized beads to yield detectable signals in flow cytometry.[17a-c,18] We used 4 μm aldehyde/sulfate latex beads to enrich EVs. The beads adsorbed with EVs were subsequently stained with anti-EpCAM or anti-HER2 and the secondary antibody for flow cytometry analysis (Figure 2c). Both TEM and scanning electron microscopy (SEM) revealed that the microbeads were densely covered with the captured EVs (Figure 2d,e), indicating the enrichment of EVs on the beads. Flow cytometry analysis showed a high percentage of EpCAM+ EV-bound beads in the breast cancer cell lines compared with that in the nontumor cell line MCF-10A (**Figure 3**a upper lane, Figure 3b left), in accordance with the expression of EpCAM in the cell lines (Figure 1a). The percentage of HER2+ EV-bound beads was the highest in the HER2-OE cell line SK-BR-3, moderate in the luminal A cell line MCF-7, and the lowest in the basal epithelial cell line MDA-MB-468 and nontumor mammary epithelial cell line MCF-10A (Figure 3a lower lane, Figure 3b right), following the same trend as the expression of HER2 in these cell lines (Figure 1b). These results were confirmed by western blot analysis that also showed high expression of EpCAM in the three breast cancer cell lines and EVs derived from them but low expression of EpCAM in the nontumor cell line MCF-10A and its EVs, and high expression of HER2 in the HER2-OE cell line SK-BR-3 and its EVs but low expression of HER2 in the other cell lines and their EVs (Figure 3b). As guided by the minimal experimental requirements for the definition and functional studies

of EVs provided by the International Society for Extracellular Vesicles,[25] β-Actin and calnexin were used as positive control for cells, and three EV-enriched marker proteins, CD81, CD63, and flotillin-1, were used as positive controls while the cell-derived calnexin was used as a negative control for EVs to show the purity of the isolated EV samples (Figure 3c; Figure S4, Supporting Information).[26] We also performed immunogold TEM using antibodies specific to EpCAM and HER2. The electron micrographs of EVs derived from the HER2-OE cell line SK-BR-3 revealed the expression of EpCAM and HER2 on the purified EVs (Figure 3d). These results demonstrated that the expression of EpCAM and HER2 in the EVs could well represent the expression of these proteins in the cells of origin. We further estimated the average expression of EpCAM and HER2 in EVs by calculating the average fluorescent intensity (AFI) of EVs adhered on the microbead. The medium fluorescence intensity measured from flow cytometry analysis was divided by the average number of EVs adhered on the microbead that was calculated from three parallel SEM images with 25K magnification. The obtained AFI represented the average expression of marker proteins in EVs. We found that the estimated average expression of EpCAM and HER2 in each EV was in good accordance with the percentage of EpCAM+ and HER2+ EV-bound beads and with the western blot analysis of these two markers in the EVs from each cell line (Figure S5, Supporting Information), indicating the validity of the estimation in evaluating the average expression of marker proteins in EV. Taken together, the microbead-assisted flow cytometry analysis was an effective method to evaluate the expression of marker surface proteins in the tumor-derived EVs and could be used for the detection and molecular phenotyping of breast cancer.

2.2. EpCAM+ EVs as a Biomarker for Breast Cancer

After establishing microbead-assisted flow cytometry for the molecular analysis of tumor-derived EVs, we tested the utility of this method in the diagnosis and molecular phenotyping of breast cancer. We first examined whether EpCAM+ EVs could be used for the detection of breast cancer. EVs were isolated from the serum of histologically validated HER2+ (n = 19) and HER2− (n = 12) breast cancer patients and healthy donors (n = 7) using differential centrifugation similar to the method used to isolate EVs from the cell lines.[18] TEM and NTA characterization showed that the size and morphology of the EVs purified from the sera of breast cancer patients were similar to those of cell line-derived EVs (**Figure 4**a,b; Figure S6, Supporting Information), indicating the success of isolating serum EVs from patients. Western blot analysis showed no expression of albumin, a serum-derived negative marker in these EVs (Figure S7, Supporting Information), confirming the purity of the EVs isolated from patient sera. We further calculated the particle/protein ratio of these purified EVs that was determined to be ≈5×10^9 particles μg^{-1} of protein (Figure S3b, Supporting Information), comparable to the previously reported ratio in serum.[24] Considering the complicated components in human serum, this purity was acceptable. Flow cytometry analysis showed that the average level of EpCAM+ serum EVs was

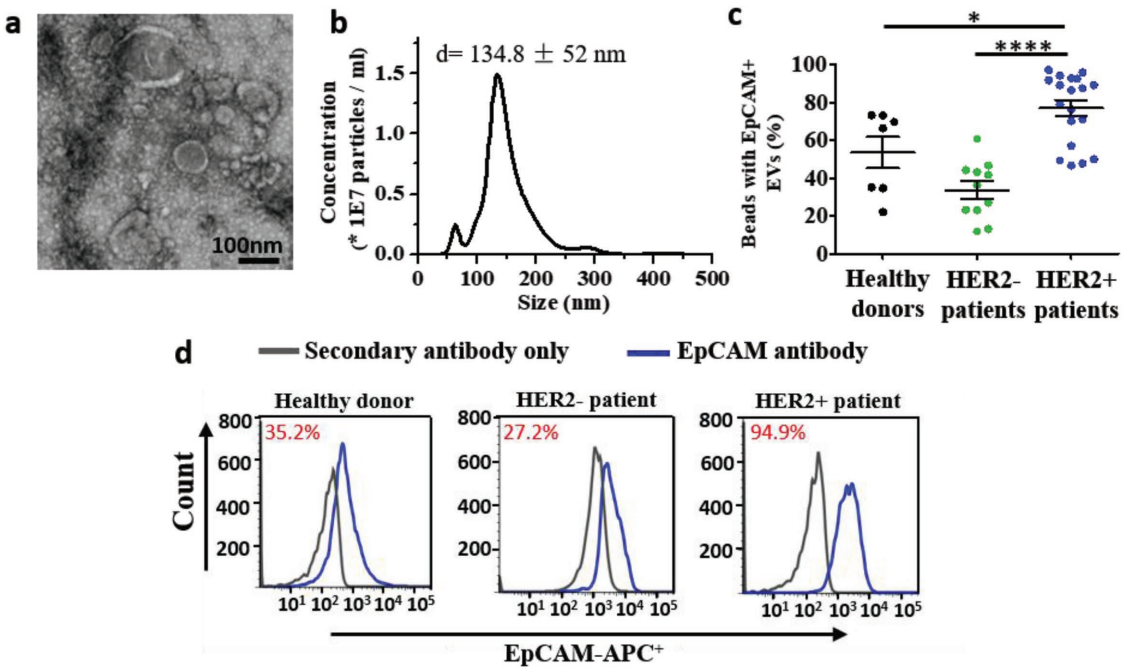

Figure 4. EpCAM+ EVs are biomarkers for breast cancer. a) TEM image of EVs from a breast cancer patient. b) Size distribution of EVs from the breast cancer patient analyzed by NTA. c) Percentage of EpCAM+ EV-bound beads from healthy donors (n = 7), and HER2− (n = 12), and HER2+ (n = 19) breast cancer patients analyzed by flow cytometry. The data are presented as the means ± S.D. *p < 0.05, ****p < 0.0001 (Mann–Whitney U test). d) Representative flow cytometry analysis of EpCAM+ EV-bound breads from healthy donors (left) and HER2− (middle) and HER2+ (right) patients. Negative control: secondary antibody only.

significantly higher in the HER2+ breast cancer cohort than in the HER2– breast cancer cohort ($p < 0.0001$) and in the healthy group ($p < 0.05$) (Figure 4c,d), in good accordance with the estimated average expression of EpCAM in EVs in each group (Figure S8a, Supporting Information). Twelve of 19 (63%) HER2+ breast cancer patients had a higher level of EpCAM+ serum EVs than healthy donors, and 14 of 19 (74%) HER2+ breast cancer patients had a higher level of EpCAM+ serum EVs than HER2– breast cancer patients (Figure 4c), indicating that EpCAM+ serum EVs was an effective biomarker to distinguish HER2+ breast cancer patients from HER2– breast cancer patients and healthy individuals. However, the level of EpCAM+ serum EVs in the HER2– breast cancer cohort was even lower ($p < 0.01$) than that in the healthy group (Figure 4c,d). This might be because most (8 of 12, 67%) of the patients recruited in the HER2– breast cancer group were triple-negative breast cancer (TNBC) patients. As the most aggressive subtype of breast cancer, TNBC tends to be closely related to epithelial to mesenchymal transition, and patients with TNBC would, therefore, have low expression of epithelial markers such as EpCAM.[27]

2.3. HER2+ EVs for HER2 Phenotyping of Breast Cancer

We next tested whether HER2+ EVs could be used for HER2 phenotyping of breast cancer. We observed that HER2– breast cancer patients had a similar level of HER2 expression in serum EVs to that in healthy donors, while the average level of HER2+ serum EVs was significantly higher in the HER2+ breast cancer cohort than in the HER2– breast cancer cohort ($p < 0.0001$) and in the healthy group ($p < 0.0001$) (**Figure 5**a,b), in good accordance with the estimated average expression of HER2 in EVs in each group (Figure S8b, Supporting Information). Thirteen of 19 (68%) HER2+ breast cancer patients had a higher level of EpCAM+ serum EVs than HER2– breast cancer patients and the healthy donors (Figure 5a). These results demonstrated the capacity of HER2+ serum EVs to differentiate HER2+ patients from HER2– patients and the healthy individuals. We further evaluated the discriminatory efficacy of HER2+ EVs in distinguishing HER2+ patients from HER2– patients and the healthy individuals using receiver operating characteristic (ROC) analysis. We found that HER2+ EVs had favorable efficacy in discriminating HER2+ breast cancer from HER2– breast cancer and the normal controls (AUC: 0.972; 95% CI: 0.927-1.000, **Figure 6**; Table S1, Supporting Information) with the cut-off value of 52.1 (Table S1, Supporting Information). This performance was remarkably better than that using the EV concentration (AUC: 0.611; 95% CI: 0.422-0.800; Figure 6; Table S1, Supporting Information). These results again indicated the high diagnostic value of HER2+ EVs in distinguishing HER2+ patients from HER2– patients and healthy individuals.

To check the correlation between flow cytometry analysis of HER2+ EVs and IHC staining of tumor tissue, we randomly selected four patients with different levels of HER2+ EVs, as

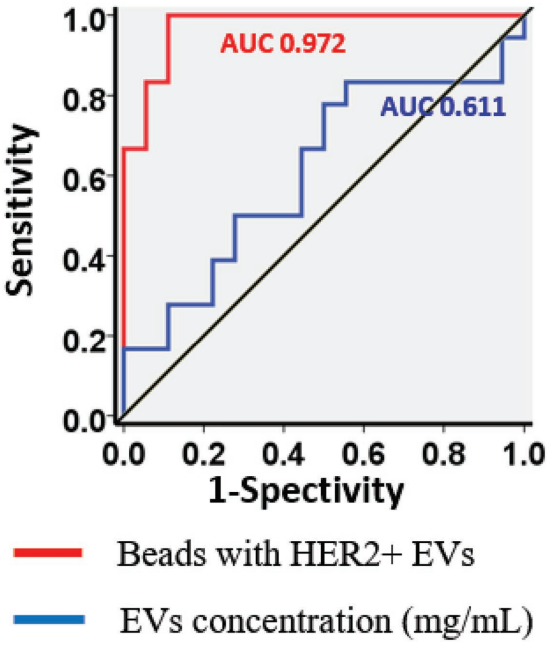

Figure 6. Receiver operating characteristic (ROC) analysis showing the discriminative efficacy of HER2+ EVs in the diagnosis of HER2+ breast cancer. ROC curve of the percentage of HER2+ EV-bound beads (red line) and the concentration of EVs (blue line) in distinguishing HER2+ patients ($n = 19$) from HER2– patients ($n = 12$) and healthy donors ($n = 7$). The area under the ROC curve (AUC) is indicated.

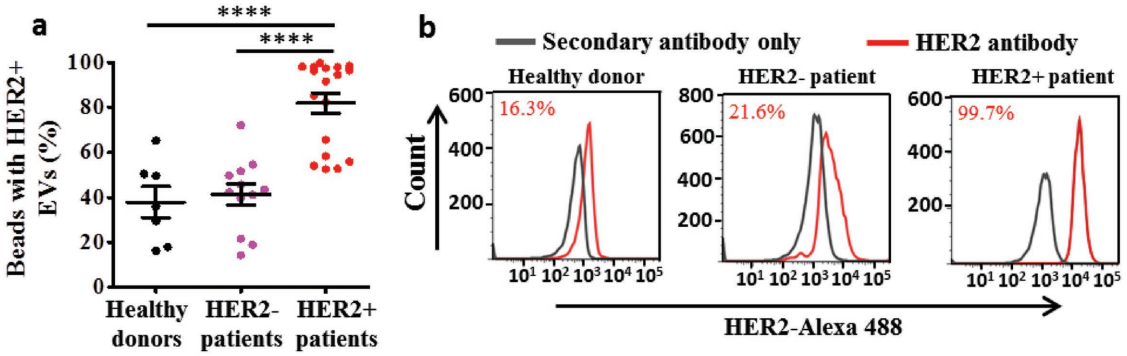

Figure 5. HER2 expression in EVs can be used for breast cancer HER2 phenotyping. a) Percentage of HER2+ EV-bound beads from healthy donors ($n = 7$), and HER2– ($n = 12$) and HER2+ ($n = 19$) breast cancer patients analyzed by flow cytometry. The data are presented as the means ± S.D. ****$p < 0.0001$ (Mann–Whitney U test). b) Representative flow cytometry analysis of HER2+ EV-bound breads from healthy donors (left) and HER2– (middle) and HER2+ (right) patients. Negative control: secondary antibody only.

assessed by flow cytometry. We found that the HER2 status in the serum EVs correlated well with the IHC staining results from the patient-matched local recurrent specimens in the breast or metastatic lesions in the chest wall or axillary lymph nodes (**Figure 7**), indicating that HER2+ serum EVs could well represent the expression level of HER2 in the tumor tissue. Patients with a percentage of ≈26–28% in flow cytometry tended to be HER2– and HER2 1+ in IHC and were clinically thought to be HER2-negative populations. The patient with a percentage of ~59% in flow cytometry tended to be HER2 2+ in IHC that was clinically suggested to be grouped into the HER2-positive population with confirmation of HER2 gene expression by FISH. The patient with a percentage of ≈95% in flow cytometry tended to be HER2 3+ in IHC that was clinically determined to be HER2 positive (Figure 7). These results, taken together with the cut-off value >52.1% as determined by ROC analysis (Table S1, Supporting Information), suggest the significance of this cutoff value in HER2 phenotyping. However, to set an accurate threshold for clinical application, larger cohorts need to be recruited and further experiments need to be performed. The microbead-assisted flow cytometry analysis of HER2+ serum EVs could, therefore, be used as an alternate to IHC staining.

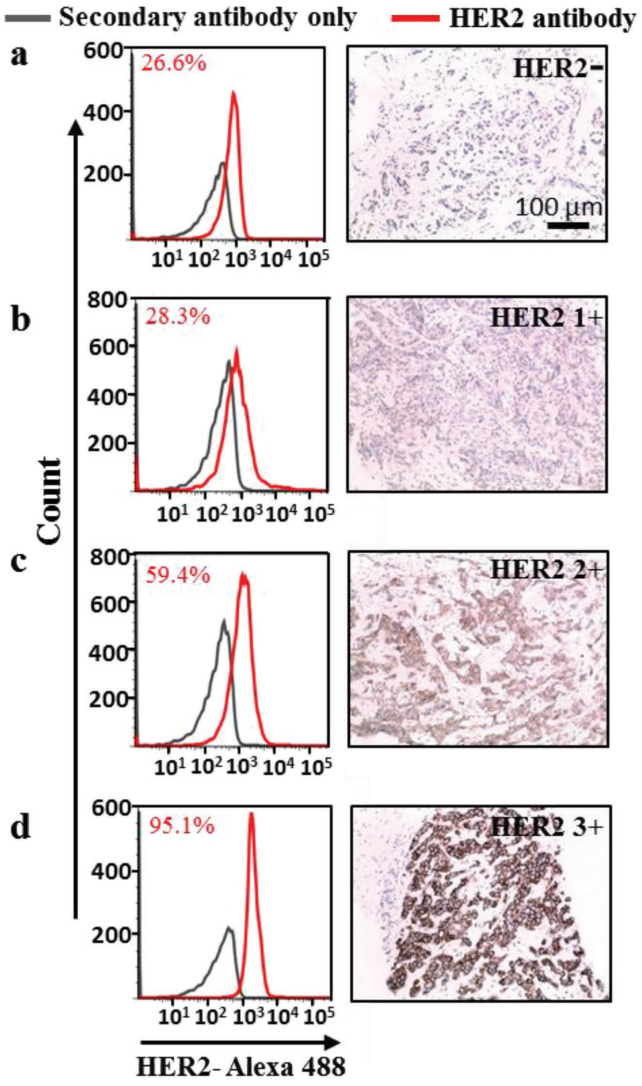

Figure 7. HER2 phenotyping in breast cancer EVs correlates with immunohistochemical (IHC) staining. Flow cytometry analysis of HER2+ EV-bound breads (left) and IHC staining (brown) for HER2 in patient-matched recurrent or metastatic tumor biopsies (right) from four individual breast cancer patients: a) chest wall, b) axillary lymph node, c) axillary lymph node, and d) breast recurrent biopsy. HER2 levels in EVs tested by flow cytometry analysis correlate with the assessments from IHC staining.

3. Conclusions

Personalized treatment is the trend in clinical management due to the heterogeneity of cancer. Noninvasive blood-based tests allow for the real-time monitoring of tumor progress and treatment efficacy and, therefore, hold great potential in clinical applications. EVs are endosomal-derived membrane vesicles that are abundant in body fluids such as blood. Because they carry molecular information such as proteins and nucleic acids from the source cells, EVs become desired liquid biopsy for the detection and molecular analysis of diseases, including cancer.[10a,28]

Numerous studies have used EVs as biomarkers for the early detection and prediction of the treatment response, prognosis and metastasis of tumors.[9b,15,18,29] EVs have been suggested to participate in the tumorigenesis, microenvironment, metastasis, and drug resistance of breast cancer.[30] An elevated concentration of tumor-derived EVs in the plasma has been reported in patients with breast cancer[31] and other types of carcinomas.[18,32] The contents of EVs and expression levels of marker proteins such as focal adhesion kinase (FAK) and epidermal growth factor receptor (EGFR) were found to be correlated with the tumor stages in breast cancer.[31] Although studies have reported the expression of EpCAM and HER2 in breast cancer cell lines and in body fluids from breast cancer patients,[11–13] EV-based HER2 phenotyping in breast cancer is even very rare, and systematic evaluation and comparison have not been performed between EV-based molecular phenotyping and the traditional IHC assessment.

Our study establishes an assessment for the detection and molecular phenotyping of tumor-derived EVs based on microbead-assisted flow cytometry and validates the clinical utility of this method in breast cancer patients. Utilizing this method, which allows for the rapid and noninvasive characterization of EV marker proteins, we demonstrate that both EpCAM+ and HER2+ EVs are effective diagnostic indicators of breast cancer, capable of distinguishing HER2+ patients from HER2– patients and healthy individuals with high sensitivity and specificity. ROC analysis reveals the excellent efficacy of HER2+ EVs in discriminating HER2+ breast cancer from HER2– breast cancer and normal controls (AUC: 0.972; 95% CI: 0.927–1.000). By contrast, the EV concentration that has been found to be increased in cancer patients[18,31,32] is much less valid (AUC: 0.611; 95% CI: 0.422–0.800) as a diagnostic indicator, consistent with the previous studies showing that EV counting alone is not sufficient in tumor detection.[18,33] Furthermore, our EV-based HER2 phenotyping has shown good correlation with the clinically

used immunohistochemistry-based HER2 phenotyping, suggesting the potential of EV-based molecular phenotyping as a surrogate to tissue assessments in routine clinical examination. Since HER2 expression may change during tumor progression, recurrence and metastasis,[4b-g] tissue-based HER2 phenotyping from the primary tumor may not represent the real-time status of HER2 to optimize treatment. Evaluation bias may also be introduced during the collection of biopsies from different locations of the tumor due to intratumoral heterogeneity.[4d,5] EV-based HER2 phenotyping, in this regard, provides a desired solution for the dynamic and integral monitoring of HER2 expression in breast cancer, and would, therefore, be beneficial to personalized treatment and eventually cancer survival. Furthermore, the discordant expression between the primary tumor and recurrent/metastatic tumor has been found not only in HER2 but also in other markers. For example, changes were observed in the expression of estrogen receptor (ER) and progesterone receptor (PR) between the primary breast cancer and metastases.[4f,34] Discordance of the EGFR mutation status has also been found between the primary tumor and lymph node or brain metastases in lung cancer.[35] Moreover, intratumoral heterogeneity in gene expression profiling has been reported in spatially distinct tumor fragments from glioblastoma patients.[36] These studies imply that the EV-based molecular phenotyping assessment can also be expanded to test other markers in different types of tumors.

Overall, microbead-assisted flow cytometry analysis of tumor-derived serum EVs provides a rapid and noninvasive method for the detection and molecular phenotyping of cancer and holds great potential in clinical applications. The EV-based molecular phenotyping provides an opportunity for the real-time monitoring of disease progress and treatment efficacy and will help with personalized treatment and eventually, cancer survival.

4. Experimental Section

Cell Culture: All the cell lines were obtained from the American Type Culture Collection (Manassas, VA, USA). The following cells lines were used: MCF10-A (human mammary epithelial cell), MDA-MB-468 (human basal epithelial breast cancer cell line), MCF-7 (human luminal A breast cancer cell line), and SK-BR-3 (human HER2-OE breast cancer cell line). All the cells were cultured in different media supplemented with 10% fetal bovine serum (GIBCO-BRL) and 1% penicillin/streptomycin (GIBCO-BRL): MEGMTM mammary epithelial cell growth medium (Lonza; CC3151) for MCF-10A, L-15 medium (GIBCO-BRL) for MDA-MB-468, and high glucose GlutaMAX Dulbecco's modified Eagle medium (Gibco-BRL Co, MD, USA) for MCF-7 and SK-BR-3. MCD-10A, MCF-7, and SK-BR-3 cells were maintained in a humidified atmosphere of 5% CO_2/95% air at 37 °C, while MDA-MB-468 cells were maintained in a humidified atmosphere of 0% CO_2/100% air at 37 °C. Subcultivation of all the cell lines was performed using 0.25% trypsin and 5×10^{-3} M ethylenediaminetetraacetic acid (EDTA) (Gibco-BRL Co, MD, USA).

Clinical Samples: The study was approved by the Medical Ethical Committee of Peking Cancer Hospital (2013KT29). All the participants, including 19 HER2+ recurrent metastatic breast cancer patients, 12 HER2− recurrent metastatic breast cancer patients, and 7 healthy volunteers were recruited with informed consent. The inclusion criteria of the breast cancer patients were histologically verified breast cancer with the first diagnosis of metastatic disease or disease progression. HER2 phenotyping was determined according to IHC staining of the local recurrent tumor tissue or metastatic lesions. Sera and metastatic tumor specimens were collected before any chemo-/radio- or anti-HER2 therapies were given to the patients after the first diagnosis of tumor recurrence and metastasis. The inclusion criteria for healthy control donors were a negative medical history for any acute, chronic, or malignant diseases. The blood drawn by venous puncture was collected in blood collection tubes containing clot activator and was allowed to clot for 30 min at room temperature. The serum was then separated by centrifugation at 3000 rpm for 10 min and stored at −80 °C. Metastatic specimens were collected by puncture biopsy. All the samples were randomly selected from larger cohorts and were analyzed in a blinded fashion. Unblinding of the clinical parameters and corresponding experimental data was performed only after finishing all the experiments.

EV Purification: EVs were purified by differential centrifugation as previously described with modification.[18] Briefly, for EV purification from the cell culture supernatant, the cells were cultured in the EV-free medium for 48 h (depletion of the contaminating vesicles and protein aggregates was performed by centrifugation overnight at 110 000*g*[37]). The medium was collected and centrifuged at 800*g* for 5 min and 2000*g* for 10 min, followed by filtration through a 0.22 µm filter (Millipore, USA) to eliminate cell debris. EVs were pelleted by ultracentrifugation at 100 000*g* for 2 h at 4 °C, followed by a wash with PBS and a second step of ultracentrifugation at 100 000*g* for 2 h at 4 °C. For EV purification from serum samples, 500 µL of human sera were centrifuged at 800*g* for 5 min and 2000*g* for 10 min, followed by dilution in 26 mL of PBS and filtration through a 0.22 µm pore filter (Millipore, USA) to eliminate cell debris. EVs were pelleted by ultracentrifugation at 150 000*g* overnight at 4 °C, followed by a wash in 26.3 mL of PBS and a second step of ultracentrifugation at 150 000*g* for 2 h at 4 °C. Thereafter, the EV pellets from the cells and sera were resuspended in 100 µL of PBS and stored at 4 °C prior to use. The total protein content of the purified EVs was determined using the BCA protein assay kit (Pierce, Rockford, IL).

Immunogold Labeling and TEM: Isolated EVs were loaded onto 200-mesh carbon/formvar-coated grids (Beijing Zhongjingkeyi Technology Co., Ltd., China) for 20 min and were negatively stained using uranyl acetate. For immunogold labeling, the grids were fixed in 4% paraformaldehyde for 10 min, washed with PBS, blocked in a drop of 10% BSA for 10 min, and incubated with anti-EpCAM (mouse mAb; Cell Signal Technology) or anti-HER2 (rabbit mAb; Cell Signal Technology) for 1 h at 4 °C. The grids were then rinsed with PBS and incubated with the secondary antibody attached to 10 nm gold particles (Aurion, BioValley, France) for 1 h at room temperature. The grids were postfixed with 2.5% glutaraldehyde for 15 min, rinsed with PBS and double-distilled water, and negatively stained with uranyl acetate. Transmission electron microscopy characterization was carried out using a Hitachi HT7700 electron microscope (Hitachi High-Tech, Japan).

SEM: Isolated EVs were loaded onto silicon wafers and dried in a drying oven. The samples were sputter-coated with a thin layer of gold prior to observation. SEM images were obtained using a Hitachi S-3400N electron microscope (Hitachi High-Tech, Japan) at an acceleration potential of 15 kV.

DLS: DLS measurements were performed using a Zetasizer Nano ZS90 system (Malvern Instruments Ltd., UK) equipped with a 633 nm HeNe laser and an avalanche photodiode detector. The samples were loaded into polymer cuvettes with a 10 mm path length. DLS determinations were made in a backscattering mode at an operating angle of 173°. The working temperature was thermostatically controlled at 25 °C.

NTA: The number and size distribution of EVs were measured using the NanoSight LM14 system with a 405 nm laser (NanoSight Technology, Malvern, UK). EVs derived from cell cultures and serum were diluted in PBS to maintain the concentration at 10^8–10^9 particles mL^{-1}. The samples were injected into the sample chamber with a syringe, measured in triplicate with a high-sensitivity scientific complementary metal-oxide semiconductor camera, at camera setting 16 with an acquisition time of 60 s and a detection threshold setting of 7. The sample chamber was rinsed three times between different samples. Finally, the data were analyzed using nanoparticle tracking analysis software (NTA version 2.3; Malvern Instruments, Malvern, UK).

Flow Cytometry Analysis: For cell analysis, cells at the logarithmic growth phase were digested with 0.25% trypsin and washed with PBS three times, followed by re-suspension in 100 µL of PBS, and staining with anti-EpCAM (mouse mAb; Cell Signal Technology) and anti-HER2 (rabbit mAb; Cell Signal Technology) or with their isotype control IgG (Cell Signal Technology) at room temperature for 40 min. After washing with PBS three times, the cells were incubated with Alexa-488- or Alexa-594-tagged secondary antibodies (Abcam). The samples were finally washed with PBS three times and resuspended in 200 µL of PBS. For EV analysis, EVs from cell lines or patient sera were enriched on 4 µm aldehyde/sulfate latex beads (Invitrogen) by incubating 5 µg of EVs with 10 µL of beads for 15 min at room temperature with continuous rotation. The suspension was then diluted with PBS to 500 µL and left for 1 h with rotation room temperature. The reaction was stopped with 100 $\times 10^{-6}$ M glycine and 0.5% BSA/PBS and was left with rotation on for 30 min at room temperature. The EV-bound beads were washed with 0.5% BSA in PBS and centrifuged for 3 min at 14 800*g*, blocked with 5% BSA in PBS with rotation at room temperature for 1 h, and washed again with 0.5% BSA in PBS and centrifuged for 3 min at 14 800*g*. The EV-bound beads were then incubated with anti-EpCAM antibody (mouse mAb; Cell Signal Technology) or anti-HER2 antibody (rabbit mAb, Cell Signal Technology) for 1 h with rotation at 4 °C, and centrifuged for 3 min at 14 800*g*. The supernatant was discarded, and the beads were washed with 0.5% BSA/PBS and centrifuged for 3 min at 14 800*g*. Thereafter, the EV-bound beads were incubated with Alexa-488- or Alexa-594-tagged secondary antibodies (Abcam) for 30 min with rotation at 4 °C. Secondary antibody incubation alone was used as the control. The samples were finally washed with 0.5% BSA in PBS three times and were resuspended in 200 µL of PBS. Flow cytometry analysis was performed using a BD Accuri TMC6 Flow Cytometer (BD Biosciences, USA).

Protein Separation and Western Blot Analysis: Cells were cultured in 6-well plates (Corning) and were scraped using scrapers (Fisherbrand). The cell suspension or EVs were lysed with lysis buffer, supplemented with protease inhibitor cocktail and phenylmethylsulfonyl fluoride (Thermo Scientific) on ice for 60 min. Protein fractions were collected by centrifugation at 15 000 rpm for 10 min at 4° C. Sample loading was normalized according to the BCA relative protein quantification kit (Solarbio). Proteins were separated in polyacrylamide gels before being transferred to poly(vinylidene difluoride) membranes (0.45 mm; Millipore, Bedford, MA, USA). The membranes were blocked with 5% nonfat milk (BD Biosciences) in Tris-buffered saline with 0.1% Tween (TBST) for 1 h at room temperature and then were incubated with anti-EpCAM (mouse mAb; Cell Signal Technology), anti-HER2 (rabbit mAb; Cell Signal Technology), anti-CD81 (mouse monoclonal antibody; Santa Cruz), anti-CD63 (mouse monoclonal antibody; Santa Cruz), antiflotillin (rabbit monoclonal antibody; abcam), anticalnexin (rabbit monoclonal antibody; abcam), and antialbumin (rabbit monoclonal antibody; abcam) overnight at 4 °C. Thereafter, the membranes were incubated with horseradish peroxidase-conjugated goat antirabbit IgG or goat antimouse IgG (Cell Signal Technology) for 1 h at room temperature in TBST containing 5% nonfat milk. The blots were developed using the Enhanced Chemiluminescence Kit (Thermo Pierce, Waltham, MA, USA) and were visualized using Image Lab (BIO-RAD, USA).

Immunohistochemistry: For immunohistochemistry, 5 µm thick sections from formalin-fixed, paraffin-embedded tissue specimens were transferred onto adhesive slides, air-dried, deparaffinized in xylene and rehydrated in graded alcohol. Antigen enhancement was performed by incubating the sections with citrate buffer (pH 6). After blocking with 5% normal goat serum (Solarbio) for 30 min at room temperature, the sections were stained with anti-HER2 (rabbit mAb; Cell Signal Technology). Avidin-biotin-peroxidase complex (Vectastain Elite ABC-HRP kit, peroxidase, rabbit IgG; Vector Laboratories, USA) and diaminobenzidine (Sigma-Aldrich) were used to detect the immunoreactivity. After rinsing and counterstaining, images of the sections were obtained using the EVOS XL Core Imaging System (Thermo Fisher Scientific, USA).

Statistical Analysis: GraphPad Prism version 6.0 (GraphPad Software) was used to analyze the flow cytometry results. ROC analysis was used to evaluate the specificity and sensitivity of HER2+ EVs and the concentration of EVs in distinguishing HER2+ breast cancer from healthy controls and HER2− breast cancer. The area under the ROC curve was estimated for each individual biomarker. All the ROC analyses were performed using GraphPad Prism 6.0 (GraphPad Software Inc.). The cutoff value was determined using the Youden index. $p < 0.05$ was taken as statistical significance.

We have submitted all the relevant data of our experiments to the EV-TRACK knowledgebase (EV-TRACK ID: EV180026)).[38]

Supporting Information

Supporting Information is available from the Wiley Online Library or from the author.

Acknowledgements

W.L. and B.S. contributed equally to this work. This work was supported by the National Natural Science Foundation of China (Nos. 31600803 and 21773042), the Beijing Natural Science Foundation (No. 2162044), and the Strategic Priority Research Program of Chinese Academy of Sciences (XDA09030306).

Conflict of Interest

The authors declare no conflict of interest.

Keywords

breast cancer, detection, extracellular vesicles, phenotyping

Received: April 17, 2018
Revised: June 3, 2018
Published online: August 1, 2018

[1] a) B. Weigelt, J. L. Peterse, L. J. van't Veer, *Nat. Rev. Cancer* **2005**, *5*, 591; b) T. Morimoto, T. Nagao, K. Okazaki, M. Kira, Y. Nakagawa, A. Tangoku, *Breast Cancer* **2009**, *16*, 2.

[2] a) L. Harris, H. Fritsche, R. Mennel, L. Norton, P. Ravdin, S. Taube, M. R. Somerfield, D. F. Hayes, R. C. Bast Jr., *J. Clin. Oncol.* **2007**, *25*, 5287; b) H. Kennecke, R. Yerushalmi, R. Woods, M. C. U. Cheang, D. Voduc, C. H. Speers, T. O. Nielsen, K. Gelmon, *J. Clin. Oncol.* **2010**, *28*, 3271; c) N. Cancer Genome Atlas, *Nature* **2012**, *490*, 61.

[3] A. C. Wolff, M. E. H. Hammond, J. N. Schwartz, K. L. Hagerty, D. C. Allred, R. J. Cote, M. Dowsett, P. L. Fitzgibbons, W. M. Hanna, A. Langer, L. M. McShane, S. Paik, M. D. Pegram, E. A. Perez, M. F. Press, A. Rhodes, C. Sturgeon, S. E. Taube, R. Tubbs, G. H. Vance, M. V. de Vijver, T. M. Wheeler, D. F. Hayes, *J. Clin. Oncol.* **2007**, *25*, 118.

[4] a) E. Munzone, F. Nole, A. Goldhirsch, E. Botteri, A. Esposito, L. Zorzino, G. Curigliano, I. Minchella, L. Adamoli, M. C. Cassatella, C. Casadio, M. T. Sandri, *Clin. Breast Cancer* **2010**, *10*, 392; b) V. Guarneri, S. Giovannelli, G. Ficarra, S. Bettelli, A. Maiorana, F. Piacentini, E. Barbieri, M. V. Dieci, R. D'Amico, G. Jovic, P. Conte, *Oncologist* **2008**, *13*, 838; c) F. Cardoso, A. Di Leo, D. Larsimont, D. Gancberg, G. Rouas, S. Dolci, F. Ferreira, M. Paesmans, M. Piccart, *Ann. Oncol.* **2001**, *12*, 615; d) D. Gancberg, A. Di Leo, F. Cardoso, G. Rouas, M. Pedrocchi, M. Paesmans, A. Verhest, C. Bernard-Marty, M. J. Piccart, D. Larsimont, *Ann. Oncol.*

2002, *13*, 1036; e) C. Liedtke, K. Broglio, S. Moulder, L. Hsu, S. W. Kau, W. F. Symmans, C. Albarracin, F. Meric-Bernstam, W. Woodward, R. L. Theriault, L. Kiesel, G. N. Hortobagyi, L. Pusztai, A. M. Gonzalez-Angulo, *Ann. Oncol.* **2009**, *20*, 1953; f) A. M. Thompson, L. B. Jordan, P. Quinlan, E. Anderson, A. Skene, J. A. Dewar, C. A. Purdie, B. R. T. S. Gr, *Breast Cancer Res.* **2010**, *12*, R92; g) Z. X. Yao, L. J. Lu, R. J. Wang, L. B. Jin, S. C. Liu, H. Y. Li, G. S. Ren, K. N. Wu, D. L. Wang, L. Q. Kong, *Med. Oncol.* **2014**, *31*, 798.

[5] a) M. Gerlinger, A. J. Rowan, S. Horswell, J. Larkin, D. Endesfelder, E. Gronroos, P. Martinez, N. Matthews, A. Stewart, P. Tarpey, I. Varela, B. Phillimore, S. Begum, N. Q. McDonald, A. Butler, D. Jones, K. Raine, C. Latimer, C. R. Santos, M. Nohadani, A. C. Eklund, B. Spencer-Dene, G. Clark, L. Pickering, G. Stamp, M. Gore, Z. Szallasi, J. Downward, P. A. Futreal, C. Swanton, *N. Engl. J. Med.* **2012**, *366*, 883; b) S. Sasada, H. Kurihara, T. Kinoshita, M. Yoshida, N. Honda, T. Shimoi, A. Shimomura, K. Yonemori, C. Shimizu, A. Hamada, Y. Kanayama, Y. Watanabe, Y. Fujiwara, K. Tamura, *Eur. J. Nucl. Med. Mol. Imaging* **2017**, *44*, 2146.

[6] a) D. J. Slamon, B. Leyland-Jones, S. Shak, H. Fuchs, V. Paton, A. Bajamonde, T. Fleming, W. Eiermann, J. Wolter, M. Pegram, J. Baselga, L. Norton, *N. Engl. J. Med.* **2001**, *344*, 783; b) C. L. Vogel, M. A. Cobleigh, D. Tripathy, J. C. Gutheil, L. N. Harris, L. Fehrenbacher, D. J. Slamon, M. Murphy, W. F. Novotny, M. Burchmore, S. Shak, S. J. Stewart, M. Press, *J. Clin. Oncol.* **2002**, *20*, 719; c) C. E. Geyer, J. Forster, D. Lindquist, S. Chan, C. G. Romieu, T. Pienkowski, A. Jagiello-Gruszfeld, J. Crown, A. Chan, B. Kaufman, D. Skarlos, M. Campone, N. Davidson, M. Berger, C. Oliva, S. D. Rubin, S. Stein, D. Cameron, *N. Engl. J. Med.* **2006**, *355*, 2733.

[7] N. V. Jordan, A. Bardia, B. S. Wittner, C. Benes, M. Ligorio, Y. Zheng, M. Yu, T. K. Sundaresan, J. A. Licausi, R. Desai, R. M. O'Keefe, R. Y. Ebright, M. Boukhali, S. Sil, M. L. Onozato, A. J. Iafrate, R. Kapur, D. Sgroi, D. T. Ting, M. Toner, S. Ramaswamy, W. Haas, S. Maheswaran, D. A. Haber, *Nature* **2016**, *537*, 102.

[8] V. Plaks, C. D. Koopman, Z. Werb, *Science* **2013**, *341*, 1186.

[9] a) N. Arraud, R. Linares, S. Tan, C. Gounou, J. M. Pasquet, S. Mornet, A. R. Brisson, *J. Thromb. Haemostasis* **2014**, *12*, 614; b) H. L. Shao, J. Chung, K. Lee, L. Balaj, C. Min, B. S. Carter, F. H. Hochberg, X. O. Breakefield, H. Lee, R. Weissleder, *Nat. Commun.* **2015**, *6*, 6999.

[10] a) C. Thery, L. Zitvogel, S. Amigorena, *Nat. Rev. Immunol.* **2002**, *2*, 569; b) C. Thery, M. Ostrowski, E. Segura, *Nat. Rev. Immunol.* **2009**, *9*, 581.

[11] a) C. Battke, R. Ruiss, U. Welsch, P. Wimberger, S. Lang, S. Jochum, R. Zeidler, *Cancer Immunol. Immunother.* **2011**, *60*, 639; b) T. M. Green, M. L. Alpaugh, S. H. Barsky, G. Rappa, A. Lorico, *Biomed Res. Int.* **2015**, *2015*, 634865; c) F. Andre, N. E. Schartz, M. Movassagh, C. Flament, P. Pautier, P. Morice, C. Pomel, C. Lhomme, B. Escudier, T. Le Chevalier, T. Tursz, S. Amigorena, G. Raposo, E. Angevin, L. Zitvogel, *Lancet* **2002**, *360*, 295.

[12] V. Ciravolo, V. Huber, G. C. Ghedini, E. Venturelli, F. Bianchi, M. Campiglio, D. Morelli, A. Villa, P. Della Mina, S. Menard, P. Filipazzi, L. Rivoltini, E. Tagliabue, S. M. Pupa, *J. Cell Physiol.* **2012**, *227*, 658.

[13] A. A. Sina, R. Vaidyanathan, S. Dey, L. G. Carrascosa, M. J. Shiddiky, M. Trau, *Sci. Rep.* **2016**, *6*, 30460.

[14] a) Z. X. Wang, H. J. Wu, D. Fine, J. Schmulen, Y. Hu, B. Godin, J. X. J. Zhang, X. W. Liu, *Lab Chip* **2013**, *13*, 2879; b) B. H. Wunsch, J. T. Smith, S. M. Gifford, C. Wang, M. Brink, R. L. Bruce, R. H. Austin, G. Stolovitzky, Y. Astier, *Nat. Nanotechnol.* **2016**, *11*, 936.

[15] H. L. Shao, J. Chung, L. Balaj, A. Charest, D. D. Bigner, B. S. Carter, F. H. Hochberg, X. O. Breakefield, R. Weissleder, H. Lee, *Nat. Med.* **2012**, *18*, 1835.

[16] a) H. Im, H. L. Shao, Y. I. Park, V. M. Peterson, C. M. Castro, R. Weissleder, H. Lee, *Nat. Biotechnol.* **2014**, *32*, 490; b) L. Zhu, K. Wang, J. Cui, H. Liu, X. L. Bu, H. L. Ma, W. Z. Wang, H. Gong, C. Lausted, L. Hood, G. Yang, Z. Y. Hu, *Anal. Chem.* **2014**, *86*, 8857.

[17] a) A. Clayton, J. Court, H. Navabi, M. Adams, M. D. Mason, J. A. Hobot, G. R. Newman, B. Jasani, *J. Immunol. Methods* **2001**, *247*, 163; b) H. Valadi, K. Ekstrom, A. Bossios, M. Sjostrand, J. J. Lee, J. O. Lotvall, *Nat. Cell Biol.* **2007**, *9*, 654; c) M. Ostrowski, N. B. Carmo, S. Krumeich, I. Fanget, G. Raposo, A. Savina, C. F. Moita, K. Schauer, A. N. Hume, R. P. Freitas, B. Goud, P. Benaroch, N. Hacohen, M. Fukuda, C. Desnos, M. C. Seabra, F. Darchen, S. Amigorena, L. F. Moita, C. Thery, *Nat. Cell Biol.* **2010**, *12*, 19; d) H. G. Lamparski, A. Metha-Damani, J.-Y. Yao, S. Patel, D.-H. Hsu, C. Ruegg, J.-B. Le Pecq, *J. Immunol. Methods* **2002**, *270*, 211; e) K. Koga, K. Matsumoto, T. Akiyoshi, M. Kubo, N. Yamanaka, A. Tasaki, H. Nakashima, M. Nakamura, S. Kuroki, M. Tanaka, M. Katano, *Anticancer Res.* **2005**, *25*, 3703.

[18] S. A. Melo, L. B. Luecke, C. Kahlert, A. F. Fernandez, S. T. Gammon, J. Kaye, V. S. LeBleu, E. A. Mittendorf, J. Weitz, N. Rahbari, C. Reissfelder, C. Pilarsky, M. F. Fraga, D. Piwnica-Worms, R. Kalluri, *Nature* **2015**, *523*, 177.

[19] a) P. T. Went, A. Lugli, S. Meier, M. Bundi, M. Mirlacher, G. Sauter, S. Dirnhofer, *Hum. Pathol.* **2004**, *35*, 122; b) W. A. Osta, Y. Chen, K. Mikhitarian, M. Mitas, M. Salem, Y. A. Hannun, D. J. Cole, W. K. Gillanders, *Cancer Res* **2004**, *64*, 5818.

[20] S. D. Soysal, S. Muenst, T. Barbie, T. Fleming, F. Gao, G. Spizzo, D. Oertli, C. T. Viehl, E. C. Obermann, W. E. Gillanders, *Br. J. Cancer* **2013**, *108*, 1480.

[21] a) T. Sorlie, C. M. Perou, R. Tibshirani, T. Aas, S. Geisler, H. Johnsen, T. Hastie, M. B. Eisen, M. van de Rijn, S. S. Jeffrey, T. Thorsen, H. Quist, J. C. Matese, P. O. Brown, D. Botstein, P. E. Lonning, A. L. Borresen-Dale, *Proc. Natl. Acad. Sci. USA* **2001**, *98*, 10869; b) T. Sorlie, Y. L. Wang, C. L. Xiao, H. Johnsen, B. Naume, R. R. Samaha, A. L. Borresen-Dale, *BMC Genomics* **2006**, *7*, 727.

[22] G. Raposo, H. W. Nijman, W. Stoorvogel, R. Leijendekker, C. V. Harding, C. J. M. Melief, H. J. Geuze, *J. Exp. Med.* **1996**, *183*, 1161.

[23] a) C. Gercel-Taylor, S. Atay, R. H. Tullis, M. Kesimer, D. D. Taylor, *Anal. Biochem.* **2012**, *428*, 44; b) S. Sitar, A. Kejzar, D. Pahovnik, K. Kogej, M. Tusek-Znidaric, M. Lenassi, E. Zagar, *Anal Chem* **2015**, *87*, 9225.

[24] J. Webber, A. Clayton, *J. Extracell. Vesicles* **2013**, *2*, 19861.

[25] J. Lotvall, A. F. Hill, F. Hochberg, E. I. Buzas, D. Di Vizio, C. Gardiner, Y. S. Gho, I. V. Kurochkin, S. Mathivanan, P. Quesenberry, S. Sahoo, H. Tahara, M. H. Wauben, K. W. Witwer, C. Thery, *J. Extracell. Vesicles* **2014**, *3*, 26913.

[26] T. H. Tran, G. Mattheolabakis, H. Aldawsari, M. Amiji, *Clin. Immunol.* **2015**, *160*, 46.

[27] a) H. Jeong, Y. J. Ryu, J. An, Y. Lee, A. Kim, *Histopathology* **2012**, *60*, E87; b) Q. Zeng, W. Li, D. Lu, Z. Wu, H. Duan, Y. Luo, J. Feng, D. Yang, L. Fu, X. Yan, *Proc. Natl. Acad. Sci. USA* **2012**, *109*, 1127.

[28] B. Fevrier, G. Raposo, *Curr. Opin. Cell Biol.* **2004**, *16*, 415.

[29] a) T. Matsumura, K. Sugimachi, H. Iinuma, Y. Takahashi, J. Kurashige, G. Sawada, M. Ueda, R. Uchi, H. Ueo, Y. Takano, Y. Shinden, H. Eguchi, H. Yamamoto, Y. Doki, M. Mori, T. Ochiya, K. Mimori, *Br. J. Cancer* **2015**, *113*, 275; b) J. Nilsson, J. Skog, A. Nordstrand, V. Baranov, L. Mincheva-Nilsson, X. O. Breakefield, A. Widmark, *Br. J. Cancer* **2009**, *100*, 1603.

[30] a) V. Luga, L. Zhang, A. M. Viloria-Petit, A. A. Ogunjimi, M. R. Inanlou, E. Chiu, M. Buchanan, A. N. Hosein, M. Basik, J. L. Wrana, *Cell* **2012**, *151*, 1542; b) D. D. Yu, Y. Wu, H. Y. Shen, M. M. Lv, W. X. Chen, X. H. Zhang, S. L. Zhong, J. H. Tang, J. H. Zhao, *Cancer Sci.* **2015**, *106*, 959; c) C. Y. Wu, S. L. Du, J. Zhang, A. L. Liang, Y. J. Liu, *Cancer Gene Ther.* **2017**, *24*, 6; d) H. W. King, M. Z. Michael, J. M. Gleadle, *BMC Cancer* **2012**, *12*, 421.

[31] O. Galindo-Hernandez, S. Villegas-Comonfort, F. Candanedo, M. C. Gonzalez-Vazquez, S. Chavez-Ocana, X. Jimenez-Villanueva, M. Sierra-Martinez, E. P. Salazar, *Arch. Med. Res.* **2013**, *44*, 208.
[32] a) G. Rabinowits, C. Gercel-Taylor, J. M. Day, D. D. Taylor, G. H. Kloecker, *Clin. Lung Cancer* **2009**, *10*, 42; b) D. D. Taylor, C. Gercel-Taylor, *Gynecol. Oncol.* **2008**, *110*, 13.
[33] Z. Zhao, Y. Yang, Y. Zeng, M. He, *Lab Chip* **2016**, *16*, 489.
[34] S. J. Aitken, J. S. Thomas, S. P. Langdon, D. J. Harrison, D. Faratian, *Ann. Oncol.* **2010**, *21*, 1254.
[35] a) K. Shimizu, T. Yukawa, Y. Hirami, R. Okita, S. Saisho, A. Maeda, K. Yasuda, M. Nakata, *Target Oncol.* **2013**, *8*, 237; b) K. M. Rau, H. K. Chen, L. Y. Shiu, T. L. Chao, Y. P. Lo, C. C. Wang, M. C. Lin, C. C. Huang, *Int. J. Mol. Sci.* **2016**, *17*, 524.
[36] A. Sottoriva, I. Spiteri, S. G. Piccirillo, A. Touloumis, V. P. Collins, J. C. Marioni, C. Curtis, C. Watts, S. Tavare, *Proc. Natl. Acad. Sci. USA* **2013**, *110*, 4009.
[37] C. Thery, M. Boussac, P. Veron, P. Ricciardi-Castagnoli, G. Raposo, J. Garin, S. Amigorena, *J. Immunol.* **2001**, *166*, 7309.
[38] E.-T. Consortium, J. Van Deun, P. Mestdagh, P. Agostinis, O. Akay, S. Anand, J. Anckaert, Z. A. Martinez, T. Baetens, E. Beghein, L. Bertier, G. Berx, J. Boere, S. Boukouris, M. Bremer, D. Buschmann, J. B. Byrd, C. Casert, L. Cheng, A. Cmoch, D. Daveloose, E. De Smedt, S. Demirsoy, V. Depoorter, B. Dhondt, T. A. Driedonks, A. Dudek, A. Elsharawy, I. Floris, A. D. Foers, K. Gartner, A. D. Garg, E. Geeurickx, J. Gettemans, F. Ghazavi, B. Giebel, T. G. Kormelink, G. Hancock, H. Helsmoortel, A. F. Hill, V. Hyenne, H. Kalra, D. Kim, J. Kowal, S. Kraemer, P. Leidinger, C. Leonelli, Y. Liang, L. Lippens, S. Liu, A. Lo Cicero, S. Martin, S. Mathivanan, P. Mathiyalagan, T. Matusek, G. Milani, M. Monguio-Tortajada, L. M. Mus, D. C. Muth, A. Nemeth, E. N. Nolte-'t Hoen, L. O'Driscoll, R. Palmulli, M. W. Pfaffl, B. Primdal-Bengtson, E. Romano, Q. Rousseau, S. Sahoo, N. Sampaio, M. Samuel, B. Scicluna, B. Soen, A. Steels, J. V. Swinnen, M. Takatalo, S. Thaminy, C. Thery, J. Tulkens, I. Van Audenhove, S. van der Grein, A. Van Goethem, M. J. van Herwijnen, G. Van Niel, N. Van Roy, A. R. Van Vliet, N. Vandamme, S. Vanhauwaert, G. Vergauwen, F. Verweij, A. Wallaert, M. Wauben, K. W. Witwer, M. I. Zonneveld, O. De Wever, J. Vandesompele, A. Hendrix, *Nat. Methods* **2017**, *14*, 228.

Received: 9 June 2020 | Revised: 3 December 2020 | Accepted: 4 December 2020

DOI: 10.1002/jev2.12047

WILEY

RESEARCH ARTICLE

Single-vesicle imaging and co-localization analysis for tetraspanin profiling of individual extracellular vesicles

Chungmin Han[1,2] | **Hyejin Kang**[2] | **Johan Yi**[1] | **Minsu Kang**[2] | **Hyunjin Lee**[1] | **Yongmin Kwon**[1] | **Jaehun Jung**[1] | **Jingeol Lee**[1] | **Jaesung Park**[1,2]

[1] Department of Mechanical Engineering, Pohang University of Science and Technology, Pohang, Gyeong-buk, Republic of Korea

[2] School of Interdisciplinary Bioscience and Bioengineering, Pohang University of Science and Technology, Pohang, Gyeong-buk, Republic of Korea

Correspondence
Jaesung Park, Department of Mechanical Engineering, Pohang University of Science and Technology, Pohang, Gyeong-buk, Republic of Korea.
Email: jpark@postech.ac.kr

Abstract

Extracellular vesicles (EVs) are secreted nano-sized vesicles that contain cellular proteins, lipids, and nucleic acids. Although EVs are expected to be biologically diverse, current analyses cannot adequately characterize this diversity because most are ensemble methods that inevitably average out information from diverse EVs. Here we describe a single vesicle analysis, which directly visualizes marker expressions of individual EVs using a total internal-reflection microscopy and analyzes their co-localization to investigate EV subpopulations. The single-vesicle imaging and co-localization analysis successfully illustrated the diversity of EVs and revealed distinct patterns of tetraspanin expressions. Application of the analysis demonstrated similarities and dissimilarities between the EV fractions that had been acquired from different conventional EV isolation methods. The analysis method developed in this study will provide a new and reliable tool for investigating characteristics of single EVs, and the findings of the analysis might increase understanding of the characteristics of EVs.

KEYWORDS

density gradient ultracentrifugation, EV heterogeneity, EV subpopulations, single-vesicle analysis, size exclusion chromatography, tetraspanin markers

1 | INTRODUCTION

Extracellular vesicles (EVs) are cell-secreted nano-sized vesicles that have important functions in diverse biological activities (Février & Raposo, 2004; Raposo & Stoorvogel, 2013). EVs are complex bodies composed of various biological materials, including proteins, lipids, and nucleic acids (Théry et al., 2002). Traditional omics approaches have identified hundreds of proteins, nucleic acids, and lipids of EVs (Choi et al., 2015; Guduric-Fuchs et al., 2012; Ji et al., 2014; Llorente et al., 2013; Simpson et al., 2008; Skotland et al., 2019). Due to the wide range of components, cells can produce various types of EVs. Consequently, EVs are expected to deliver more comprehensive and specific messages than soluble molecules (Kao & Papoutsakis, 2019; Krämer-Albers & Hill, 2016). However, most conventional analytical methods for EVs consider ensemble averages of heterogeneous populations, so much remains unknown about the heterogeneity of EVs. The ensemble methods such as western blotting (WB) and omics approaches require lysis of EVs, and only provide pooled information about the whole population, so information from individual EVs is lost (Margolis & Sadovsky, 2019). As a result, despite the vast amount of existing information about EV components, the characteristics of individual EVs and heterogeneity of EV samples cannot be discerned.

Some studies have attempted to elucidate the heterogeneity of EVs, and have suggested the presence of different EV subpopulations depending on isolation methods (Shu et al., 2020). Investigations using density gradient ultracentrifugation (DG) and

size exclusion chromatography (SEC) has revealed the presence of EV populations having different densities and sizes (Böing et al., 2014; Kowal et al., 2016). Studies that exploit asymmetric-flow field-flow fractionation suggested distinct EV subpopulations having different sizes ranging from approximately 35 to 120 nm that also have different biological compositions (Sitar et al., 2015; Zhang et al., 2018). Although such isolation-oriented approaches have successfully separated EV populations into relatively smaller populations, the implications of these studies were mostly limited to the evaluation of physical characteristics (Gardiner et al., 2013; Höög & Lötvall, 2015; Yuana et al., 2013). Therefore, to better understand the correlation between EV subpopulations and biological implications, biological properties and heterogeneity of refined EV populations should be further investigated.

A few advanced analytical methods have also developed for characterizing biological properties of individual EVs. High resolution flow cytometers and imaging flow cytometers have been proposed to overcome the limitations of conventional cytometers that are optimized for single-cell analysis, but they still have technical limitations such as swarm detection and low detection sensitivity (detection limits are often > 200 nm) (Erdbrügger et al., 2014; Van Der Pol et al., 2012). NTAs equipped with fluorescence units were developed for probing biological properties of individual EVs, but the technical principle exploits diffusion, and therefore cannot reliably investigate the co-expression of multiple markers. Recently, studies have used advanced fluorescence microscopies such as super resolution microscopies and con-focal microscopy to analyse multiple protein expressions of individual EVs (Chen et al., 2016; Lee et al., 2018; Nizamudeen et al., 2018). In addition, technologies that do not exploit fluorescence have also been proposed to investigate individual EVs; examples include single-particle interferometric reflectance imaging sensing (SP-IRIS), nano-plasmonic sensors and Raman spectroscopic analysis (Daaboul et al., 2016; Im et al., 2014; Lee et al., 2018). Although such single-EV analysis approaches have provided important findings regarding EV heterogeneity and subtypes, this field of study still needs a method that can precisely analyse multiple biological markers of individual EVs without the bias that may arise during sample preparation and analyses.

Recently, technological advances in biophysical methods have enabled observation of the behaviour of single biological molecules (Aggarwal & Ha, 2016; Roy et al., 2008). Applications of single-molecule imaging techniques have been used to characterize interactions between biological molecules, and have revealed many phenomena that had been obscured by ensemble-averaging methods (Jain et al., 2011; Myong et al., 2006). Particularly, single-molecule pull-down (SiMPull) and single-molecule blotting (SiMBlot) assays overcome the limitation of conventional ensemble averaging biochemical analysis such as WB, which have enabled us to quantitatively characterize biochemical properties of individual biomolecules (Jain et al., 2011; Kim et al., 2016). The techniques have also been applied to relatively large biological complexes, such as viruses and liposomes, but they have rarely been used to explore the characteristics of EVs (Brandenburg & Zhuang, 2007; Choi et al., 2010).

In this study, to overcome the technical pitfalls of conventional EV analyses, we developed a single-vesicle imaging analysis method that uses total internal reflection fluorescence microscopy (TIRFM). The analysis can visualize multiple marker expressions of individual EVs by using fluorescent probes, and can also investigate EV subpopulations by analysing co-localization of markers. We used the single-EV tetraspanin co-localization analysis to investigate EV fractions that were isolated by three frequently-used EV isolation methods. The analysis revealed that individual EVs had distinct tetraspanin expression patterns that could not be characterized by conventional analyses, and this capability enabled us to deduce similarities and dissimilarities among the conventional methods to isolate EVs.

2 | METHODS

2.1 | Cell culture

The HEK293 WT (# 21573), MCF-7 (# 30022) and B16BL6 (# 80006) cell line was purchased from Korean Cell Line Bank (KCLB). The HEK293 WT cells were maintained in Dulbecco's modified Eagle's medium (DMEM, Gibco, 12100046) supplemented 10% (v/v) fetal bovine serum (FBS, Gibco, 12483020) and 1x antibiotic-antimycotic (anti-anti, Gibco, 15240062) at 37°C and 5% CO_2 in a humidified incubator. MCF-7 and B16BL6 cells were maintained in minimum essential medium (MEM, Gibco, 41500-034) supplemented 10% (v/v) FBS and 1x anti-anti at 37°C and 5% CO_2 in a humidified incubator. When cells were ~ 90% confluent, culture media were changed to supplement-free base medium and cultured for 24 h under the same incubation condition. After 24 h, cultured media were collected and then centrifuged at 500 × *g* for 10 min to remove detached cells and at 3000 × *g* for 20 min to eliminate cellular debris. The pre-cleaned media (supernatants) were stored at −80°C until they were used. A total of 6 L of cell cultured media (CM) was pooled and processed for EV isolation to minimize batch to batch variation.

2.2 | Antibodies and labelling reagents

A CD9 (MEM-61, sc51575), CD63 (MX-49.129.5, sc5275), CD81 (1.3.3.22, sc7637), Calnexin (H-70, sc11397) and ribosomal protein S6 (C-8, sc-74459) primary antibodies and HRP-conjugated anti-mouse IgG_1 secondary antibody (sc2005) were purchased from Santa Cruz Biotechnology for western blotting. Alexa-Fluor 488 (A-21121), 546 (A-21123), and 647 (A-21240) conjugated

anti-mouse IgG_1 secondary antibodies were purchased from Invitrogen. Fluorescent dye-conjugated primary antibodies for CD9, CD63, and CD81 (MEM-61, MX-49.129.5, and 1.3.3.22 clones, respectively) were purchased from Novus biologicals, BioLegends, and Santa Cruz Biotechnology, and lot to lot variations of labelling efficiency was tested before use. Specifically, the signal counts of conjugated antibodies were compared with the counts of same clones of primary antibodies and secondary antibodies, and the conjugated antibodies that yielded > 90% of the counts of indirect labelling were selected for further multi-colour single-vesicle analyses. A recombinant CTB protein (NBP2-61449) and anti-CTB rabbit polyclonal antibody (NB100-63067) were purchased from Novus Biological. A Di-dye cell labelling kit (V22889) and Alexa-Fluor 488 conjugated annexin V (A13201) were purchased from Invitrogen.

2.3 | EV preparation: concentration, biotinylation and purifications

For differential ultracentrifugation (DUC) concentration, Type 45 Ti (Beckman) fixed-angle titanium rotor was used for first and second rounds of EV pelleting. The procedures of DUC concentration were derived from previous literature (Théry et al., 2006). The 6 L of pooled cultured media (CM) was centrifuged at 500 × *g* for 10 min to remove cells then centrifuged again at 3000 × *g* for 20 min to remove cellular debris. The pre-cleaned CM was them ultra-centrifuged at 100,000 × *g* for 2 h, and the resulting pellets were re-suspended in total 12 ml filtered-PBS solution. After first-round pelleting, the sample was biotinylated with approximately 100-times molar excess of sulfo-NHS-biotin (Thermo scientific, 21217) according to the manufacturer's instruction. The biotinylated sample was ultra-centrifuged again at 100,000 × *g* for 2 h to remove protein contaminants and residual biotins. The pellet was suspended again in 4 ml filtered-PBS and centrifuged again at 3000 × *g* for 20 min to remove EV aggregates formed during ultracentrifugation; 1 ml of the EV solution was kept for the characterization of DUC method (DUC-EVs) and 3 ml of the solution was used for further purification. Each purification method was performed using 1 ml of DUC-EVs. Because 1 ml of DUC samples was prepared from 1.5 L CM, each purification method can be considered to isolate EVs from initial 1.5 L CM. In addition, the DUC sample had already been biotinylated during the concentration process, so purification methods did not require a biotinylation process.

For density gradient ultracentrifugation (DG) and buoyant DG (BDG) purification, different densities of Opti-Prep iodixanol density-gradient medium (AXIS-SHIELD) were prepared according to the manufacturer's instruction. The overall procedures of DG and BDG purifications were based on the previous literature with minor modifications (Hong et al., 2009; Tauro et al., 2012; Wubbolts et al., 2003). In the DG method, a sample is loaded on top of the density layers, thus the DUC sample was diluted with PBS (0%) and layered on top of 30%, 20% and 10% Opti-Prep layers. On the contrary, in the BDG method, a sample is loaded at the bottom with the highest-density layers, so the DUC sample was diluted in 30% Opti-Prep layers and layered at the bottom of tube with 20% and 10% Opti-Prep and PBS (0%) layers. The DG and BDG samples were centrifuged at 100,000 × *g* for 2 h using a SW55 Ti swinging-bucket rotor (Beckman) with no-brake option. All fractions between the layers (DG/0-10, DG/10-20, DG/20-30, BDG/0-10, BDG/10-20 and BDG/20-30) were collected and stored for further analyses.

We performed SEC purification as described previously (Böing et al., 2014). Approximately ~7.5 ml bed volume of Sepharose CL-2B (GE Healthcare) gel-filtration matrix was packed into a 10-ml plastic disposable column (Pierce). The packed columns were washed using more than three bed volumes (~ 30 ml) of filtered-PBS solution before use. A 1-ml of DUC sample was loaded on the column and then eluted with filtered-PBS solution. The eluates were collected in 20 fractions of 0.5 ml and stored for further analyses.

2.4 | Conventional EV characterizations

All fractions of EVs were characterized by western blotting (WB, Bio-Rad), nano-particle tracking analysis (NTA, ExoCope, ExosomePlus), and transmission electron microscopy (TEM, JEOL) according to the guideline provided by international society for extracellular vesicles (ISEV) (Théry et al., 2018).

EV-positive (CD9, CD63, CD81) and EV-negative (Calnexin and ribosomal protein S6) markers were used for WB analysis. In WB analysis, the same volumes (25 μl) of samples were lysed and separated by SDS-PAGE in a non-reducing condition (Bio-Rad). The separated proteins were transferred to a PVDF membrane, and blocked for 1 h at room temperature (RT) using a solution of 3% (w/v) BSA in TBS supplemented with 0.05% (w/v) Tween-20. The membrane was then incubated with primary antibodies (200 ng/ml) in the blocking solution overnight at 4°C, and subsequently incubated with HRP-conjugated secondary antibodies (200 ng/ml, Santa Cruz Biotechnology) for 1 h at RT. The membrane was exposed to a chemiluminescent substrate (ECL, Thermo Scientific) for detection. The signals were captured using a c-Digit western blot scanner (LI-COR). The WB results presented in the same figure set were all detected under the same condition for valid comparison. Quantification of WB bands was performed using ImageJ software. Briefly, a scan of WB gel was inversed and a fixed size of rectangular region of interest (ROI) that include each WB band was selected. The intensities of bands were measured as mean intensity of ROIs.

Particle concentrations and sizes of samples were measured using NTA (Exocope, Exosomeplus). All samples were diluted ~1,000 to 3,000 times with filtered-PBS solution to achieve appropriate particle concentration (~100 particles/imaging field). Images of all samples were recorded for 15 s at least six times in different imaging fields. The size distribution of EVs was plotted using mean values of six measurements.

For TEM analysis, each EV fraction was loaded onto formvar carbon film (Electron Microscopy Science) for 30 min at RT. The sample-loaded grids were then negatively stained with 2% uranyl acetate (Sigma) for ~ 10 s for image contrasting. The grids were then completely dried overnight and imaged using a TEM (JEOL).

2.5 | Surface preparation and EV immobilization

The detailed procedure used to prepare the DDS-tween 20 surface was explained previously, and used with minor modification (Hua et al., 2014). Briefly, cover and slide glasses were extensively cleaned with acetone, methanol (Samchun Chemicals), and ultra-pure water. The glasses were then incubated in piranha solution (three parts sulfuric acid; one part 30% H_2O_2) for surface cleaning and activation, and then rinsed thoroughly with ultra-pure water. The activated glasses were incubated with DDS (Sigma) solution in cyclohexane for 1.5 h at RT, and then rinsed with clean cyclohexane and completely dried under N_2 gas in a fume hood. The DDS-treated glasses were then sealed with N_2 gas and stored at −20°C for up to 2 weeks.

For EV immobilization, DDS-treated glasses were first assembled in a simple flow chamber by using double-sided tape (3 M) and epoxy bond (Devcon). After the seal of each chamber had completely cured, it was incubated with 0.2 mg/ml biotin-BSA (Sigma) for 5 min at RT to introduce biotin sites to the surface, then incubated with 0.2% Tween-20 (Sigma) solution for 10 min at RT to passivate the remaining surface. To prepare a control surface without biotin anchor, DDS-treated glasses were directly passivated with 0.2% Tween-20 solution. BSA and Tween-20 solutions were both prepared in tris buffer (50 mM Tris). The passivated chambers were incubated with 0.4 mg/ml NeutrAvidin (Thermo Scientific) solution for 5 min at RT, and then biotinylated EVs were introduced to the chambers and incubated for 10 min at RT. NeutrAvidin and EV samples were prepared with filtered-PBS supplemented with 0.5 mg/ml BSA. For surface-tethered CD81 antibody immobilization of EVs, the surface was prepared in the same way with DDS-Tween surface up to the avidin incubation step. Then, biotinylated-CD81 antibodies were incubated for 10 min, then EV samples were introduced to the chamber and incubated for 10 min at RT for immobilization.

2.6 | Scanning probe microscopy and scanning electron microscopy

Surfaces with immobilized-EVs were fixed with 3% (v/v) electron microscopy grade glutaraldehyde (Sigma) for 15 min at RT. Surfaces were then washed with PBS at least three times. Fixed samples were stained with 1% (w/v) osmium tetroxide (OsO4, Sigma) for 30 min at RT, and the OsO_4 was removed by thorough washing with distilled water (DW) at least three times. Samples were then incubated with 1% carbohydrazide (Sigma) for 20 min at RT, and washed with DW at least three times. Then, samples were dehydrated by sequential immersion in 20%, 40%, 60%, 80%, and 100% ethanol solution (v/v) over 30 min at RT. Dehydrated samples were completely dried using a critical point dryer for at least 30 min. For the SPM analysis, the dehydrated surface analyzed using an AFM (Veeco Dimension 3100, VEECO) for an area of 5 × 5 μm with tapping mode in 512 lines at a scan rate of ~0.7 Hz (Skliar & Chernyshev, 2019). An AppNano Si probe (ACT-50, AppNano) was used for the analysis (rectangular-shaped cantilever with nominal length = 125 μm and width = 30 μm; and a pyramidal-shaped tip with height 14–16 μm, and tip radius < 10 nm, spring constant 13–77 N/m and f = 300 kHz). For SEM analysis, the sample was further sputter-coated with platinum (20 mA, 10 s) and analyzed using a JSM7401F high resolution FE-SEM (JEOL).

2.7 | Individual EV visualization and co-localization analysis

EV-immobilized surfaces were fluorescently visualized using antibodies. For indirect antibody labelling, 2 μg/ml (~13.3 nM) primary antibodies were first introduced to the chamber for 10 min at RT, and then 1 μg/ml (~6.6 nM) fluorescent conjugated secondary antibodies were introduced for 8 min at RT. When conjugated antibodies were used, 5 μg/ml (~33.2 nM) conjugated antibodies were incubated for 10 min at RT. When multiple conjugated antibodies were used for labelling, all antibodies were mixed together, and then used for EV labelling (cocktail staining). After the labelling, the chambers were thoroughly washed with filtered PBS three times. The fluorescent labelled EVs were visualized using a laboratory-built objective-type TIRF microscope (Olympus, IX73) equipped with an EMCCD (Andor, iXon 888), four diode lasers (Cobolt, 405-nm, 488-nm, 638-nm MDL series, and 561-nm DPL series), and a four-channel simultaneous-imaging system (Photometrics, QV2). Average signal count per field was measured from 2,000 μm (Février & Raposo, 2004) imaging areas.

For co-localization analysis, we built image processing software in MATLAB by reference to previous literature (Jain et al., 2011; Kim et al., 2016; Ulbrich & Isacoff, 2008). Briefly, the coordination of each multi-channel images was precisely corrected using

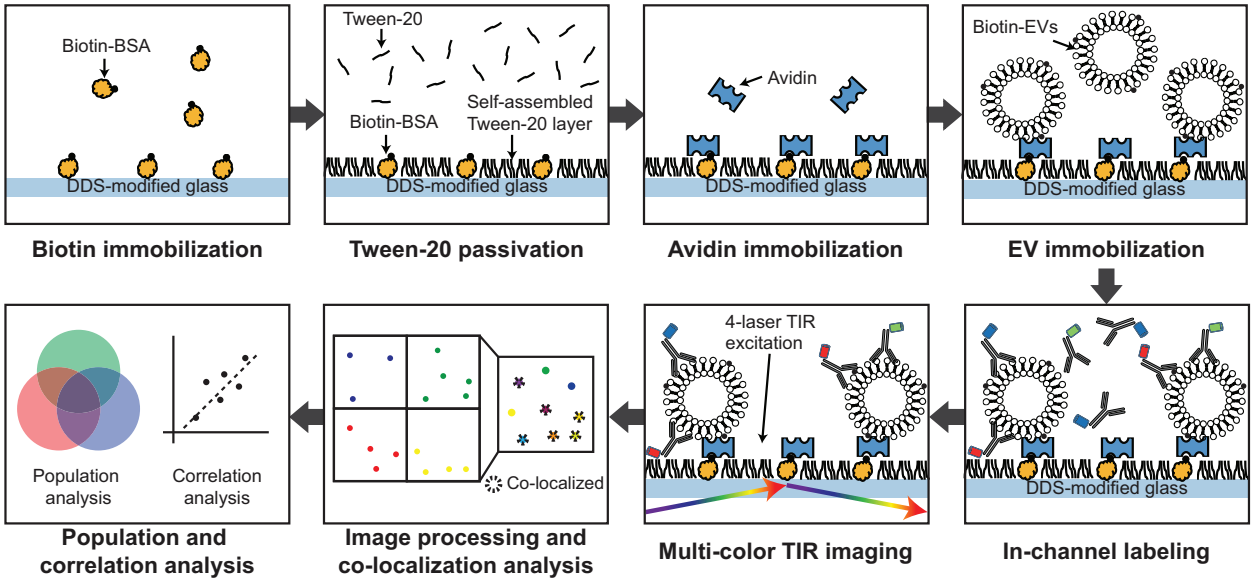

FIGURE 1 Procedure of single-vesicle imaging and co-localization analysis. A simple fluidic channel made of DDS functionalized cover and slide glasses was incubated with biotinylated BSA, then passivated with Tween-20. Avidins were then introduced to the surface to immobilize biotinylated EVs. Unbound molecules were washed out after each step to prevent unwanted interactions among the molecules. Immobilized EVs were labelled with probes, and the EVs were imaged with multiple excitation lasers and a multi-colour simultaneous fluorescence imaging device equipped with EMCCD camera. Acquired signals were analyzed for signal counts and co-localizations for investigating EV heterogeneity and subpopulation

a MATLAB-coded image processing program. The coordinates were corrected using the coordinates of the signals acquired from the full-range fluorescent bead for calibration (Spherotech, FP-0257-2). Then the centers of each tetraspanin signals of coordinate-corrected images were determined with sub-pixel accuracy using Gaussian fitting methods. Using the acquired center coordinates of each signals, the distances between the signals were calculated, and the signals located within 3 pixels (~300 nm) were considered to be co-localized.

2.8 | Multi-dimensional analysis

Populations of samples were compared using two different multi-dimensional analyses: t-stochastic neighbour embedding (t-SNE) and a clustered heat map based on Euclidean distances. In t-SNE, nine independent population data of 11 different fractions were plotted as a single point in two-dimensional space with different perplexity values, and the value that best illustrated the clusters and that had low error was selected. The analysis was performed using a computer code derived from the tsne library of the R package. In clustered heat map analysis, Euclidean distances between the 11 different population data were calculated, and the clusters were formed based on the similarity and dissimilarity values, which were calculated using a computer code derived from ggplot2 and pheatmap libraries of the R package ('pheatmap' and 'tsne') (Donaldson, 2016; Kolde, 2019; R Core Team 2020)

2.9 | Statistical analysis

Data visualization were performed using Excel (Microsoft) and packages in R statistics software. The data were presented as mean ± SD. When statistical analysis was required, two-tailed unpaired Student's t-test was performed. Pairs that had $P < 0.05$ and $P < 0.01$ were considered statistically significant, and noted using a single asterisk and double asterisk, respectively.

3 | RESULTS

3.1 | Schematic of single vesicle imaging and co-localization analysis

The analysis method (Figure 1) visualizes individual EVs and analyzes their co-localization by immobilizing them to a surface that can stably anchor EVs and effectively repel non-specific adsorptions of probes. To achieve such characteristics, we

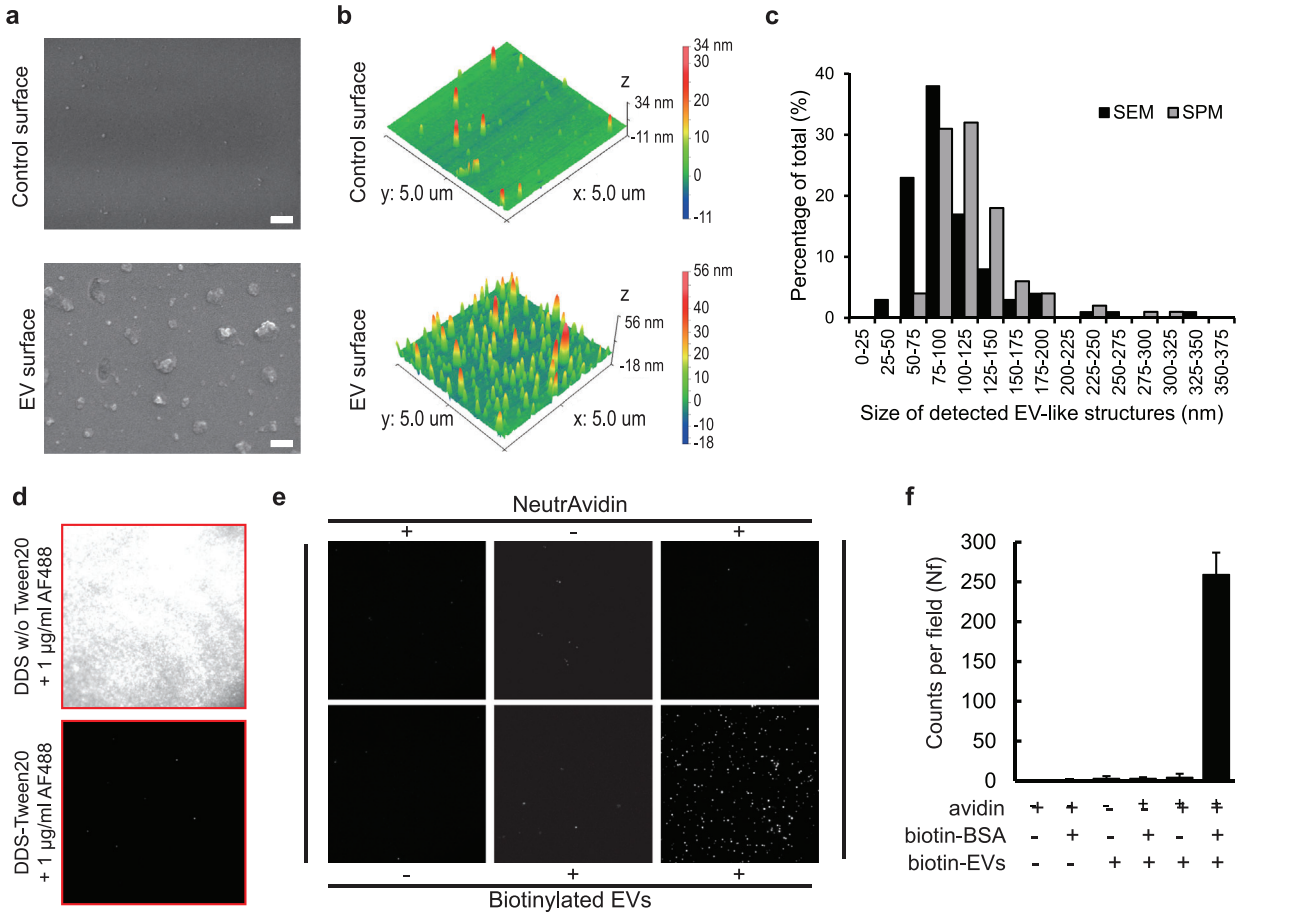

FIGURE 2 Validation of single-EV imaging surface. (a) Scanning electron microscopy (SEM) images of control surface (top) and EV immobilized surface (bottom). Only the EV immobilized surface showed vesicle-like structures, x 50k magnification, bars: 200 nm. (b) Scanning probe microscopy (SPM) results of control surface (top) and EV immobilized surface (bottom). Only the EV immobilized surface exhibited vesicle-like structures. Scanning area is 5 × 5 μm. Scanning mode is tapping mode, scanned for 512 lines with 10-nm tip-radius cantilever. (c) Size analyses of EM images. Sizes of detected EV-like structures were analyzed using ImageJ software. Black bars = SEM, gray bars = SPM. $n > 200$ EV-like structures. (d) Surface passivation test. The DDS surface passivated with 0.2% Tween-20 showed an excellent protein repelling ability (top), whereas the surface without passivation showed a large amount of non-specific antibody adsorption (bottom). (e) Demonstration of single-EV imaging conditions, and (f), average EV signal counts per imaging field. Six combinations of surfaces were tested for single-EV imaging. EVs were visualized using Alexa Fluor 488 (AF488) conjugated CD9 antibody. Only the triple positive (biotin-BSA+/NuetrAvidin+/biotin-EV+) condition exhibited substantial amounts of CD9 signals from immobilized EVs. Size of images: 45 × 45 μm, Bars = mean ± S.D. ($n = 8$)

utilized a glass substrate functionalized with dichlorodimethylsilane (DDS) and Tween-20 passivation that had been developed for single-molecule imaging (Hua et al., 2014). Due to the characteristics of the imaging surface, EVs can be efficiently labelled with fluorescent probes within 20 min. The expressions of multiple markers on individual EVs were detected using a multi-colour fluorescence imaging system that consists of multiple TIR-aligned excitation lasers and an electron-multiplying CCD (EMCCD) camera. The co-localizations of detected signals were analyzed with sub-pixel accuracy by using an computer-coded image processing program described in previous studies (Kim et al., 2016). The 0.2% Tween-20 solution only acted as passivation layer; redundant Tween-20 was thoroughly washed out using sample buffer (PBS). According to the previous literature both the microvesicles (MVs) and exosomes are not lysed even when 5% Tween-20 is added (Osteikoetxea et al., 2015). Therefore, the use of Tween-20 does not disrupt the structure or characteristics of EVs and also does not compromise antibody activities.

3.2 | Validation of single vesicle imaging surface

To ascertain that the surface actually immobilized EVs, a surface was incubated with HEK293 EVs that had been isolated using differential ultracentrifugation (DUC-EVs). The surface was examined using a scanning electron microscope (SEM) and a scanning probe microscope (SPM). Both images of control surfaces revealed only tiny speckles; that is, EVs were not present on the surfaces (Figure 2a,b, control surface). In contrast, the both EM images of the EV-immobilized surfaces showed distinct

EV-like structures (Figure 2a,b, EV surface). The SEM analysis detected ~5.3 EV-like structures per μm (Février & Raposo, 2004) scanning area, and the footprint size of detected EVs was approximately 99 ± 46 nm (Figure 2c, **black bars**). SPM identified ~4.3 signals EV-like signals per μm (Février & Raposo, 2004) scanning area, and the footprint size of the signals was approximately 118 ± 41 nm (Figure 2c, **gray bars**); both numbers are similar to those obtained using SEM analysis. Both EM analyses showed similar amounts of EV-like structures having similar size distributions, and these results agree well with previously-known EV sizes, so we conclude that the DDS-Tween surface successfully immobilized a significant number of EVs.

The protein-repelling ability of the surface was then assessed by binding of Alexa Fluor 488 conjugated secondary antibodies (2 μg/ml) in the absence of EVs: if the surface can effectively repel binding of non-specific proteins, it will show only a small number of fluorescent signals. A control surface without passivation showed a large amount of fluorescent signals from non-specifically adsorbed antibodies (Figure 2d, DDS w/o Tween20), whereas the Tween-passivated DDS surface exhibited almost no non-specific adsorption of antibodies (average counts per field < 10) (Figure 2d, DDS-Tween20).

To demonstrate whether the single-EV imaging surface works properly, all combinations of components that are used for EV immobilization (biotin-BSA, avidin, biotin-EV) were tested. When biotinylated BSA was not introduced to the surface, very few of fluorescent signals were detected from the surface because it bore no anchors (Figure 2e). Even when the surface was properly coated with biotinylated BSA, fluorescence signals from CD9 antibodies were observed only when both the avidin and biotinylated EV were introduced to the surface (Figure 2e). When the numbers of signals from all six combinations were quantified, only the combination that used all three components showed substantial amounts of fluorescence signals from CD9-labeled single EVs (Figure 2f). To confirm whether the detected CD9 signals were came from CD9-positive EVs or from soluble CD9 molecules, we performed a detergent lysis analysis. As a result, the numbers of CD9 signals were decreased when EV samples were treated with SDS, indicating the vesicle structure of detergent-treated EVs were disrupted (Figure S1a,b). Therefore, from this observation, we could conclude that the detected signals of CD9 staining were actually coming from surface-immobilized EVs.

3.3 | Characterization of single-vesicle imaging conditions

EV labelling and EV immobilization conditions affect the results of the single-EV analysis, so the effects of such conditions were first characterized. First, to characterize the effect of antibody concentration, a fixed quantity of DUC-EVs was immobilized to the prepared surfaces, then labelled with different concentrations of tetraspanin antibodies (CD9, CD63 and CD81). In the results, the EV signal counts began to saturate from 1.1 μg/ml in the case of CD9 antibody and from 3.3 μg/ml in the cases of the other two antibodies. The imaging surface appeared to effectively block the nonspecific adsorption of antibodies up to 10 μg/ml because the signals almost stopped increasing after the binding had saturated (Figure 3a,b). Because of this result, all subsequent single-EV analyses performed in this study were conducted using an antibody concentration of 5 μg/ml.

In previous single-molecule studies, multi-colour analyses were often difficult due to steric hindrance (Wang et al., 2014). Therefore, whether the antibodies used in this study interfered with each other was experimentally determined. The signal counts of the cocktail labelling (labelled with all three kinds of antibodies at the same time) were not significantly different from the signal counts of single labelling (one kind of antibody for one sample); this result indicates that the tetraspanins antibodies do not interfere with each other (Figure 3c,d).

Then we characterized the effect of EV concentration on single-vesicle analysis using DUC-EVs. The EV signals of single-vesicle imaging were distinguishable from the background at an EV concentration of 5×10^6 particles/ml; the signals started to saturate at ~10^8 particles/ml (Figure 3c,d). In a few cases, the trend varied noticeably depending on batches of EV samples. From the results of further purity analysis, we determined that the purity of samples might affect the results of the single-vesicle analysis (Figure S2a,b). For example, low-purity EV samples contain a relatively large amount of protein contaminants that compete with EVs for binding sites on the imaging surface (Figure S2c). However, in an additional experiment we confirmed that that proportions of each tetraspanin-positive EVs were not affected by the total EV counts of the analysis. For example, while total EV counts were changed from ~250 to ~80, the proportions of CD9, CD63, and CD81-positive signals were almost unchanged (Figure S3a,b).

We also tested effect of Opti-Prep density gradient medium for single-EV analysis; the analysis result was not affected by addition of up to 3% Opti-Prep (Figure S4a,b). All subsequent single-EV analyses in this study were performed based on the conditions that were characterized here (EV concentration > 10^7 particles/ml and Opti-Prep concentration < 3%).

3.4 | Comparison of different EV-immobilization strategies

To effectively capture EVs on the surface regardless of their antigen expressions, we exploited a direct biotin-avidin interaction. The EV-immobilization strategy could critically affect the result of the EV analyses, so the immobilization should be demonstrated to be valid for the purpose of analysis. For example, if EVs are immobilized using surface-tethered CD9

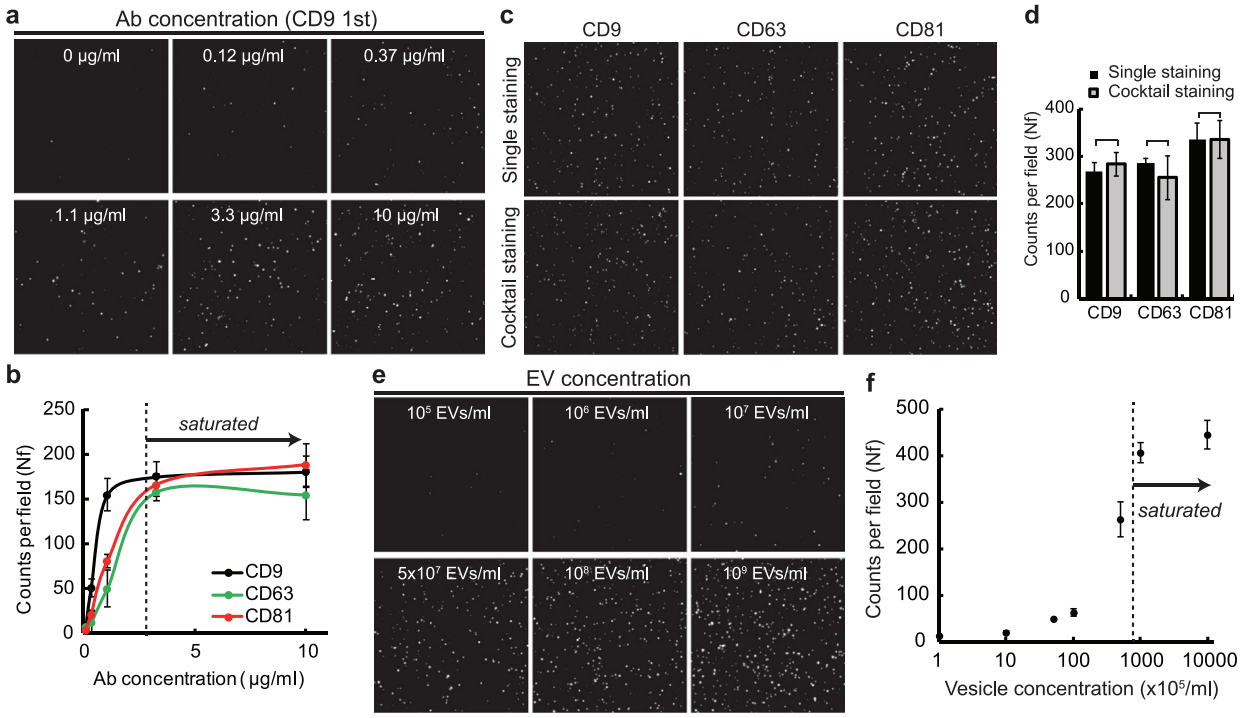

FIGURE 3 Characterization of single vesicle imaging conditions. (a,b), Characterization of antibody concentrations. The numbers of detected EV signals plateaued after 1.1 μg/ml in the case of CD9 antibody and 3.3 μg/ml in the case of CD63 and CD81 antibodies. Black line: CD9; green line: CD63; red line: CD81. Error bars = S.D. ($n = 5$). (c,d), Comparison of single staining and multiple staining of tetraspanin antibodies. The result of single and cocktail staining of CD9, CD63, and CD81 antibodies did not show significant differences in average EV signal counts. Bars = mean ± S.D. Student's t-test, $P > 0.1$ ($n = 8$). Size of all images: 45 × 45 μm. (e,f) Characterization of EV concentration. The numbers of detected EVs plateaued at 108 particles/ml EV concentration. The linear range of detection was from ~107 to ~108 particles/ml. Error bars = S.D. ($n = 8$)

antibody, the result will only reflect the characteristics of CD9-positive EVs, instead of the whole population. Therefore, using a surface-tethered antibody strategy for studying EV diversity might provide a biased result that could distort our understanding of EV diversity. For this reason, prior to analysing the diversity of EVs, we tested experimentally whether our immobilization strategy provides unbiased analysis of EV diversity.

The DUC-isolated EVs were immobilized on surfaces using the biotin-avidin interaction and surface-tethered CD81 antibody, and the surfaces were imaged using CD9, CD63, and CD81 tetraspanin antibodies (Figure 1: biotin-avidin, Figure S5a: surface-tethered CD81). The EV-immobilized surfaces using biotin-avidin interaction and surface-tethered antibody showed clear single-EV images in all three tetraspanin labellings (Figure S5b). When the numbers of each EV signals were quantified and compared with the WB of the same DUC-EVs using the same set of antibodies, the biotin-avidin sample showed the most similar tetraspanin expressions to the WB results (Figure S5c,d). The surface-tethered CD81 immobilization showed distinctly lower counts of CD63-positive EV signals than the counts CD9- or CD81-positive EV signals. Therefore, we determined that the biotin-avidin strategy can provide the most unbiased result that also agreed well with the results of the conventional method.

3.5 | Characterization of tetraspanin expressions in individual EVs by co-localization analysis

To investigate tetraspanin marker expression profiles in individual EVs, multi-channel imaging and co-localization analysis of the marker signals in individual EVs is essential. The reliability of the co-localization analysis was first demonstrated using EV-sized nanoparticles (multi-colour, blue and red nanoparticles, all 100 nm in diameter). From the multi-channel images of multi-colour nanoparticles (emission: ~400 to 700 nm), we first confirmed that the microscope setup could reliably detect all four colour channels without bias (Figure S6a,b). When the co-localizations of the signals acquired from the different colour channels were analyzed, the signals detected from the multi-colour nanoparticle sample showed ~100% co-localizations, whereas the signals detected from a blue and red nanoparticle mixture sample showed only ~15% co-localizations (Figure S6c,d). In addition to the nanoparticle demonstrations, DUC-EVs labelled with CD9 primary antibody and three different coloured secondary antibodies (Alexa Fluor 488, 546, and 647) were also subjected to the multi-colour co-localization analysis. The results showed at least 85% of detected signals were triple-positives (co-localized); this result confirms that co-localization analysis is also valid for real EV samples (Figure S6e,f).

The DUC EV-immobilized surfaces were then labelled with CD9, CD63, and CD81 tetraspanin antibodies having different colours, and the acquired tetraspanin signals were subjected to a multi-colour co-localization analysis to investigate how tetraspanins were expressed in individual EVs. All detected tetraspanin signals were analyzed for co-localization and classified into seven EV subpopulations according to their tetraspanin expression patterns (Figure 4a,b). For example, the signals detected in a yellow-boxed image showed three different HEK293 DIUC-EV subpopulations: (i) CD9•CD63•CD81 triple-positive EV; (ii) CD63 single-positive EVs; and (iii) CD9•CD81 double-positive EVs (Figure 4b). In the result, ∼51% of the tetraspanin signals were not co-localized (Figure 4c). Most of these single-positive EVs were CD63 single-positives (∼34%) (Figure 4c). As for co-localized signals, ∼38% of the tetraspanin counts were double-positive EVs, most of which were CD9•CD81 double-positive EVs (∼34%) (Figure 4c). The proportions of CD9•CD63 and CD63•CD81 double-positive EV were negligible (<3%). However, CD9•CD63•CD81 triple-positive EVs comprised a substantial portion (∼11%) of total EVs (Figure 4c). When all correlations among tetraspanin expressions of HEK293 DUC-EVs were simplified as a Venn diagram, the populations were roughly divided into two groups: one mainly composed of CD9•CD81 double-positive EVs, and one composed of CD63 single-positive EVs (Figure 4d).

However, EVs that are double-positive and triple-positive for tetraspanin could be EV aggregates, rather than individual EVs. To test this possibility, we analyzed a 0.20-μm filtered DUC-EV sample for tetraspanin co-localizations. This 0.20-μm filtration significantly decreased total detected EV counts but did not alter the tetraspanin expression profiles of individual EVs (Figure S7a-c). Therefore, we concluded that the EV aggregates had been removed during the sample preparation process by aggregate-cleaning centrifugation step performed after the DUC (Methods section), and that co-localized tetraspanin signals were unlikely to be EV aggregates.

To evaluate whether the analysis is broadly applicable for different EV samples, the tetraspanin co-localization analysis was applied to EVs that had been produced by different cell lines. The EVs were isolated using the DUC method from MCF-7 human breast cancer and B16BL6 mouse melanoma cell cultures, and both types of EV were analyzed using the same set of tetraspanin antibodies that had been used for the HEK293 EV analysis. The analysis of DUC-isolated MCF-7 EV showed a similar result to that of HEK293 DUC-EV analysis (Figure 4e,f). The MCF-7 EVs had slightly higher proportions of CD9 and CD81 single-positive EVs and slightly lower proportions of CD63 single-positive EVs, but the overall profile of the tetraspanin expressions in individual EVs was almost the same as in HEK293 EVs (Figure 4d and g). In contrast, the analysis of DUC-isolated B16BL6 EV showed a distinctively different result; only < 10% of total tetraspanin-positive EV signals were co-localized and most of them were single-positive EVs (Figure 4h,i). The overall tetraspanin expression profile of the B16BL6 EVs was completely different than those of to the other two cell lines (Figure 4d, g, and j). These results suggest that the TIRF-based single-EV analysis can successfully detect multiple marker expressions in individual EVs from various cell types.

3.6 | Characterization of lipid expressions in individual EVs by co-localization analysis

Lipids are another major components of EVs, so analysis of lipid expressions in individual EVs may provide insight into the nature of EVs. Therefore, HEK293 DUC-EVs were labelled using three different lipid probes, and the acquired lipid signals were then analyzed for co-localizations. The three lipid specific probes were cholera toxin-β (CTB), annexinV (AV) and Di-dye. CTB molecules bind to ganglioside GM1, which is one of the representative components of the membrane micro-domain, called lipid rafts (Blank et al., 2007). AV molecules have an affinity to phosphatidylserines (PS), which are mainly located at the inner leaflet of plasma membrane, so AV molecules are used to detect apoptotic cells (Van Engeland et al., 1998). Di-dyes are lipophilic carbocyanine tracers that are used to label plasma membrane, but specific targets and labelling mechanisms are not well defined. Although these lipid-labelling probes have different targets and mechanisms, all of them have been used for EV labelling in previous literature (Lai et al., 2015; Yost et al., 2007).

When the co-localization of lipid probe positive signals were analyzed, all detected EVs that expressed the lipids were classified into three major subpopulations. This result indicates that the lipid expressions in DUC-EVs were less heterogeneous than the tetraspanin expressions (Figure S8a,b). Most of the single-positive EVs were CTB single-positives (∼60%), whereas only ∼2% of DiI-positive EVs and AV-positive EVs were single-positive (Figure S8b). Among the double-positive EVs, only CTB•DiI double-positive EVs were substantially common (∼29%); but CTB•AV and DiI•AV double-positive EVs were not observed (both 0%). Finally, ∼5% of EVs were positive for all three probes. When all correlations between lipid expressions were simplified as a Venn diagram, the EV populations classified by lipid expressions exhibited a distinct hierarchical structure [AV ⊂ DiI ⊂ CTB] (Figure S8c).

Further analysis of the correlation between CTB-labelled EVs and tetraspanin-positive EVs could confirmed that almost half of the CTB-labelled EVs were negative for tetraspanin expression (Figure S8d). Although this population was not further investigated in this study, it was presumed to be an EV subpopulation that is enriched with GM1 lipids but does not express tetraspanins. Similarly, the single-EV co-localization analysis can be further used to investigate the correlation of numerous combinations of markers. However, in this study, instead of using other combinations of markers, we decided to use the three tetraspanin combinations to further investigate how different EV isolation methods affect the population of isolated EVs.

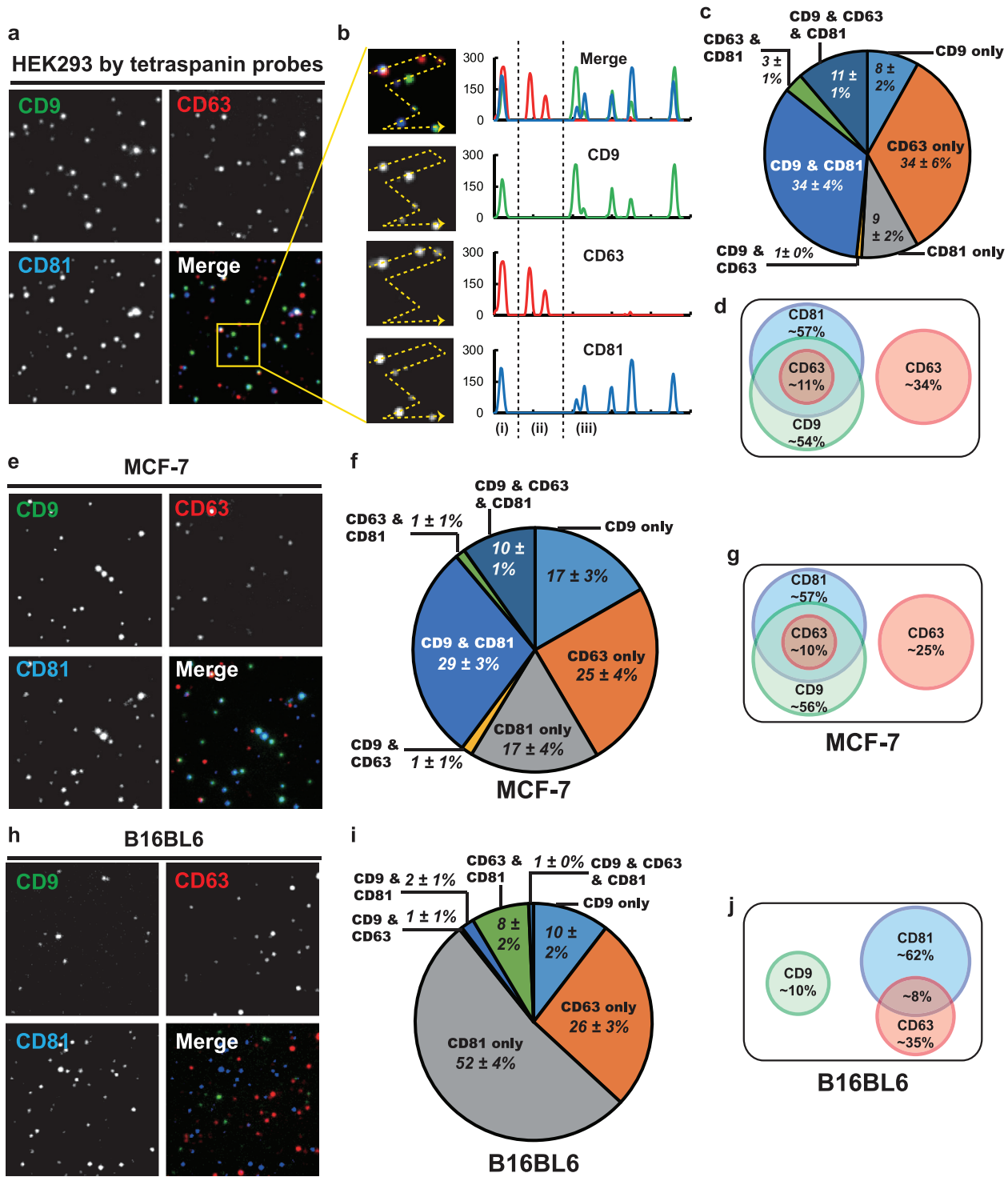

FIGURE 4 Characterization of EV populations by tetraspanin co-localization analysis. (a), Representative single-vesicle fluorescence images of HEK293 DUC-EVs. The CD9, CD63, and CD81 images were coloured in green, red and blue, respectively. Size of images: 17 × 17 μm. (b) Intensity line scan of selected area (yellow box). Region (i) CD9•CD63•CD81 triple-positive EV, region (ii) CD63 single-positive EVs, and region (iii) CD9•CD81 double-positive EVs. Size of enlarged images: 5 × 5 μm. (c) Pie chart of EV populations expressing different combinations tetraspanins. (d) Venn diagram depicting tetraspanin relationships in individual HEK293 EVs. The EV populations were roughly divided into two distinct groups: CD63 single-positive and CD9•CD81 double-positive EVs. (e-g) Tetraspanin co-localization analysis of MCF-7 EVs. The population of MCF-7 EVs were overall similar to HEK293 EVs. Size of images: 17 × 17 μm. (h-j) Tetraspanin co-localization analysis of B16BL6 EVs. The population of B16BL6 EVs was completely different compared to the other two cell lines; it showed higher single-positive EV proportion than the other two cases. Numbers in pie charts: mean ± S.D. ($n > 8$). Numbers in Venn diagrams: percentages of total EVs

3.7 | Conventional characterization of EV fractions acquired from different isolation methods

We then use the tetraspanin co-localization analysis to investigate the EVs that had been isolated using three frequently-used isolation methods: DG, buoyant DG (BDG) and size exclusion chromatography (SEC) (Figure S9). DG and BDG purify EVs according to sedimentation number (Sv) and density, and SEC purifies EVs according to size. Small impurities like proteins have small Sv, so they stay in the sample fractions in DG and BDG, but have low mobility in an SEC column, so will be eluted in the later fractions. Due to these differences in separation principles, the methods are expected to isolate different EVs. In this study, for DG and BDG, we used 0%, 10%, 20% and 30% Opti-Prep as density-gradient media, and acquired all fractions and subjected them to single-EV tetraspanin analysis. When SEC was used, we tested all acquired fractions (#5 to #20) for protein amount, particle amount and tetraspanin expressions, then selected the four fractions that expressed the largest amount of tetraspanins (#8, #9, #10 #11) for further analysis (Figure S10a-c). All fractions were obtained as 500-μl final volume from the same amount of initial culture medium.

Before being used for the conventional and single-EV analysis, all acquired fractions were first analyzed using nanoparticle tracking analysis (NTA) and TEM to test whether or not the fractions actually contained isolated EVs. The size distributions measured using NTA confirmed that all acquired fractions contained EV-sized particles (Figure S11a-c); the fractions that had heaviest density (DG/20-30 and BDG/20-30) showed noticeably larger particles than the other fractions (Figure S11a,b). However, the fractions acquired from SEC did not show any significant difference in size distribution; this result suggests that the SEC might not have sufficient resolution to isolate different sizes of EVs (Figure S11c). The TEM observations confirmed that all fractions included numerous EV-like structures (Figure S11d-f).

All acquired fractions were first analyzed using conventional EV analyses. Protein and particle yield of EVs from 1 L cultured media (CM) were quantified for each fraction, and the numbers of particles per microgram protein in each were calculated to estimate the purities. Tetraspanin WB was performed using the same 25 μl of each fraction, and the resulting bands were detected under the same detection conditions. The intensities of the bands were quantified using ImageJ software (Figure 5d,e). Protein quantifications indicated that the DG/0-10 fraction isolated the largest number of EVs, whereas particle quantifications indicated that the BDG/10-20 fraction isolated the largest number of EVs (Figure 5a,b). The purity index also indicated that the BDG/10-20 fraction isolated the purest EVs (Figure 5c). However, the WB results only partially agreed with the protein quantifications; WB indicated that the DG/0-10 and DG/10-20 fractions isolated the largest number of EVs and that other six fractions except DG/20-30 and BDG/0-10 fractions showed a similar intermediate levels of tetraspanin expression. When the correlations between the conventional quantifications of all fractions were investigated, the 'protein and WB' pair and the 'particle and purity' pair showed a moderate and statistically significant correlation ($R^2 > \sim 0.6$, $P < 0.01$) (Figure 5h,i). However, the protein yield did not show any correlation with either particle yield or purity index, and particle yield and purity index also did not show any correlations with WB intensity (Figure 5f,g and j,k). To summarize the results of these analyses, either the correlation among the results of the conventional analyses is low, or the different EV fractions isolated different subpopulations of EVs. In contrast, when the WB intensities of each tetraspanin results were compared, all of the pairs showed strong and statistically significant linear correlations ($R^2 > \sim 0.75$, $P < 0.01$) (Figure 5l-n). The results of analysis did not show consistent conclusions, so further analyses using single-EV imaging and co-localization were performed in the following sections.

3.8 | Single-EV tetraspanin co-localization analysis of the EV fractions acquired from different isolation methods

To experimentally confirm whether the isolated EV fractions contain different subpopulations or not, we analyzed the fractions using the single-EV tetraspanin analysis. In the results, the DG/10-20 fraction showed the highest counts for all three tetraspanins (Figure 6a,b). The SEC fractions also showed relatively high tetraspanin counts, whereas DG/20-30 and BDG/0-10 fraction showed low tetraspanin counts which were even lower than the counts of DUC-EVs (Figures 4a and 6a). The DG/0-10 and BDG/20-30 fractions showed similar numbers of tetraspanin, which were also similar to the numbers of DUC-EVs (Figures 4a and 6a). Before analysing co-localizations of tetraspanin signals detected from each fraction, the correlations between the results of tetraspanin counts and conventional analyses were first investigated. As a result, the quantifications of protein, particle and tetraspanin WB did not show significant correlations with the counts from the single-EV tetraspanin analyses (Figure 6c-e). Even when each tetraspanin count of the fractions was then separately compared with the WB intensities, none of the pairs showed a significant correlation ($P > 0.05$) (Figure 6f-h). However, similar to the case of the WB results, each single-EV tetraspanin count of the fractions showed very strong and statistically significant linear correlations ($R^2 > \sim 0.87$ and $P < 0.0001$) (Figure 6i-k). These results confirm that the simple tetraspanin counts of single-EV analysis did not provide new insights, and also had little correlation with the results of conventional analyses.

Therefore, tetraspanin co-localizations analysis of each fractions were performed to further investigate the differences and similarities among the fractions. In the case of DG fractions, EV populations in DG/10-20 fraction showed a distinctively different pattern of tetraspanin expressions compared to the other two DG fractions (Figure 7a). More than 50% of EVs isolated

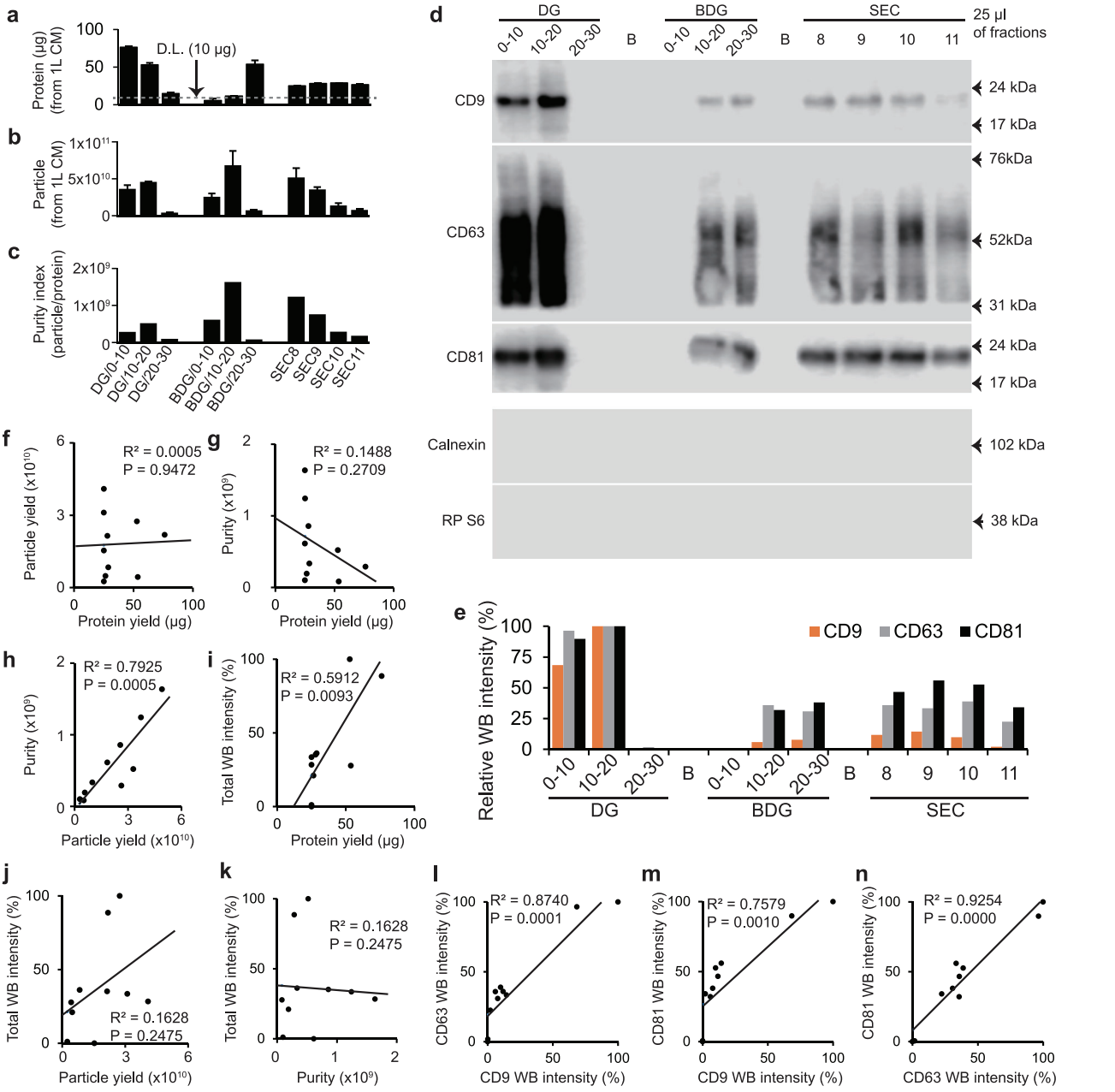

FIGURE 5 Characterization of EV fractions using conventional analyses. (a) Protein amount of EVs per 1L CM and (b), particle amount of EVs per 1L CM of all fractions. Protein amount < 10 μg could not be detected by Bradford protein assay. Bars = mean ± S.D. ($n = 3$ for protein, $n = 6$ for particle). DL, detection limit. (c) Purity index of the fractions. Purity of samples was calculated as particles per microgram protein. (d) Western blot analysis (WB) of EV fractions and (e), quantification of WB intensities. Expressions of EV-positive markers (CD9, CD63, and CD81) and -negative markers (Calnexin and ribosomal protein S6) were analysed using WB. Same volumes (25 μl) of each fraction were analyzed under the same condition. Different fraction showed different tetraspanin expressions, but none of the fractions showed EV-negative markers. (f-k), Correlation analyses between conventional analyses and l-m, correlation analysis between the each tetraspanin results of WB. All correlation analyses were investigated using linear regression. In all linear regressions, individual points represented mean values of each fractions. Solid lines: linear regressions; R2: determination coefficient of the regression. Regressions that have $P < 0.05$ are considered statistically significant

from DG/0-10 and DG/20-30 fractions were CD63 single-positive EVs, whereas the largest population of DG/10-20 fraction was CD9•CD81 double-positive EVs (Figure 7a). The BDG fractions also showed distinct differences in tetraspanin co-localization analysis (Figure 7b). The BDG/10-20 fraction contained mostly CD9•CD81 double-positive EVs, whereas the BDG/20-30 fraction contained mostly CD63 single-positive EVs (Figure 7b).

On the contrary, the result of SEC fractions did not show many differences among fractions: some statistically-significant differences were observed between the fractions, but the extent was less significant than the cases of the DG or BDG fractions (Figure 7c). The SEC fractions showed comparatively evenly-distributed populations, and the proportions of CD9, CD63, and CD81 single-positive and CD9•CD81 double-positive EV populations were the four major populations (Figure 7c).

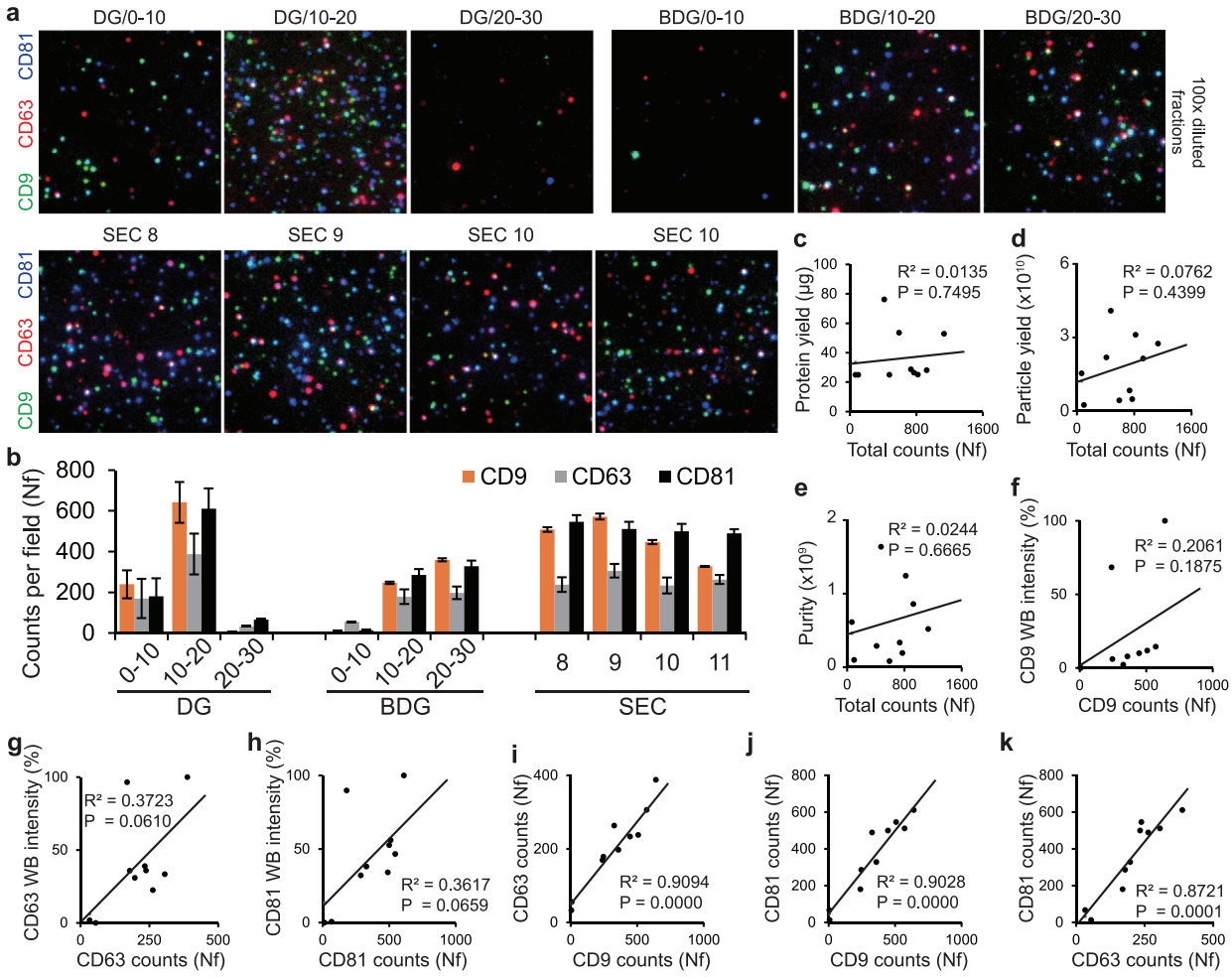

FIGURE 6 Single-EV tetraspanin analysis of EV fractions from DG, BDG and SEC. (a), Single EV tetraspanin expression images of EV fractions. EVs expressing tetraspanin markers were analyzed using single-EV imaging. The CD9, CD63, and CD81 signals were coloured in green, red and blue, respectively. Size of images: 17 × 17 μm. (b) Quantification of tetraspanin signals detected from EV fractions. Numbers of tetraspanin signals were quantified from the images (45 × 45 μm). Bars = mean ± S.D. ($n = 9$). (c-h) Correlation analyses between conventional analyses and single-EV tetraspanin analysis. The correlation between conventional analyses and single-EV tetraspanin counts were investigated using linear regression. None of the analyses showed statistically significant correlation. (i-k) Correlation analyses between tetraspanin counts of single-EV analysis. The correlation between tetraspanin counts of single-EV analysis were investigated using linear regression. All three regressions showed statistically significant correlations. In all linear regressions, individual points represented mean values of each fraction. Solid lines indicated linear regressions and R2 indicated determination coefficient of the regression. Regressions that have $P < 0.05$ are considered statistically significant

EVs in each fraction were classified into seven populations that had different tetraspanin expression profiles, it is difficult to investigate correlations among them by direct comparison. Therefore, the results were further visualized using t-distributed stochastic neighbour embedding (t-SNE) and clustered heat map analyses (Figure 7d,e). In both analyses, some of the fractions clustered together; that is, these fractions have similar population compositions. For example, the DG/10-20 and BDG/10-20 fractions were clustered together in both analyses but the DG/0-10 fraction was not; this result suggest that the DG/10-20 and BDG/10-20 fractions isolated similar populations of EVs, and that they were different than the EVs in the DG/0-10 fraction.

The heat map result showed four clusters. The first and third clusters were exactly matched with the C1 and C3 clusters of tSNE analysis; this clusters indicated that isolation methods that exploit density most effectively separated CD9•CD81 double-positive and CD63 single-positive EVs, which were the two major populations of DUC-EVs (Figures 4d and 7e). The fourth cluster and C4 cluster of tSNE showed that all SEC fractions isolated similar populations of EVs, and also showed that the SEC isolation separated different populations of EVs compared to the methods that exploit density gradients (Figure 7d,e).

Lastly, to reinvestigate the correlation between the conventional analyses and single-EV analysis that failed in the previous section, we performed the correlation analysis again, but only with the fractions that were confirmed to have similar populations in the tetraspanin co-localization analysis (SEC8, SEC9, SEC10, SEC11, and BDG/0-10 fractions) (Figure 7e, **bottom five fractions**). As a consequence, the correlation between the single-EV tetraspanin counts and tetraspanin WB became strong and statistically

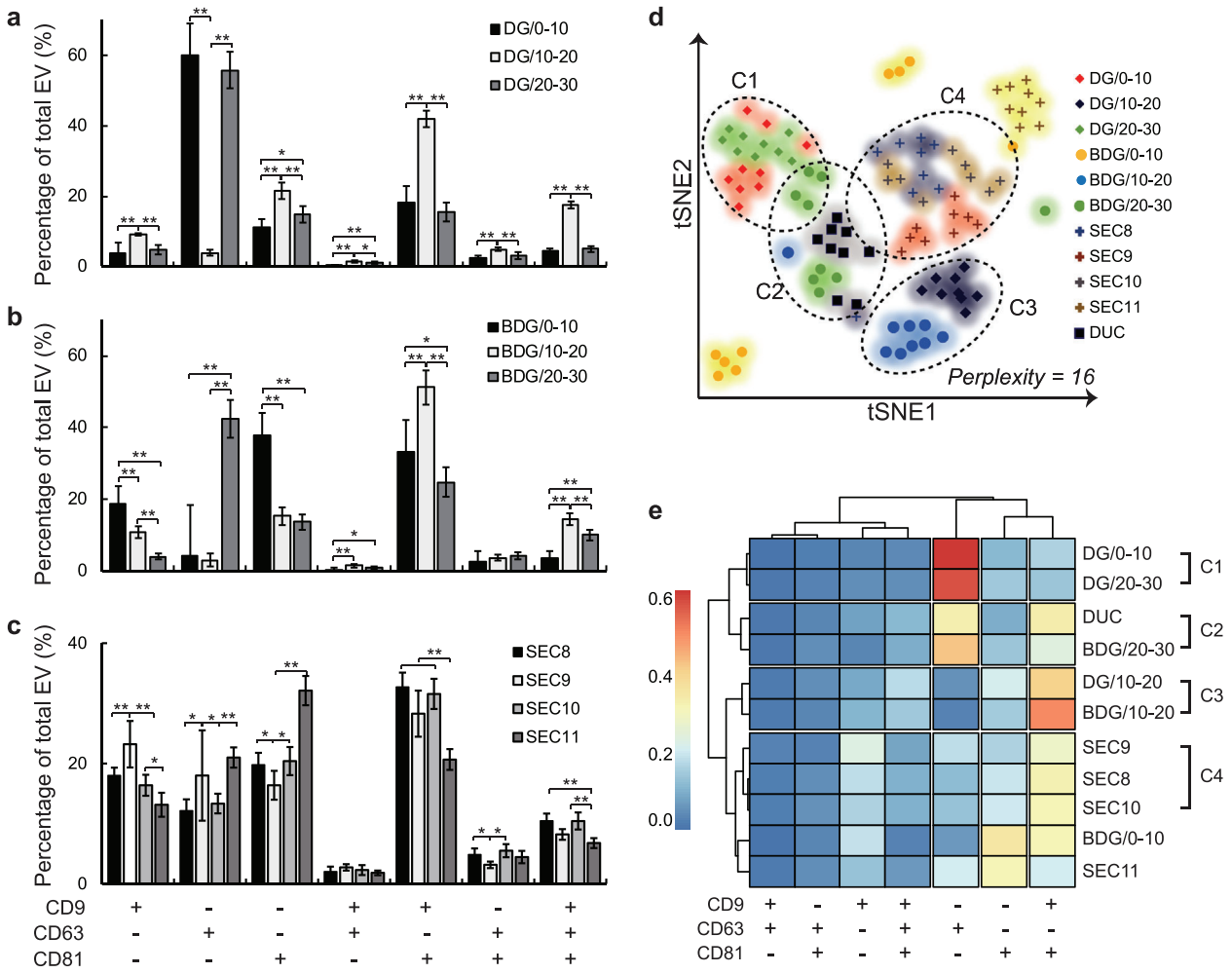

FIGURE 7 Single EV tetraspanin co-localization analysis of all EV fractions. Tetraspanin co-localization analysis of (a) DG fractions, (b) BDG fractions, and (c) SEC fractions. Co-localization analysis of all fractions showed seven different EV populations by tetraspanin expression profiles. Bars = mean ± S.D., Student's t-test, pairs showed statistical significant differences were indicated by brackets with *: $P < 0.05$, **: $P < 0.01$ ($n > 9$). (d) t-distributed stochastic neighbour embedding (t-SNE) visualization of all EV fractions. Seven-dimensional population information of each fraction was reduced to two-dimensional space by t-SNE with perplexity value = 16. Fractions that were close to each other were grouped into clusters (c1-c4). ($n = 9$). (e) Clustering heat map analysis of EV fractions. Average proportions of each population were expressed as coloured block (high: red, low: blue) ($n = 9$). Similarities between the EV fractions were calculated using the Euclidean distance and the similar fractions were grouped and separated by the gaps. The clusters identified in tSNE analysis are also indicated on the right side of the heat map

significant (Figure S12d-f). However, the tetraspanin counts still did not show any correlations with protein yield, particle yield or purity (Figure S12a-c).

4 | DISCUSSION

Although the diversity of EVs and the presence of their subpopulations have been well demonstrate by previous studies, analytical methods that can quantitatively investigate this feature have rarely been developed. Available EV analysis methods have not been able to answer critical questions about EV biology, such as which EV subpopulations exert specific biological functions, or which subpopulations of EVs from blood provide information for disease diagnostics. Although some of the recently-developed technologies have provided tools to investigate subpopulations of EVs, the use of such advanced technologies has often been limited. In this study, to establish the technical foundation to find answers for these important questions, we introduced a new single- vesicle analysis method that can visualize individual EVs and characterize their marker expressions. The method uses a TIRF microscope, which is already widely used, so various researchers can easily apply the method to their own research. For a reliable and reproducible analysis, every aspect of the analysis such as imaging surface-EV interaction, imaging surface-probe interaction, EV labelling conditions and accuracy of co-localization analysis were thoroughly characterized in the manuscript.

The method can be used along with conventional EV analyses because it only requires a simple biotinylation of EVs that is compatible with most of existing analysis methods. The strong EV-anchoring property of the surface allows a reliable co-localization analysis of multiple markers, and the effective protein-repelling property of the surface enables rapid and efficient fluorescent labelling of EVs. With these advantages, the entire analysis, including EV labelling, took only approximately 1 h. This rapid and efficient EV analysis is a great advantage over conventional methods, which all require lengthy EV labelling and washing steps that also affect the diversity of EV samples.

From the results of the application of our single-EV analysis to HEK293 EVs, we identified unprecedented expression patterns of tetraspanins and lipids in individual EVs. The analysis revealed two distinct subpopulations from the DUC-isolated HEK293 EVs by tetraspanin expression pattern: one is CD9•CD81 double-positive EVs and the other is CD63 single-positive EVs. Although we did not further investigate to identify the biological implications of these populations, similar observations have been reported previous literatures. A study that used flow cytometry showed co-partitioning of CD9 and CD81 tetraspanin molecules into HIV-1, and another showed that EVs that express CD9 and CD81 had similar sizes using size-based EV separation technique (Dahmane et al., 2019; Jeong, Han, Cho, Gianchandani, & Park, 2018). Our analysis also showed that most of the CD63-positive EVs were CD63 single-positive, but once co-localized, they were CD9•CD63•CD81 triple-positives. This unique pattern was also observed in the control experiment using the surface-tethered CD81 antibody; the number of detected CD63-positive EVs was significantly reduced in EVs immobilized by CD81 antibody compared to EVs immobilized by biotin-avidin interaction. However, from the analysis result of EVs isolated from the B16BL6 cell line, we also confirmed that these tetraspanin expression patterns were not always observed in all types of cells. For example, a previous literature that investigated tetraspanin expression profiles of porcine seminal plasma EVs reported that CD9 and CD63 were co-expressed in exosomes in their flow cytometric EV analysis (Barranco et al., 2019). In addition, the co-localization analysis result of lipid probes and tetraspanins implied possibility that there might be plenty of undetected EVs on the imaging surface. Therefore, to verify biological meanings of the identified EV subpopulations and to identify surface-immobilized but undetected EV populations, further investigations with a wide variety of additional EV markers are required.

To demonstrate the advantages of the single-EV analysis in a real EV applications, we performed population analysis of EV fractions acquired from three most frequently used EV isolation methods. The tetraspanin co-localization analysis effectively showed the similarity and dissimilarity between the fractions, which could not be revealed by any of conventional analyses. For example, tetraspanin WB analysis of the BDG/10-20 and SEC #10 fractions showed almost the same tetraspanin expression profiles, whereas single-EV co-localization analysis clearly illustrated their differences in tetraspanin expression profiles. The fractions acquired from different density gradient layers showed distinctively different tetraspanin expression patterns, which is indicating density-based isolation methods were effective in separating a heterogeneous DUC-EV sample into more refined subpopulations. On the contrary, the fractions acquired from SEC did not show much difference in tetraspanin expression profiles, and from this result, we can confirm that the SEC methods might have difficulty separating EVs that express different tetraspanins.

In summary, we demonstrated a single-EV analysis that can visualize expressions of multiple EV-related markers in individual EVs. By analysing the co-localizations of tetraspanin signals, we revealed distinct EV populations expressing different combinations of tetraspanin. Although we tested only a limited number of EV markers, the analysis successfully revealed that the different isolation methods yielded different characteristics of EV fractions. Further investigations using different sets of antibodies or EVs from different sources will provide more valuable information regarding the biology of EVs. We expect that the proposed analysis method will be a powerful tool to investigate the characteristics of EVs.

ACKNOWLEDGEMENTS

The authors are grateful to Mrs. Wonjung Kwak of the Department of Mechanical Engineering at POSTECH for invaluable support regarding cell culture and EV isolation, and Dr. Jong-Bong Lee of the Department of Physics at POSTECH for essential discussions concerning the microscope setup. This work was supported by the National Research Foundation of Korea (NRF) grant funded by Korean government (MSIP) (No. 2018R1A2B3006280) and partial support from ExosomePlus, Inc., Republic of Korea.

CONFLICTS OF INTEREST

The authors declare the following competing interests: J.P. is a founder of ExosomePlus, Inc. that partially supported this work.

AUTHOR CONTRIBUTIONS

Chungmin Han and Jaesung Park designed the overall experiments. Chungmin Han, Jaehun Jung and Hyunjin Lee performed surface treatment and microfluidic channel preparations. Chungmin Han, Johan Yi, Hyunjin Lee, Yongmin Kwon, Hyejin Kang carried out EV isolation and electron microscopy. Hyejin Kang and Minsu Kang cultured cells and performed western blotting. Johan Yi and Jingeol Lee conducted nanoparticle tracking analysis. Chungmin Han established overall methods, built the TIRF microscope system, performed individual EV analysis, wrote the MATLAB script for image processing, analyzed data, prepared figures, and wrote the manuscript. Jaesung Park managed the project and helped figure preparation, and manuscript writing.

The manuscript was written through contributions of all authors. All authors have given approval to the final version of the manuscript.

DATA AVAILABILITY STATEMENT

The authors confirm that the data supporting the findings of this study are available within the article and its supplementary materials.

REFERENCES

Aggarwal, V., & Ha, T. (2016). Single-molecule fluorescence microscopy of native macromolecular complexes. *Current Opinion Structure Biology*, *41*, 225–232

Barranco, I., Padilla, L., Parrilla, I., Álvarez-Barrientos, A., Pérez-Patiño, C., Peña, F. J., Martínez, E. A., Rodriguez-Martínez, H., & Roca, J. (2019).Extracellular vesicles isolated from porcine seminal plasma exhibit different tetraspanin expression profiles. *Scientific Reports*, *9*(1), 11584. https://doi.org/10.1038/s41598-019-48095-3

Blank, N., Schiller, M., Krienke, S., Wabnitz, G., Ho, A. D., & Lorenz, H.-.M. (2007). Cholera toxin binds to lipid rafts but has a limited specificity for ganglioside GM1. *Immunology Cell Biology*, *85*, 378–382

Böing, A. N., Van Der Pol, E., Grootemaat, A. E., Coumans, F. A. W., Sturk, A., & Nieuwland, R. (2014). Single-step isolation of extracellular vesicles by size-exclusion chromatography. *Journal of Extracellular Vesicles*, *3*, 1–11

Brandenburg, B., & Zhuang, X. (2007). Virus trafficking - Learning from single-virus tracking. *Nature Reviews Microbiology*, *5*, 197–208

Chen, C., Zong, S., Wang, Z., Lu, Ju, Zhu, D., Zhang, Y., & Cui, Y. (2016). Imaging and intracellular tracking of cancer-derived exosomes using single-molecule localization-based super-resolution microscope. *ACS Applied Materials & Interfaces*, *8*, 25825–25833

Choi, D.-.S., Kim, D.-.K., Kim, Y.-.K., & Gho, Y. S. (2015). Proteomics of extracellular vesicles: exosomes and ectosomes. *Mass Spectrometry Reviews*, *34*, 474–490

Choi, U. B., Strop, P., Vrljic, M., Chu, S., Brunger, A. T., & Weninger, K. R. (2010). Single-molecule FRET-derived model of the synaptotagmin 1-SNARE fusion complex. *Nature Structural & Molecular Biology*, *17*, 318–324

Daaboul, G. G., Gagni, P., Benussi, L., Bettotti, P., Ciani, M., Cretich, M., Chiari, M., Freedman, D. S., Ghidoni, R., Ozkumur, A. Y., Piotto, C., & Prosperi, D. (2016). Digital detection of exosomes by interferometric imaging. *Scientific Reports*, *6*, 1–10

Dahmane, S., Doucet, C., Le Gall, A., Chamontin, C., Dosset, P., Murcy, F., Fernandez, L., Salas, D., Rubinstein, E., Mougel, M., Nollmann, M., & Milhiet, P.-.E. (2019). Nanoscale organization of tetraspanins during HIV-1 budding by correlative dSTORM/AFM. *Nanoscale*, *11*, 6036–6044

Donaldson, J. (2016). Tsne: T-Distributed Stochastic Neighbor Embedding for R (t-SNE). R package version 0.1-3. https://CRAN.R-project.org/package=tsne

Erdbrügger, U., Rudy, C. K., E. Etter, M., Dryden, K. A., Yeager, M., Klibanov, A. L., & Lannigan, J. (2014). Imaging flow cytometry elucidates limitations of microparticle analysis by conventional flow cytometry. *Cytometry. Part A*, *85*, 756–770

Février, B., & Raposo, G. (2004). Exosomes: endosomal-derived vesicles shipping extracellular messages. *Current Opinion Cell Biology*, *16*, 415–421

Gardiner, C., Ferreira, Y. J., Dragovic, R. A., Redman, C. W. G., & Sargent, I. L. (2013). Extracellular vesicle sizing and enumeration by nanoparticle tracking analysis. *Journal of Extracellular Vesicles*, *2*, (1)

Guduric-Fuchs, J., O'connor, A., Camp, B., O'neill, C. L., Medina, R. J., & Simpson, D. A. (2012). Selective extracellular vesicle-mediated export of an overlapping set of microRNAs from multiple cell types. *BMC Genomics*, *13*, 357

Hong, B., Cho, Ji-H., Kim, H., Choi, E.-.J., Rho, S., Kim, J., Kim, J. H., Choi, D. H., Kim, Y. K., Hwang, D., & Gho, Y. (2009). Colorectal cancer cell-derived microvesicles are enriched in cell cycle-related mRNAs that promote proliferation of endothelial cells. *BMC Genomics*, *10*, 1–13

Höög, J. L., & Lötvall, J. (2015). Diversity of extracellular vesicles in human ejaculates revealed by cryo-electron microscopy. *Journal of Extracellular Vesicles*, *4*, 28680

Hua, B., Han, K. Y., Zhou, R., Kim, H., Shi, X., Abeysirigunawardena, S. C., Jain, A., Singh, D., Aggarwal, V., Woodson, S. A., & Ha, T. (2014). An improved surface passivation method for single-molecule studies. *Nature Methods*, *11*, 1233–1236

Im, H., Shao, H., Park, Y. I.l, Peterson, V. M., Castro, C. M., Weissleder, R., & Lee, H. (2014). Label-free detection and molecular profiling of exosomes with a nano-plasmonic sensor. *Nature Biotechnology*, *32*, 490–495

Jain, A., Liu, R., Ramani, B., Arauz, E., Ishitsuka, Y., Ragunathan, K., Park, J., Chen, J., Xiang, Y. K., & Ha, T. (2011). Probing cellular protein complexes using single-molecule pull-down. *Nature*, *473*, 484–488

Jeong, H., Han, C., Cho, S., Gianchandani, Y., & Park, J. (2018). Analysis of extracellular vesicles using coffee ring. *ACS Applied Materials & Interfaces*, *10*, 22877–22882

Ji, H., Chen, M., Greening, D. W., He, W., Rai, A., Zhang, W., & Simpson, R. J. (2014). Deep sequencing of RNA from three different extracellular vesicle (EV) subtypes released from the human LIM1863 colon cancer cell line uncovers distinct mirna-enrichment signatures. *PLoS One*, *9*, e110314

Kao, C.-.Y., & Papoutsakis, E. T. (2019). Extracellular vesicles: exosomes, microparticles, their parts, and their targets to enable their biomanufacturing and clinical applications. *Current Opinion in Biotechnology*, *60*, 89–98

Kim, K. L., Kim, D., Lee, S., Kim, S. J., Noh, J. E., Kim, J. H., Chae, Y. C., Lee, J. B., & Ryu, S. H. (2016). Pairwise detection of site-specific receptor phosphorylations using single-molecule blotting. *Nature Commununications*, *7*, 1–10

Kolde, R. (2019). Pheatmap: Pretty Heatmaps. R package version 1.0.12. https://CRAN.R-project.org/package=pheatmap

Kowal, J., Arras, G., Colombo, M., Jouve, M., Morath, J. P., Primdal-Bengtson, B., Dingli, F., Loew, D., Tkach, M. & Théry, C. (2016). Proteomic comparison defines novel markers to characterize heterogeneous populations of extracellular vesicle subtypes. *Proceedings of the National Academy of Sciences of the United States of America*, *113*, E968–E977

Krämer-Albers, E.-.M., & Hill, A. F. (2016). Extracellular vesicles: interneural shuttles of complex messages. *Current Opinion in Neurobiology*, *39*, 101–107

Lai, C. P., Kim, E. Y., Badr, C. E., Weissleder, R., Mempel, T. R., Tannous, B. A., & Breakefield, X. O. (2015). Visualization and tracking of tumour extracellular vesicle delivery and RNA translation using multiplexed reporters. *Nature Commununications*, *6*, 1–12.

Lee, K., Fraser, K., Ghaddar, B., Yang, K., Kim, E., Balaj, L.,, Chiocca, E A., Breakefield, X, O., Lee, H., Weissleder, R., &- Weissleder, R. (2018). Multiplexed profiling of single extracellular vesicles. *ACS Nano*, *12*, 494–503

Lee, W., Nanou, A., Rikkert, L., Coumans, F. A. W., Otto, C., Terstappen, L. W. M. M., & Offerhaus, H. L. (2018). Label-free prostate cancer detection by characterization of extracellular vesicles using raman spectroscopy. *Analytical Chemistry*, *90*, 11290–11296

Llorente, A., Skotland, T., Sylvänne, T., Kauhanen, D., Róg, T., Orłowski, A., Vattulainen, I., Ekroos, K., & Sandvig, K. (2013). Molecular lipidomics of exosomes released by PC-3 prostate cancer cells. *Biochimica et Biophysica Accta*, *1831*, 1302–1309

Margolis, L., & Sadovsky, Y. (2019). The biology of extracellular vesicles: the known unknowns. *PLoS Biology*, *17*, 1–12

Myong, S., Stevens, B. C., & Ha, T. (2006). Bridging conformational dynamics and function using single-molecule spectroscopy. *Structure*, *14*, 633–643
Nizamudeen, Z., Markus, R., Lodge, R., Parmenter, C., Platt, M., Chakrabarti, L., & Sottile, V. (2018). Rapid and accurate analysis of stem cell-derived extracellular vesicles with super resolution microscopy and live imaging. *Biochimica et Biophysica Acta. Molecular Cell Research*, *1865*, 1891–1900
Osteikoetxea, X., Sódar, B., Németh, A., Szabó-Taylor, K., Pálóczi, K., Vukman, K. V., Tamási, V., Balogh, A., Kittel, A., Pállinger, E., & Buzás, E. I. (2015). Differential detergent sensitivity of extracellular vesicle subpopulations. *Organic and Biomolecular Chemisty*, *13*, 9775–9782
R Core Team. (2020). *R: A language and environment for statistical computing*. R Foundation for Statistical Computing, Vienna, Austria. https://www.R-project.org/
Raposo, G., & Stoorvogel, W. (2013). Extracellular vesicles: exosomes, microvesicles, and friends. *Journal of Cell Biology*, *200*, 373–383
Roy, R., Hohng, S., & Ha, T. (2008). A practical guide to single-molecule FRET. *Nature Methods*, *5*, 507–516
Shu, S. L.a, Yang, Y., Allen, C. L., Hurley, E., Tung, K. H., Minderman, H., Wu, Y., & Ernstoff, M. S. (2020). Purity and yield of melanoma exosomes are dependent on isolation method. *Journal of Extracellular Vesicles*, 1692401, *9*
Simpson, R. J., Jensen, S. S., & Lim, J. W. E. (2008). Proteomic profiling of exosomes: current perspectives. *Proteomics*, *8*, 4083–4099
Sitar, S., Kejžar, A., Pahovnik, D., Kogej, K., Tušek-Žnidarič, M., Lenassi, M., & Žagar, E. (2015). Size characterization and quantification of exosomes by asymmetrical-flow field-flow fractionation. *Analytical Chemistry*, *87*, 9225–9233
Skliar, M., & Chernyshev, V. S. (2019) Imaging of extracellular vesicles by atomic force microscopy. *Journal of Visualized Experiments : JoVE*, 1–13. https://doi.org/10.3791/59254
Skotland, T., Hessvik, N. P., Sandvig, K., & Llorente, A. (2019). Exosomal lipid composition and the role of ether lipids and phosphoinositides in exosome biology. *Journal of Lipid Research*, *60*, 9–18
Tauro, B. J., Greening, D. W., Mathias, R. A., Ji, H., Mathivanan, S., Scott, A. M., & Simpson, R. J. (2012). Comparison of ultracentrifugation, density gradient separation, and immunoaffinity capture methods for isolating human colon cancer cell line LIM1863-derived exosomes. *Methods*, *56*, 293–304
Théry, C., Amigorena, S., Raposo, G., & Clayton, A. (2006). Isolation and characterization of exosomes from cell culture supernatants and biological fluids. *Current Protocols in Cell Biology*, *30*(1), 3–22
Théry, C., Witwer, K. W., Aikawa, E., Alcaraz, M. J., Anderson, J. D., Andriantsitohaina, R., Antoniou, A., Arab, T., Archer, F., Atkin-Smith, G. K., Ayre, D. C., Bach, J. M., & Zuba-Surma, E. K. (2018). Minimal information for studies of extracellular vesicles 2018 (MISEV2018): a position statement of the International Society for Extracellular Vesicles and update of the MISEV2014 guidelines. *Journal of Extracellular Vesicles*, *7*, 1535750
Théry, C., Zitvogel, L., & Amigorena, S. (2002). Exosomes: composition, biogenesis and function. *Nature Reviews Immunology*, *2*, 569–579
Ulbrich, M. H., & Isacoff, E. Y. (2008) Rules of engagement for NMDA receptor subunits, *105*, 14163–14168. https://www.pnas.org/content/105/37/14163
Van Der Pol, E., Van Gemert, M. J. C., Sturk, A., Nieuwland, R., & Van Leeuwen, T. G. (2012). Single vs. swarm detection of microparticles and exosomes by flow cytometry. *Journal of Thrombosis Haemostasis*, *10*, 919–930
Van Engeland, M., Nieland, L. J. W., Ramaekers, F. C. S., Schutte, B., & Reutelingsperger, C. P. M. (1998). Annexin V-affinity assay: a review on an apoptosis detection system based on phosphatidylserine exposure. *Cytometry*, *31*, 1–9
Wang, Y., Liu, Y., Deberg, H. A., Nomura, T., Hoffman, M. T., Rohde, P. R., Schulten, K., Martinac, B., & Selvin, P. R. (2014). Single molecule FRET reveals pore size and opening mechanism of a mechano-sensitive ion channel. *Elife*, *3*, 1–21
Wubbolts, R., Leckie, R. S., Veenhuizen, P. T. M., Schwarzmann, G., Möbius, W., Hoernschemeyer, J., Slot, J. W., Geuze, H. J., & Stoorvogel, W. (2003). Proteomic and biochemical analyses of human B cell-derived exosomes: potential implications for their function and multivesicular body formation. *Journal of Biological Chemistry*, *278*, 10963–10972
Yost, E. A., Mervine, S. M., Sabo, J. L., Hynes, T. R., & Berlot, C. H. (2007). Live cell analysis of G protein β5 complex formation, function, and targeting. *Molecular Pharmacology*, *72*, 812–825
Yuana, Y., Koning, R. I., Kuil, M. E., Rensen, P. C. N., Koster, A. J., Bertina, R. M., & Osanto, S. (2013). Cryo-electron microscopy of extracellular vesicles in fresh plasma. *Journal of Extracellular Vesicles*, *2*, 21494
Zhang, H., Freitas, D., Kim, H. S., Fabijanic, K., Li, Z., Chen, H., Mark, M. T., Molina, H., Martin, A. B., Bojmar, L., Fang, J., & Lyden, D. (2018). Identification of distinct nanoparticles and subsets of extracellular vesicles by asymmetric flow field-flow fractionation. *Nature Cell Biology*, *20*, 332–343

SUPPORTING INFORMATION

Additional supporting information may be found online in the Supporting Information section at the end of the article.